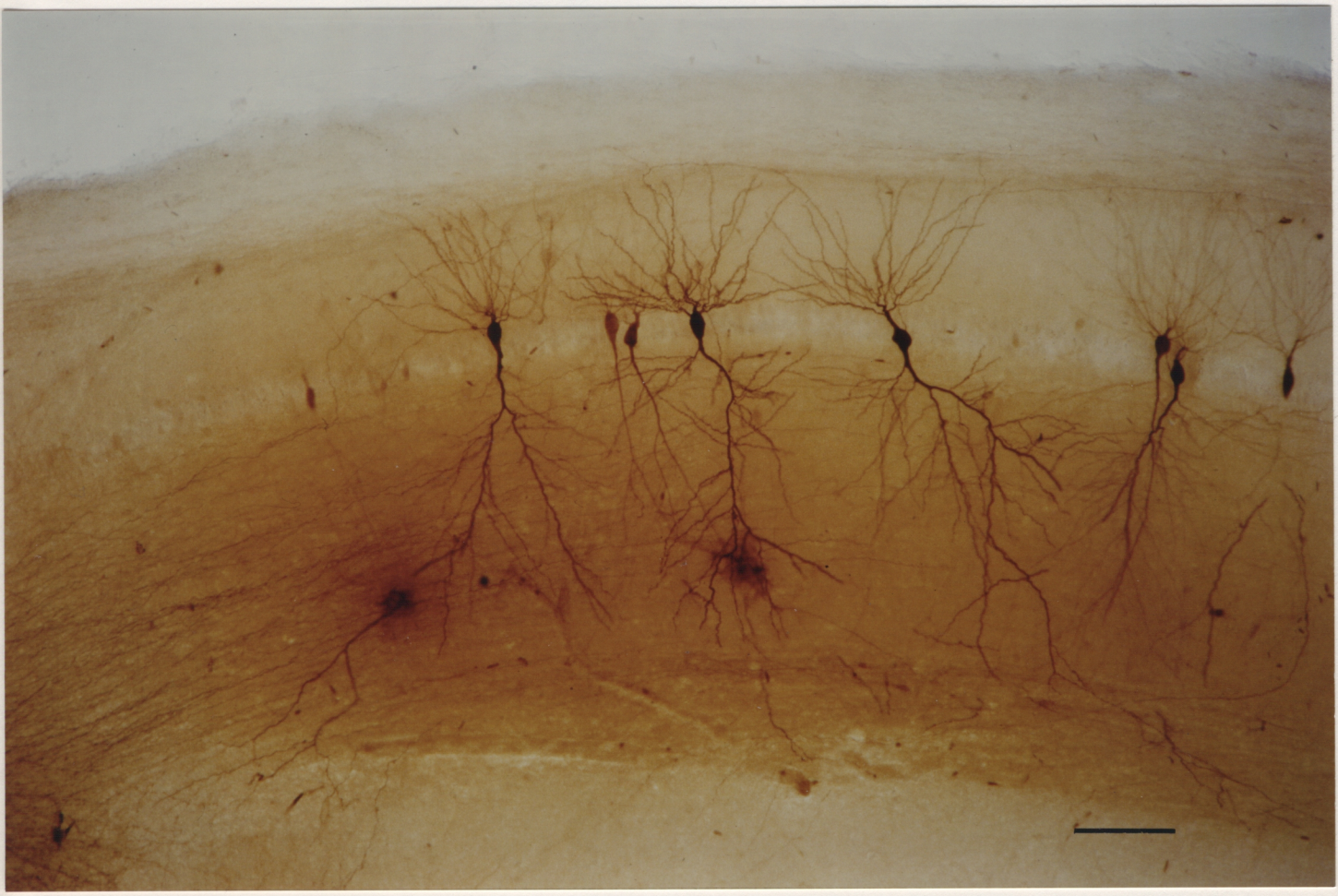
Frontspiece. Schaffer collateral/commissural axons and CA1 pyramidal cells stained with horseradish peroxidase (HRP) in the guinea pig hippocampal slice. In this orientation, which is the same as for Figs. 3.1, 3.3 and 4.2, the apical dendrites of the pyramidal cells project downwards. The CA3 region is beyond the lefthand edge of the photograph. The scale bar represents 100 μm.

Methods. Hippocampal slices were prepared and maintained as described in Chapter 2. The Schaffer collateral/commissural axons were filled from a deposit of HRP solution (10% in 0.5 M KCl/0.1 M Tris/HCl, pH 7.6) applied to the CA3 stratum pyramidale through a broken glass micropipette. The CA1 pyramidal cells were filled by ejecting the same HRP solution from a glass micropipette (tip diameter 0.5-1.0 μm) impaled into the distal CA1 stratum radiatum at a depth of 100-150 μm (no attempt was made to record from this electrode). The HRP was ejected by passing 1 μA 200 ms pulses, in a 300 ms cycle, for 2 min. Three ejections were made in this slice (HRP spill can be seen from two of them). The slice was maintained *in vitro* for a further four hours and was then fixed in 2% paraformaldehyde/2% glutaraldehyde in phosphate buffer for six hours. After a further ten hours in 30% sucrose/phosphate buffer, the slice was sectioned at 50 μm on a freezing microtome. The sections were reacted for HRP by the method of Hanker et al (1977) and were then mounted on glass slides, dehydrated and coverslipped. A single section is shown in this photograph.

Adriatic Bookbinde
P/L



SYNAPTIC TRANSMISSION BETWEEN CA3 AND CA1 NEURONES IN THE GUINEA PIG HIPPOCAMPAL SLICE

Rodney John Sayer

B.Med.Sc., M.B. Ch.B. (Otago)

Experimental Neurology Unit

The John Curtin School of Medical Research

Canberra

A thesis submitted for the degree of Doctor of Philosophy

of the Australian National University

September, 1988.

The work described in this thesis is original, and the experiments and the analysis were performed by me between February 1985 and August 1988, under the supervision of Dr Stephen J. Redman. Two visitors to the Experimental Neurology Unit were collaborators at different stages. Professor Per Andersen, from the University of Oslo, was involved with the initiation of the project (February-April, 1985), and he supervised my experiments when I visited Oslo in November and December 1985. Dr Michael J. Friedlander, from the University of Alabama in Birmingham, was involved as an equal collaborator during the final six months of experiments and analysis.

Where others have been responsible for development of experimental procedures or analysis routines, acknowledgement has been given.



R. J. Sayer

ACKNOWLEDGEMENTS

I am especially grateful to my supervisor, Dr Steve Redman, for his interest, advice and encouragement.

I would like to thank Prof. Per Andersen for his involvement with this study and for teaching me the hippocampal slice technique. I was very fortunate to have the opportunity to work with him.

Thanks are due to both Steve and Per for initiating a project which turned out to be so interesting and worthwhile.

I am indebted to Dr Mike Friedlander for his help during the final six months of this investigation. The productiveness of this period is in part due to his energy and enthusiasm. I am grateful to Mike for both his practical help and for the many useful discussions.

I would also like to thank Dr Frank Edwards and Dr Bruce Walmsley for advice and discussion relating to quantal analysis.

I would like to acknowledge those who have contributed to various aspects of the computer-based collection and analysis system. Some of programs and hardware used in this project were developed by Frank Edwards, John Clements, Dimitri Kullmann, Greg Quinn and Richard Friend.

I am grateful to the many others in the John Curtin School of Medical Research who have helped me at various times, including:

- the technical and secretarial staff of the

Experimental Neurology unit; Ken Collins, Terrina Thompson, Garry Rodda and Rosemary Enge,

- the Electron Microscopy and Histology Service; Lesley Maxwell, Helen Geier, Sue Bell and Geoff Osborne,
- the Photographic Section; Stuart Butterworth and staff,
- the staff of the Animal Breeding Establishment.

The support provided by an Australian National University Medical Scholarship (1985) and by the National Health and Medical Research Council of Australia (Medical Postgraduate Research Scholarship, 1986-1988) is gratefully acknowledged.

ABSTRACT

Excitatory synaptic transmission from CA3 to CA1 pyramidal cells has been investigated in the guinea pig hippocampal slice. In simultaneous intracellular recordings from CA3 and CA1 cells, unitary EPSPs were obtained in CA1 neurones on 71 occasions. The CA3 neurones were activated by short pulses of depolarizing current, adjusted to elicit single action potentials and delivered at 2 Hz. The average amplitude of the unitary EPSPs was 131 μV, with a range of 30-665μV. The mean 10-90% rise time was 3.93 ms and the mean half-width was 19.50 ms. On three occasions, hyperpolarizing responses were seen in the CA1 neurones in response to activation of single CA3 neurones.

The trial-to-trial variations in amplitude were examined for 12 of the unitary EPSPs, and also for 25 small compound EPSPs (mean amplitudes ranging 67-396 μV) evoked by low-intensity stimulation of the stratum radiatum. The unitary EPSPs showed greater variability in amplitude than could be accounted for by the levels of baseline noise. Intermittent failure of the presynaptic terminals to release transmitter was implicated as one source of the variability by the presence of distinct 'failures' peaks in some of the noise-contaminated EPSP amplitude histograms. An unconstrained deconvolution method of quantal analysis was applied to the amplitude variations of both the unitary EPSPs and the small compound EPSPs evoked in CA1 neurones. In three cases the signal to noise ratios of the results gave confidence that discrete amplitudes were accurately resolved from the noise-

contaminated EPSP amplitude histograms. For the three EPSPs the quantal size estimates were 278 μV, 224 μV and 193 μV (for one unitary EPSP and two compound EPSPs respectively). The failure to resolve discrete amplitudes in the other noise-contaminated EPSP amplitude histograms may have been due to (1) the small amplitude of the quantal EPSPs relative to the noise, (2) significant variance in the quantal amplitude from trial-to-trial, or (3) significant differences between the amplitudes of the quantal EPSPs originating from different release sites in the synaptic connections.

Paired-pulse facilitation was investigated for 10 unitary EPSPs. The mean facilitation at the 25 ms inter-pulse interval was 35%. Long-term potentiation (LTP) was examined for unitary EPSPs and small compound EPSPs. A surprising finding was the low incidence of LTP observed in small compound and unitary EPSPs after induction protocols which caused sustained enhancements of larger compound EPSPs. It is argued that this is unlikely to be secondary to any problems associated with the testing or induction protocols. The possible mechanisms for LTP which would be consistent with this finding are discussed. LTP was demonstrated for one unitary EPSP. The time course parameters and the noise-contaminated amplitude histograms are compared for the control EPSP and the enhanced EPSP.

PUBLICATIONS ARISING FROM THIS WORK

(to September 1988)

The following paper has recently been accepted for publication by the Journal of Neuroscience:

Sayer, R.J., S.J. Redman, and P. Andersen. Amplitude fluctuations in small EPSPs recorded from CA1 pyramidal cells in the guinea pig hippocampal slice.

Preliminary results from this project have been presented at meetings in Australia. The following abstracts were published in conjunction with these presentations:

Andersen, P., R.J. Sayer, and S.J. Redman (1985) Fluctuations in the amplitude of excitatory postsynaptic potentials evoked in hippocampal CA1 pyramidal cells *in vitro*. Proceedings of the Australian Physiological and Pharmacological Society 16:100P.

Sayer, R.J., and S.J. Redman (1988) EPSPs in CA1 pyramidal cells evoked by activation of single CA3 neurones in the guinea pig hippocampal slice. Neuroscience Letters Suppl. 30:S120.

The following abstracts have been submitted to the Society for Neuroscience for presentation at the November 1988 meeting in Toronto:

Friedlander, M.J., R.J. Sayer, and S.J. Redman (1988) Synaptic transmission between individual CA3 and CA1 neurons in the hippocampus.

Sayer, R.J., M.J. Friedlander, and S.J. Redman (1988) Long-term potentiation compared for unitary and compound EPSPs in CA1 neurons.

CONTENTS

		Page
1	GENERAL INTRODUCTION	1
1.1	The classification of areas CA1 and CA3	2
1.2	Efferents from the CA3 region	4
1.3	The anatomy of the Schaffer collaterals	4
1.4	Ultrastructural studies of the CA1 stratum radiatum	6
1.5	Synaptic pharmacology and physiology of the CA3-CA1 connection	7
1.5.1	Excitatory synaptic transmission	7
1.5.2	Inhibitory influences of the CA3-CA1 projection	9
1.6	Synaptic integration in CA1 pyramidal cells	11
1.7	Trial-to-trial variations in EPSP amplitude: Quantal analysis of synaptic transmission in the CNS	15
1.8	Quantal analysis of EPSPs in the hippocampal formation	21
1.9	Synaptic plasticity: long-term potentiation	25
1.9.1	The induction of LTP	26
1.9.2	The expression of LTP: suggested mechanisms	31
1.10	The aims of this project	34
2	METHODS	37
2.1	Preparation and maintenance of the hippocampal slices	37

page

2.2 Stimulating electrodes 38

2.3 Recording electrodes 39

2.4 Recording techniques and equipment 40

3 CHARACTERISTICS OF UNITARY POSTSYNAPTIC POTENTIALS EVOKED IN CA1 NEURONES 42

3.1 Introduction 42

3.2 Methods 43

3.3 Results 47

3.3.1 General 47

3.3.2 Intracellular parameters 49

3.3.3 Locations of the CA3 and CA1 neurones 50

3.3.4 Schaffer collateral conduction velocities and delays to onset of EPSPs 51

3.3.5 Amplitudes of the averaged unitary EPSPs 52

3.3.6 The time courses of the unitary EPSPs 54

3.3.7 Relationship between time course and amplitude 55

3.3.8 An atypical CA1 neurone 55

3.3.9 Hyperpolarizing responses 57

3.3.10 Convergent inputs to CA1 58

3.3.11 Divergent outputs from CA3 59

3.4 Discussion 61

3.4.1 The monosynaptic nature of the EPSPs 61

3.4.2 Conduction delays and latencies to onset of the CA1 EPSPs 63

3.4.3 Amplitudes of the unitary EPSPs 65

3.4.4 The time courses of the unitary EPSPs 68

page

3.4.5 Hyperpolarizing PSPs 73

3.4.6 Convergent and divergent connections 75

4 AN ANALYSIS OF THE FLUCTUATIONS IN AMPLITUDE OF UNITARY EPSPS AND SMALL COMPOUND EPSPS EVOKED IN CA1 NEURONES 77

4.1 Introduction 77

4.2 Methods 79

4.2.1 Simultaneous CA3-CA1 intracellular recordings 79

4.2.2 EPSPs evoked in CA1 neurons by stimulation of stratum radiatum 82

4.2.3 Determination of EPSP variability 84

4.2.4 Estimation of quantal parameters by the variance method 85

4.2.5 The unconstrained deconvolution method 89

4.2.6 Monte Carlo testing of the deconvolution procedure 90

4.3 Results 93

4.3.1 EPSP variability from trial-to-trial 93

4.3.2 Estimation of quantal parameters by the variance method 94

4.3.3 Quantal analysis by the deconvolution method 96

4.4 Discussion 102

4.4.1 EPSP variability from trial-to-trial 102

4.4.2 Quantal analysis by the method of variance 106

page

4.4.3 Quantal size obtained by the deconvolution method 108

4.4.4 Quantal size of EPSPs evoked at different dendritic locations 109

4.4.5 Possible models for release underlying the EPSP amplitude distributions 109

4.4.6 Further comments on quantal analysis by the deconvolution method 111

5 SYNAPTIC PLASTICITY: PAIRED-PULSE FACILITATION AND LONG-TERM POTENTIATION INVESTIGATED FOR SMALL EPSPS IN CA1 NEURONES 114

5.1 Introduction 114

5.2 Methods 115

5.2.1 Paired-pulse facilitation 115

5.2.2 Long-term potentiation 116

5.3 Results 120

5.3.1 Paired-pulse facilitation 120

5.3.2 LTP - extracellular field recordings 120

5.3.3 LTP - large compound EPSPs 121

5.3.4 LTP - small compound EPSPs 122

5.3.5 LTP - unitary EPSPs 125

5.4 Discussion 133

5.4.1 Paired-pulse facilitation 133

5.4.2 LTP compared for small and large EPSPs 135

5.4.3 Features of the unitary EPSP which showed LTP 153

page

6 CONCLUSIONS AND SUGGESTIONS FOR EXTENSIONS OF THIS STUDY 158

REFERENCES 166

Chapter One:
GENERAL INTRODUCTION

The hippocampal formation is an attractive brain structure to neurophysiologists for several reasons. In the whole animal, it appears to have a role in memory formation and emotional expression, and it is a challenging long-term goal to gain an understanding of these processes from the behaviour of elements at the cellular or neuronal network level. For those interested in the functional intricacies of different kinds of neurone, the hippocampus provides a highly ordered and readily studied arrangement of cell types. The hippocampus is particularly convenient for *in vitro* techniques, the most notable of these being the hippocampal slice preparation, which was first shown to be viable by Skrede & Westgaard (1971).

In the study presented here, the guinea pig hippocampal slice has been used to investigate excitatory synaptic transmission between the two major regions of the hippocampus, areas CA3 and CA1. The emphasis of this report is on experiments in which simultaneous intracellular recordings were made from synaptically-connected CA3 and CA1 neurones. These experiments, while difficult enough to perform in the slice, would have been impossible in the whole animal. The three most important features of the hippocampal

slice preparation which made the experiments feasible, were (1) mechanical stability, which allowed long duration intracellular impalements, (2) direct visualisation of the different regions within the slice, which enabled accurate positioning of the stimulating and recording electrodes, and (3) the laminar nature of the circuitry within the hippocampus (see below), which allowed a proportion of the CA3-CA1 projection to remain intact despite the slicing.

For the purposes of this thesis, *unitary* excitatory postsynaptic potentials (EPSPs) are defined as monosynaptic EPSPs evoked by activation of a single presynaptic neurone. *Compound* EPSPs are evoked by activation of multiple presynaptic cells (or their axons). Even when the compound EPSPs are so small as to be probably due to activation of only a single afferent, they are still referred to as compound because the method by which they are activated makes it uncertain that they are unitary.

The following sections of the introduction summarise the relevant features of previous investigations into the anatomy and physiology of the CA3-CA1 projection, as a background to the experiments detailed in the subsequent chapters. More general sections on quantal analysis and long-term potentiation (LTP) are included.

1.1 The classification of areas CA1 and CA3

The regions of the hippocampal formation were first described and named by Ramon y Cajal (1893, 1911). The hippocampus proper (i.e. distinct from the dentate gyrus) was divided into two regions: regio superior, adjacent to the

subiculum, and regio inferior, adjacent to the dentate gyrus. The border between the regio inferior and the regio superior was distinguished by the different morphology of the strata pyramidale (soma layers) of the two regions. The pyramidal somata of the regio inferior were noted to be larger and more loosely packed than those in the regio superior (see also Blackstad, 1956).

Lorente de No (1934) introduced the classification CA1-CA4 to the subregions of the hippocampus. CA1 corresponded to the regio superior of Ramon y Cajal (1893), while the regio inferior was divided into areas CA2 and CA3. Area CA2 was named as that portion of regio inferior containing the large pyramidal somata, but not reached by the mossy fibres, which originate from the dentate gyrus and form a distinct layer (the stratum lucidum) in the apical dendritic field of CA3. The diffuse pyramidal cell region between the blades of the dentate gyrus was named CA4.

More recent investigations have suggested that area CA2 is considerably narrower than indicated by Lorente de No (1934). Blackstad et al (1970) found that the mossy fibres reached exactly to the border between regio inferior and regio superior. Blackstad et al (1970) proposed that the distal mossy fibres may not have been fully revealed by the silver impregnation method as used by Lorente de No (1934), and they implied that the CA2 zone may not exist, at least in the rodent. Swanson et al (1978) have suggested that there is only a very narrow transition zone (100-150 μm) between CA3 and CA1, which corresponds to the CA2 region. The most common classification, which is followed in this study, now

regards areas CA3 and CA1 as vitually synonymous to Ramon y Cajal's (1893) regio inferior and regio superior respectively. If a narrow transition zone does exist at the CA3/CA1 border, it is an open question as to whether it is worthy of separate classification as area CA2.

Please note that the data presented here ~~is~~ are for the rodent hippocampal formation unless stated otherwise.

1.2 Efferents from the CA3 region

While the projection from CA3 to the ipsilateral CA1 region (the Schaffer collateral pathway) is the focus of attention for this study, it should be noted that efferents are also supplied to other regions. Swanson and Cowan (1977) have shown that the CA3 field projects to the subiculum and entorhinal cortex ipsilaterally, to the contralateral CA3 and CA1 regions (via the ventral hippocampal commissure) and to the septal nuclei of both sides. Simultaneous retrograde labelling with different fluorescent dyes has indicated that individual CA3 cells may send collaterals to three or more of these target regions (Swanson et al, 1980). Injection of horseradish peroxidase (HRP) into single CA3 pyramidal cells has revealed extensive axonal arborizations into areas CA3 and CA1 of both sides, and into the septum (Tamamaki et al, 1984).

1.3 The anatomy of the Schaffer collaterals

Within the stratum radiatum of CA1, the major branches of the Schaffer collaterals generally course parallel to the stratum pyramidale, perpendicular to the main dendritic axis

(Golgi, 1886, Schaffer, 1892 - cited in Andersen et al, 1980a; Ramon y Cajal, 1893, 1911; Andersen et al, 1987c; see also the frontspiece). Some fibres from CA3 project to the stratum oriens of CA1, but this is more prominent for the commissural pathway to the contralateral CA1 region (Swanson et al, 1978; Groen & Wyss, 1988). There is no evidence for any connection in the reverse direction, from CA1 to CA3 (Hjorth-Simonsen, 1973).

From HRP staining of axons running in the stratum radiatum from CA3 to CA1 in the guinea pig hippocampal slice (unpublished observations, see frontspiece), it is apparent that the filled branches generally conform to the laminar organization of the hippocampus, as established by Andersen et al (1971) for the rabbit. The direction of the laminae is not strictly transverse to the longitudinal axis of the hippocampus, but at an angle of 20-30^{o}, with the origin of the axons in CA3 being closer to the septal pole. Some departure from the laminar arrangement is to be expected for individual Schaffer collaterals, and single CA3 cells may send more than one collateral into the CA1 region (Finch et al, 1983; Tamamaki et al, 1984). Not all of these follow the same laminar course.

There is little information available about the pattern of terminations in CA1 for single CA3 neurones. Reports based on reconstructions of HRP-filled CA3 cells (Finch et al, 1983; Tamamaki et al; 1984) do not describe the distribution of boutons within CA1, presumably because the resolution by light microscopy is inadequate or because the terminations are not sufficiently filled with HRP.

1.4 Ultrastructural studies of the CA1 stratum radiatum

Serial electron microscopy has been used by Andersen (1975) to reconstruct segments of the Schaffer collaterals in the stratum radiatum of the rabbit. The 'parent' fibres were myelinated and had Ranvier nodes every 60-70 μm, from which one to three unmyelinated axons emerged. These unmyelinated axons had synaptic swellings 3-5 μm apart, which formed *en passant* synapses with dendritic spines.

Westrum and Blackstad (1962) examined the CA1 stratum radiatum in the rat by serial electron microscopy. They followed unmyelinated axons for short distances (<5 μm); the axons mostly had diameters of 0.12-0.20 μm and gave rise to *en passant* synaptic terminals (diameter 0.4-1.0 μm) about every 3 μm. The synapses onto spines were Gray's type 1 (asymmetrical). More than 95% of synapses in the stratum radiatum are onto dendritic spines (Lee et al, 1980; Chang & Greenough, 1984).

Harris and Stevens (1987) have made three-dimensional reconstructions of synapses onto dendritic spines in CA1 stratum radiatum of the rat. Important findings from their study were (1) all of the spines they reconstructed had only one synaptic junction, although some of these were perforated by electron-lucent regions (and so might appear like multiple release sites on a single section), and (2) the majority of presynaptic varicosities made a connection with a single dendritic spine, and on the occasions when the varicosities were shared by two spines (they estimate 5-13% of varicosities), the spines originated on different dendrites (probably, but not necessarily on different neurones).

No single study has been able to reconstruct the Schaffer collateral(s) originating from a single CA3 pyramidal cell, in combination with reconstruction of a postsynaptic CA1 neurone. For this reason, both the number of terminals involved in a single CA3 cell projection to area CA1 (i.e. divergence), and the number of synapses involved in a single CA3-CA1 cell (unitary) connection remain unknown.

1.5 Synaptic pharmacology and physiology of the CA3-CA1 connection

1.5.1 Excitatory synaptic transmission

In recent years, rapid progress has been made towards an understanding of excitatory synaptic transmission in the hippocampus, both because of the interest in its modification during LTP and because hippocampal *in vitro* preparations have allowed pharmacological manipulations which were previously impossible in the whole animal.

There is good evidence that the amino acids glutamate and aspartate mediate excitatory synaptic transmission between CA3 and CA1 neurones. When isolated slices of CA1 are treated with depolarizing agents (e.g. raised K^+ or veratridine), there is a Ca^{2+}-dependent rise in glutamate and aspartate release (Cotman & Nadler, 1981). The increase in firing rate of CA1 neurones in response to iontophoretically-applied glutamate and aspartate is inhibited by the excitatory amino acid antagonist γ-D-glutamylglycine (Collingridge et al, 1983a), and this antagonist also supresses synaptic responses evoked by stimuli to the stratum radiatum (Collingridge et al, 1983b).

It is now clear that the actions of excitatory amino acids in the central nervous system (CNS) are mediated by several distinct receptor sub-types (for reviews see Cotman & Iversen, 1987; Watkins & Olverman, 1987; Cotman et al, 1987). Four classes have been characterized; N-methyl-D-aspartate (NMDA), quisqualate, and kainate (named after their selective agonists), and L-AP4 (after the antagonist L-2-amino-4-phosphonobutyrate). The sub-types differ in their anatomical distributions, which have been mapped by a variety of histochemical methods. Particularly high levels of NMDA receptors are present in the stratum radiatum and stratum oriens of CA1 (Monaghan et al, 1983). This class of receptors has some special properties, which will be discussed below. In general, the distribution of quisqualate receptors overlaps that of the NMDA sites, and high levels are found in CA1 strata radiatum, pyramidale and oriens (Rainbow et al, 1984; Monaghan et al, 1984). Kainate receptors are found in the same regions as NMDA sites in some cases (e.g. in the dentate gyrus) but often they occur where the NMDA receptor levels are low, such as in the stratum lucidum of CA3 (Monaghan & Cotman, 1982).

The specific NMDA antagonist D-2-amino-5-phosphonovalerate (AP5) does not suppress excitatory synaptic transmission under normal conditions (Collingridge et al, 1982, 1983b; Wigstrom et al, 1985; but see Hablitz et al, 1986), implying that the responses are mediated by the quisqualate and/or kainate rather than the NMDA receptor type. However, in low Mg^{2+} solutions (Wigstrom et al, 1985; Herron et al, 1986; Coan & Collingridge, 1987), or if cells

are sufficiently depolarized by current injection (Wigstrom et al, 1986b; Collingridge et al, 1988a) or with repetitive activation at 10 Hz or greater (Herron et al, 1986; Collingridge et al, 1988b), an additional AP5-sensitive component to the EPSP becomes apparent. The time course of this component is considerably slower than the normal 'fast' EPSP (e.g. time to peak 30 ms compared with 10 ms for single responses in CA1 cells depolarized to about -25 mV, Collingridge et al, 1988a).

The conditions required to reveal the slow EPSP in CA1 pyramidal cells are consistent with the properties of the NMDA receptor and its associated ion channels as characterised in other preparations (for reviews see MacDermott & Dale, 1987; Ascher & Nowak, 1987). The two most important features of relevance here are (1) the NMDA ion channel is almost fully blocked by Mg^{2+} at membrane potentials near rest(-60 to -70 mV), but the block is progressively relieved by depolarization (Nowak et al, 1984; Mayer and Westbrook, 1985) and (2) the NMDA channel is permeable to Ca^{2+} as well as to Na^{+} and K^{+} (Ascher & Nowak, 1986; MacDermott et al, 1986). The significance of these findings will be made apparent in the section relating to the induction of LTP (1.9.1).

1.5.2 Inhibitory influences of the CA3-CA1 projection

Besides their monosynaptic excitatory input, afferents in the stratum radiatum have polysynaptic inhibitory actions on CA1 pyramidal cells. These are mediated by two known pathways, termed recurrent and feedforward inhibition. Recurrent inhibition requires discharge of local (CA1)

pyramidal cells; these in turn activate interneurones which have inhibitory connections back to the same population of pyramidal cells (Andersen et al, 1963, 1964a, 1964b; Knowles & Schwartzkroin, 1981). Feedforward inhibition occurs more directly. The stratum radiatum afferents monosynaptically activate the interneurones, which then exert their inhibitory influence on the pyramidal cells (Buzaki & Eidelberg, 1982; Alger & Nicoll, 1982a; Ashwood et al, 1984).

Simultaneous intracellular recordings from CA1 pyramidal cells and physiologically-identified interneurones have revealed reciprocal excitatory/inhibitory connections which would be consistent with recurrent inhibitory circuits (Knowles & Schwartzkroin, 1981; Lacaille et al, 1987). These interneurones, which are located in the stratum pyramidale ('basket' cells) and at the border between the strata oriens and alveus (O/A interneurones), also receive excitatory input from stratum radiatum afferents at short latency and with low stimulus intensities, suggesting that they may participate in feedforward as well as recurrent inhibition (Schwartzkroin & Mathers, 1978; Knowles & Schwartzkroin, 1981; Buzsaki & Eidelberg, 1982; Ashwood et al, 1984; Lacaille et al, 1987). Physiologically-identified basket cells and O/A interneurones have been filled with HRP and shown by electron microscopy to make Gray's Type 2 symmetric synaptic contacts with pyramidal cell somata and dendrites (Schwartzkroin & Kunkel, 1985; Lacaille et al, 1987).

The inhibitory postsynaptic potential (IPSP) evoked in CA1 pyramidal cells by stimulation of stratum radiatum

afferents comprises both early and late components. The early phase results from a $GABA_A$ receptor-mediated Cl^- conductance, primarily at the soma, and both feedforward and recurrent circuits are probably involved (Newberry & Nichol, 1984, 1985). The later phase of the IPSP is resistant to $GABA_A$ antagonists (e.g. bicuculline), and is believed to result from a $GABA_B$-mediated increase in K^+ conductance in the dendrites (Alger & Nicoll, 1982a,b; Newberry & Nicoll, 1984, 1985; Dutar & Nicoll, 1988). Lacaille & Schwartzkroin (1988a,b) have recently suggested that the late IPSP may comprise feedforward inhibition via a third class of nonpyramidal cell in CA1, the lacunosum-moleculare interneurone. The IPSPs evoked in CA1 pyramidal cells in simultaneous intracellular recordings with these interneurones, were similar in time course to the late phase of the IPSP.

1.6 Synaptic integration in CA1 pyramidal cells

The extensiveness of the apical dendritic trees of CA1 pyramidal cells has raised questions about the relative effectiveness of synapses at different distances from the soma. Synaptic potentials are attentuated and their time courses are slowed according to the cable properties of the dendritic tree (Redman, 1973; Rall & Rinzel, 1973; Rall, 1977;), so those originating from more distal sites would be expected to contribute less to depolarization at the soma, which is close to the presumed site of action potential generation (but see below).

Suprisingly, Andersen et al (1980a) found that neurones in CA1 were equally likely to generate action potentials following stimulation of afferents running through narrow bridges of intact tissue, in either the proximal or distal regions of the stratum radiatum. The two inputs also gave equally large synaptic field potentials, and the corresponding intracellular EPSPs (about 5 mV mean peak amplitude) had similar time courses.

Subsequently, theoretical analyses have been made of the cable properties of CA1 pyramidal cells, based on reconstruction of HRP-filled neurones and estimations of the effects of spines (Turner, 1984a,b, 1988). These predicted that distal and proximal inputs separated by 300-400 μm would correspond to an electrotonic separation of 0.6-0.7 space constants, in an average apical dendritic tree of length 0.9 space constants. Turner (1988) then tested these predictions, and found that when small (<1 mV) EPSPs were evoked in CA1 pyramidal cells, there was clear differentiation between the time courses of EPSPs evoked by proximal and distal stimulation. The ratios of mean proximal to distal rise times (0.44) were close to those of the model (0.43) (Turner, 1988). However for larger EPSPs (mean peak amplitude about 2 mV), the differences between those evoked by proximal and distal stimulation were less, although still significant (Turner, 1988). A recent study by Andersen et al (1987c) found a small but significant difference in the rise times of EPSPs near threshold (mean peak amplitude > 10 mV) evoked by proximal and distal stimuli. The proximal to distal rise time ratio for these was 0.79.

Several mechanisms have been suggested to explain the discrepancies in the results for the EPSPs of different amplitudes. One possibility is that the axons or their collaterals in the stratum radiatum deviate from their course parallel to the stratum pyramidale, and that as more are recruited by stratum radiatum stimulation the regions of input to the dendritic tree become less discrete (Turner, 1988). Alternatively, it may be that inhibitory pathways are activated (and recruited) differentially by the proximal and distal stimulating electrodes (Andersen et al, 1987c). The onset of feedforward inhibition is rapid enough to affect the rising phases of EPSPs (Turner, 1985).

A further possibility is that the larger EPSPs are suprathreshold for active membrane processes in the dendrites, and that these boost the amplitudes of the distal EPSP and shorten their time courses. Regenerative processes were first suggested for the dendrites of hippocampal pyramidal cells following observations of pre-potentials (i.e. depolarizations immediately before the action potentials, but distinct from the EPSPs) and small all-or-nothing spikes assumed to be of dendritic origin, in somatic intracellular recordings *in vivo* (Spencer & Kandel, 1961; Andersen & Lomo, 1966). Similar phenomena have been noted in impalements of dendrites in hippocampal slices (Wong & Prince, 1979; Wong et al, 1979; Schwartzkroin & Prince, 1980). Regenerative potentials have been detected in isolated dendrites of CA1 neurones (Benardo et al, 1982; Masukawa & Prince, 1984).

Andersen et al (1987c) have found that the threshold amplitude for triggering of action potentials is smaller for EPSPs evoked by stimulation of distal afferents than for those evoked by proximal stimuli (mean 12 mV c.f. 16 mV). Although the differential effects of inhibition could again be a complicating factor, this finding would also be consistent with a separate trigger site for action potential initiation in the distal dendrites.

On the other hand, the most recent current source-density analysis of evoked extracellular field potentials in the CA1 region of the hippocampal slice does not support the concept of action potential generation within the dendrites. Richardson et al (1987) report that the initial site for generation of action potentials, in response to stratum radiatum stimulation, is in the region of the cell body layer (either soma or axon hillock). Invasion of the action potential into the dendrites always followed, rather than preceeded, initiation at the stratum pyramidale (Richardson et al 1987). However, this does not rule out the possibility of regenerative processes within the dendrites, as these may boost depolarization without actually promoting action potential discharge. Note also that Miyakawa and Kato (1986) found that the current sink associated with antidromic action potentials recorded over the proximal to mid-dendritic regions was tetrodotoxin sensitive, suggesting that Na^+ conductances in the dendrites could be activated by sufficient depolarization.

1.7 Trial-to-trial variations in EPSP amplitude: Quantal analysis of synaptic transmission in the CNS

The quantal theory of synaptic transmission, as first formulated by del Castillo & Katz (1954), stated that normal synaptic responses resulted from the simultaneous release of many individual quanta of transmitter from the presynaptic terminal. It explained the trial-to-trial fluctuations in postsynaptic response by assuming that there are a number (n) of presynaptic quanta capable of release in response to a nerve impulse, and that each of these has an independent probability of release (p). The evoked release is therefore probabilistic, and the distribution of response amplitudes should follow statistics determined by n and p.

Numerous studies of synaptic transmission in the peripheral nervous system have provided support for the quantal hypothesis, and application of the quantal theory has provided a great deal of useful information about normal synaptic mechanisms and synaptic plasticity. Rather than focussing on those studies (for reviews see Martin, 1966, 1977; McLachlan, 1978), some of the issues concerning quantal analysis at CNS synapses will be briefly presented.

The EPSP evoked in cat spinal motoneurones by activation of group Ia afferents was the first in the CNS to be investigated by quantal analysis (Kuno, 1964). The analysis for this preparation suffered an immediate disadvantage in comparison with that at the neuromuscular junction: the spontaneous potentials originating from the synapses under scrutiny could not be distinguished from those originating from all the other connections to the same cell.

Consequently, the spontaneous synaptic potentials could not be used to determine the amplitude and the variability of the quantal EPSP. The quantal size (v_1) and mean quantal content (m) of the group Ia EPSPs were instead estimated from the probability of the failures ('method of failures') or from the variance of the amplitude fluctuations ('method of variance')(Kuno, 1964; Burke & Nelson, 1966; Burke, 1967). These methods assumed Poisson statistics for the distribution of the quantal content (see Martin, 1966; McLachlan, 1978 for details of the techniques). Poisson statistics provided a good description of release at the neuromuscular junction when transmisson was suppressed in low Ca^{2+}/high Mg^{2+} media, but not under normal conditions when the probabilities for release of individual quanta are higher. Perhaps for the same reason (innappropriate assumption of uniformly low probabilities for release), Poisson statistics did not give in general a satisfactory account of the fluctuations in amplitude of group Ia EPSPs (McLachlan, 1978; Redman, 1979).

To avoid making assumptions about the underlying probabilites of release, Redman and co-workers applied a deconvolution method to the distributions of evoked EPSP amplitudes in cat motoneurones (Edwards et al, 1976a,b; Wong & Redman, 1980; Jack et al, 1981). This method aimed to extract distributions of discrete amplitudes underlying the noise-contaminated EPSP amplitudes. Background noise distributions were sampled from the same neurones as the evoked EPSPs, and it was assumed that the noise summed linearly with the EPSPs and was statistically independent from the fluctuations in the EPSP.

Given adequate signal to noise ratios, the variations in amplitude of most group Ia EPSPs could be modelled by fluctuations between discrete amplitudes which were obscured by the noise. The amplitude of the quantal EPSPs estimated by this method averaged about 90 μV (Jack et al, 1981). On the other hand, several EPSPs were found which did not fluctuate in amplitude by more than could be attributed to the superimposed noise. From these examples, it was estimated that the coefficient of variation of the quantal EPSP in this system was less than 0.05 (Jack et al, 1981), compared with about 0.3 for the quantal response at the neuromuscular junction (Martin, 1977). As a possible explanation for the small coefficient of variation, it was suggested that release of a single quantum from a terminal may saturate all the postsynaptic receptors at that release site (Jack et al, 1981).

Two other lines of evidence have been used to argue that for the group Ia connection to the motorneurone, the quantal EPSP is generated when release occurs at a single bouton, and is all-or-none for that synapse. Firstly, in a few cases, the EPSPs comprising each discrete amplitude had different time courses, indicating that that were generated at different dendritic locations (Jack et al, 1981). Secondly, in experiments which combined quantal analysis with HRP staining and light microscopic reconstruction of the presynaptic and postsynaptic elements, there were never more discrete amplitudes in the fluctuation pattern for the EPSP than boutons in the corresponding connection (Redman & Walmsley, 1983b). This would not be expected if a single

bouton could contribute more than one quantal EPSP to the postsynaptic response. Another interesting aspect of this result was the implication that some synapses were inactive (i.e. did not release transmitter over a large number of trials) with the stimulus regime used in those experiments.

A subsequent ultrastructural finding that some Ia boutons contacting motoneurones consist of more than one release site (Fyffe & Light, 1984), suggests quantal EPSPs might be better associated with single release sites, rather than boutons *per se*. It also reinforced the evidence that some release sites were inactive.

Another opportunity to test the association between quantal EPSPs and single release sites ~~(or for boutons)~~ may arise from the initial studies of the connection between group Ia afferents and dorsospinocerebellar (DSCT) cells in the cat. Some of the boutons in this connection are large, elongated structures containing multiple release sites (Rethelyi, 1970; Walmsley et al, 1985). Investigations to date in this system have indicated that the signal to noise ratios are superior to those obtained in motoneurones and that for some EPSPs the different amplitudes in the fluctuation pattern can be seen as distinct peaks in the amplitude histograms (Tracey & Walmsley, 1984; Walmsley et al, 1987, 1988). The discreteness of these peaks indicates that the coefficient of variation of the quantal EPSP is also low in this system (<0.1; Walmsley et al, 1988). The quantal EPSPs determined by the deconvolution method for the Ia/DSCT connection averaged 144 μV (range 90-200 μV, Walmsley et al,

1987). Combined quantal analysis with morphological reconstruction has not yet been done.

One of the controversial issues for quantal analysis in the CNS is whether or not the different release sites in a synaptic connection have equal probabilities for transmitter release following a presynaptic nerve impulse. If the release probabilities were equal, the distribution of discrete EPSP amplitudes would follow a (simple) binomial distribution; if they differed, a compound binomial (i.e. combination of more than one binomial) distribution would instead be appropriate. This has an important bearing on which methodologies are appropriate for quantal analysis in the CNS, and also on the possibilities for control of the effectiveness of individual release sites or boutons (e.g. in presynaptic inhibition; Clements et al, 1987).

For both the group Ia connection to the motoneurone and to the DSCT cell, compound binomial distributions describe the probabilities associated with each discrete amplitude better than simple binomial distributions (Jack et al, 1981; Walmsley et al, 1987). Nevertheless, Korn et al (1981, 1982), have analysed the fluctuations in amplitude of reversed IPSPs evoked in the goldfish Mauthner cell, by a deconvolution method which constrained the probabilities in the result to follow the binomial distribution and which assumed negligible variance in the quantal EPSP. In these experiments the analysis was combined with HRP injections into the pre- and postsynaptic cells, and the morphology of the synaptic connections was subsequently reconstructed. The result was a close correlation between the binomial parameter

n and the number of synaptic ~~terminations~~ boutons for each synaptic connection. As most of these terminations have only one release site (Triller & Korn, 1982), this suggests that the active site in each termination releases no more than one quantum of transmitter (provided the assumption of equal probabilities for release at different sites is correct). No alternative hypotheses to those which required uniformity of p were examined. More recently, an analysis of spontaneous inhibitory currents at the inhibitory interneurone-Mauthner cell connection determined a coefficient of variation for the quantal current averaging 0.11 (Korn et al, 1987), which supports the earlier assumption of minimal quantal variability.

The single club ending synapses formed between saccular afferents and the Mauthner cell are particularly interesting for the analysis of fluctuations in EPSP amplitude. These synapses have the morphological features of both electrical and chemical synapses (Kohno & Noguchi, 1986; Tuttle et al, 1986). Two important findings have come from experiments involving simultaneous intracellular recordings from the saccular afferent and the Mauthner cell (Lin & Faber, 1988a,b). Firstly, for connections where both chemically-mediated EPSPs and electrotonic coupling potentials were present, there was no correlation between the amplitudes of the two responses, for individual trials. This indicates that the variations in amplitude of the chemically-mediated EPSP (including failures) were not due to variable invasion of the nerve terminal by the presynaptic action potential. Secondly, while all the club endings generated postsynaptic

coupling potentials, an associated chemically-mediated EPSP was only observed for about 20% of the synapses. The presence of the structural correlates for chemical transmission in all afferents suggests that in most cases the chemical synapses were inactive.

A mismatch between the binomially-determined n and the number of identified synapses in cultures of fetal mouse spinal cord and dorsal root ganglion cells, has also been proposed as evidence for inactive synapses (Neale et al, 1983; Pun et al, 1986).

1.8 Quantal analysis of EPSPs in the hippocampal formation

There have been very few investigations of synaptic transmission in the dentate gyrus or hippocampus which have involved quantal analysis. McNaughton et al (1981) analysed the variations in amplitude of compound EPSPs evoked in dentate granule cells by perforant path stimulation. Two methods based on Poisson statistics were used; the method of variance and the method of failures. The mean quantal contents determined for the compound EPSPs (average amplitude 560 μV, n=15) by the two methods were 4.7 and 2.2 respectively (McNaughton et al, 1981). The corresponding mean quantal sizes were 119 μV for the method of variance, and 255 μV for the method of failures.

The mossy fibre input to CA3 pyramidal cells has also been analysed by the method of variance. Trains of presumed unitary EPSPs have been evoked in the CA3 neurones by short iontophoretic ejections of DL-homocysteate (Yamamoto, 1982) or glutamate (Higashima et al, 1986; Yamamoto et al, 1987)

onto dentate granule cells. For the first EPSP in each train, the mean quantal size estimated by the method of variance for 11 cells was 610 μV (Higashima et al, 1986). The mean quantal content was 4.4, the mean EPSP amplitude being approximately 2.5 mV. When this technique was applied to determine the changed parameters underlying the facilitation of the second EPSP in the evoked train, the mean quantal content was found to be increased, with little change in the quantal size (Yamamoto, 1982). A similar result was obtained for the potentiated EPSP amplitudes induced by application of the protein kinase C activator phorbol diacetate (Yamamoto et al, 1987). These findings were used as support for presynaptic mechanisms being responsible for the enhancement of the EPSP amplitudes.

Miles and Wong (1986) obtained unitary EPSPs in simultaneous recordings from pairs of CA3 pyramidal cells in the hippocampal slice (these cells have recurrent monosynaptic excitatory connections). The presynaptic neurones were discharged by injection of steady depolarizing current. For one of the pairs, the fluctuations in the amplitude of the EPSP were analysed by the method of variance and the method of failures. The mean amplitude of this EPSP was 1300 μV, and the quantal sizes estimated by the two methods were 600 μV and 400 μV respectively (Miles & Wong, 1986). Note that 'failures' were defined as those responses which could not be distinguished above the background noise, and that the threshold for discrimination above the noise was about 400 μV.

Brown et al (1979) have recorded spontaneous EPSPs in CA3 neurones, in slices treated with tetrodotoxin and Mn^{2+} to prevent evoked release. These EPSPs presumably represented spontaneous release from both the mossy fibres and the other inputs, including the recurrent excitatory collaterals. The mean peak amplitude of the spontaneous EPSPs, sampled from eight cells, was 2.1 mV. However, the mean was biased because only those EPSPs discriminable above the background noise (about 750 μV or greater) were included. The distributions were skewed, with the modes always buried in the background noise (Brown et al, 1979). These results are therefore not inconsistent with the amplitudes of the quantal EPSPs as estimated by Higashima et al (1986) and Miles and Wong (1986); on the other hand, the results do not provide sufficient information to be considered supportive.

The only previous quantal analysis of EPSPs in CA1 pyramidal cells is that of Hess et al (1987). EPSPs were evoked by stimuli to the strata radiatum or oriens in the guinea pig hippocampal slice. The mean amplitude of the EPSPs was 314 μV (15 cells). The quantal size was estimated by three methods: (1) from the mean distance between peaks observed in the raw amplitude histograms. It is pertinent here that the number of responses sampled for each EPSP was only about 100, and that the appearance of peaks in such histograms is highly dependent on the sample size and the width of the histogram bins (Hess et al, 1987, make no comment on this point), (2) by the method of variance, and (3) by the method of failures. It is not clear how the failures were distinguished from the smallest responses.

For the 15 EPSPs, the three methods gave mean quantal sizes of 240 μV, 286 μV and 297 μV respectively (Hess et al, 1987). The corresponding mean quantal contents were 1.5, 1.29 and 1.13. As part of the same study, EPSPs were evoked by paired stimuli (40-50 ms interval) to investigate paired-pulse facilitation. The above results were from analysis of the first EPSP in each pair. For the second EPSP in each pair, the mean increase in peak amplitude was 146%. Surprisingly, all of the methods of quantal analysis gave increases in quantal size (to mean values of 306, 348 and 329 μV for methods 1-3) as well as increases in quantal content (to mean values of 2.61, 2.36 and 2.23) for the second EPSP. Note that this is the only reported example at any synapse of facilitation being associated with a change in quantal size.

The above analyses of the variations in amplitude of EPSPs in the hippocampal formation suffer from two main weaknesses. Firstly, methods based on Poisson statistics have been used without any independent means of ascertaining their applicability to the system being investigated. Poisson statistics are only appropriate for connections where a large number of quanta are available for release and where the probability of release for each one of them is very small (Martin, 1966, McLachlan, 1978). This is the case for the neuromuscular junction in conditions of raised Mg^{2+} or lowered Ca^{2+}, but there is no reason to expect this to be so at normal CNS synapses. The main attractiveness of the Poisson-based methods would seem to be their ease of use.

Secondly, with the exception of the protocol of Miles and Wong (1986), the methods of eliciting the EPSPs are insecure, in that intermittent failures to excite the afferents cannot be ruled out. If these were occurring, there would be a disproportionate number of failures in the responses. This would lead directly to errors in the case of the method of failures, and by affecting the variance of the amplitude histograms, would also introduce errors to the method of variance. The method of failures as used by Miles and Wong (1986) could be subject to the same source of uncertainty, because there was no sure means of distinguishing failures from small responses hidden by the noise.

In an investigation of the time courses of small EPSPs evoked in CA1 cells by stimulation of the stratum radiatum, Turner (1988) observed that the variations in EPSP amplitude were greater than could be attributed to the baseline noise. It was noted that failures could not be reliably distinguished from the smallest responses, and that the prevailing noise levels prevented further discrimination of the components underlying the EPSPs.

1.9 Synaptic plasticity: long-term potentiation

Long-term potentiation (LTP) is a sustained enhancement in the synaptic response of neurones following tetanic activation of their afferents. Its onset following tetanization occurs with a delay of several seconds and its maximal effect occurs after a further 15-20 s (McNaughton, 1983; Gustafsson & Wigstrom, 1988). The duration of the

enhanced response is variable depending upon the conditions in which it is induced; it may last for days or weeks in the whole animal (Racine et al, 1983), or only a few minutes after weak stimulation in hippocampal slices (Gustafsson et al, 1987). Even then, it outlasts the shorter-duration plastic phenomena seen at central synapses, such as facilitation, post-tetanic augmentation and potentiation, which all decay within 1-2 min (McNaughton, 1982; Gustafsson & Wigstrom, 1988). Although LTP is most readily demonstrated in the hippocampal formation, enduring changes in synaptic efficacy have been seen in many other regions of the brain (reviewed by Teyler & DiScenna, 1987).

Since the first descriptions of LTP in the dentate gyrus of the rabbit (Bliss & Lomo, 1973; Bliss & Gardner-Medwin, 1973), there has been a burgeoning interest in the topic, mainly due to the belief that it represents a neurophysiological correlate of memory formation. As there are several recent reviews of the field (Teyler & DiScenna, 1987; Smith, 1987; Gustafsson & Wigstrom, 1988), an extensive summary will not be attempted here. However, some the more recent findings related to LTP are presented below.

1.9.1 The induction of LTP

It is probably fair to say that our understanding of the mechanisms underlying the induction (or triggering) of LTP is somewhat in advance of our understanding of the processes for its expression and maintenance. The evidence relating to induction mechanisms will be considered first.

Any putative induction mechanism needs to explain two fundamental properties of LTP; (1) the specificity of the

enhanced postsynaptic responses to those inputs which were active during the tetanus (Dunwiddie & Lynch, 1978; Andersen et al, 1980b), and (2) the associative interaction (or cooperativity) between excitatory inputs in which a weak input is unchanged if tetanized alone, but shows LTP if tetanized in combination with a strong input (McNaughton et al, 1978; Levy & Steward, 1979; Lee, 1983, Kelso & Brown, 1986).

The first clues for possible induction mechanisms arose from evidence that the crucial triggering steps were postsynaptic. It seemed difficult to explain associativity by a presynaptic mechanism, because it would have required rapid interactions (e.g. by transmitter diffusion) between the widely separated terminals of different inputs (McNaughton et al, 1978; Levy & Steward, 1983; Gustafsson & Wigstrom, 1986). Further, blockade of postsynaptic inhibition was shown to facilitate the induction of LTP (but not to alter the degree of enhancement), and this suggested that postsynaptic depolarization during the tetanus might be important (Wigstrom & Gustafsson, 1985). Intracellular recordings confirmed the importance of the postsynaptic membrane potential; LTP could be induced in weak inputs if they were tetanized in conjunction with depolarizing current injections (Kelso et al, 1986; Gustafsson & Wigstrom, 1988), and strong inputs were prevented from showing LTP by tetanization paired with hyperpolarizing current (Malinow & Miller, 1986). In fact, presynaptic tetanization did not appear to be necessary at all, as LTP could be shown for inputs which were continued at the test stimulus rate, but

paired for 20-30 events with postsynaptic depolarizing pulses (Wigstrom et al, 1986a; Gustafsson et al, 1987).

There is some evidence, although indirect, for postsynaptic Ca^{2+} influx as a step in the triggering process. Injection of the Ca^{2+} chelator EGTA into the postsynaptic neurone blocks the generation of LTP (Lynch et al, 1983) and there is increased dendritic binding of calcium following tetanization (Kuhnt et al, 1985). However, these results did not enable confirmation of a role for Ca^{2+} during the induction rather than the maintenance phase of LTP. Lowered extracellular levels of Ca^{2+} prevented LTP while leaving synaptic transmission intact (Dunwiddie & Lynch, 1979), but these concentration changes may have compromised postsynaptic depolarization during the tetani.

An important step forward occurred when it was found that the NMDA antagonist AP5 blocked the induction of LTP, but had no effect on already-established LTP (Collingridge et al, 1983b; Wigstrom et al, 1986a,b; but note that LTP of the mossy fibre input to CA3 is not blocked by AP5, Harris & Cotman, 1986). From the properties of the NMDA receptor-channel complex (section 1.5.1), the features of LTP induction listed above can be explained. Postsynaptic depolarization, whether provided by tetanic activation of a sufficient number of afferents (associativity), or by injection of depolarizing current, relieves the Mg^{2+} block of the NMDA channels over a region of the dendritic tree. The spread of the depolarization is limited only by the cable properties of the neurone, and hippocampal pyramidal cells are relatively compact electotonically (Turner &

Schwartzkroin, 1980; Johnston, 1981; Turner, 1984a,b). However, these channels additionally require binding of neurotransmitter to the NMDA receptor before they will conduct. Both of the required conditions (depolarization and transmitter release) only occur at those synapses which are active during the postsynaptic depolarization, and the consequence is a Ca^{2+} influx through the NMDA channels at the site of the active synapses. In order to explain the specificity of LTP, it has been proposed that the dendritic spine geometry and intracellular buffering systems limit the spread of Ca^{2+} (Gamble & Koch, 1987; Wickens, 1988). The presumed activation of LTP mechanisms by the elevation of intracellular Ca^{2+} is therefore confined to the active synapses.

Although the above scheme is attractive, there are still some aspects of it which are uncertain. It is not known whether the NMDA and the non-NMDA receptors coexist at the same synapses, or in the same part of the spines. The possible involvement of other voltage sensitive Ca^{2+} channels in the induction of LTP has not been ruled out. Wickens (1988) has argued for at least some of the Ca^{2+} influx during the tetanization being carried by such channels. Certainly the NMDA receptor hypothesis is not applicable to the mossy fibre input to CA3 neurones.

One recently proposed intermediary between Ca^{2+} influx and the (unknown) mechanisms which enhance transmission, is the calcium, diacylglycerol and phosholipid-dependent protein kinase known as protein kinase C (PKC). When activated, PKC

becomes associated with the cell membrane, where it catalyses the phosphorylation of substrate proteins (Kazmarek, 1987). The evidence which has implicated PKC involvement in LTP includes (1) a doubling of membrane-bound PKC activity when measured 1 hour after the induction of LTP in the dentate gyrus (but not when measured 1 min after induction; Akers et al, 1986), (2) application of PKC-activating phorbol esters to hippocampal slices potentiated synaptic transmission in CA1 (Malenka et al, 1986), (3) PKC ejected through intracellular electrodes enhanced EPSP amplitude and firing probability in CA1 pyramidal cells (Andersen et al, 1987b), (4) inhibitors of PKC applied to the dentate gyrus either before or within 10 min following tetanization caused the decay of LTP within 1 hour, although the initial magnitude of the LTP was not affected (Lovinger et al, 1987), and (5) another activator of PKC, oleate, produced a persistent potentiation of synaptic transmission in the dentate gyrus when applied in combination with a weak tetanus which otherwise caused a shorter (<1 hour) potentiation (Linden et al, 1987).

Note that (1), (4) and (5) above all point to the involvement of PKC in a later phase rather than the initial stages of LTP. This in itself suggests that there may be several different processes underlying LTP, with overlapping time courses. Presumably there are other substances which may mediate the more rapidly-activated processes; the Ca2+/calmodulin-dependent kinase would be one candidate (Gustafsson & Wigstrom, 1988).

1.9.2 The expression of LTP: suggested mechanisms

LTP is not associated with any measurable changes in postsynaptic resting membrane potential or input resistance (Andersen et al, 1980b; Barrionuevo & Brown, 1983); neither is it due to a reduction in synaptic inhibition (Haas & Rose, 1984; Wigstrom & Gustafsson, 1985; Abraham et al, 1987; Taube & Schwartzkroin, 1987). Tetanization of the stratum radiatum does not change the number of synapses onto dendrites, although it is associated with a persistent increase in the number of synapses onto dendritic shafts (Lee et al, 1980; Chang & Greenough, 1984). However, synapses on dendritic shafts make up less than 5% of the total number of synapses, and it is not clear whether they are new synapses or transformed spine synapses, and whether they are synapses onto interneurones or pyramidal cells. Changes in the shape of the spine head have been reported following tetanization in CA1 (Lee et al, 1980; Chang & Greenough, 1984), although one group reported these to last for less than two hours (Chang & Greenough, 1984). Andersen et al (1987a) found significant widening of the dendritic spine necks associated with LTP in the dentate gyrus, although it is not yet clear to what extent this change would reduce the attenuation of the EPSP between the spine head and the soma.

One line of evidence which points to a presynaptic mechanism for the expression of LTP is the finding that the release of excitatory amino acids is enhanced following tetanization. This has been shown for hippocampal slices following tetanization of the stratum radiatum (Skrede & Malthe-Sorenssen, 1981) and for the dentate gyrus, both in

anaesthetised rats (Dolphin et al, 1982; Bliss et al, 1986) and in slices (Lynch & Bliss, 1986). The enhanced release was not seen for animals in which tetani were given, but failed to induce LTP (Dolphin et al, 1982), or in animals in which the induction of LTP was blocked by AP5 (Errington et al, 1987). The maximum increase in glutamate release occurred about 8-15 min after the induction of LTP, but the released levels remained above baseline for at least 1-2 hours.

The existence of a presynaptic mechanism for the expression of LTP, triggered by a postsynaptic induction mechanism, would require a retrograde messenger substance to carry the signal from the postsynaptic side to the presynaptic side of the terminal. Williams and Bliss (1988) suggest that small lipid-soluble metabolites of arachadonic acid could perform this role, because they pass easily through both cytoplasmic and membrane compartments of the cell. Futhermore, they have shown that norhydroguaiaretic acid, which inhibits the production of these metabolites, prevents the LTP-like increase in synaptic efficacy induced by transiently raising the extracellular Ca^{2+} concentration (dentate gyrus and CA1 *in vitro*, Williams & Bliss, 1988). Norhydroguaiaretic acid did not block the maintenance of the synaptic enhancement after it had been induced.

A scheme for postsynaptic expression of LTP has been proposed, based on an increased number of glutamate receptors in the postsynaptic membrane (Baudry et al, 1980; Lynch et al, 1982; Lynch & Baudry, 1984). This paradigm involves activation of calpain I (a thiol proteinase) by the tetanus-

induced elevation of intracellular Ca^{2+}. The calpain I then acts on structural proteins such as fodrin or microtubule-associated proteins, to uncover previously inactive glutamate receptors of the non-NMDA type. There is some basis for such a scheme; high levels of membrane-bound calpains are found in the hippocampus (Simonson et al, 1985), and fodrin antibodies block the Ca^{2+}-induced increase in glutamate binding to hippocampal synaptosomal membranes. However, there is no supporting electrophysiological evidence. The response to iontophoretically-applied glutamate is not enhanced in LTP (Lynch et al, 1976; Taube & Schwartzkroin, 1988), which is against expectations for the hypothesis.

Connor et al (1988) have recently suggested that a postsynaptic modification of voltage-sensitive Ca^{2+} channels might underly LTP. Their evidence comes from measurement of intracellular Ca^{2+} gradients in isolated adult CA1 neurones, using the fluorescent Ca indicator fura-2. Sustained Ca^{2+} gradients were induced in the apical dendrites following local applications of glutamate or NMDA. The sustained gradients (but not the initial brief Ca^{2+} influx) were blocked by previous treatment with sphingosine, a PKC inhibitor. They were also suppressed by application of GABA, which was assumed to hyperpolarize the neurones. Both the initial and the sustained Ca^{2+} gradients were blocked by addition of AP5 to the bathing medium. The initial gradients were attributed to Ca^{2+} influx through NMDA channels, and it was proposed that the sustained gradients were due to a PKC-mediated modification of previously inactive voltage-sensitive Ca^{2+} channels (Connor et al, 1988). The

implications of this scheme as they may relate to the findings presented in this thesis, are discussed in Chapter Five.

1.10 The aims of this project

At the outset of this study, the primary aim was to apply quantal analysis to the fluctuations in amplitude of small EPSPs evoked in CA1 pyramidal cells. While interesting in itself, the motive for quantal analysis was the information it ought to provide about the mechanisms underlying synaptic plasticity. If quantal analysis coud be performed before and after the induction of LTP, it would be possible to determine whether the enhanced amplitude of the averaged EPSP was due to an increase in the quantal size or in the quantal content (or both). A change in the quantal content would imply a presynaptic mechanism for the expression of LTP, whereas an increased quantal size would be consistent with a postsynaptic mechanism, provided that a change in vesicular content could be ruled out.

In order to determine the statistics of transmitter release, it is preferable to use a technique which activates the afferent(s) reliably from trial-to-trial. This is difficult to achieve in the hippocampal slice, as direct stimulation of the afferent pathways runs the risk of activating some axons near to their threshold, which would introduce an additional source of variability in the amplitude of the evoked EPSPs. A further concern at the commencement of this study was that the amplitude range for unitary CA3-CA1 EPSPs was unknown. It was therefore

impossible to know how many afferents were activated by stimuli to the stratum radiatum. For quantal analysis, it is best to activate as few inputs as possible, as this minimises the range of EPSP amplitudes. This is advantageous because for a given number of trials, the number of entries in each bin of the EPSP amplitude histogram is maximised, thereby reducing the effects of finite sampling error.

For these reasons, it was decided to undertake simultaneous intracellular recordings from the CA3 and CA1 regions. Intracellular access to the presynaptic neurone allowed reliable activation of a single presynaptic cell. These experiments were much more difficult than single intracellular recordings in CA1 (with EPSPs evoked by stimuli to the stratum radiatum), but they promised information which would be especially useful. Several other groups have searched for synaptically-connected CA3 and CA1 neurones in dual intracellular recording experiments, without success (Andersen, 1986). However, simultaneous intracellular recordings have been used to study excitatory or inhibitory connections between pairs of neurones *within* CA3 (MacVicar & Dudek, 1980; Miles & Wong, 1984, 1986, 1987a,b) or *within* CA1 (Knowles & Schwartzkroin, 1981; Lacaille et al, 1987; Lacaille & Schwartzkroin, 1988a,b).

In experiments preliminary to the simultaneous CA3-CA1 recordings, afferents in the stratum radiatum and some CA1 cells were stained with horseradish peroxidase. One of the purposes of these experiments was to examine the course of the Schaffer collaterals so as to determine the optimum angle for cutting the slices. The results from these experiments

are not formally presented here, but a photomicrograph of some horseradish peroxidase-stained material is included as a frontspiece to this thesis.

Besides their variations in amplitude, there were many previously unreported features of the unitary responses in CA1 cells, and these are described in Chapter Three. Chapter Four details the analysis of the variations in amplitude of both unitary EPSPs and small compound EPSPs evoked in CA1 neurones. Two methods of quantal analysis are applied to the EPSPs: the method of variance and an unconstrained deconvolution technique. Chapter Five concerns synaptic plasticity; paired-pulse facilitation is demonstrated for unitary EPSPs and LTP is compared for large compound, small compound and unitary EPSPs. The final conclusions drawn from this study are presented in Chapter Six.

Chapter Two:
METHODS

This chapter describes the methods which were common to all of the experiments. Chapters Three, Four and Five each have their own methods sections which deal with the specific aspects of the experimental protocols and the analysis relating to those chapters.

2.1 Preparation and maintenance of the hippocampal slices

Albino guinea pigs of either sex and weighing 600-900 g were used in these experiments. The animals were supplied by the Animal Breeding Establishment at the John Curtin School of Medical Research (JCSMR).

Each guinea pig was exposed to ether until a surgical level of anaesthesia was achieved (relaxed muscle tone, regular breathing and no response to paw-pinch). The carotids were sectioned immediately before opening the skull, to ensure that the animal would not be aroused from the anaesthesia. The brain was removed and placed in artificial cerebrospinal fluid (ACSF) at 2-4^{o}C for 3-5 min. The hippocampus was then dissected out from one side and 450-500 μm slices were cut with a McIlwain tissue chopper (Mickle Laboratory Engineering Co.). The hippocampus was

aligned on the chopper so that the slices were cut parallel to the lamellae, 20-30° from the transverse plane with the rostral end of the blade turned medially.

The slices were transferred to an Oslo-type chamber (see Dingledine, 1984, p 392). The recording chamber was constructed in the workshops of the University of Oslo and was kindly donated by Prof. P. Andersen. The slices lay on netting covered with lens tissue (Kodak), and were maintained at 32-33°C at the interface between ACSF and humidified gas (95% O_2/5% CO_2). The ACSF consisted of (in mM): NaCl 124, KCl 2, $MgSO_4$ 2, $CaCl_2$ 2, KH_2PO_4 1.25, $NaHCO_3$ 26 and glucose 11, saturated with 95% O_2/5% CO_2. The slices were usually allowed to recover for about 1 hour before recording was commenced. They usually remained viable for about 8-10 h.

2.2 Stimulating electrodes

The stimuli delivered to the stratum radiatum were constant-current cathodal pulses of duration 0.1 ms. Two kinds of monopolar stimulating electrode were used:

(1) For antidromic activation of CA3 cells and for eliciting large compound EPSPs, the electrodes used were made from 25 μm diameter tungsten wire (Goodfellow Metals). The wire was threaded through glass capillary tubing, which was then pulled to a fine tip by hand-pulling it past a heated element. The glass was broken back to allow the tungsten wire to protrude about 10-30 μm through the tip. The outside of the electrode was coated with Sylgard (Dow Corning) as close to the tip as possible. This prevented a fluid

meniscus forming between the slice surface and the outer walls of the electrode.

(2) For prolonged recordings of small compound EPSPs (mean peak amplitude <400 μV), it was especially important that the current density around the tip of the stimulating electrode remained constant. The type of electrode used for these experiments was designed to cause a minimum of trauma and to reduce fluid accumulation around the tip where it made contact with the tissue. Capillary tubing (1.8 mm outer diameter, Kimax-51) was pulled to a fine tip, then broken back and heat polished to form a tip with an inside diameter of 5-15 μm. The shanks were coated with Sylgard (to the tip) and the shafts were shielded with conductive paint. The electrodes were filled with 1 M NaCl in gelatine. The gelatine prevented the electrolyte from flowing out of the tip. (Agar was tried, but it tended to contract inside the electrode over the course of a few days.)

2.3 Recording electrodes

Micropipettes were pulled from 1.5 mm outer diameter glass capillary tubing on a Brown-Flaming puller (Sutter Instrument Co.). For the simultaneous CA3-CA1 recordings, glass with an inner diameter of 1.12 mm was used (cat no. 6175, A-M Systems). These electrodes had resistances of 40-70 MΩ when filled with 2 M potassium methylsulphate. For the experiments with small compound EPSPs, glass with an inner diameter of 1.17 mm (GC150TF-15, Clark Electromedical Instruments) was used to pull electrodes of resistance 30-40 MΩ. The advantage of these was lower electrode noise levels,

but the yield of satisfactory intracellular penetrations was reduced.

The electrodes were filled with 2 M potassium methylsulphate in all experiments. For many of the simultaneous CA3-CA1 recordings, the electrodes were coated with Antispread M2 (Etsyntha Chemie). This agent lowers the surface tension of the glass, and has been reported to improve the yield and stability of intracellular recordings (Jarvilehto et al, 1986). It is not clear from our experience whether Antispread was beneficial, as we did not test it in a controlled way (it may have improved the duration of recordings slightly).

The reference electrode was a chlorided silver wire in contact with the ACSF inside the recording chamber.

2.4 Recording techniques and equipment

The slices were visualised at 50x magnification through a binocular microscope (Wild M5A). The recording electrodes were advanced by mechanical manipulators (Leitz).

The headstage preamplifiers and amplifiers (ASF1, an early version of the Axoclamp) were operated in bridge mode, except when measuring the input resistance of neurones. Input resistance was measured using discontinuous current mode (also known as discontinuous current clamp, DCC), with a switching rate of 3-5 Hz. The input resistance was determined from the maximum voltage response to a 0.1 nA hyperpolarizing current of 100 ms duration.

The signals from the amplifiers were routed via the analog output of an oscilloscope (Tektronix 5223) to a 12 bit

A/D board in a microcomputer (Cromemco CS2). The A/D board was designed and constructed by Mr R. Friend of the JCSMR electronics workshop, and the collection programs for the microcomputer were written by Dr F. Edwards. The hard disk on the microcomputer was configured to provide a storage capacity of about 20 Mbytes. For the standard A/D board sampling rate of 4 KHz, this was sufficient to save about 25,000 individual records of 100 ms duration. At the end of each experiment, the data was transferred to a mainframe computer (Pyramid 90x) for off-line analysis. The software for the analysis routines which performed averaging, graphics plotting and various aspects of the deconvolution analysis (Chapter 4) was developed by various people, including the author, Dr J. Clements, Dr F. Edwards, Mr G. Quinn and Dr D. Kullmann.

Chapter Three:
CHARACTERISTICS OF UNITARY POSTSYNAPTIC POTENTIALS EVOKED IN CA1 NEURONES

3.1 INTRODUCTION

This chapter describes some of the basic features of synaptic potentials evoked in CA1 pyramidal cells by activation of single CA3 cells. The emphasis is on the peak amplitudes and time courses of the averaged unitary EPSPs, as these are fundamental to an understanding of synaptic integration in these large and complex neurones. Other properties of the EPSPs, such as trial-to-trial variations in amplitude and changes in synaptic strength (plasticity), are examined in the subsequent chapters.

The only other comparable study of small EPSPs in CA1 is that of Turner (1988), in which 'minimal' EPSPs were evoked in pyramidal cells by grading the stratum radiatum stimuli to produce the smallest responses which could be discriminated from the baseline noise. Although Turner (1988) was able to provide some valuable comparisons of the time courses of EPSPs evoked by afferents to proximal and distal regions of the apical dendrites, the method of eliciting the EPSPs meant that conclusions about the strength of single afferents could not be drawn from the EPSP amplitudes. An advantage of the

protocol adopted here is that the EPSP amplitude is relevant, as it indicates the effectiveness of a single presynaptic neurone in bringing the postsynaptic cell closer to its discharge threshold.

Some ~~chance~~ unusual findings of this study are presented and discussed in this chapter. One neurone is described which had some atypical features, although it did not satisfy all the criteria for classification as 'non-pyramidal' (Schwartzkroin & Mathers, 1978). It was a surprise to discover three instances of PSPs which were predominantly hyperpolarizing, as it was initially assumed that a single action potential in a CA3 pyramidal cell would have only monosynaptic excitatory effects. In a few cases more than one postsynaptic CA1 neurone was found which received an input from an individual CA3 cell (divergence) or more than one input was found for a given CA1 cell (convergence), and the characteristics of these connections are compared.

3.2 METHODS

Guinea pig hippocampal slices were prepared and maintained as described in the previous chapter. In these experiments, no attempt was made to block $GABA_A$-mediated synaptic inhibition with bicuculline methiodide, for two reasons, (1) because in the absence of inhibition, polysynaptic excitatory connections between CA3 neurones are revealed (Miles and Wong, 1987b), and this might allow polysynaptic connections between CA3 and CA1 cells, and (2)

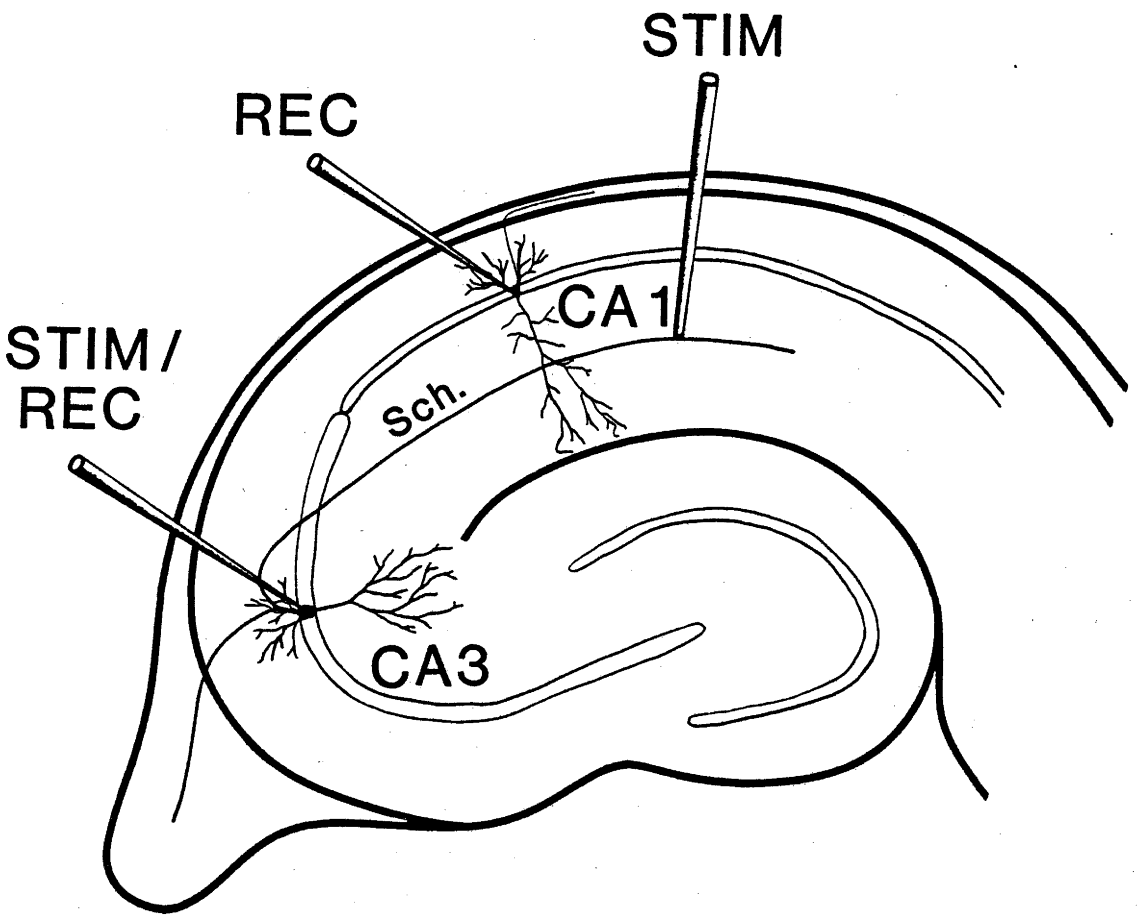
because we wanted to observe any IPSPs which might be evoked in the CA1 neurones.

The protocol for electrode placement is illustrated in Fig. 3.1. Although not shown in this figure, a platinum foil shield was attached to the CA3 electrode holder, and this extended between the two glass microelectrodes to within 1-2 mm of the slice surface. The shield was connnected to ground and it greatly reduced the coupling artifact betwen the two electrodes.

To improve the chances of finding a connected CA3-CA1 pair, we first impaled CA3 cells and looked for one which could be antidromically activated by the tungsten stimulating electrode placed in the CA1 stratum radiatum (constant current cathodal stimuli, 100 μS, <100 μA). This ensured that the CA3 neurone had a Schaffer collateral running in the plane of the slice through the CA1 apical dendritic field. Antidromic action potentials in the CA3 neurone were identified by (a) their direct rise from the baseline, earlier in onset than the recurrent CA3 EPSP, and (b) the insensitivity of the stimulus threshold to hyperpolarizing or depolarizing current injected into the CA3 cell.

Each time a CA1 neurone was impaled, the CA3-CA1 pair was tested for a synaptic connection by activating the CA3 cell at 2 Hz with an intracellular depolarizing current pulse (0.5-5 nA, 3-5 ms). The current pulse injected into the CA3 neurone was adjusted to evoke a single action potential. Usually 100-200 records were averaged to determine the presence or absence of a PSP in the CA1 neurone. If there was any suggestion of a PSP, care was taken to optimise the

Figure 3.1. Electrode placements for CA3-CA1 simultaneous recordings. Glass micropipettes impaled somata in the CA3 and CA1 strata pyramidale (STIM/REC and REC). The tungsten cathode was placed in the CA1 stratum radiatum (STIM). STIM, stimulating electrodes; REC, recording electrodes (the CA3 intracellular electrode is used for both).


STIM
REC
CA1
STIM/
REC
Sch.
CA3

quality of the penetration of the CA1 cell. Often the electrode was advanced or pulled back slightly to a position where the membrane was most polarized. In some cases a small hyperpolarizing current (<0.5 nA) was maintained for the duration of the recording, to hold the membrane potential more hyperpolarized than 60 mV.

Both presynaptic and postsynaptic records were digitised at 4 kHz and saved on disk. They were saved as individual records, typically 100 ms in duration, and averages were reconstructed off-line. Allowance was made for variations in the latency of the CA3 action potential by determining the time of the peak of the action potential on each presynaptic record. Each corresponding postsynaptic record was adjusted relative to that time before being incorporated in the cumulative average (i.e. software "spike triggering"). Before the timing of each record was adjusted, the region which was contaminated by the capacitive coupling artifact from the CA3 electrode was "masked", and excluded from the average. Failure to evoke an action potential in the CA3 neurone was also detected and the corresponding postsynaptic record was excluded from the average.

The time course parameters of the averaged EPSPs were determined by a computer program which made the following calculations: (a) latency; time from the peak of the CA3 action potential to the time at which the CA1 EPSP reached 10% of its peak amplitude, (b) rise time; the time taken by the EPSP to rise from 10% to 90% of its peak amplitude, (c) half-width; the time between the EPSP reaching 50% of its peak amplitude and falling again to the same amplitude, and

(d) the decay time constant; determined by making a semi-log plot of the EPSP, then fitting a straight line to the final linear portion of the decay phase. The time constant was the absolute value of the slope of this line.

At the end of recording, an extracellular average was taken from immediately outside the CA1 cell, while continuing to activate the CA3 cell. (This was not possible if the CA3 cell was lost first.) Any extracellular field which might contaminate the intracellular EPSP was detected by this average. Before the electrodes were withdrawn from the slice, the slice was sketched and measurements were made with the microscope eyepiece scale. The locations of the two recording electrodes and the stimulating electrode were recorded. In some cases when the CA3/CA1 border was difficult to distinguish, visualisation was improved by a drop of methylene blue stain diluted in ACSF applied to the surface of the slice. On many occasions, and especially when there was any doubt about the position of the electrodes, small cuts were made at the recording sites with a knife made from pieces of razor blade, and the slice was removed from the bath and fixed in 2% glutaraldehyde overnight. The whole slice was then stained with thionine, dehydrated, mounted and coverslipped. The sites of the lesions were then localised with respect to the CA3/CA1 border by microscopy.

3.3 RESULTS

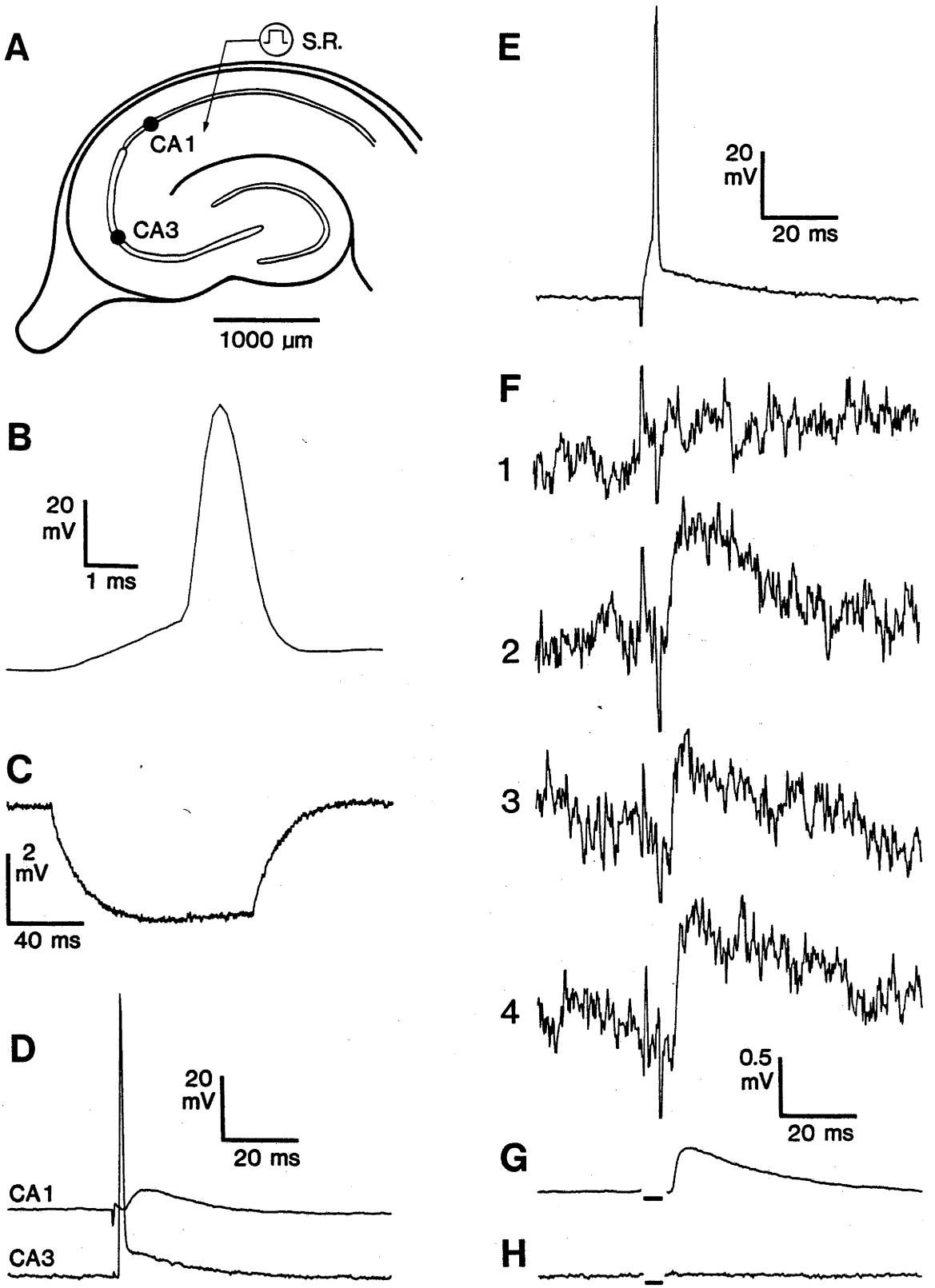
3.3.1 General

One thousand, one hundred and seventy-eight simultaneous recordings were made from CA3 and CA1 neurones, in 55 experiments. On 74 occasions, postsynaptic potentials (PSPs) were seen on the averaged CA1 records, in response to activation of the CA3 neurone. The yield of unitary PSPs obtained by this method was therefore approximately one for every 16 pairs tested. Seventy-one of the PSPs were EPSPs (depolarizing only), but three had prominent hyperpolarizing components and will be analysed separately.

The 74 PSPs were obtained from 72 neurones in the CA1 stratum pyramidale. For each of two CA1 cells, synaptic connections were obtained from two CA3 cells (i.e convergent inputs). Only 63 CA3 neurones were involved for the 74 unitary PSPs. On seven occasions, two postsynaptic CA1 cells were found for single CA3 neurones; and three postsynaptic targets were found on two occasions (i.e. divergence).

Fig. 3.2 introduces some representative features of the CA3-CA1 simultaneous recordings. The CA3 and CA1 recording sites are indicated in Fig. 3.2A, as is the position of the stimulating electrode in the CA1 stratum radiatum. The CA1 action potential in Fig. 3.2B was elicited in the CA1 neurone from the stimulating electrode (cathodal 20 μA, 100 μs). Its duration of 1.6 ms is typical for a pyramidal cell (range 1.4 - 2.0 ms, Schwartzkroin & Mathers, 1978). The response of this neurone to a 0.1 nA, 100 ms hyperpolarizing current pulse (discontinuous current mode, 4.0 kHz) is shown in Fig.

Figure 3.2. Simultaneous recordings from a CA3 neurone and a CA1 neurone with a synaptic connection. **A**, Approximate locations of the electrodes. S.R., stratum radiatum recording electrode. **B**, Action potential evoked in the CA1 cell by a 20 μA, 0.1 ms cathodal stimulus delivered through S.R. (the stimulus artifact is cut off to the left of the figure). **C**, Response of the CA1 neurone to a 0.1 nA, 100 ms hyperpolarizing current pulse. **D**, Responses of both cells to a 10 μA S.R. stimulus. **E**, The CA3 neurone was activated by short
depolarizing current pulses, adjusted to evoke single action potentials. These were repeated at 2 Hz; one example is shown. **F**, Examples of individual responses in the CA1 neurone. Record **F1** was the CA1 record taken concurrently with the CA3 record in **E**. **G**, Average of 1780 CA1 responses, after adjustment for latency variations of the CA3 action potential. The capacitive coupling artifact has been masked. The bar indicates the duration of the CA3 current pulses (4 ms). **H**, Average of 150 records taken on exit from the CA1 cell, while continuing to activate the CA3 neurone.


A
S.R.
CA1
CA3
1000 µm
B
20
mV
1 ms
C
2
mV
40 ms
D
20
mV
20 ms
CA1
CA3
E
20
mV
20 ms
F
1
2
3
4
0.5
mV
20 ms
G
H

3.2C, and the voltage change of 3.1 mV indicates that the input resistance was 31 MΩ. Fig. 3.2D shows the responses in both cells to a 10 μA stratum radiatum stimulus. At this stimulus strength the EPSP elicited in the CA1 neurone was subthreshold for action potential discharge. The CA3 cell was activated antidromically, indicating that it had an intact axon collateral in the CA1 stratum radiatum. The straight line distance between the stimulating electrode in the stratum radiatum and the CA3 recording electrode was 1600 μm, and the latency from the stimulus to the onset of the action potential was 1.25 ms. This implied a conduction velocity of at least 1.3 ms^{-1} for this axon, depending on the extent to which it deviated from a direct line between the electrodes.

The right-hand column of Fig. 3.2 shows records obtained while evoking unitary EPSPs. The stratum radiatum electrode was no longer used. The CA3 neurone was instead activated by a depolarizing current pulse, in this case 4 ms duration (Fig. 3.2E). Examples of individual responses in the CA1 neurone are shown in Fig 3.2 (F1-F4). An average was constructed from 1780 individual records (Fig. 3.2G). The averaging procedure included adjustments for latency variations of the CA3 action potential and masking of the capacitive coupling artifact. On exit from the CA1 neurone, and from immediately outside the cell, 150 extracellular records were averaged while continuing to activate the CA3 cell. The flat trace in Fig. 3.2H indicates that there was no extracellular field potential. This was typical, in that extracellular fields were tested for whenever possible (but

not if the CA3 neurone was lost first); however none were ever observed.

3.3.2 Intracellular parameters

Stable intracellular penetrations of CA3-CA1 pairs with synaptic connections were commonly maintained for 10-60 min, and sometimes for longer (maximum 3 h). For the CA1 cells, the average action potential amplitude was 82 ± 9 mV (mean ± S.D.). The mean resting membrane potential, with no current applied and determined on exit from these neurones was 64 ± 8 mV (n=42, as this could not be obtained for penetrations which were lost suddenly in the presence of steady current). The average input resistance was 20.2 ± 10.8 MΩ (measured for 54 of the CA1 neurones). These values are comparable to other reports for guinea pig CA1 pyramidal cells *in vitro* (e.g. Turner (1988), mean resting potential and input resistance 63 mV and 22.5 MΩ respectively).

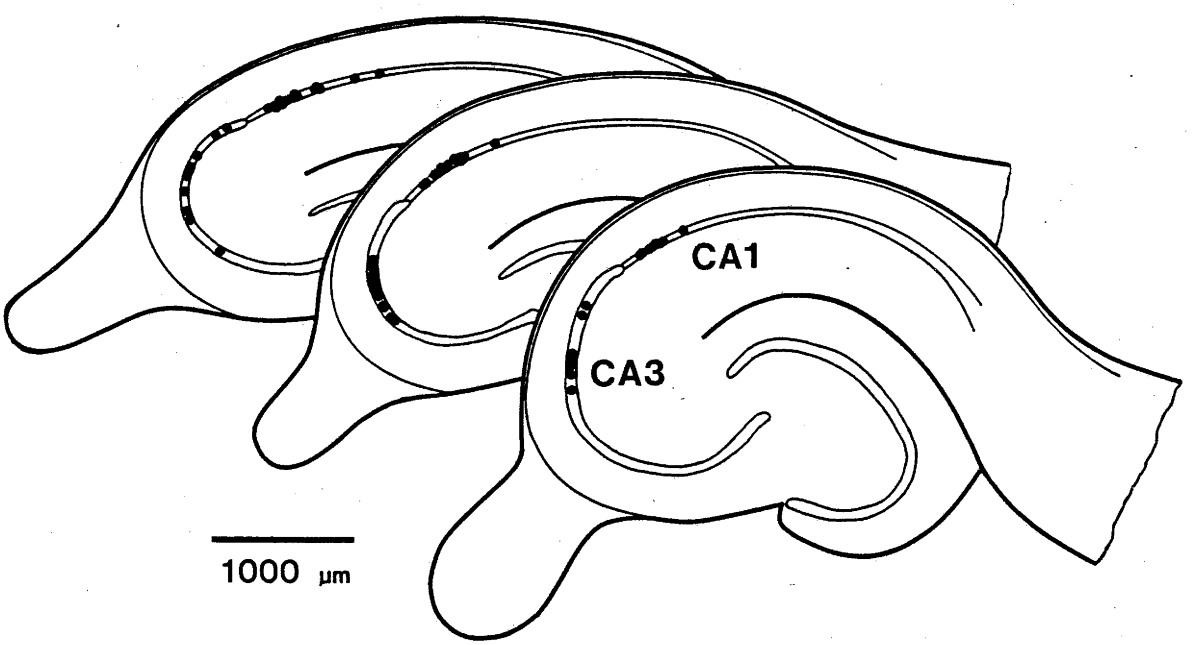
The CA3 pyramidal cells were generally more robust than CA1 neurones, and stable intracellular recordings were often maintained for several hours while searching for postsynaptic (CA1) cells. The stability of the penetrations was usually improved by a small continuous hyperpolarizing current (< 1.0 nA). CA3 neurones were discarded if their action potential amplitudes declined to 60 mV or less, if they could not be reliably activated by the depolarizing current pulse, or if more than about 15 pairs were tested without any synaptic connections being found. The input resistances and membrane potentials of the CA3 neurones were not routinely recorded.

3.3.3 Locations of the CA3 and CA1 neurones

CA3 neurones which were activated antidromically from the CA1 stratum radiatum were mostly found in the two thirds of the CA3 region nearest to the CA1 region. As the stimulating electrode in the CA1 stratum radiatum was moved towards the subicular end of CA1, fewer antidromically-activated CA3 neurones were found. This implied that fewer intact Schaffer collaterals remained within the slice as the distance from CA3 was increased. For this reason, we preferentially impaled CA1 neurones in the stratum pyramidale within a few hundred μm from the CA3/CA1 border, believing this would give us the highest yield of synaptically-connected pairs.

Fig. 3.3 illustrates the recording sites for CA3-CA1 pairs with synaptic connections, in slices which were subsequently fixed and stained with thionine (n=41). The locations have been superimposed onto three representative sections, which vary in shape according to their positions along the septo-temporal axis of the hippocampus (shown with the closest to the temporal end in the foreground). The recording sites have been marked on these sections with respect to their distances from the CA3/CA1 border, and the measurements have been adjusted for the shrinkage caused by histological processing. The shrinkage was determined for each slice by comparing the distances between the lesions measured *in vitro* with those after processing, and was on average 19%. For this group of CA3-CA1 pairs, the distance between the CA3 and CA1 recording sites (measured around the stratum pyramidale, not the straight line distance) ranged

Figure 3.3. Recording sites for CA3-CA1 simultaneous recordings in which unitary EPSPs were obtained, in slices which were subsequently fixed and stained with thionine. The slices varied in shape according to their position along the septo-temporal axis of the hippocampus; they are here superimposed onto three representative sections, with the closest to the temporal end in the foreground.


CA1
CA3
1000 µm

from 500 to 1835 μm (mean 1030 μm). The CA3 electrode to CA3/CA1 border distance ranged from 135 to 1075 μm (mean 675 μm), and the distance from the CA1 electrode to the CA3/CA1 border ranged from 130-970 μm (mean 355 μm).

3.3.4 Schaffer collateral conduction velocities and delays to onset of EPSPs

The latency from the stratum radiatum stimulus to the onset of the antidromic action potential, and the distance between the stratum radiatum and CA3 electrodes, were both recorded for 27 CA3 neurones. The conduction velocities determined for the Schaffer collaterals from these parameters ranged from 0.33 to 1.70 ms^{-1}, with a mean of 1.01 ms^{-1}. However, note that these values are likely to be underestimates, depending on how far the axons deviate from the direct line between the CA3 somata and the stimulating electrode in the stratum radiatum. In addition, as CA3 axons emerge from the basal dendritic side of the soma, a variable amount of extra axon length must be involved before crossing the stratum pyramidale and reaching the stratum radiatum. (At present there is insufficient information available in the literature to make any useful estimate of the average extra length involved.)

For all 71 unitary EPSPs, the latency was measured from the peak of the CA3 action potential (in this case activated by an intracellular current pulse) to the time at which the averaged CA1 EPSP reached 10% of its peak amplitude. The mean latency was 3.4 ± 1.2 ms, with a range from 0.7 to 5.8 ms. Any errors in these measures, due to encroachment of the

capacitive coupling artifact into the rising phase of the EPSP, would affect the shortest latency EPSPs most and would tend to prolong them. The value for the mean latency given above should therefore be regarded as an approximation, and the true mean may be slightly less.

3.3.5 Amplitudes of the averaged unitary EPSPs

When EPSPs were present on the CA1 records, the largest responses were visible on single oscilloscope traces (Fig. 3.2F). However, the baseline noise levels often required 100-200 records to be averaged before the presence of a unitary PSP could be established. We estimate that under typical recording conditons, the noise levels on averages of 100-200 records allowed us to detect EPSPs with mean peak amplitudes greater than 20 μV.

Measurements of the mean peak amplitude of the EPSPs, evoked at 2 Hz, were made from averages of 230-3000 records. These were taken after stable penetrations of the cells had been achieved, and before any further experimental manipulations (e.g. tetanic stimuli). Fig. 3.4 is a histogram showing the distribution of mean peak amplitudes for the 71 unitary EPSPs. They ranged in amplitude from 30 to 665 μV, with an overall mean of 131 μV. The mode occurs in the 50-75 μV bin.

Fig. 3.5 shows the scatter plot for mean peak EPSP amplitude versus the CA1 neurone input resistance. The correlation coefficient between these parameters was 0.34.

Figure 3.4. The distribution of the mean peak amplitudes of the 71 unitary EPSPs. The bin size is 25 μV.

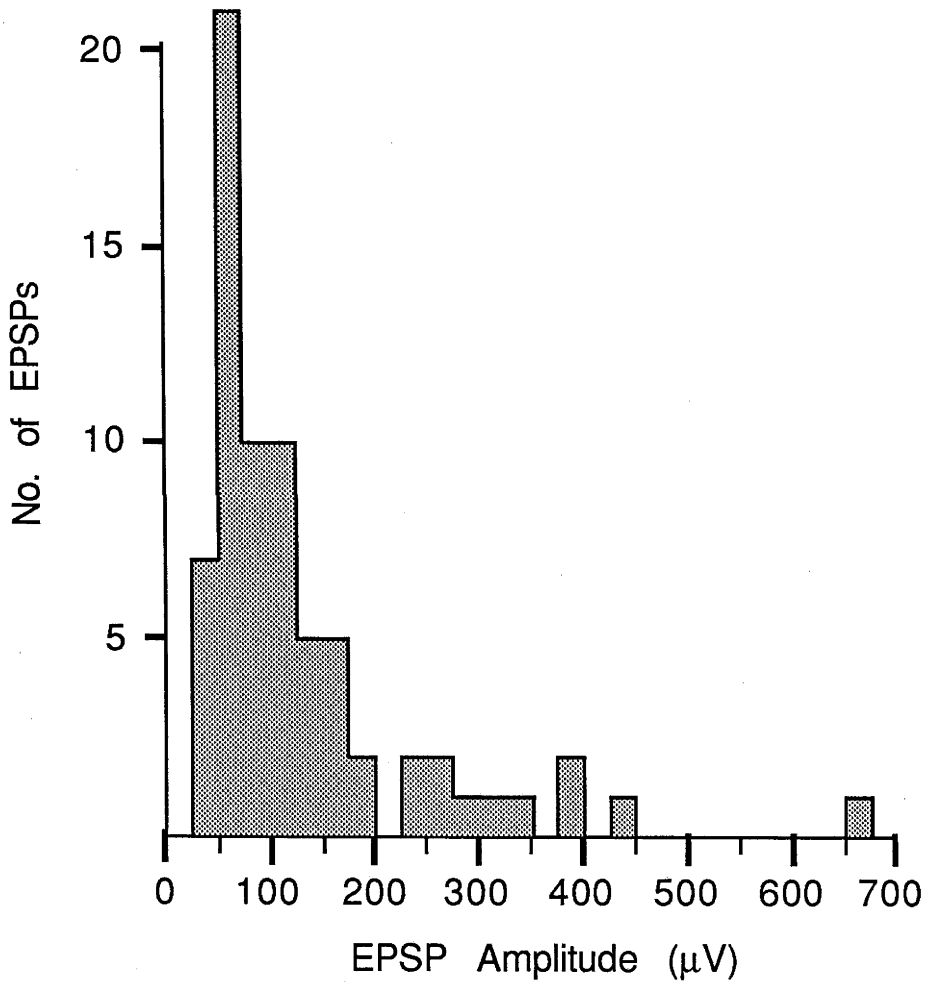
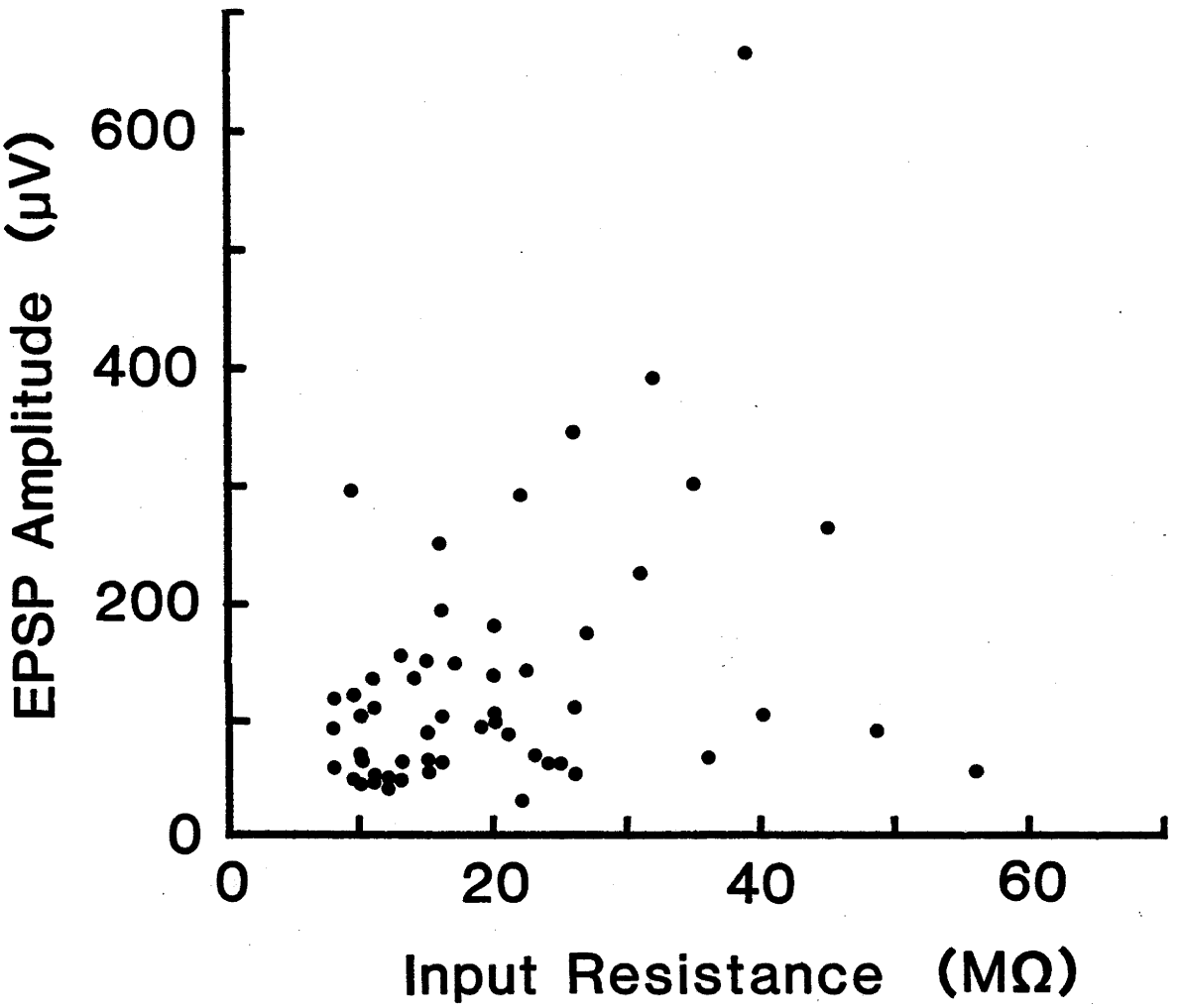

20
15
10
5
No. of EPSPs
0
100
200
300
400
500
600
700
EPSP Amplitude (μV)

Figure 3.5. The mean peak amplitude of the unitary EPSPs versus the input resistance of the CA1 neurones (n=54).


EPSP Amplitude (μV)
600
400
200
0
0
20
40
60
Input Resistance (MΩ)

The variability of the unitary EPSPs from trial-to-trial is apparent from the single records in Fig. 3.2F. This feature of the unitary EPSPs is analysed in the following chapter. However, when the EPSPs were averaged over sequential one minute intervals (120 records per average, at 2 Hz), their mean peak amplitudes rarely showed any consistent drift from the overall mean. Of 23 unitary EPSPs held for more than 10 minutes and not manipulated experimentally in any way, 20 showed no trend towards a decline or increase in mean peak amplitude.

Two examples of stable EPSPs in CA1 pyamidal neurones are shown in Fig. 3.6. The points represent the average peak amplitudes for successive minute intervals. The outer dashed lines indicate the 95% confidence intervals (two standard errors from the mean) calculated from the mean and standard deviation of the whole sample of EPSPs for each cell. The overall means are shown by the inner dashed lines. As expected for stationary conditions, most of the points fall within the 95% confidence intervals. A counter-example is given in Fig. 3.7. The unitary EPSP in this CA1 pyramidal cell increased in amplitude (at least for the first 7-10 minutes), with no concurrent hyperpolarization of the membrane potential, and an increase in the input resistance of less than 10%. Two other EPSPs in CA1 pyramidal neurones showed a gradual decline in EPSP amplitude, which in only one case was coincident with a slow depolarization of the cell.

Figure 3.6. Minute-averages for two EPSPs which showed no drift in mean peak amplitude over a 15 min recording period. Each point represents the mean peak amplitude over a one min interval (120 individual records). The outer dashed lines indicate the 95% confidence intervals, and the inner dashed lines indicate the overall mean peak amplitudes for the recording periods.

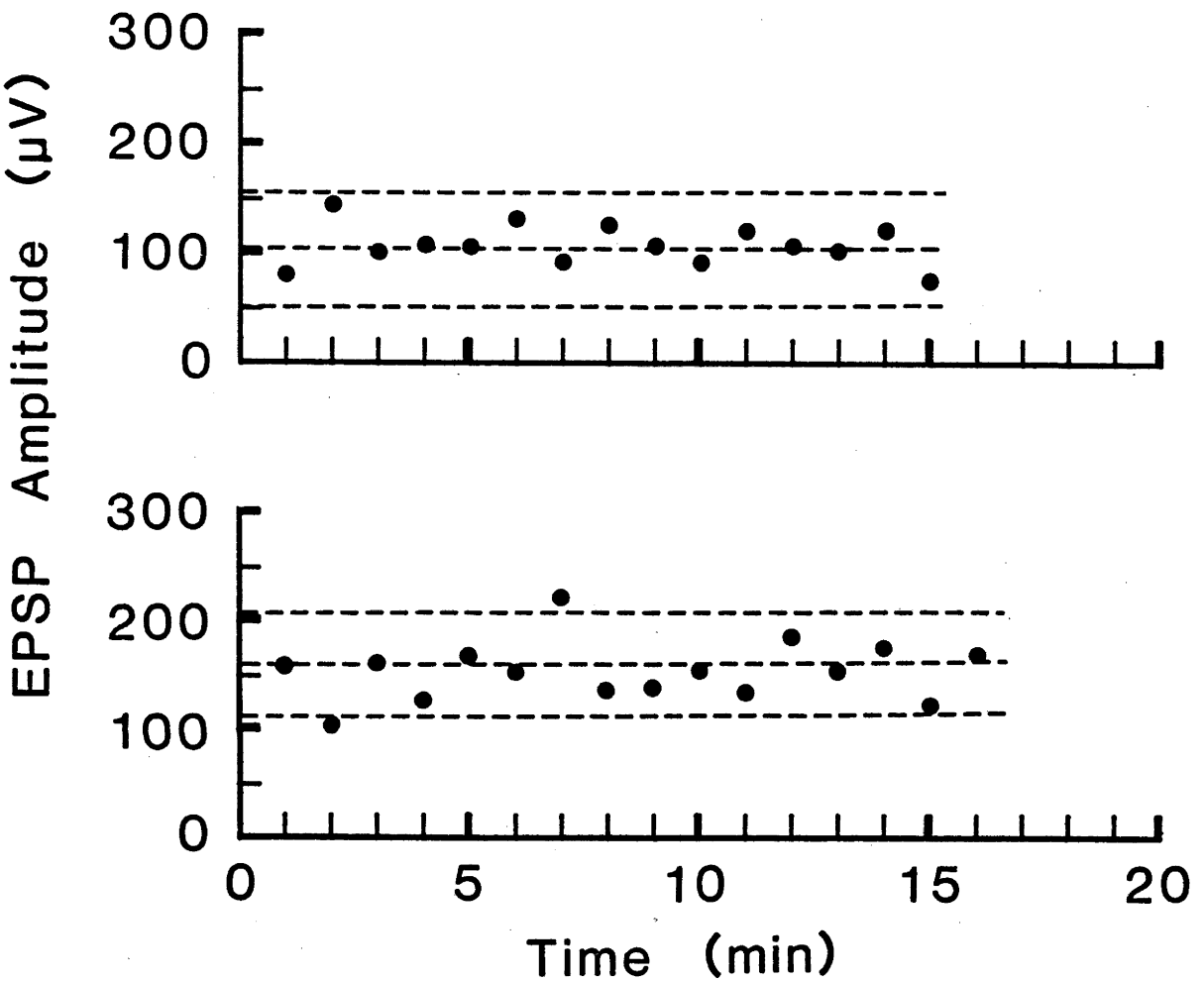
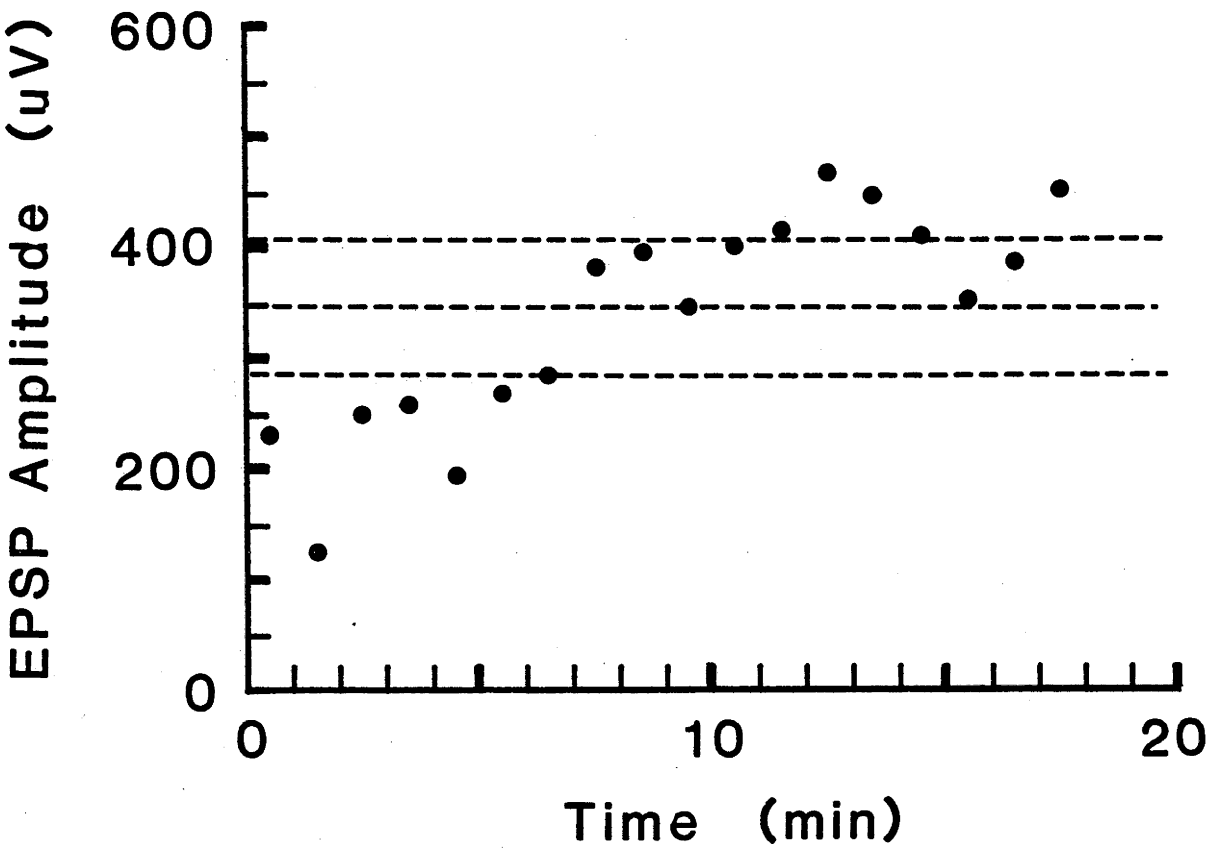

EPSP Amplitude (μV)
300
200
100
0
300
200
100
0
0
5
10
15
20
Time (min)

Figure 3.7. The minute-average for a unitary EPSP which increased in mean peak amplitude over a 10-15 min period. The outer dashed line indicates the 95% confidence interval, and the inner dashed line the mean peak amplitude, calculated from the whole sample of EPSPs in this recording.


EPSP Amplitude (uV)
600
400
200
0
0
10
20
Time (min)

3.3.6 The time courses of the unitary EPSPs

Fig. 3.8 shows a sample of six averaged unitary EPSPs, to illustrate a range of time courses and amplitudes. They are arranged in order of slow to fast rise times. The rise times and half-widths were measured for all 71 EPSPs, and these values are plotted in Fig. 3.9A. The average rise time was 3.93 ± 1.84 ms, with a range from 0.8 to 9.0 ms. The average half-width was 19.50 ± 7.96 ms, ranging from 3.7 to 43.0 ms. To ensure that these values had not been biased by encroachment of the capacitive coupling artifact onto the rising phases of the EPSPs, 11 EPSPs were selected which had a short segment of flat baseline immediately before rising phase. Examples of such EPSPs can been seen in Figs. 3.2G and 3.8D. The mean rise time and half-widths of this group (n=11) were then compared with those of the other 60 EPSPs. There was little difference between the groups; their mean rise times were 3.87 and 3.94 ms (n=11 and n=60 respectively) and their mean half-widths were 21.48 and 19.15 ms. These differences were not significant (p=0.90 for rise time and p=0.35 for half-width), and it was considered appropriate to combine the two data groups.

The linear fit to the log plot of the final decay of the EPSPs was judged to be adequate for 66 of the 71 EPSPs. In general the fits were very good; some examples are illustrated in Fig. 3.10. This figure shows a range of time courses, from slow to fast, and it indicates the regions over which the rise times, half-widths and time constants were calculated. The average time constant of decay for the 66 EPSPs was 22.6 ± 11.0 ms.

Figure 3.8. Six examples of averaged unitary EPSPs. They are arranged in order of slowest (**A**) to fastest (**F**) rise times. The number of individual records comprising each average was 579, 900, 1049, 1879, 581 and 673 for for **A-F** respectively. The capacitive coupling artifacts have been masked and the bars indicate the durations of the depolarizing current pulses in the CA3 neurones. The (time-adjusted) CA3 action potentials occurred close to the end of the depolarizing pulses.

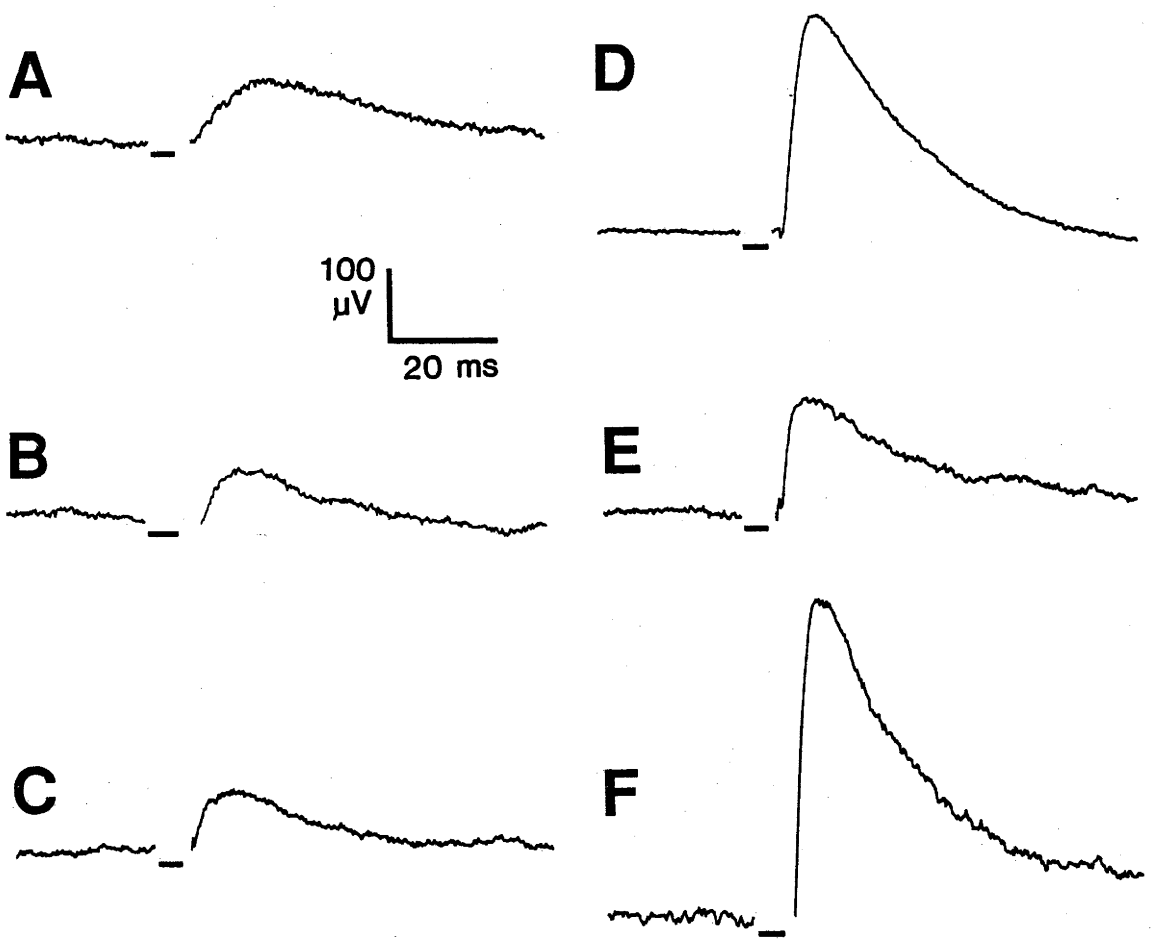
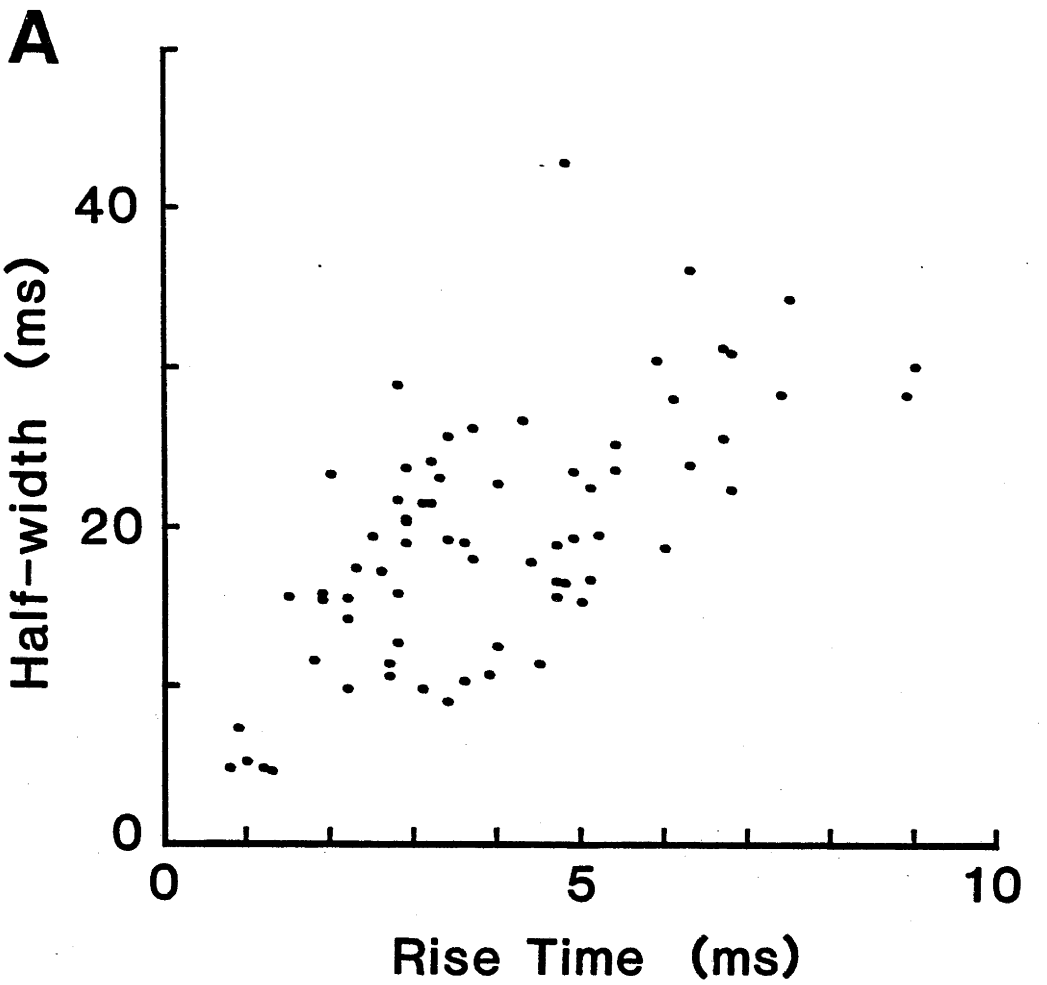

A
B
C
D
E
F
100
µV
20 ms

Figure 3.9. Scatter plots of the time course indicies for the unitary EPSPs. **A**, Raw half-widths and rise times. **B**, Half-widths and rise times normalized by the time constant of decay for each EPSP.


A
40
20
0
Half-width (ms)
0
5
10
Rise Time (ms)

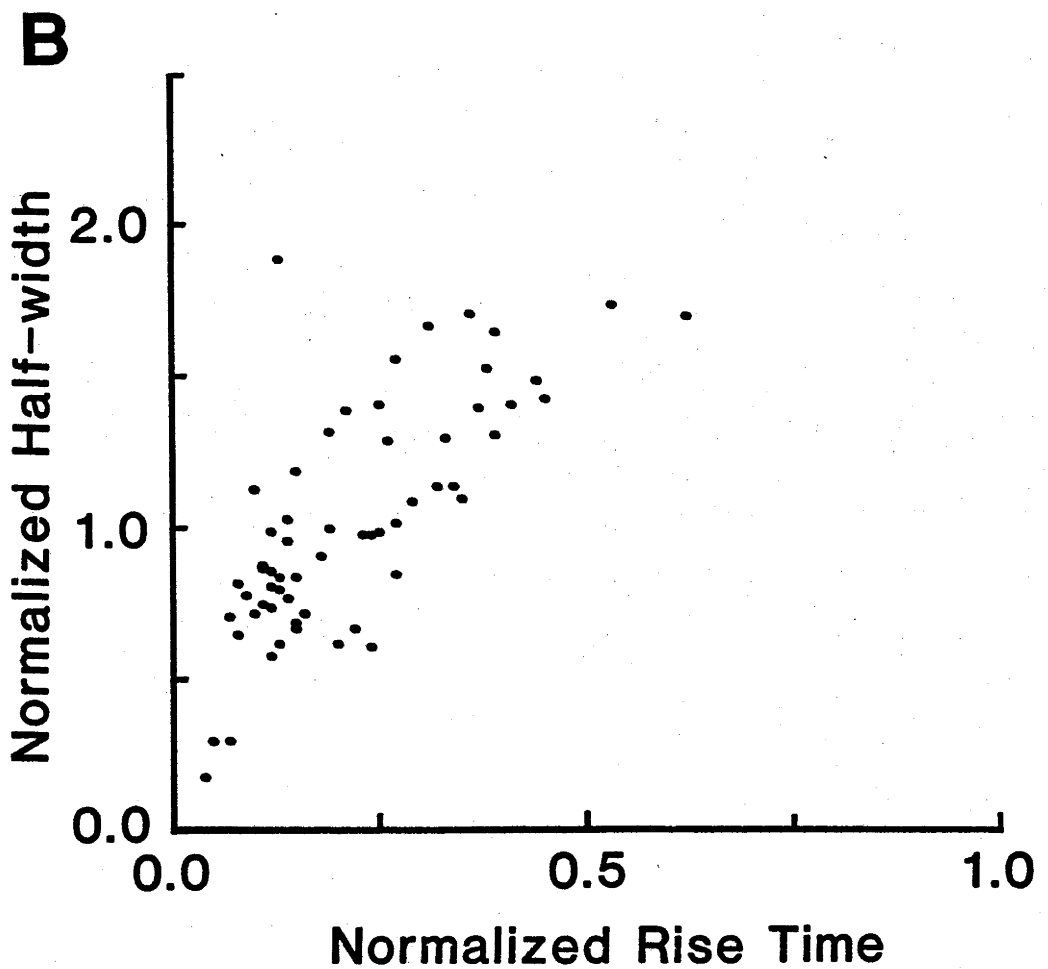

B
2.0
1.0
0.0
Normalized Half-width
0.0
0.5
1.0
Normalized Rise Time

Figure 3.10. Regions for measurement of time course parameters. The four EPSPs **A-D** illustrate a range of time courses, from slow to fast. The arrows on the rising phases indicate the points at 10% and 90% of the peak amplitude; the time difference between these is the rise time (RT). The filled circles indicate the points on the rising and decay phases which are at 50% of the peak amplitude. The time difference between these is the half-width (HW). **E-H**, corresponding log plots for EPSPs for EPSPs A-D. The vertical scale bar (100 μV) does not apply to these. The filled squares indicate the beginning and end of the log linear regions used for measurement of the time constant (T).

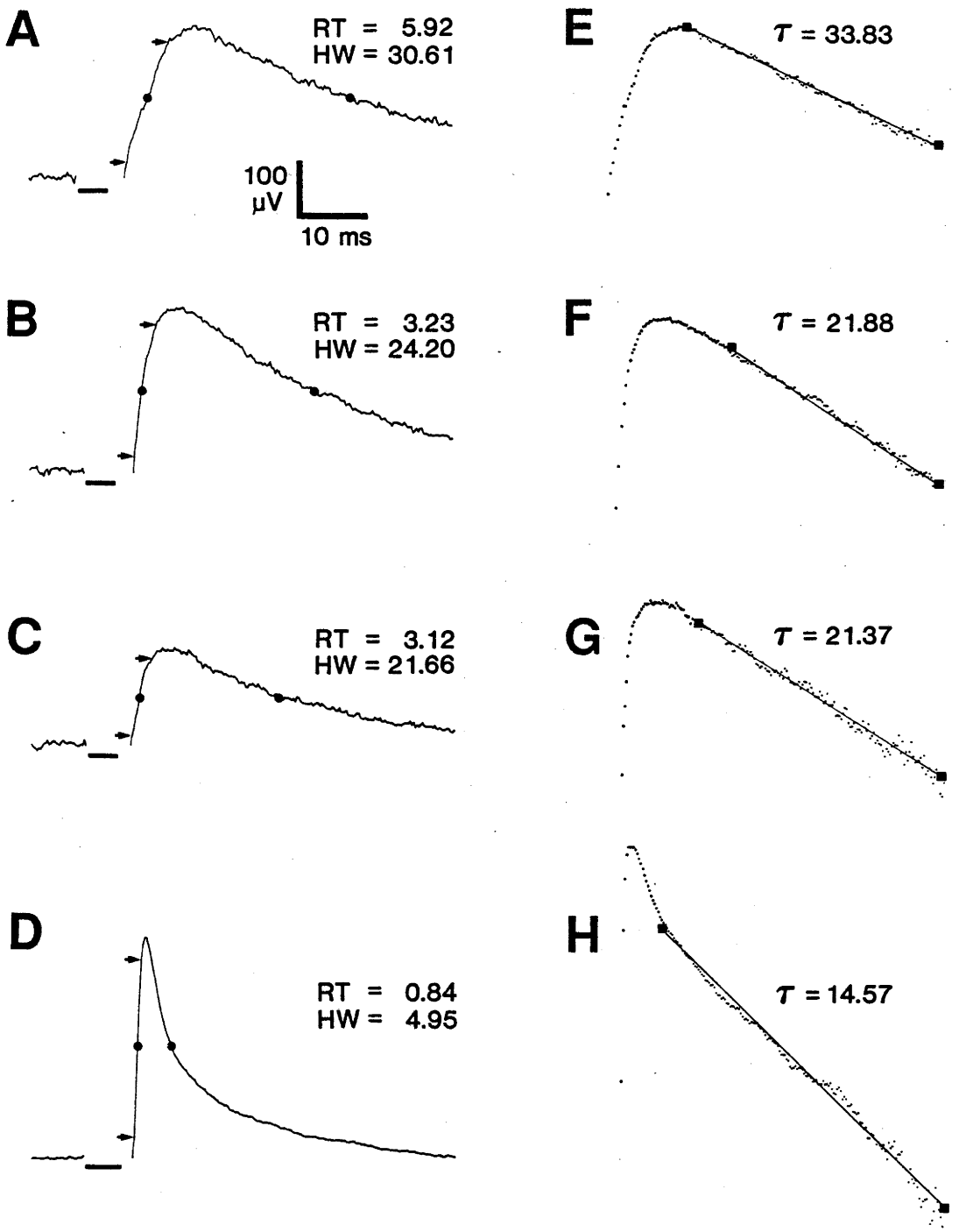

A
RT = 5.92
HW = 30.61
100
μV
10 ms
B
RT = 3.23
HW = 24.20
C
RT = 3.12
HW = 21.66
D
RT = 0.84
HW = 4.95
E
τ = 33.83
F
τ = 21.88
G
τ = 21.37
H
τ = 14.57

Fig. 3.9B shows the rise times plotted against the half-widths for the above 66 EPSPs, after both have been normalized by the time constant of decay for the EPSP (normalized shape-index plot, Jack et al, 1971). Most of the results are clustered between normalized rise times of 0.1 to 0.5 and normalized half-widths of 0.5 to 2.0.

3.3.7 Relationship between time course and amplitude

Mean EPSP amplitude has been plotted against normalized rise time in Fig. 3.11A. Note that small EPSP amplitudes are associated with the full range of normalized rise times, and that short rise times are associated with a wide range of EPSP amplitudes. However, there are no cases of longer rise times with large amplitude EPSPs.

The scatter of mean EPSP amplitude against normalized half-width is more widely spread (Fig. 3.11B), although there is a suggestion that the longest normalized half-widths are associated with only small amplitude EPSPs.

3.3.8 An atypical CA1 neurone

One CA1 neurone requires specific mention because it had some characteristics which distinguished it from the other CA1 cells. The most obvious of these was the short duration of its action potential, evoked either synaptically (Fig. 3.12B) or by intracellular current injection (Fig. 3.12C). At 1.2 ms (measured at the base), this action potential duration lies at the upper end of the range characterised for the non-pyramidal neurone type (0.5-1.2 ms, Schwartzkroin & Mathers, 1978). However, it did not have some of the other

Figure 3.11. Scatter plots of the mean peak amplitude of the unitary EPSPs versus normalized rise time (**A**) and versus normalized half-width (**B**).

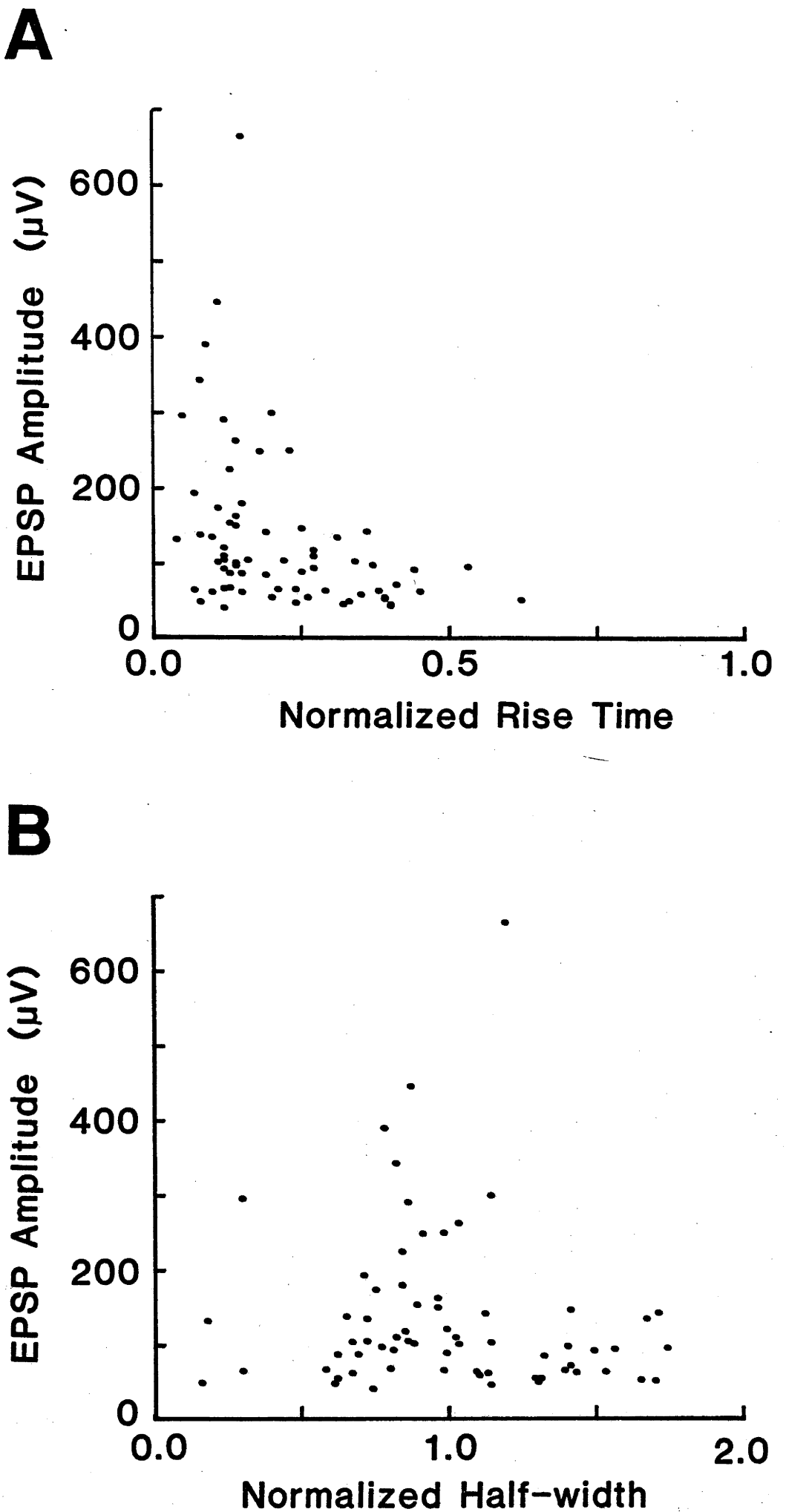
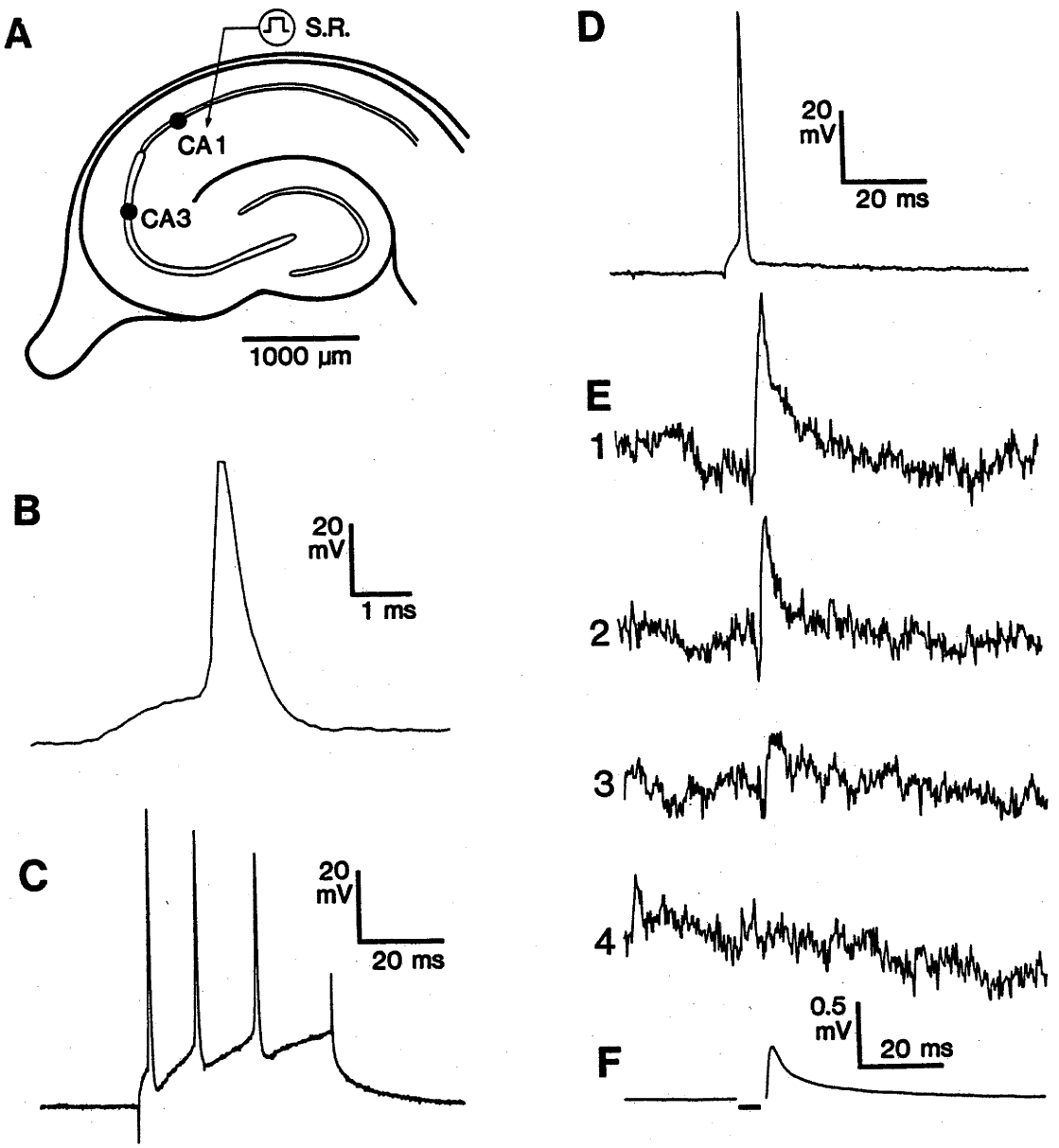

A
EPSP Amplitude (μV)
600
400
200
0
0.0
0.5
1.0
Normalized Rise Time
B
EPSP Amplitude (μV)
600
400
200
0
0.0
1.0
2.0
Normalized Half-width

Figure 3.12. Simultaneous recordings from a CA3 neurone and an atypical CA1 neurone. **A**, Approximate locations of the electrodes. S.R., stratum radiatum recording electrode. **B**, Action potential evoked in the CA1 cell by a 28 μA, 0.1 ms cathodal stimulus delivered through S.R. (the stimulus artifact is cut off to the left of the figure). **C**, Response of the CA1 neurone to a 2.6 nA, 45 ms depolarizing current pulse. **D**, Action potential evoked in the CA3 neurone by a short duration depolarizing current pulse. **E**, Examples of individual records from the CA1 neurone, showing the responses to activation of the CA3 neurone. **F**, average of 2953 CA1 records, after adjustment for latency variations of the CA3 action potential. The capacitive coupling artifact has been masked. The bar indicates the duration of the CA3 current pulse (4 ms).

This unitary EPSP is no. A12 analysed in Chapter 4.


A
S.R.
CA1
CA3
1000 µm
B
20
mV
1 ms
C
20
mV
20 ms
D
20
mV
20 ms
E
1
2
3
4
0.5
mV
20 ms
F

features expected for this kind of cell, such as a high spontaneous firing rate, large spike after-hyperpolarizations, and a high frequency non-decrementing spike train in response to a depolarizing current injection (Schwartzkroin & Mathers, 1978; Schwartzkroin & Kunkel, 1985).

Another distinctive feature of this neurone was the short time courses of the two unitary EPSPs which were obtained by activation of two different CA3 cells. Single records and an average for one of these EPSPs are shown in Fig. 3.12E and Fig. 3.12F respectively. The short time course, and the large amplitude of some of the individual responses, made them clearly visible above the baseline noise. This EPSP had the shortest rise time (0.8 ms) and half-width (5.0 ms) of all EPSPs analysed. The regions over which these parameters were measured are shown in Fig. 3.10D. The average for the other EPSP obtained in this CA1 cell is shown in Fig. 3.14A (these EPSPs will be referred to again in the section on convergent inputs). This EPSP also had a very short rise time (1.24 ms) and half-width (4.9 ms).

The exceptionally short time courses of the EPSPs were not simply due to a short time constant for the CA1 neurone, because when normalized, the parameters were still particularly small. On the plot of the normalized shape-indices (Fig. 3.9B), these two EPSPs are represented by the two filled circles closest to the origin of the axes.

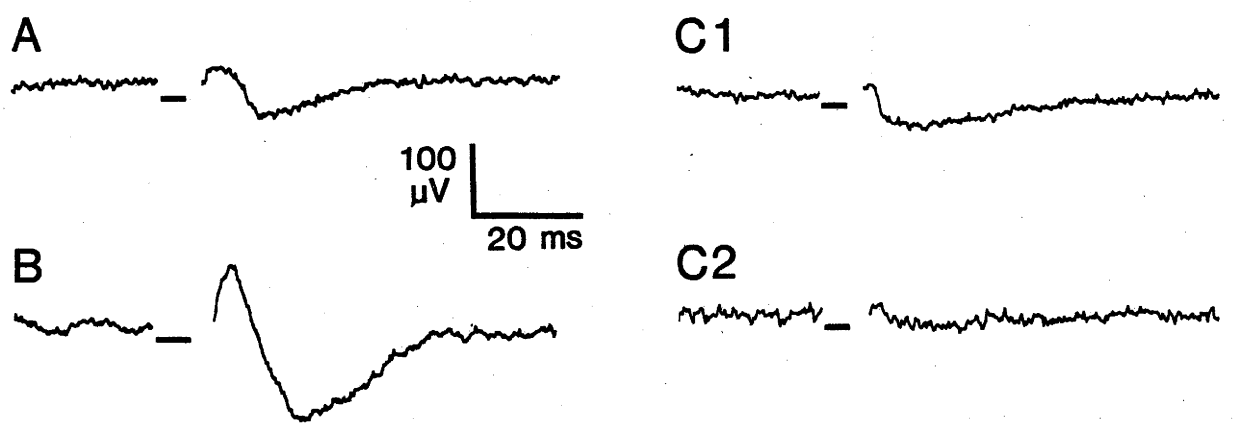
The log plots of the final decays for the two EPSPs in this CA1 neurone were both linear, but suprisingly, their time constants were quite different. For the EPSP in Fig.

3.10D (the same as Fig. 3.12F and Fig. 3.14B), the time constant of the final decay was 14.6 ms (Fig. 3.10H). This was close to the charging and decay time constants for the 100 ms hyperpolarizing pulse used to measure the input resistance of this neurone, which were 17.2 and 14.6 ms respectively. However, the decay time constant for the other EPSP (Fig. 3.14) was more prolonged, being 27.6 ms. This difference cannot be explained from the available data. There was no significant change in either the membrane potential or the input resistance in the time between recording the two EPSPs. It seems unlikely (but not impossible) that an EPSP prolonged by a slow underlying component from a distal synapse, or by regenerative currents, would still show a pure exponential decay.

3.3.9 Hyperpolarizing responses

On three occasions PSPs were seen which were predominantly hyperpolarizing (Fig. 3.13). In two cases the responses appeared to be biphasic (Fig. 3.13A and Fig. 3.13B); i.e. they consisted of a smaller depolarization followed shortly by a larger hyperpolarization. Latencies from the CA3 action potential to the time at which the hyperpolarizing phase reached 10% of its maximum, were 8.5, 9.8 and 5.7 ms for the PSPs in Fig. 3.13A, B and C1 respectively. The corresponding maximum hyperpolarizations, measured from the pre-stimulus baseline, were -40, -118 and -42 μV. The times taken for the PSPs to fall from 10% to 90% of their peak (negative) amplitudes were 4.7, 7.8 and 5.8 ms, and half-widths were 16.4, 29.5 and 27.9 ms for the

Figure 3.13. Averaged PSPs with hyperpolarizing components, evoked in CA1 neurones by activation of single CA3 cells. **A**, **B** and **C** are from three different CA3 neurones. **C1**, 0.6 nA and **C2**, 1.0 nA continuous hyperpolarizing current was applied through the CA1 intracellular electrode.


A
100
µV
20 ms
B
C1
C2

hyperpolarizations of Fig. 3.13A, B and C1 respectively. The duration of the hyperpolarization was about 30-35 ms in each case.

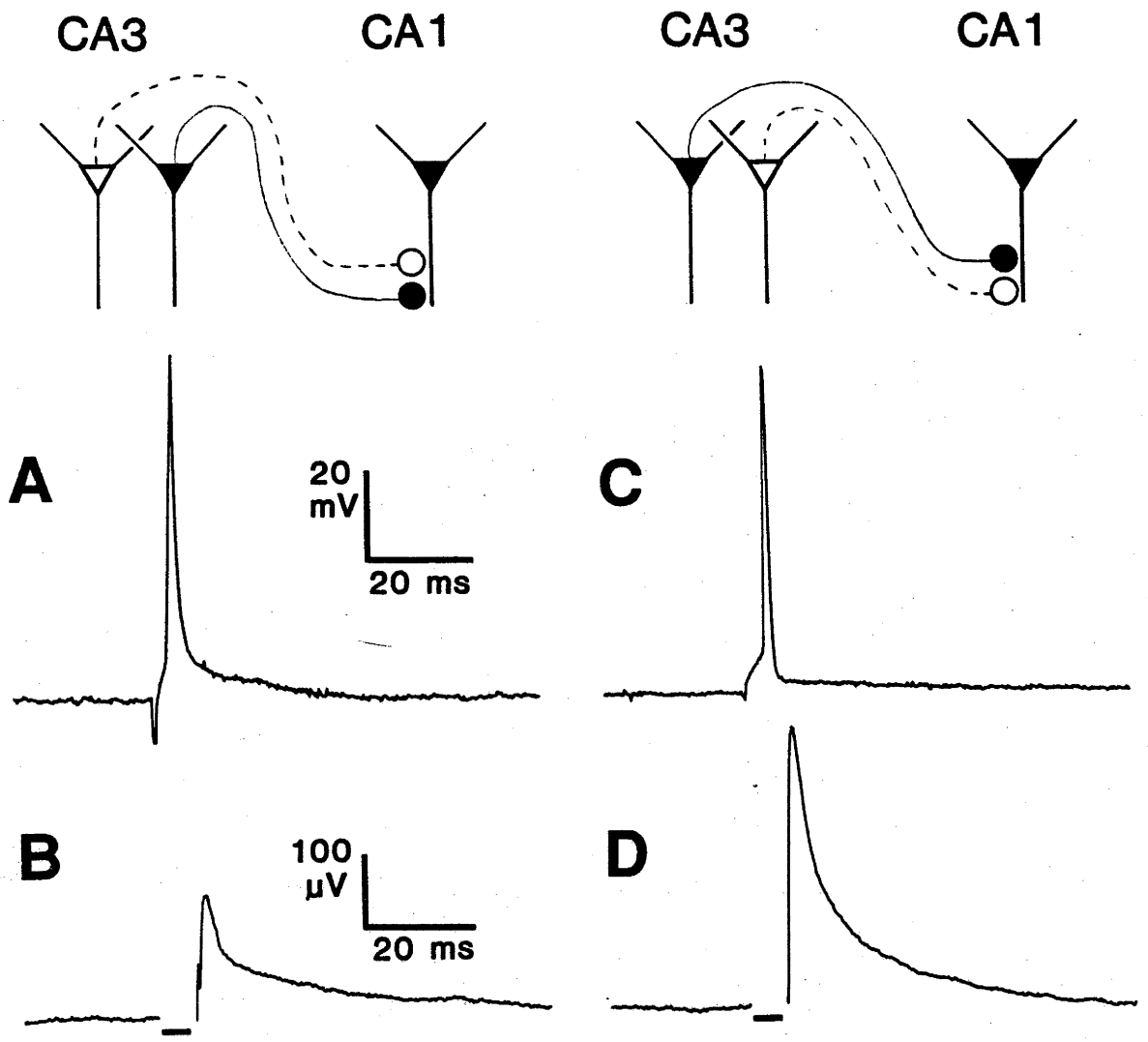
These CA3-CA1 recordings were unfortunately not held for long enough for a thorough examination of the hyperpolarizing PSPs. For one PSP, an average was obtained for two different levels of continuous hyperpolarizing current, 0.6 and 1.0 nA (Fig. 3.13, C1 and C2). The input resistance of this CA1 neurone was 12 MΩ, so the additional 0.4 nA would have hyperpolarized the cell by about 5 mV (assuming linear membrane properties over this membrane potential change). This voltage change was sufficient to greatly reduce the amplitude of the PSP, and would suggest that the membrane was brought close to the reversal potential for the synaptic current. The membrane potential with no current applied, measured shortly after these records were obtained and taking into account the offset on exit from the neurone, was -56 mV. Again assuming linear membrane properties, the steady hyperpolarizing current of 1.0 nA would have produced a membrane potential of -68 mV at the soma.

It was intended to add bicuculline methiodide to the ACSF to determine whether these hyperpolarizations were $GABA_A$-mediated IPSPs. However none of the simultaneous CA3-CA1 recordings were maintained long enough for this to be done.

3.3.10 Convergent inputs to CA1

In two experiments, a CA1 penetration was held long enough for two presynaptic CA3 cells to be found. Fig. 3.14

Figure 3.14. Convergent inputs to a single CA1 neurone. This CA1 cell was the atypical neurone described in section 3.3.8. **A** and **C** are examples of action potentials from the two presynaptic CA3 cells which were found for the CA1 neurone. **B** and **D** are the averaged EPSPs evoked by the two inputs. **C** and **D** are from the CA3-CA1 pair featured in Fig. 3.14.


CA3
CA1
CA3
CA1
A
20
mV
20 ms
C
B
100
µV
20 ms
D

shows CA3 action potentials and the averaged EPSPs from the CA1 neurone, for one of these examples. This CA1 cell is the one discussed above in section 3.3.8 ('atypical CA1 neurone') and some of the features of this cell were illustrated in Fig. 3.12. The two CA3 neurones involved were found in nearby tracks in CA3; the positions of both would be covered by the filled circle indicating the position of the CA3 cell in Fig. 3.12. The rise times for these EPSPs were different, but the half-widths were similar (actual values were given in section 3.3.6). The most marked difference between the two EPSPs was their peak amplitudes, which were 170 μV and 377 μV Fig. 3.14, B and D).

In the other example of convergent input to a CA1 neurone, the amplitudes of the two EPSPs were also quite different, being 446 μV and 193 μV (not illustrated). Their rise times were 2.5 ms and 1.5 ms, and their half-widths were 19.5 ms and 15.7 ms respectively. As for the other example of convergence, the two presynaptic cells were near each other in CA3. In contrast to the other example, the time constants of the final decay of the two EPSPs were almost identical, being 22.0 and 22.5 ms respectively.

3.3.11 Divergent outputs from CA3

It was a more common occurrence to find multiple postsynaptic CA1 neurones for a single CA3 cell, as CA3 neurones could often be held without deterioration for several hours. This happened on nine occasions; in seven experiments two postsynaptic CA1 neurones were found for

single CA3 cells, and in two experiments, three postsynaptic cells were found.

Fig. 3.15 shows where pairs of EPSPs from CA1 neurones with a common CA3 cell lie on the plot of normalized rise time versus EPSP amplitude. The inset illustrates two examples of these pairs. Note that for six of the nine sets of related EPSPs (with a common presynaptic cell), the mean peak amplitudes are similar for EPSPs within the set, even though their rise times are different.

One of the two instances of three postsynaptic neurons for a single CA3 cell is illustrated in Fig. 3.16. In this case the three postsynaptic responses are quite different in time course and amplitude. The PSP shown in Fig. 3.16E is one of those presented above in section 3.3.9 and Fig. 3.13B. For the other case of divergence to three neurons, the mean peak amplitudes of the three CA1 EPSPs were 135 μV, 67 μV and 110 μV. Corresponding rise times were 3.6 ms, 6.7 ms and 6.3 ms, while the half-widths were 19.1 ms, 31.4 ms and 24.0 ms respectively.

In general, the CA1 neurones postsynaptic to a common CA3 cell were found close to each other in the CA1 stratum pyramidale. Having found one connection in a given area, and therefore knowing that there was an axon collateral with terminals nearby, we tended to search for others in the vicinity.

Figure 3.15. Divergent outputs from CA3. On the scatter plot of mean peak amplitude versus normalized rise time, EPSPs with a common presynaptic CA3 neurone are joined by lines. In two cases, three unitary responses were found for a single CA3 cell. One of these is marked on the plot by the open triangles. In the other case, one of the CA1 responses had a hyperpolarizing component, so only the two EPSPs are indicated on the plot (open diamonds). The three postsynaptic responses for this example are shown in Fig. 3.16. **Inset**, Two examples of divergence. Each pair of averaged EPSPs had a common CA3 cell. Scale bars: 100 μV and 20 ms.

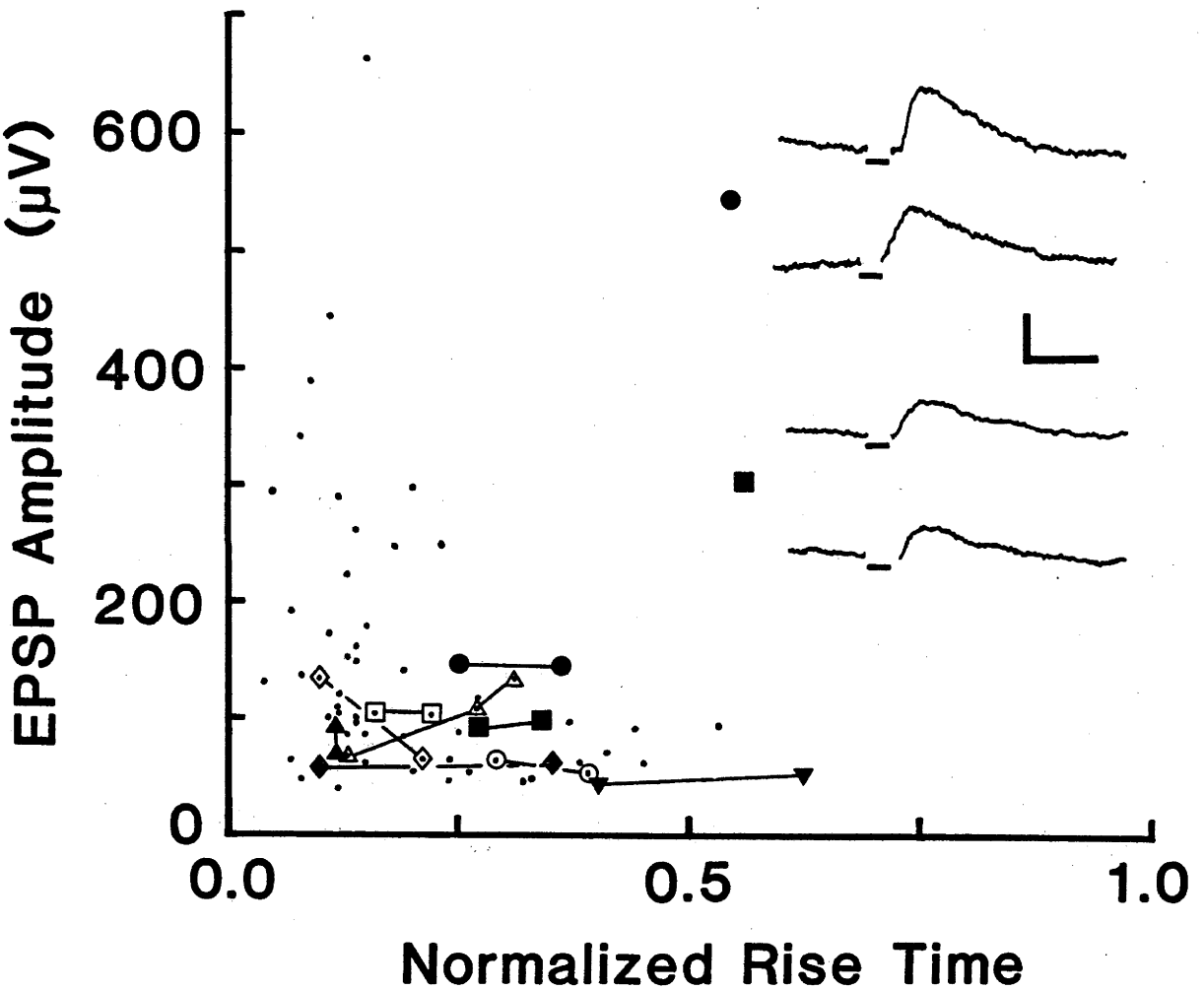
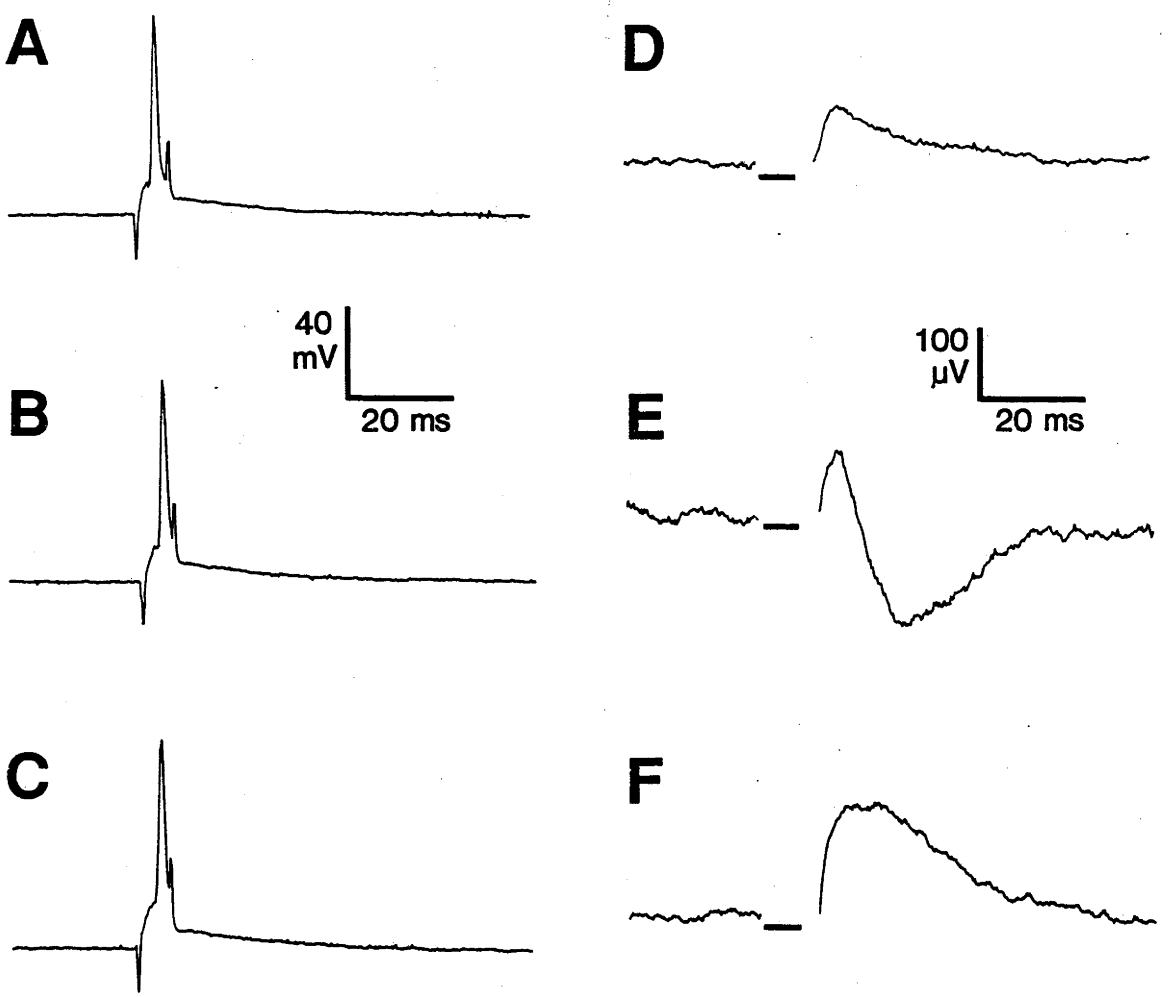

EPSP Amplitude (μV)
600
400
200
0
0.0
0.5
1.0
Normalized Rise Time

Figure 3.16. Divergence from a single CA3 neurone. **A**, **B** and **C**, Examples of action potentials associated with each of the postsynaptic responses. All three action potentials are from the same CA3 cell. **D**, **E** and **F**, Averaged responses from three different CA1 neurones, evoked by activation of the same CA3 cell. E corresponds to response B in Fig. 3.13.


A
B
C
40
mV
20 ms
D
E
F
100
µV
20 ms

3.4 DISCUSSION

3.4.1 The monosynaptic nature of the EPSPs

Throughout this chapter it has been assumed that the EPSPs evoked in CA1 neurones by activation of single CA3 neurones are monosynaptic, unitary EPSPs. It is worth questioning this assumption for a moment, because there are alternative interpretations. For example, monosynaptic excitatory connections have been found between CA3 pyramidal cells, in simultaneous intracellular recording experiments (MacVicar & Dudek, 1980; Miles & Wong, 1986). These reports indicated that these connections may occasionally have been powerful enough for a single presynaptic action potential to discharge the postsynaptic neurone, but were not specific about how often this occurred. If a strongly connected pair of CA3 cells such as this was involved in our experiment, and if the postsynaptic CA3 neuron projected to the neurone impaled in CA1, the connection observed between the first CA3 cell and the CA1 neurone would be disynaptic, rather than monosynaptic.

The strongest evidence that this did not occur for the EPSPs presented here, comes from the studies by Miles and Wong (1987a,b) of the polysynaptic connections between CA3 pyramidal cells which were revealed when inhibition was blocked by picrotoxin. The polysynaptic events within CA3 were evoked with latencies of at least 8 ms (Miles & Wong, 1987a), whereas the EPSPs in this study all had latencies of less than 5.8 ms. If the responses in CA1 were polysynaptic,

they would be expected to occur even later than those in CA3, due to a greater distance for action potential conduction.

It can also be argued that the monosynaptic excitatory connections between CA3 pyramidal cells are not likely to be sufficiently powerful to cause postsynaptic action potentials, when recurrent inhibition is functional. With inhibition intact, Miles and Wong (1987b) observed polysynaptic connections between CA3 pyramidal cells in only 5 out of 550 simultaneous recordings. These responses, which were evoked by current injections which generated a burst of action potentials in the (first) presynaptic cell, indicated that at least one intermediate CA3 cell was being discharged, and are therefore sensitive tests for the existence of powerful monosynaptic connections. Polysynaptic responses to single presynaptic action potentials should occur even less frequently, as the temporal summation of the postsynaptic responses caused by the burst firing (Miles & Wong, 1986) cannot occur. Even when latent polysynaptic pathways were revealed by blockade of inhibition (with picrotoxin), postsynaptic events were only rarely elicited by single action potentials (Miles & Wong, 1987a). These observations imply that when inhibition is intact, single CA3 action potentials are unlikely to activate other CA3 pyramidal cells, and just as this makes polysynaptic responses unlikely within CA3, it makes polysynaptic events unlikely to be transmitted to CA1.

The question may also arise as to whether recurrent excitatory pathways within CA1 could produce responses which might be mistakenly identified as monosynaptic. Although one

study which made simultaneous recordings from pairs of CA1 pyramidal cells failed to find excitatory interactions (Knowles & Schwartzkroin, 1981), a recent report of EPSPs evoked in CA1 neurons by local applications of glutamate (Christian & Dudek, 1988), suggests that they may exist. However, the EPSPs obtained in CA1 pyramidal cells in our study were all clearly subthreshold for action potential discharge, so we have no evidence for unitary inputs to CA1 pyramidal cells which would be powerful enough to activate recurrent excitatory circuits.

The possibility that the CA1 EPSPs were really synaptic field potentials, recorded through the cell membrane, can be excluded. Whenever possible, extracellular recordings were made immediately on exit from CA1 neurones in which EPSPs had been obtained, but there were no occasions when even a suggestion of a field potential was observed.

3.4.2 Conduction delays and latencies to onset of the CA1 EPSPs

In this study, the mean conduction velocity of the antidromic action potentials in the Schaffer collaterals was 1.0 ms^{-1}. The mean distance between the CA3 and CA1 recording sites was 1030 μm, which would imply an expected delay due to conduction of the action potential of about 1 ms (depending on the true distance to the site of the synaptic connection). The synaptic delay at the CA3-CA1 connection is unknown, but about 0.3 ms would be a reasonable assumption for mammalian CNS synapses (Eccles, 1964). Because the latency has been measured to the time the EPSP reaches 10% of

its peak amplitude, rather than its true onset, there must be some delay while the EPSP attains that amplitude. By analysing a subsample of EPSPs in which the capacitive coupling artifact was short enough to allow a short period of flat baseline before the rising phase, this delay has been estimated to be 0.25-0.75 ms (say mean 0.5 ms).

These factors account for an average delay of less than 2 ms, and yet the mean latency of the CA1 EPSPs was 3.4 ms. In case the mean latency had been overestimated due to contamination by the coupling artifact, the differences between the expected conduction time and the EPSP latency were calculated for a subsample of EPSPs (n=21). The EPSPs in this subsample had short coupling artifacts and measurements had been made of the distances between all three electrodes in the slice. A mean of 2.1 ± 1.1 ms was obtained for these differences in this group. This time includes synaptic delay and time taken for the EPSP to rise to 10% of its peak amplitude, and when these are subtracted, there is still an mean delay of just over 1 ms (range 0-3.5 ms) to be accounted for.

One cause of this delay might be the existence of fine terminal branches from the main Schaffer collaterals, with slower conduction velocities. In the rabbit, fine umyelinated axons (with *en passant* synaptic boutons) emerge from the nodes of Ranvier of large myelinated Schaffer collaterals in the stratum radiatum (Andersen, 1975). Although no equivalent study has been done for the rodent, there are likely to be similarities. The conduction velocities determined in our experiments (by antidromic

activation of CA3 neurones) may have predominantly measured the velocities in larger myelinated axons. In addition to the time taken for an orthodromic action potential to conduct along such an axon, there would be a variable delay for conduction along the finer branches before reaching the synapse(s). The duration of this delay would depend upon the conduction velocity of the terminal branch and upon the distance of the synapse(s) from the main axon. Clearly, further anatomical studies in the rodent are required before the feasibility of this scheme can be adequately assessed.

3.4.3 Amplitudes of the unitary EPSPs

This study is the first to directly measure the synaptic strength of a single CA3-CA1 connection. The only previous estimate of the CA1 unitary EPSP amplitude (Andersen, 1982) was, at 100 μV, ~~remarkably~~ reasonably close to our mean amplitude (131 μV). Andersen (1982, 1986) based his estimate on the proportion of intact fibres in the stratum radiatum required to discharge a CA1 pyramidal cell, and took into account factors such as the number of terminals per unit length of axon, the packing density of CA1 cells, and the approximate number of spines on the apical dendrites of CA1 pyramidal cells.

Note that our mean amplitudes are specific for the membrane potentials of the CA1 cells, which averaged -63 mV in this series. The voltage dependence of the EPSP amplitudes was not investigated in this study. They are also specific to the regular 2 Hz timing of the CA3 neurone activation. This rate of stimulation is too slow to expect the responses

to show frequency facilitation (Creager et al, 1980), but the effects of different rates were not explored here. Certainly the timing is artificial, and the effects of different patterns of CA3 neurone discharge will be discussed in Chapters 5 and 6.

The consequences of impalement of the CA1 neurones by the microelectrodes should also be considered. Because of the low yield of connected CA3-CA1 pairs, CA1 cells were not routinely discarded if their input resistances were below some arbitrary value. Although there was only a very weak correlation (0.34) between input resistance and EPSP amplitude, it can be seen from Fig. 3.5 that the larger EPSP amplitudes are less common for the lower input resistances (e.g. 8-15 mΩ). It is not clear to what extent the lower input resistances are due to natural differences in the neurones, or to greater damage from the microelectrode. It is conceivable that in their undisturbed state the CA1 neurones have a higher input resistance, and therefore a greater voltage response to the synaptic current. Future investigations using the whole-cell patch technique in slices ought to give useful information on this matter, as the tight seal formed by patch electrodes should reduce the somatic shunt caused by the imperfect seal of conventional microelectrodes.

It is interesting to compare the amplitudes of the CA3-CA1 EPSPs with other unitary EPSPs in the hippocampal formation. The recurrent excitatory connections within CA3, which presumably are collaterals of the same axons which project to CA1, are about one order of magnitude more

powerful than the CA3-CA1 EPSPs (in terms of somatic depolarization). Miles and Wong (1986), using simultaneous intracellular recordings from pairs of CA3 pyramidal cells, obtained monosynaptic EPSPs at the cell body with mean peak amplitudes of 1-2 mV (average 1.4 mV). There is no clear explanation for this dissimilarity to the CA3-CA1 projection. It may be that there are anatomical differences between the connections, perhaps in the number of synapses or release sites, or in the quantal currents. Alternatively there could be differences in the electrotonic parameters of the two kinds of pyramidal cell (CA1 and CA3) which influence the postsynaptic voltage change. The time courses of the two kinds of unitary EPSP will be compared in the next section.

The amplitude of unitary EPSPs in granule cells of the rat dentate gyrus has been estimated to be 100 μV, for input from the medial perforant path (McNaughton et al, 1981). This estimate was obtained by looking for the first plateaux on plots of mean EPSP amplitude versus stimulus voltage. These plateaux were believed to represent the responses to the first fibre recruited.

Presumed unitary responses have been obtained in CA3 pyramidal cells by iontophoretic ejection of excitatory amino acids onto dentate granule cells in the guinea pig hippocampal slice (Yamamoto, 1982; Higashima et al, 1986). This technique evoked trains of EPSPs in the CA3 cells, and the mean amplitude of the first EPSP in the train (presumptive unitary) was 2.5 ± 1.0 mV.

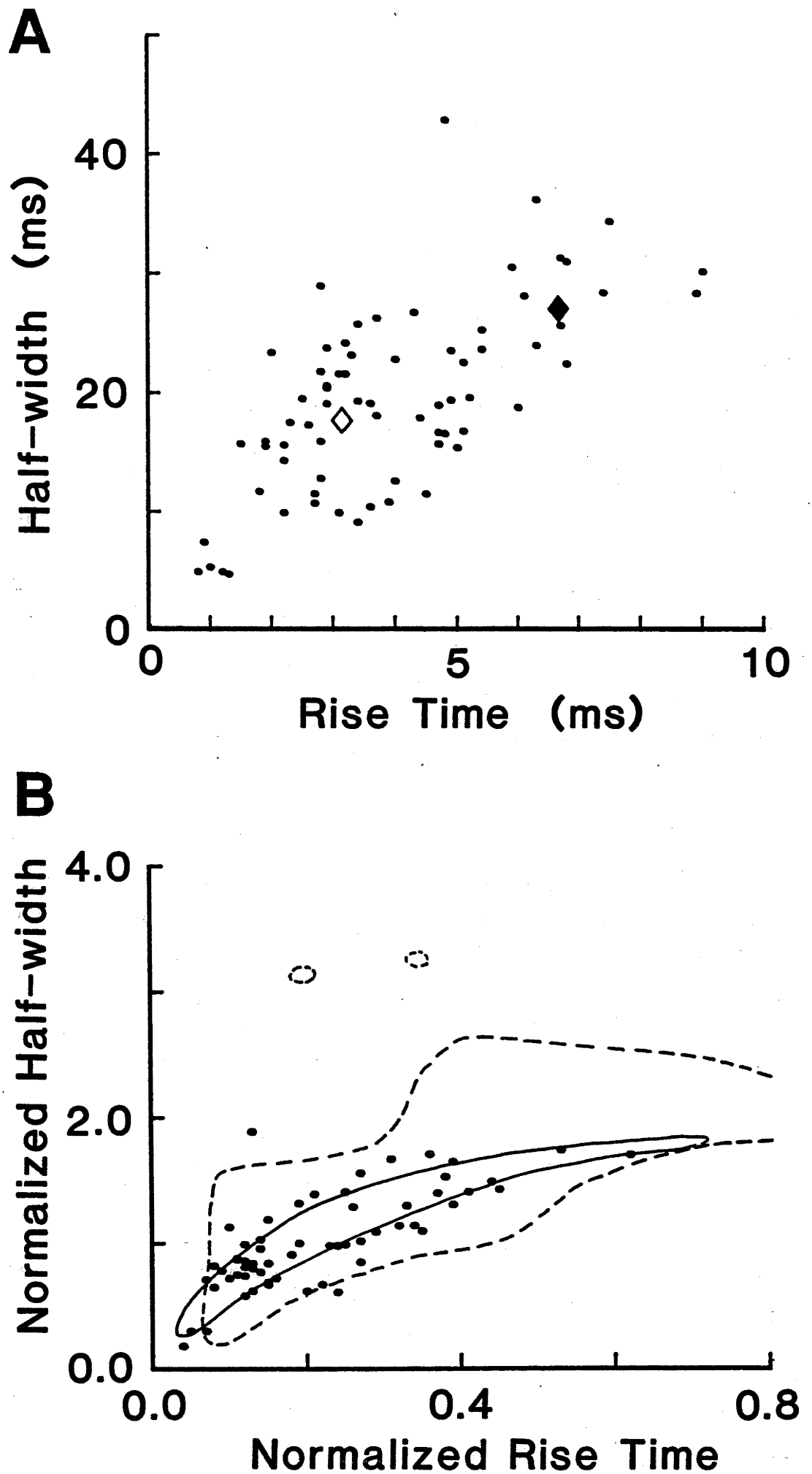
More similar in amplitude to the CA3-CA1 unitary EPSP is the single group Ia afferent EPSP in the cat motoneurone.

Kuno (1964) found that the smallest of the EPSPs obtainable by graded nerve stimulation were 100-250 μV in mean peak amplitude. The median value for peak amplitude obtained for 574 presumed single-fibre EPSPs in this system by Jack et al (1971) was 230 μV. This similarity to the CA3-CA1 unitary EPSP is perhaps surprising considering the extensive morphological differences between the motoneurone and the CA1 pyramidal cell. However, the time courses of the EPSPs are quite different for the two cell types (see below).

3.4.4 The time courses of the unitary EPSPs

Turner (1988) compared the time courses of minimal EPSPs evoked by proximal and distal stimuli to the stratum radiatum (mean peak amplitudes 470 μV and 400 μV respectively) . The mean rise time of the unitary EPSPs obtained in the present study (3.93 ms), lies between the mean rise times of 3.20 ms for proximal, and 6.66 ms for distal inputs obtained by Turner (1988). Similarly, the mean half-width of 19.5 ms for the unitary EPSPs was within the half-width values of 17.8 ms (proximal) and 27.2 ms (distal) obtained by Turner (1988). For comparison with our results, the mean time course values from Turner (1988) for proximal and distal EPSPs have been superimposed on the data for the unitary EPSPs in Fig. 3.17A. Note that the rise time and half-width parameters for the unitary EPSPs tend to cluster more around the mean point for the proximal minimal EPSPs (open diamond) than that for the distal minimal EPSPs (filled diamond). This suggests that the unitary EPSPs sampled in this study may have involved

Figure 3.17. Comparison of data from the present study with that of Turner (1988). **A**, The filled circles are the raw time course indicies for the unitary EPSPs (as in Fig. 3.9A). The diamonds are the mean values (n= 34) obtained by Turner (1988, Table 1) for minimal EPSPs evoked by proximal and distal stimulation to the stratum radiatum (open diamond, proximal; closed diamond, distal). **B**, The filled circles are the normalized time course indicies for the unitary EPSPs in the present study (as in Fig. 3.9B). Envelopes have been drawn around the results of Turner (1988, Fig 7A,B); the interrupted lines surround his results for the minimal EPSPs (including two outlying points above), and the solid line encloses the results from his model of single spine inputs.


A
Half-width (ms)
40
20
0
0
5
10
Rise Time (ms)
B
Normalized Half-width
4.0
2.0
0.0
0.0
0.4
0.8
Normalized Rise Time

proximal synaptic connections more frequently than distal ones.

This impression is confirmed when the plot of normalized rise time versus normalized half-width for the unitary EPSPs is compared to the corresponding plot for the minimal EPSPs (Turner, 1988). In Fig. 3.17B, the field occupied by the data for the minimal EPSPs (interrupted lines; constructed from Turner, 1988, Fig. 7B) has been superimposed on the values for the unitary EPSPs obtained in the present study (filled circles; re-scaled plot of Fig. 3.9B). The two groups of data occupy similar fields, especially for normalized rise times of less than 0.5 and normalized half-widths of less than 2.0. However, Turner (1988) had more EPSPs with longer normalized time courses, which were all evoked by distal stratum radiatum stimuli.

The shape-index plot for the unitary EPSPs also differs from that of the minimal EPSPs in being less scattered in the vertical (half-width) axis (Fig. 3.17B). In this sense it is closer to the theoretically-predicted plot for single dendritic synapses (Turner, 1988), based on cable models of horseradish peroxidase-stained CA1 pyramidal cells (Turner, 1984a,b). The field occupied by the theoretically-predicted plot is indicated by the solid lines in Fig. 3.17B. As Turner (1988) suggests, the scatter of the shape indices for the minimal EPSPs may occur because the EPSPs are composed of synapses which terminate on different regions of the dendrites. There may also be differences in the arrival time of the action potentials at the different synapses. The composite time course characteristics of these EPSPs would

therefore be less uniform than in the modelling situation. Although it is not known how many synapses are involved in single CA3-CA1 connections, there must have been fewer on average for the unitary EPSPs (mean peak amplitude 131 μV), than for the minimal EPSPs (mean peak amplitude 470 μV for proximal inputs, 400 μV for distal inputs; Turner,1988). This difference is therefore consistent with the smaller degree of scatter in the shape index plot for the unitary EPSPs when compared to the minimal EPSPs.

Time course data for larger EPSPs in CA1 pyramidal cells are scarce, but Andersen et al (1980a) reported 10-90% rise times of about 4 ms for EPSPs of approximately 5 mV peak amplitude. In a more recent report, Andersen et al (1987c) gave mean rise times of 1.65-2.10 ms for 10-14 mV EPSPs. They attributed the shorter rise time to both a more synchronised afferent volley, as the stimulating electrodes were closer to the dendrites, and a slightly higher tissue temperature.

The unitary EPSPs obtained in simultaneous intracellular recordings from CA3 cells (Miles & Wong, 1986) had normalized rise times of 0.3-0.5, and normalized half-widths of 1.0-1.5. Note that the rise time in this case was the time to peak, not the 10-90% rise time. These are within the range of values obtained here for CA3-CA1 unitary EPSPs. The synaptic location of recurrent excitatory inputs to CA3 pyramidal cells is not known.

Minimal Ia EPSPs in motoneurones have a much more rapid time course than the CA1 EPSPs; most have rise times less than 2 ms and half-widths less than 10 ms (Jack et al, 1971).

Nevertheless, when normalized by the time constant, there is overlap with the shape indices for CA1 unitary EPSPs. The slowest (normalized) Ia EPSPs have normalized rise times of 0.25-0.4 and normalized half-widths of 1.0-1.5, which is within the range for CA1 EPSPs. However, the Ia EPSPs fall more predominantly in the faster rise times (<0.2) and half-widths (<1.0).

The possibility that the time courses of some EPSPs could have been contaminated by IPSPs will be considered in the following section. Except for the three cases of PSPs which were predominantly hyperpolarizing, no hyperpolarizations were seen to be associated with the CA1 unitary EPSPs. Specifically, the 'undershoots' observed to follow Ia EPSPs (Ito & Oshima, 1965; Jack et al, 1971) and unitary recurrent EPSPs in CA3 (Miles & Wong, 1986), were never seen in the CA1 EPSPs.

The relationship between the normalized rise time and the peak amplitude of the unitary CA1 EPSPs was shown in Fig. 3.11A. The shape of this scatter plot is interesting because the EPSPs with the longer rise times, and therefore presumably the more remote dendritic origins, also have on average smaller peak amplitudes. This agrees with the cable model predictions for dendritic synapses, which describe how time courses are prolonged and EPSP amplitudes attenuated, for increasing electrotonic distances from the soma (Rall, 1967; Redman, 1973). Note however that short rise times are associated not just with large EPSP amplitudes, but with the full range of amplitudes. Assuming that similar rise times are a reliable indication of a similar electrotonic distance

from the synapse(s) to the soma, this implies differences in the number of active release sites, in the probablities of transmitter release, or in the amplitudes of the quantal EPSPs at those release sites.

If these factors were the causes of variability in mean EPSP amplitude for the EPSPs with short rise times, they might also be expected to occur for the more distal synapses. It may be that a range of different amplitudes does occur for distal synapses, but that the largest distal responses are small compared to the largest proximal ones, and the smallest may not have been discriminated above the noise. As mentioned above, responses of less than 20 μV may have been missed on averaging 100-200 records.

There was a suggestion of a similar relationship, although less clear, between the normalized half-widths and the amplitudes of the unitary EPSPs (Fig. 3.11B). The longest half-widths (i.e. 1.5-1.75) were associated with a smaller range of peak amplitudes than those of about 1.0. However, as discussed above, the half-width is a less reliable indicator of dendritic location when more than one synaptic contact is involved. In addition, the half-width can be prolonged out of proportion to the dendritic location of the synapse(s) if it is near the termination of a dendritic branch (Jack & Redman, 1971).

Note that the above points assume passive properties for the dendritic membrane, and that the interpretation of these results would be complicated by the activation of voltage-dependent conductances. Although there is evidence for regenerative processes in the dendrites of CA1 neurones (see

section 1.6), it is at present unknown whether the change in membrane potential associated with a unitary EPSP, at its dendritic or spine origin, would be sufficient to activate them. This question is raised again in the discussion for Chapter Five.

3.4.5 Hyperpolarizing PSPs

Although IPSPs are commonly associated with small EPSPs (500 μV or less) elicited by stratum radiatum stimuli (Turner, 1985, 1988), it was a surprise to find what appeared to be IPSPs or EPSP/IPSP sequences in CA1 cells, on activation of single CA3 neurones. It seems unlikely that these could be mediated by recurrent inhibitory circuits (Andersen et al, 1963, 1964a,b; Knowles & Schwartzkroin, 1981), because the unitary EPSPs seen in this study were far too small to cause CA1 pyramidal cell discharge. A more feasible mechanism would be via feedforward inhibition (Buzaki & Eidelberg, 1982; Alger & Nicoll, 1982a; Ashwood et al, 1984). This would require discharge of an inhibitory interneuron in CA1 by a single afferent from CA3. There is no information from this study which would confirm this possibility, as we have not recorded unitary EPSPs in CA1 interneurones. However the EPSPs evoked in interneurones by activation of single pyramidal cells (both in CA1) have been recorded in other dual-intracellular experiments (Knowles & Schwartzkroin, 1981; Lacaille et al, 1987), and they were sufficiently large to discharge the interneurone in some cases. The latencies to the hyperpolarizing phases of the PSPs in the present study, at 5.7-9.8 ms, were longer than

those for the unitary EPSPs (mean 3.4 ms) and would be consistent with a disynaptic connection from CA3.

Two of the responses appeared to have an early depolarizing phase (Fig. 3.12, A & B). These could be explained by the coexistence of monosynaptic excitatory connections from CA3, with the disynaptic inhibitory inputs. The question then needs to be asked whether the other responses obtained in this study, initially assumed to be purely excitatory, could have also been contaminated by IPSPs. Inhibitory potentials might have gone unnoticed if they had similar time courses to the EPSPs, or if they were very small. This would be most likely if the membrane potential was near to the IPSP equilibrium potential, which is about -70 mV for the recurrent IPSP in CA1 pyramidal cells (Alger & Nicholl, 1982b). The clearest answer would be provided by comparing the PSP waveforms at different membrane potentials. Injection of steady depolarizing current should reveal IPSPs, provided they are generated close enough to the soma. This was not done in the present study, because the first priority was to use the limited time (while simultaneous recordings were held) for the plasticity experiments (Chapter Five).

It can be argued that IPSPs were unlikely to be commonly present with the EPSPs, because they were so rarely seen alone. Interneurones account for only a small proportion of CA1 neurones (0.5-2%; Schwartzkroin & Mathers, 1978) but their efferents are highly divergent (Knowles & Schwartzkroin, 1981; Schwartzkroin & Kunkel, 1985; Lacaille et al, 1987). CA3 neurones were often held for long periods

while testing many CA1 cells in a localised region. If a CA3 cell was causing discharge of an inhibitory interneuron, pure IPSPs ought to be seen in some of the CA1 impalements, near impalements in which EPSPs were seen. However, clear IPSPs (or EPSP/IPSP sequences) were only seen in three out of 1178 paired recordings. Probably the two requirements for the disynaptic IPSP, namely (1) a synaptic connection between the impaled CA3 pyramidal cell and a CA1 inhibitory interneurone in that slice, and (2) for that connection to be powerful enough to cause discharge of the interneurone following a single presynaptic action potential, were both satisfied only rarely.

Unfortunately, the above interpretation gains little support from the one example of divergence which included a hyperpolarizing PSP (Fig. 3.16). In that case there were no obvious signs of IPSPs on the other responses (Fig. 3.16, D & F). The same CA3 neurone was subsequently tested with other CA1 cells in the same region, but there were no further signs of any IPSPs. For the other hyperpolarizing PSPs (Fig. 3.12, A & C), the CA3 impalements were not held long enough to be tested with other CA1 neurones.

3.4.6 Convergent and divergent connections

The two examples of convergence to single CA1 neurones illustrated how inputs from CA3 vary in synaptic strength. Obviously, a large number of factors could combine to create these disparities, ranging from presynaptic (number of synapses in the connection, number and area of release sites per connection, transmitter content and release probabilities

of the vesicles) to postsynaptic (area/density of the postsynaptic receptors, differences in spine and local dendritic geometry, electrotonic distance from the synaptic site to the soma). These cannot be distinguished in this kind of study, but some information may eventually be gained by simultaneous pre- and postsynaptic staining experiments along the lines of Korn et al (1981, inhibitory interneurone to the goldfish Mauthner cell) or Redman & Walmsley (1983a,b; Ia afferents to the motoneurone).

An interesting feature of the divergent examples was that some CA3 efferents evoked EPSPs of similar amplitude in different CA1 neurones, even though the time courses of those EPSPs were different. These were shown in Fig. 3.15 as the nearly-horizontal lines, and two examples were given in the inset for Fig. 3.15. It is tempting to speculate that individual Schaffer collaterals might be able to regulate the strength of their connections to compensate for their dendritic locations. However, the sample size is small, and there are counter-examples in which the amplitudes of the PSPs evoked by a single CA3 cell are quite different (see Fig. 3.16), so it would be premature to attach much significance to this finding. Furthermore, the overall shapes of the mean amplitude versus time course plots (Fig. 3.11) suggest that for the whole group of EPSPs (in different CA1 cells), there is at least an upper constraint on the amplitude of EPSPs related to their electrotonic distance from the soma.

Chapter Four:
AN ANALYSIS OF THE FLUCTUATIONS IN AMPLITUDE OF UNITARY EPSPS AND SMALL COMPOUND EPSPS EVOKED IN CA1 NEURONES

4.1 INTRODUCTION

This chapter concerns one of the most basic functional details of synaptic transmission, the trial-to-trial variability in the evoked postsynaptic potentials. The successful application of quantal analysis to the amplitude variations of EPSPs in CA1 neurones would be particularly useful, because the measurement of quantal parameters would be expected to give clues to the mechanisms underlying synaptic plasticity. However, the technical difficulties involved are daunting and have so far precluded satisfactory analysis. In comparison with the neuromuscular junction, quantal analysis at the CA3-CA1 synapse is made more difficult by:

(a) the higher level of intracellular recording noise, due to both the fine electrodes needed for stable penetrations and a high level of spontaneous synaptic activity,

(b) the spontaneous events cannot be used to determine quantal size because they arise from widely spread dendritic

locations, and furthermore they are generally obscured by the noise,

(c) there has been no easy means to activate single afferents; the afferents to any given pyramidal cell are diffusely spread through the apical and basal dendritic zones and are too fine to be penetrated intra-axonally, while conventional extracellular stimulation of the axons is likely to be near threshold for several fibres, so introducing another source of EPSP variability,

(d) the quantal components of the EPSPs cannot be directly observed, so statistical procedures for determining quantal parameters must be used. These methods have been successfully applied to other preparations, but they are all to some extent model-dependent and there is no *a priori* means of determining their applicability to the CA3-CA1 synapse.

Although no single protocol has been found to eliminate all of these problems, two kinds of experiment were undertaken in this study, each having particular advantages. The first used simultaneous recordings from CA3 and CA1 neurones, as decribed in the previous chapters. This achieved reliable presynaptic activation, and eliminated two concerns inherent with extracellular stimulation - that more than one afferent might be activated and that some fraction of the variability in the response might be produced by the afferent fibres being activated intermittently. The second experimental protocol used low intensity extracellular stimulation of the afferent fibres in the stratum radiatum to evoke small EPSPs of comparable amplitude to the unitary

EPSPs. This method had the advantage of lower noise levels on most occasions, since a larger number of CA1 cells could be sampled to find those with lowest intracellular noise. In addition, the smaller stimulus artefact with this protocol allowed more favourable selection of amplitude measurement regions (see below), and this also reduced contamination of the EPSPs by noise.

The first questions under consideration in this chapter are whether these synapses show probabilistic behaviour (variability from trial to trial), and at the same time, whether any of the EPSPs can be shown not to fluctuate. Two methods for quantal analysis are then applied to the noise-contaminated EPSPs, (1) the method of variance, which assumes Poisson statistics and (2) the unconstrained noise deconvolution method, which has been developed for EPSPs in spinal motoneurones. The latter method has the advantage that it does not impose any overall probability distribution upon the amplitudes of the evoked EPSPs. It does require two assumptions, that variance in quantal size is negligible compared with the noise variance and that the processes generating the intracellular noise are statistically independent of the processes causing fluctuations in the evoked EPSP.

4.2 METHODS

4.2.1 Simultaneous CA3-CA1 intracellular recordings

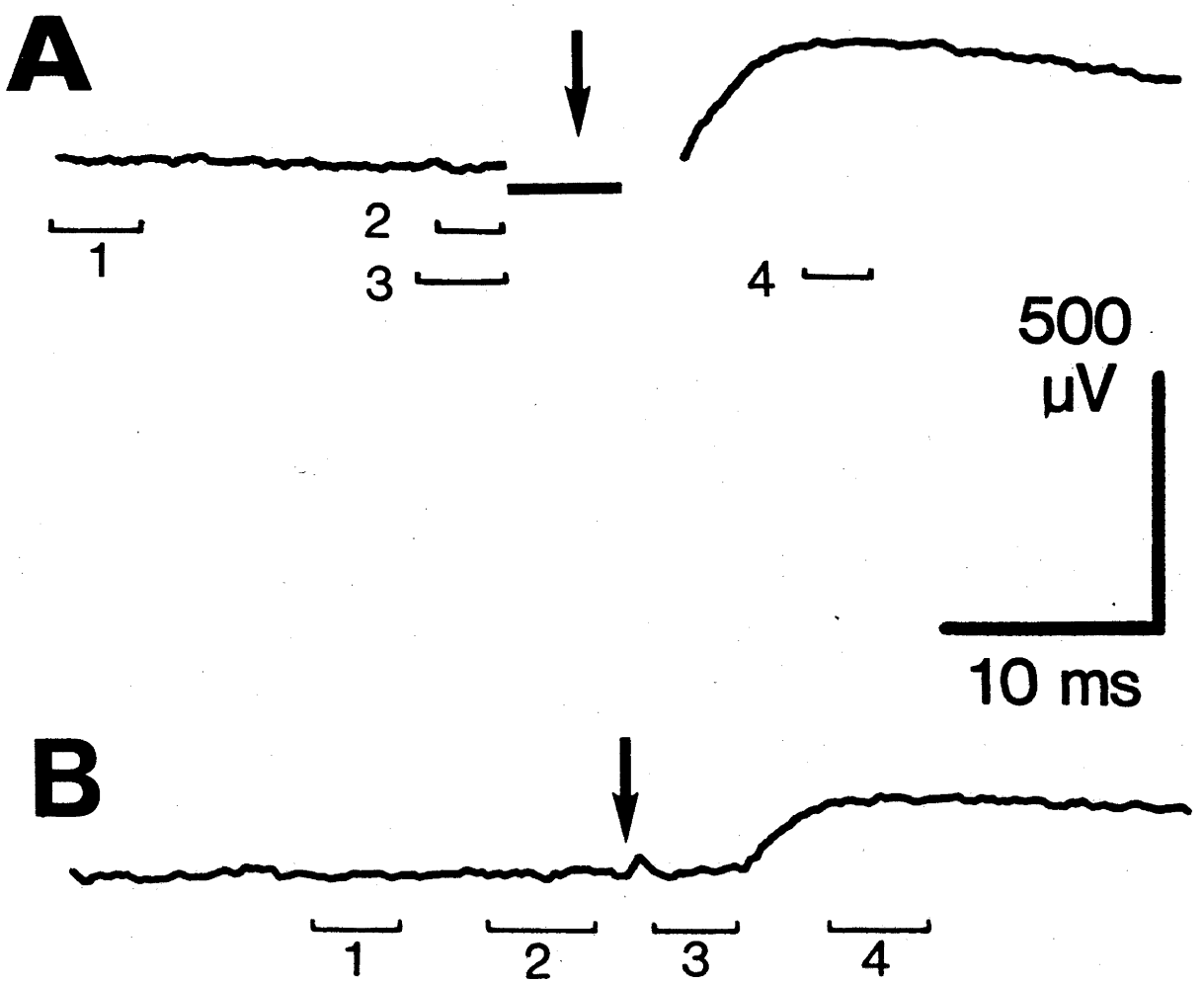
Hippocampal slices were prepared and maintained as described in Chapter 2. The 12 unitary EPSPs analysed in

this chapter are referred to as group 'A' EPSPs (numbered A1-A12), to avoid confusion with the other EPSPs used for fluctuation analysis. The presynaptic cells were activated at 2 Hz by 3-5 ms depolarizing current pulses (0.5 - 5.0 nA) and both pre- and postsynaptic records were digitised at 4 kHz and saved on disk. More than 2000 trials were obtained for each of the EPSPs included in this analysis, and records were only used from periods where there had been no drift in the mean EPSP amplitude (see below).

During the off-line analysis the time of the peak of the presynaptic (CA3) action potential was determined for each trial and was reassigned as t = 0 for that record (i.e. software "spike triggering"). Any failure to evoke an action potential was also detected and the corresponding postsynaptic record was then excluded from the analysis.

Fig. 4.1 shows how the regions were selected for measurement of EPSP and noise voltages. The individual records were averaged (Fig. 4.1A,B) and two regions were selected for the measurement of peak amplitude (regions 3 and 4). For the unitary EPSPs, the baseline region (3) immediately preceded the coupling artefact (blanked out in Fig. 4.1A) and a peak region (4) straddled the maximum of the EPSP. Region 4 was chosen such that throughout this period the amplitude of the averaged EPSP always exceeded 90% of its peak value. The duration of these regions was usually 3-4 ms. For each trial, the average voltages over regions 3 and 4 (V_3 and V_4) were calculated, and (V_4-V_3) was used to construct an amplitude histogram of the noise-contaminated EPSP. The same regions were used to measure the mean EPSP amplitude for

Figure 4.1. Examples of regions selected for measurement of noise amplitudes (1 and 2) and noise-contaminated EPSP amplitudes (3 and 4). **A**, averaged unitary EPSP (980 records). The bar indicates the duration of the depolarizing current pulse injected into the CA3 neurone, and the arrow indicates the time of the peak of the action potential. **B**, averaged small compound EPSP (1718 records). The arrow indicates the time of the stratum radiatum stimulus.


A
1
2
3
4
500
µV
10 ms
B
1
2
3
4

sequential sets of 100-120 records. These sequential mean amplitudes were plotted against time to check that no drift had occurred in the EPSP amplitude during recording.

Similarly, a histogram of the noise present during the recording was obtained by selecting regions before the coupling artifact (regions 1 and 2 in Fig. 4.1A,B) to have identical durations to regions 3 and 4 respectively, and to be separated by the same period as regions 3 and 4. The average voltages in regions 1 and 2 (V_1 and V_2) were calculated for each record, and (V_2-V_1) was used to construct the noise amplitude histogram.

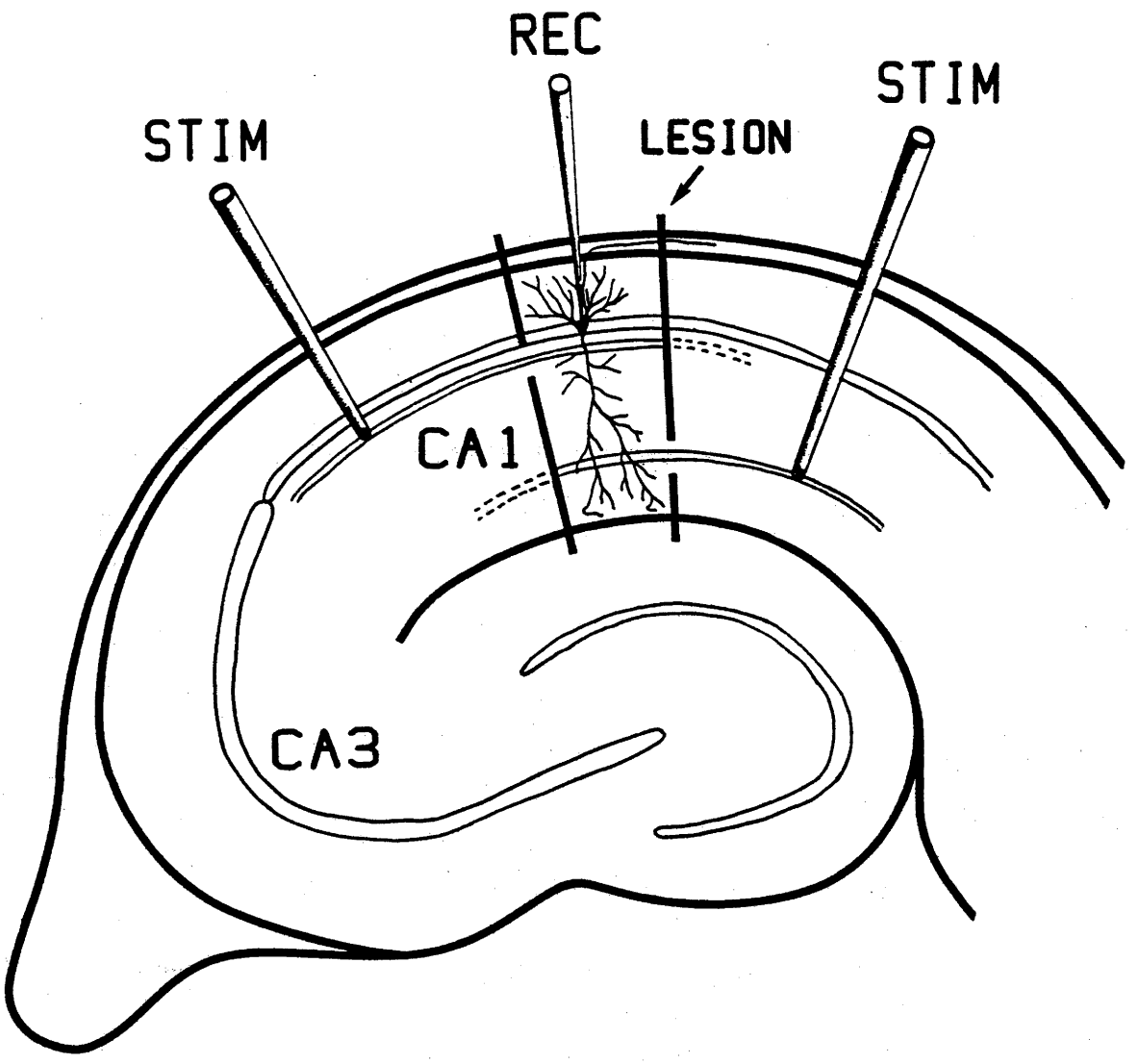
The program for making amplitude histograms from the voltage measurements was written by Clements (Ph.D. thesis, 1986). The range of measured amplitudes was divided into intervals of equal width (the bin size). A bin size of 20 μV was used for all of the histograms in this study. The program also incorporates a facility for smoothing the histograms. Each amplitude measure is represented by a triangular function centered on that amplitude, and a fraction of a count is added to each bin covered by any portion of the triangle. The smoothing used for the histograms analysed here was minor - the base of the smoothing triangle was never more than one bin width. The advantage of smoothing is that more information is conserved from the raw data. For example, an amplitude measure falling on the boundary between two bins has an equal fraction added to both bins, rather than adding a whole count to one bin and none to the other.

Special care was taken when lumping together records collected before and after the tetanic stimuli given during the LTP experiments (Chapter 5), even though the mean amplitude of the EPSPs did not change. It is conceivable that quantal size and release probabilities might change in opposition so that the mean amplitude remained constant. To ensure that this did not happen, histograms were made of the before and after records and then superimposed to ensure that their overall shapes were similar (they always were.) The records were then combined into a single histogram. The first few hundred records after a tetanus were routinely discarded to avoid the interval over which post-tetanic potentiation might be expected to occur.

4.2.2 EPSPs evoked in CA1 neurons by stimulation of stratum radiatum

Twenty-five EPSPs have been analysed in these experiments. The first ten, identified as group 'B', were obtained from five CA1 cells in slices in which cuts were made to restrict the Schaffer collateral/commissural input to regions of the stratum radiatum which were either proximal or distal with respect to the stratum pyramidale (Andersen et al, 1980a). The cuts were made with fragments of razor blade mounted so that a 50 μm bridge of tissue remained intact after the knife was lowered through the slice. Two cuts were made in each slice, leaving proximal and distal bridges in the stratum radiatum through which stimulated fibres passed before making contact with dendrites of the impaled pyramidal cell (Fig. 4.2). Distances from the stratum pyramidale were

Figure 4.2. Experimental protocol for EPSPs in group B. Pyramidal cells were impaled by the recording electrode (REC) in the stratum radiatum. EPSPs were evoked by stimulating electrodes (STIM) positioned to alternately excite fibres running distally and proximally (with respect to the stratum pyramidale) in the stratum radiatum. Synaptic input to the cells was restricted to the proximal and distal regions by cuts made across the slice (solid lines), leaving intact bridges of tissue 50 μm wide.


REC
STIM
STIM
LESION
CA1
CA3

<50 μm and 350-450 μm for the proximal and distal bridges respectively. This protocol was used because we were interested to compare the quantal size of EPSPs evoked at the two locations. However, note that some departure from strictly orthogonal connectivity could be caused by (a) Schaffer collaterals which do not run exactly parallel to the stratum pyramidale, or (b) connections made with dendritic branches extending laterally from the proximal apical dendrites. These factors would reduce the discreteness of the proximal and distal inputs.

One apparent advantage of the microsurgery was that obvious contamination of the EPSPs by IPSPs was only rarely seen, perhaps because the inhibitory interneurone collaterals in the strata pyramidale and oriens were cut. In non-lesioned slices, IPSPs can be evoked at very low stimulus intensities (unpublished observations, and Turner, 1988). However, the possibility of IPSP contamination could not be completely ruled out for these EPSPs. Bicuculline methiodide (1 μM, Sigma) was added to the ACSF to reduce $GABA_A$-mediated inhibition in some experiments (EPSPs B1, B2, B5 and B6).

The 15 EPSPs in group 'C' were obtained from 15 CA1 cells in slices which were not cut with the razor blades. The stimulating electrode was placed in mid stratum radiatum, towards the CA3 end of CA1, 840-1500 μm from a line extending from the recording site normal to the stratum pyramidale. These EPSPs were also among those obtained during the LTP experiments (Chapter 5). $GABA_A$-mediated inhibition was reduced in all of these experiments by the addition of 10 μM bicuculline methiodide to the ACSF. In order to eliminate

the propagation of spontaneous activity in the disinhibited CA3 region to the CA1 region (which would increase the intracellularly recorded noise), the CA3 region was trimmed from the slices with a scalpel blade before they were put into the recording chamber.

The stimulating electrodes used in these experiments were the gelatin/NaCl-filled micropipettes described in Chapter 2. Stimuli were constant-current cathodal pulses of 100 μs duration at an intensity sufficient to evoke an EPSP of 50-400 μV (typically 1 -10 μA).

The regions for measurement of peak amplitude were chosen as above except that the stimulus artefact was always short enough to allow region 3 to be placed between the artefact and the rising phase of the EPSP (Fig. 4.1B). Minimising the separation between regions 3 and 4 (and therefore between 1 and 2) reduced contamination of the histograms by the lower frequencies of the noise spectrum.

4.2.3 Determination of EPSP variability

Only unitary EPSPs (group A) were used for this analysis, because EPSPs evoked by stratum radiatum stimuli might have an extra component of fluctuation due to some afferents being near to threshold for activation. Two methods were used to determine whether the unitary EPSPs showed amplitude fluctations on a trial-to-trial basis in excess of that expected from the level of baseline noise. The first of these was visual inspection of a standard deviation record calculated for each EPSP, with the variability due to the noise subtracted. These were

constructed by subtracting the mean EPSP from each evoked response, squaring the difference, subtracting the noise variance record, and then taking the square root of the result (Jack et al, 1981).

The second method compared the standard deviation of the noise-contaminated EPSP amplitude distribution with the standard deviation of the noise amplitude distribution. If the only source of EPSP fluctuation was the noise, the standard deviations of the two distributions would be the same, except for the differences caused by finite sampling of the two distributions. The expected discrepancies due to finite sampling can be estimated by Fisher's z-approximation to the F-distribution, $z = \sqrt{N} \log(\sigma_E/\sigma_N)$ (Johnson & Kotz, 1970, p 81), where N is the sample size and z is normally distributed with mean = 0 and standard deviation = 1. The null hypothesis under test is that both the noise distribution and the noise-contaminated EPSP distribution have been sampled from distributions having the same standard deviation.

4.2.4 Estimation of quantal parameters by the variance method

If Poisson statistics are assumed, the quantal content distribution is given by the formula for the Poisson distribution:

$$p_x = e^{-m} m^x/x! \qquad (1)$$

This gives the probability of x quanta being released on a single trial. m is the mean of this distribution, i.e. the

average quantal content over a large number of trials. A useful simplification arises for determination of m because the standard deviation of a Poisson distribution is equal to the square root of its mean, i.e.:

$$\sigma = \sqrt{m} \qquad (2)$$

The coefficient of variation (CV) is:

$$CV = \sigma/m = 1/\sqrt{m}$$

$$\text{therefore} \qquad m = 1/(CV)^2 \qquad (3)$$

The coefficient of variation is used because it is dimensionless and is therefore the same for both the quantal content distribution and the EPSP amplitude distribution, which is the distribution sampled in the experiment. m can then be determined from the coefficient of variation of the EPSP amplitude distribution, which is

$$CV = \sigma_E/\bar{v}$$

where $\bar{v}$ and σ_E are the mean and standard deviation of the EPSP amplitude distribution.

Substituting for CV in equation 3:

$$m = \bar{v}^2/\sigma_E^2 \qquad (4)$$

The means of the two distributions (quantal content and EPSP amplitude) are related by

$$m = \bar{v}/v_1 \qquad (5)$$

where v_1 is the quantal size. v_1 can be obtained by substituting for m in equation 4:

$$\bar{v}/v_1 = \bar{v}^2/\sigma_E^2$$

$$v_1 = \sigma_E^2/\bar{v}$$

i.e. the quantal size is the variance of the EPSP distribution divided by its mean.

Because the EPSP amplitude distribution is contaminated by noise, which contributes to its coefficient of variation, the appropriate variance measure (σ_E^2) to use is the ~~the~~ variance of the noise-contaminated EPSP distribution minus the variance of the noise distribution (Hubbard, Llinas & Quastel, 1969, p 133).

Allowance can also be made for variability in the quantal size. This increases the observed coefficient of variation of the amplitude distribution by $\sqrt{(1 + CV_q^2)}$ (where CV_q is the coefficient of variation of the quantal unit), and

the quantal size estimate should be divided by this factor (Martin, 1966).

To determine whether our noise-contaminated amplitude distributions could be modelled by the Poisson distribution, the parameters m and v_1 were estimated by the above method for the 12 unitary EPSPs. (The EPSPs evoked by stratum radiatum stimulation are considered less reliable for this analysis, because they may have an inappropriate number of failures if some fibres are activated near threshold). In the absence of information about quantal variability for this synapse, m and v_1 were estimated twice, (a) with the assumption of no quantal variance, and (b) assuming a coefficient of variation for the quantal unit of 0.3, which is a typical value for the frog and mammalian neuromuscular junction (Martin, 1966). The relative frequency of failures, single unit responses, two unit responses and so on was then calculated according to equation 1.

This quantal content distribution was converted to an EPSP amplitude distribution (each quanta multiplied by v_1) and reconvolved with the noise distribution (represented as the sum of two Gaussian distributions, see below). For CV_q = 0.3, a Gaussian distribution with the appropriate variance ($x.(0.3v_1)^2$) was convolved with each EPSP amplitude, in addition to the convolution with the noise. The reconvolved distributions were compared with the experimentally obtained noise-contaminated EPSP distribution, both visually and by chi-square criteria.

4.2.5 The unconstrained deconvolution method

Probability densities of EPSP amplitudes were obtained by deconvolving the noise-contaminated EPSP amplitude histogram with the histogram for the noise voltage using a recently developed deconvolution procedure. This particular version was implemented by Dr Dimitri Kullmann (University Laboratory of Physiology, Oxford). The statistical task was to determine, by maximum likelihood estimates, the optimal set of discrete amplitudes making up the fluctuation of the EPSP amplitude. The maximum likelihood estimator (MLE), a variant of the Estimation-Maximization (E-M) algorithm (Dempster, Laird & Rubin, 1977), first described by Hasselblad (1966), was applied in two stages. The noise histogram was approximated by a continuous monotonic distribution made up from the sum of two Gaussian curves, using the MLE to find their optimal probabilities, standard deviations and positions relative to zero on the voltage axis. (The noise histogram was approximated by two Gaussian distributions rather than one to allow for skew.) The MLE was then applied to the histogram of the evoked EPSP, this time treating the noise fit as the contaminating distribution, and allowing only the probabilities and positions of the underlying discrete amplitudes of the EPSP to vary. In all other respects the technique follows the procedures outlined in Jack et al (1981) and Wong & Redman (1980). The discrete amplitudes determined by this procedure are not constrained to be equally spaced, nor are the probabilities assigned to them forced to conform to any overall probability distribution (e.g. the binomial

distribution), except that the sum of probabilities for all values must be equal to one. All discrete amplitudes were included in the result, regardless of their probabilities of occurrence. However, when calculating the mean separation between adjacent discrete amplitudes (mean quantal amplitude) only those amplitudes with probabilities of occurrence >0.05 were included, as amplitudes with smaller probabilities are likely to be unreliably located (Jack et al, 1981).

4.2.6 Monte Carlo testing of the deconvolution procedure

The Monte Carlo testing described by Wong and Redman (1980) and Clements et al (1987) was extended to cover a wider range of signal to noise ratios. A noise amplitude histogram was made from a sample of 32,000 records of real noise taken from a CA1 neurone. Noise-contaminated EPSP amplitude histograms were also constructed from these records, by adding discrete voltages to the real noise records in multiples of the chosen quantal size, in proportion to their desired frequency. Records were then drawn at random from the distribution of 32,000 EPSP records to form subsamples of a size representative of the number of records obtained in an experiment (e.g. 2000). Amplitude histograms were then made from these subsamples, with a bin size equal to 10% of the quantal size and the smoothing factor equal to the bin size. The bin size was kept at a constant proportion of the quantal size to maintain a constant mean number of entries per bin as the quantal size was varied. Otherwise, the errors introduced by finite

sampling would vary not only with sample size, but also with quantal size.

Monte Carlo simulations were performed for EPSP distributions of two, three and four discrete amplitudes (representing failures and one, two or three quantal increments). The relative frequencies of each discrete amplitude were equal within each distribution, i.e. 0.5, 0.333 and 0.25 respectively. For each group a range of signal to noise ratios was tested, by varying the separation between the discrete amplitudes (i.e. varying quantal size). The signal to noise ratios tested, expressed as v_1/σ_N (where v_1 = quantal size and σ_N = standard deviation of the noise distribution), were 0.5, 0.7, 0.9, 1.1, 1.3, 1.6, 2.0, 2.5 and 3.0. For each of these, 30 different samples of size 2000 were drawn at random to construct EPSP amplitude histograms. Thirty different noise samples of 2000 noise records were also drawn at random to make noise amplitude distributions. The deconvolution procedure was then applied to each of these pairs of noise and noise-contaminated EPSP amplitude histograms.

The results of the Monte Carlo testing of the deconvolution procedure will be described here so that they can be used for interpretation of the deconvolution analysis in the results section (4.3). The aspect of the deconvolution procedure's performance we were most interested in was its ability to recover the discrete amplitudes underlying the original distributions. For each deconvolution, the mean separation between adjacent components in the result was compared with the separation in

the original distribution. (Amplitudes in the result with a probability of occurrence <0.05 were not included.) The mean separations were normalized with respect to the standard deviation of the noise distribution (i.e. converted to a signal-to-noise ratio, $\bar{v}_1/\sigma_N$) and were plotted against the signal-to-noise ratio of the original distribution (Fig. 4.3). Points on the diagonal line indicate instances where the true discrete amplitudes have been exactly recovered. The features to note from these graphs are:

(1) Although discrete amplitudes separated by 1.6 σ_N tend to be reliably recovered, as they are brought closer together (< 1.6 σ_N), the separations between the recovered peak amplitudes become more divergent. The true amplitudes are less accurately identified and there is a predominence of overestimates of the separation between them (sometimes these exceed 1.6 σ_N). The overestimates are largely due to the recovery of too few amplitudes, which results in an increase in the mean separation between them.

(2) As the signal to noise ratio improves, the results generally become more tightly grouped around the correct separation, but a significant number of errors do still occur. These are due to too many components being included in the result, which reduces the mean separation. It can be argued that this error is less serious, because discrete amplitudes separated by more than 2.0-2.5 σ_N are visible by eye in the noise-contaminated EPSP amplitude histograms. Errors of this kind should therefore be obvious and would lead to these results being discarded, rather than being mistakenly accepted.

Figure 4.3. Testing the unconstrained deconvolution method by Monte Carlo simulations. Simulated noise-contaminated EPSP amplitude histograms were composed of two discrete amplitudes (**A**), three discrete amplitudes (**B**) or four discrete amplitudes (**C**) separated by the quantal size and with equal probabilities, convolved with real noise recorded from a CA1 neuron. The true quantal sizes and the quantal sizes in the deconvolution results have been normalized with respect to the standard deviation of the noise distribution. Perfect deconvolution results would lie on the diagonal lines, which indicate equivalence between the true underlying quantal sizes and the quantal sizes given in the results.

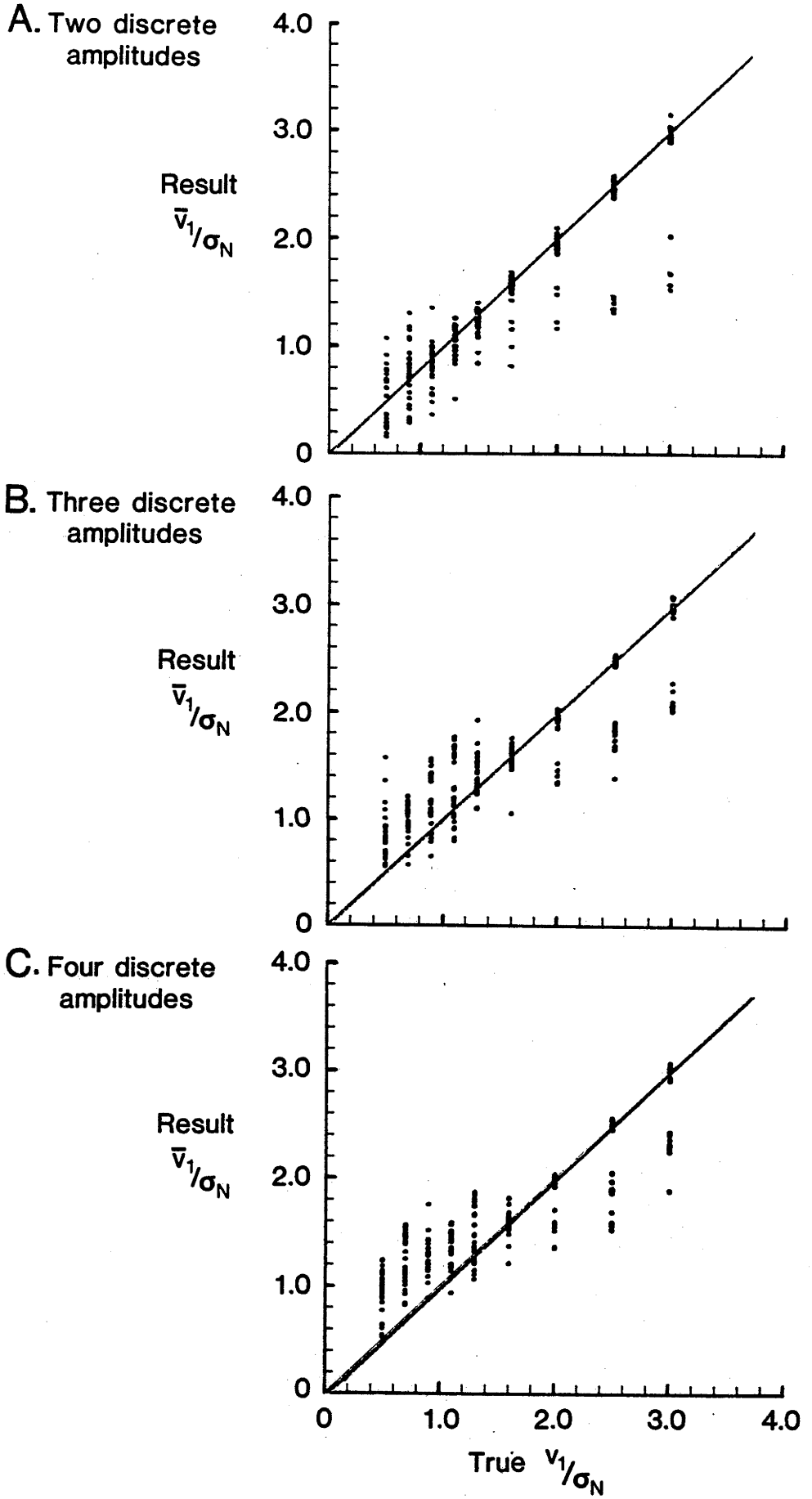

A. Two discrete amplitudes
B. Three discrete amplitudes
C. Four discrete amplitudes
Result $\bar{v}_1/\sigma_N$
4.0
3.0
2.0
1.0
0
0
1.0
2.0
3.0
4.0
True v_1/σ_N

Fig. 4.4 shows the results of some other Monte Carlo tests presented in a different way. In these examples there are three discrete amplitudes in the original distribution (indicated by the vertical bars), but two have been assigned equal probabilities of 0.4 while the third has a probability of 0.2. The deconvolution results are indicated by filled circles (discrete amplitude values and probabilites). Thirty deconvolutions were performed for each of four sample size (N) and signal-to-noise (v_1/σ_N) conditions. Firstly, note that even under the most favourable conditions (v_1/σ_N = 2.0 and 1.6), the two higher probability components are more reliably recovered than the third. Secondly, this figure illustrates the importance of sample size. A signal-to-noise ratio of 2.0 σ_N is adequate for a sample of 2000 records, but not for 500 (Fig 4.4A,B).

4.3 RESULTS

4.3.1 EPSP variability from trial-to-trial

Fig. 4.5 shows the average and standard deviation record for each of the 12 unitary EPSPs used for this analysis. All the standard deviation records show clear increases in variability during the EPSP. With the exception of EPSP A9, the maxima of the standard deviation records occur at almost the same time as the peaks of the averaged EPSPs. The standard deviation record for A9 has its peak during the rising phase of the averaged EPSP.

Figure 4.4. Testing the unconstrained deconvolution method by Monte Carlo simulations. The true noise-free EPSP amplitude distributions are indicated by the vertical bars. The filled circles represent the deconvolution results (discrete amplitude values and probabilities). Thirty simulations were deconvolved for each of the each of four sample size (N) and signal/noise (v_1/σ_N) conditions. **A, C** and **D,** The separation of the discrete amplitudes was decreased from 2.0 to 1.6 and 1.3 σ_N respectively for a constant sample size of 2000 EPSPs. **B,** The separation of discrete amplitude values is the same as for **A,** but the sample size has been decreased to 500.

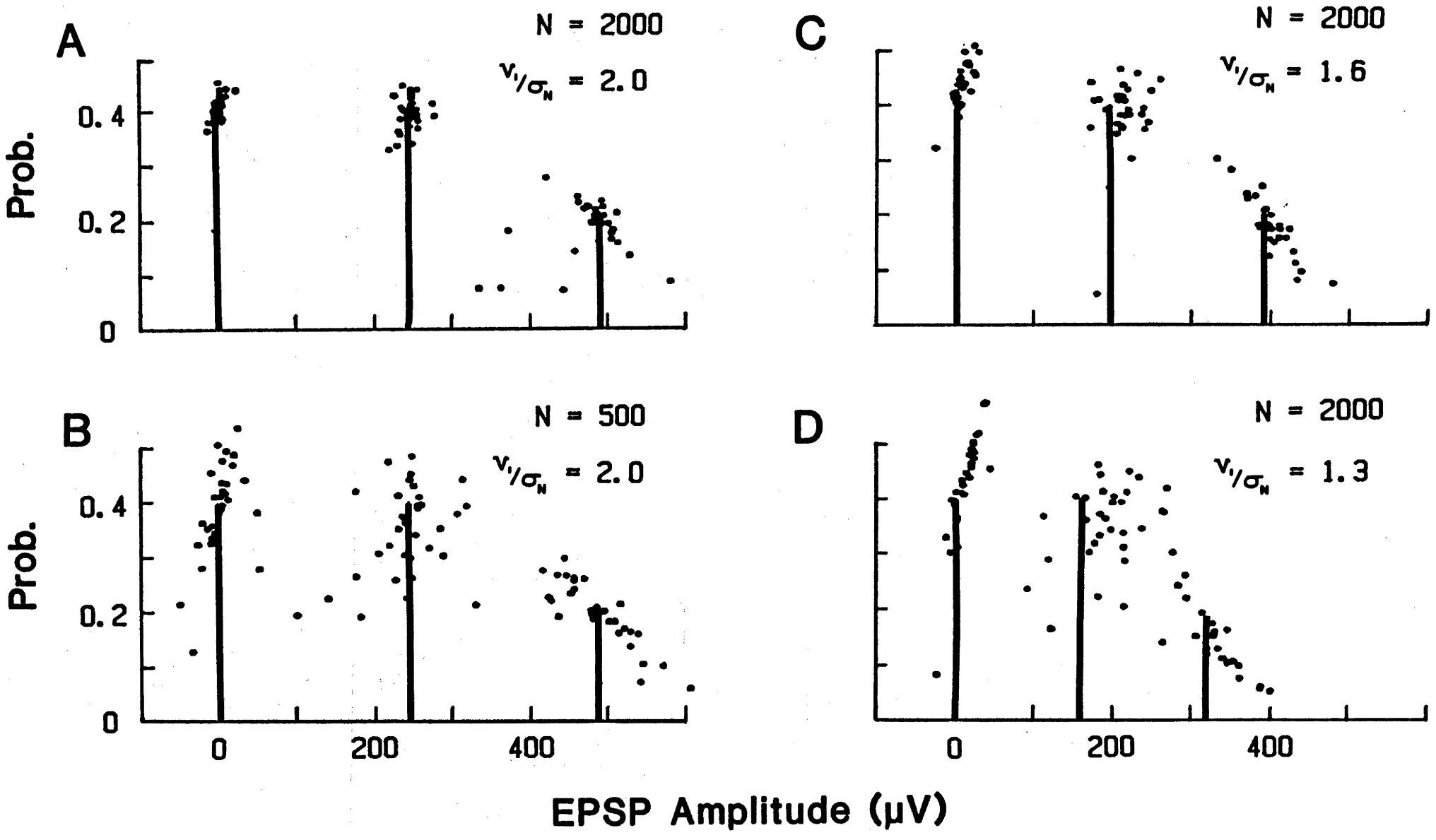
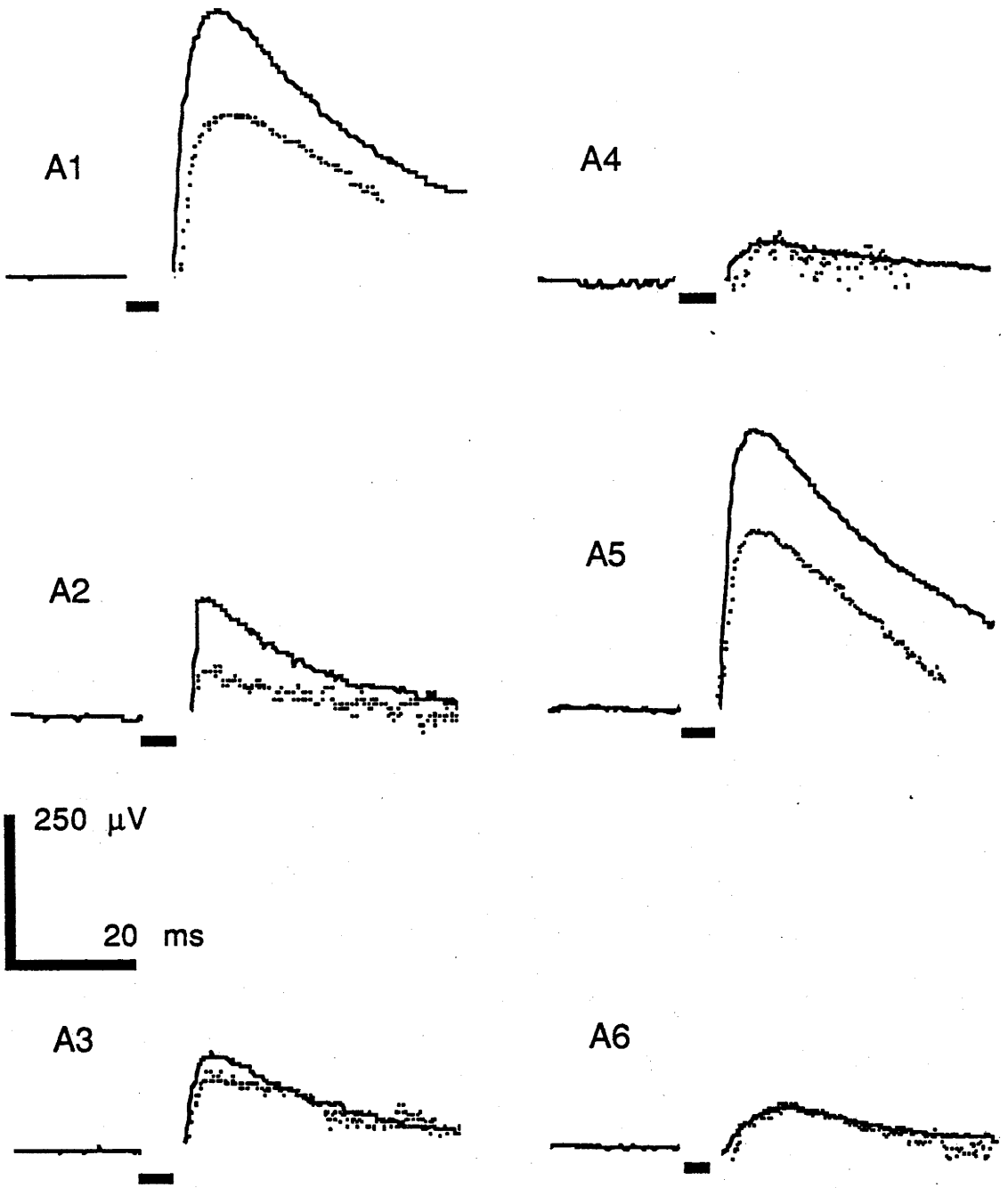
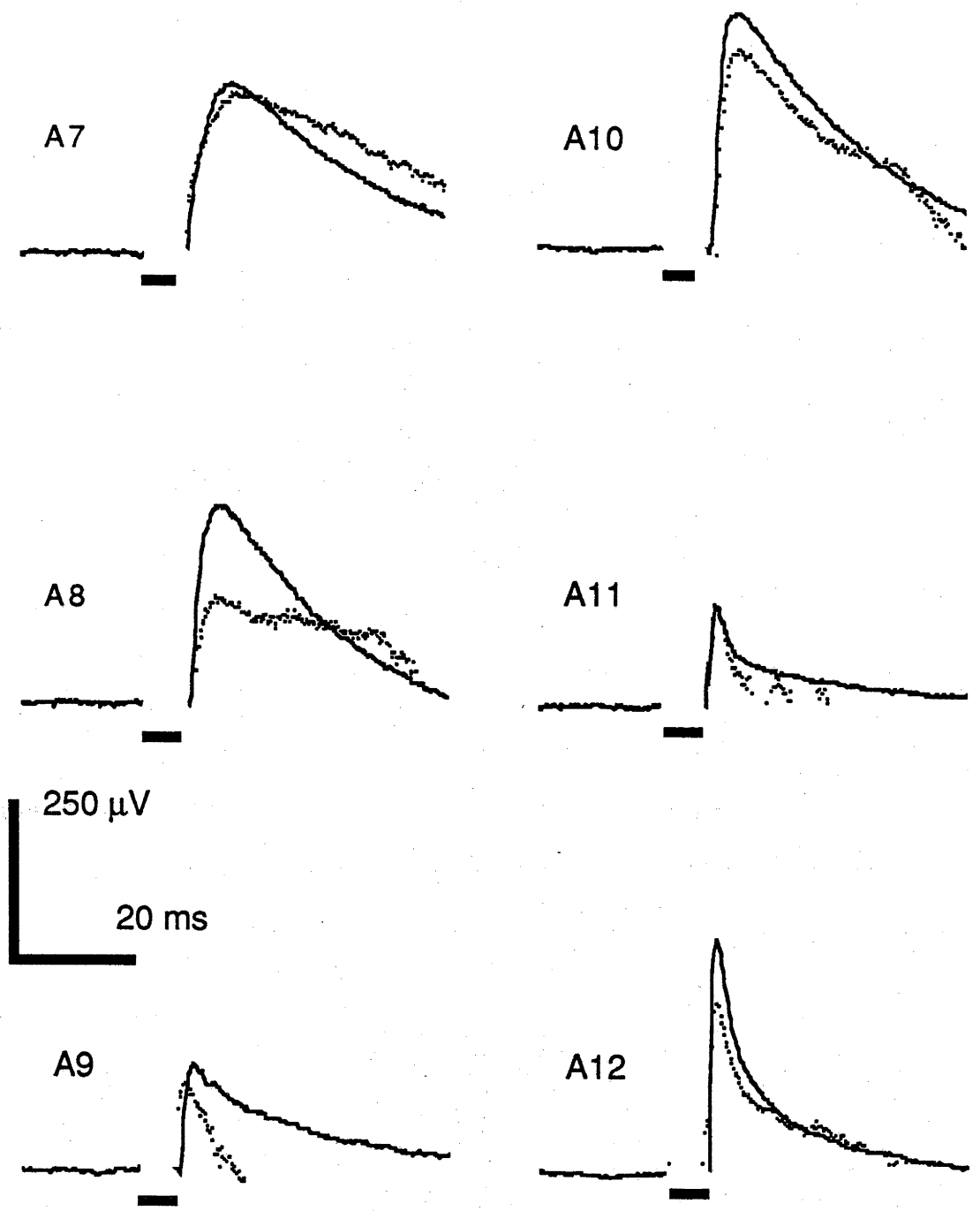

A
N = 2000
v_1/σ_N = 2.0
B
N = 500
v_1/σ_N = 2.0
C
N = 2000
v_1/σ_N = 1.6
D
N = 2000
v_1/σ_N = 1.3
Prob.
0.4
0.2
0
0
200
400
EPSP Amplitude (μV)

Figure 4.5. (Following two pages) Comparison of the average and standard deviation time courses for the group A (unitary) EPSPs. The solid lines are the averages (the number of records for each is given in Table 4.3) and the dotted lines are the standard deviation records, which were calculated as described in section 4.2.3.


A1
A4
A2
A5
250 µV
20 ms
A3
A6

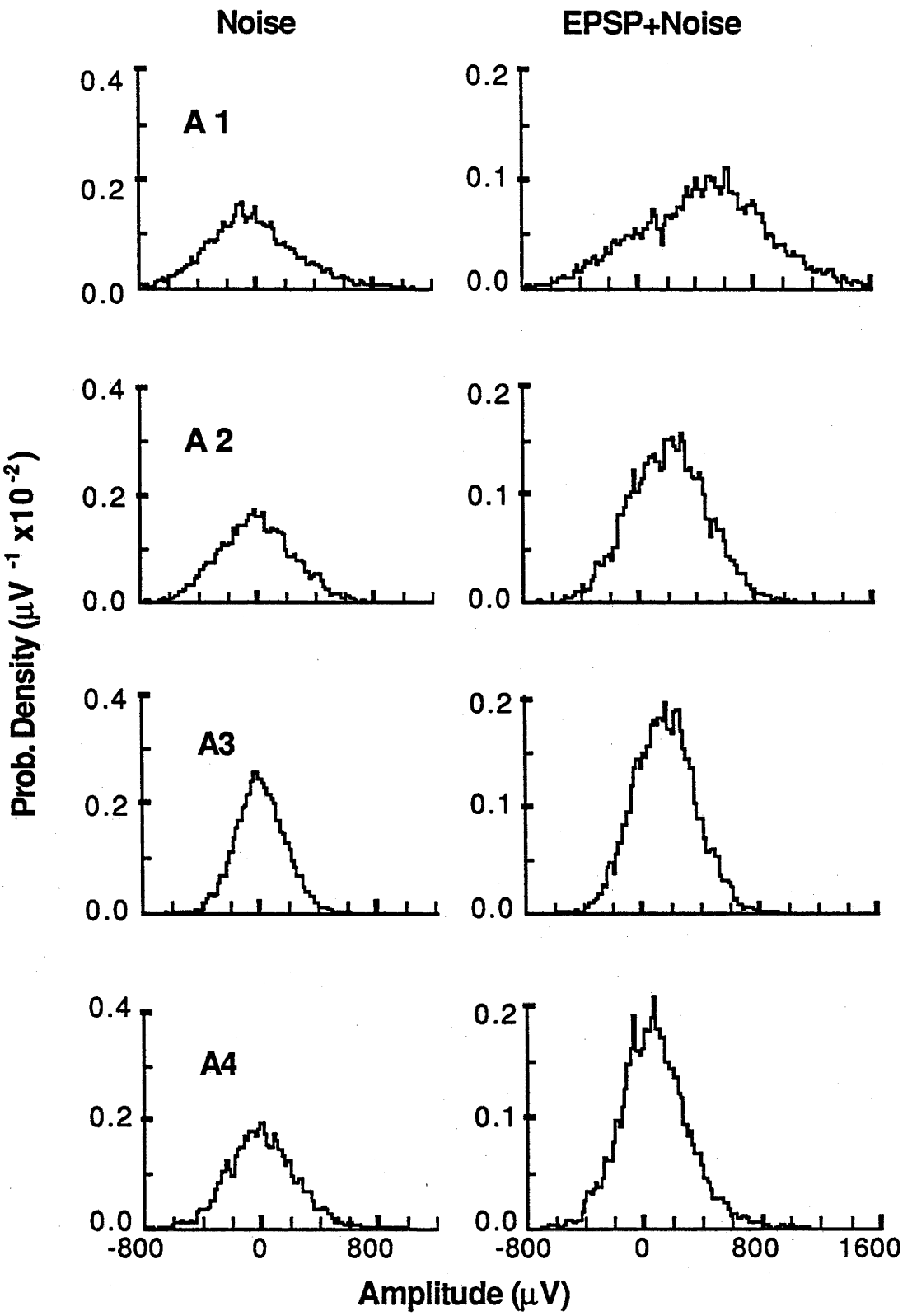

A7
A10
A8
A11
250 µV
20 ms
A9
A12

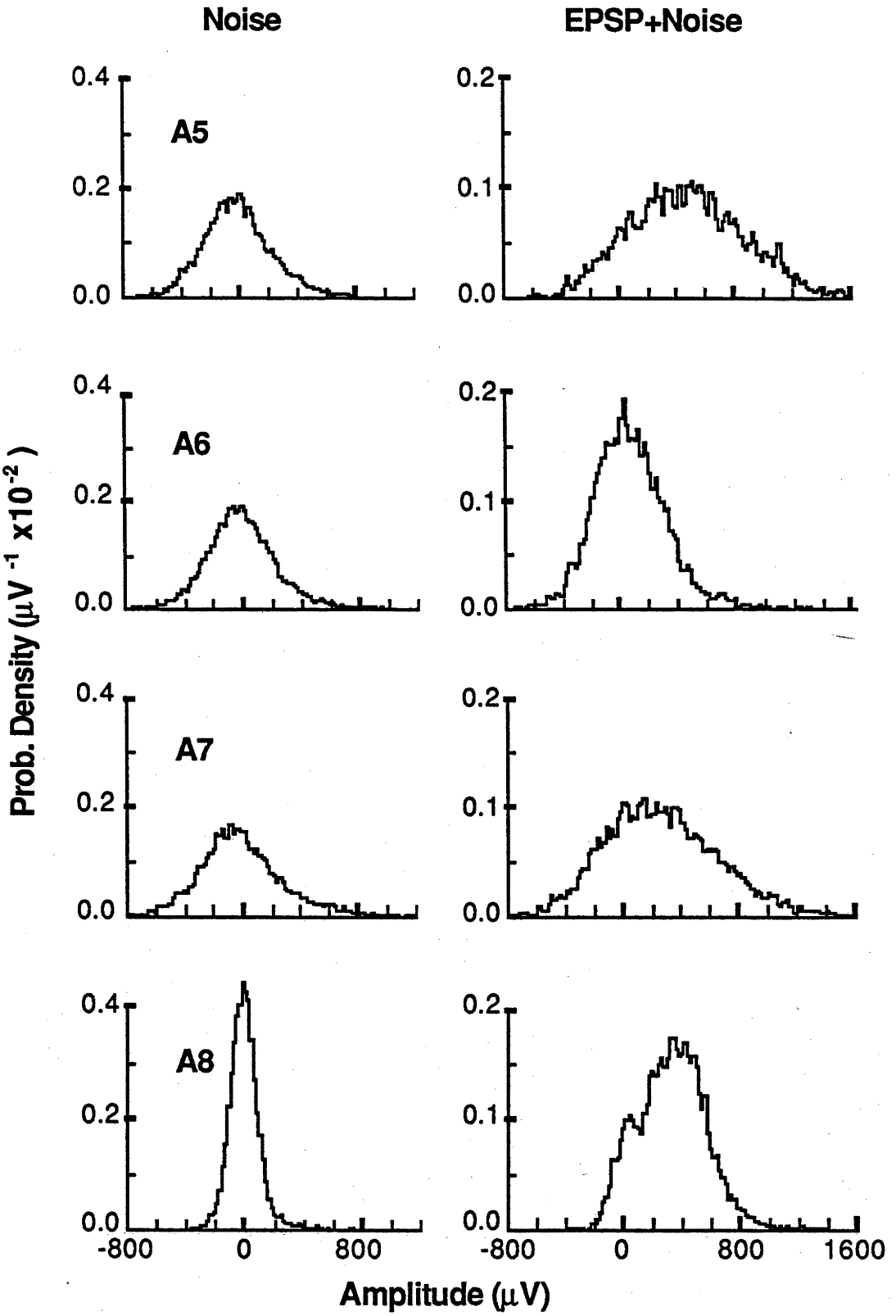
One way of quantifying the degree of fluctuation in these EPSPs is to compare the standard deviations of the noise-contaminated amplitude histograms with the standard deviations of the noise histograms. The histograms for the 12 unitary EPSPs are illustrated in Fig. 4.6. The standard deviations of these histograms are listed in Table 4.1, where it can be seen that the standard deviation of the EPSP amplitude histogram is greater than that of the noise histogram in every case. The significance of these differences has been estimated by Fisher's z-approximation to the F-distribution, and the z and P values are listed in Table 4.1. The null hypothesis, which is that both the noise distribution and the noise-contaminated EPSP distribution have been sampled from distributions with the same standard deviation, can be rejected at the 0.0001 level of confidence for 9 of the 12 EPSPs. The P values for the other three EPSPs (no.s A2, A4 and A6) indicate that if the null hypothesis were correct, then differences of this magnitude in the standard deviations would commonly occur by chance. The data from the amplitude histograms for these three EPSPs is therefore consistent with either the presence or absence of intrinsic variability.

4.3.2 Estimation of quantal parameters by the variance method

Table 4.2 gives the values for quantal size (v_1) and mean quantal content (m) for the 12 unitary EPSPs analysed by the method of variance. The results are given for both the assumption of no quantal variance ($CV_q = 0$) and for the

Figure 4.6. (Following three pages) Noise and noise-contaminated EPSP amplitude histograms for the group A (unitary) EPSPs. The bin size for all histograms (in this and all subsequent figures) is 20 μV. The number of records used to construct the histograms (same for noise and noise-contaminated EPSP) is listed in Table 4.3.


Noise
EPSP+Noise
A 1
A 2
A3
A4
0.4
0.2
0.0
0.1
-800
0
800
1600
Prob. Density (μV -1 x10-2)
Amplitude (μV)


Noise
EPSP+Noise
A5
A6
A7
A8
0.4
0.2
0.0
0.1
-800
0
800
1600
Prob. Density (μV -1 x10-2)
Amplitude (μV)

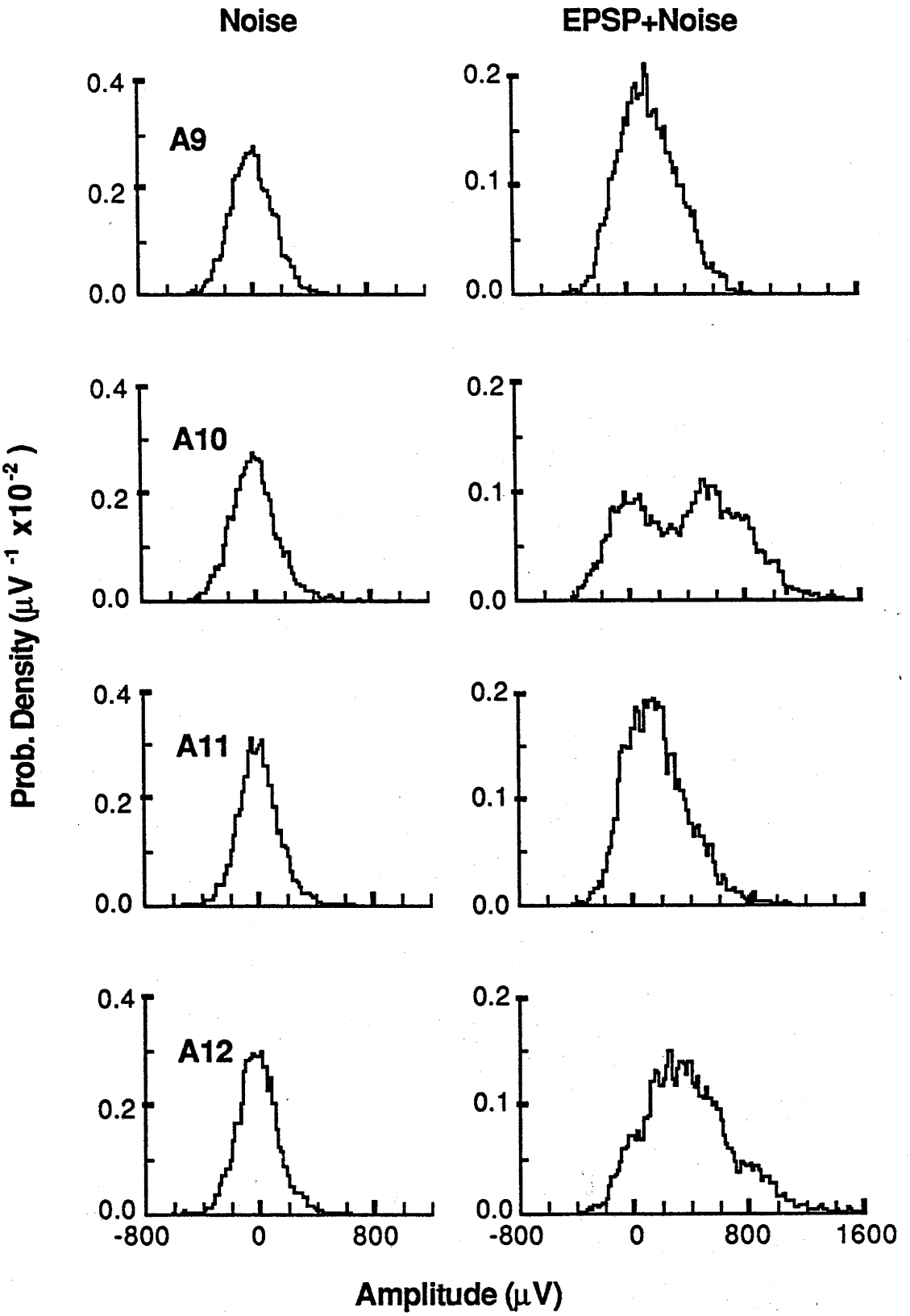

Noise
EPSP+Noise
A9
A10
A11
A12
0.4
0.2
0.0
0.1
-800
0
800
1600
Prob. Density (μV -1 x10-2)
Amplitude (μV)

Table 4.1. Unitary EPSP variability from trial-to-trial: parameters derived from the standard deviations of the histograms of the noise-contaminated EPSP amplitudes and the histograms of the noise amplitudes.

EPSP No.	$\bar{v}$ (μV)	σ_E (μV)	σ_N (μV)	CV	z	P
A1.	451	446	349	0.62	7.55	<0.0001
A2.	205	268	257	0.37	0.97	0.33
A3.	155	210	169	0.80	6.32	<0.0001
A4.	67	237	233	0.65	0.48	0.63
A5.	471	402	254	0.66	9.76	<0.0001
A6.	69	255	246	0.97	0.92	0.36
A7.	274	416	308	1.02	8.35	<0.0001
A8.	324	236	127	0.61	17.72	<0.0001
A9.	159	211	158	0.88	7.49	<0.0001
A10.	380	375	169	0.88	20.17	<0.0001
A11.	170	222	147	0.98	8.32	<0.0001
A12.	377	309	145	0.72	16.69	<0.0001

$\bar{v}$ = mean amplitude of EPSP

σ_E = standard deviation of the noise-contaminated EPSP amplitude histogram

σ_N = standard deviation of the noise amplitude histogram

CV = $\sqrt{(\sigma_E^2 - \sigma_N^2)}/\bar{v}$, the coefficient of variation for the noise-free EPSP. This measure assumes that σ_E and σ_N are accurate (i.e. not subject to sampling error), and that their difference is caused by the variability of the underlying noise-free EPSP.

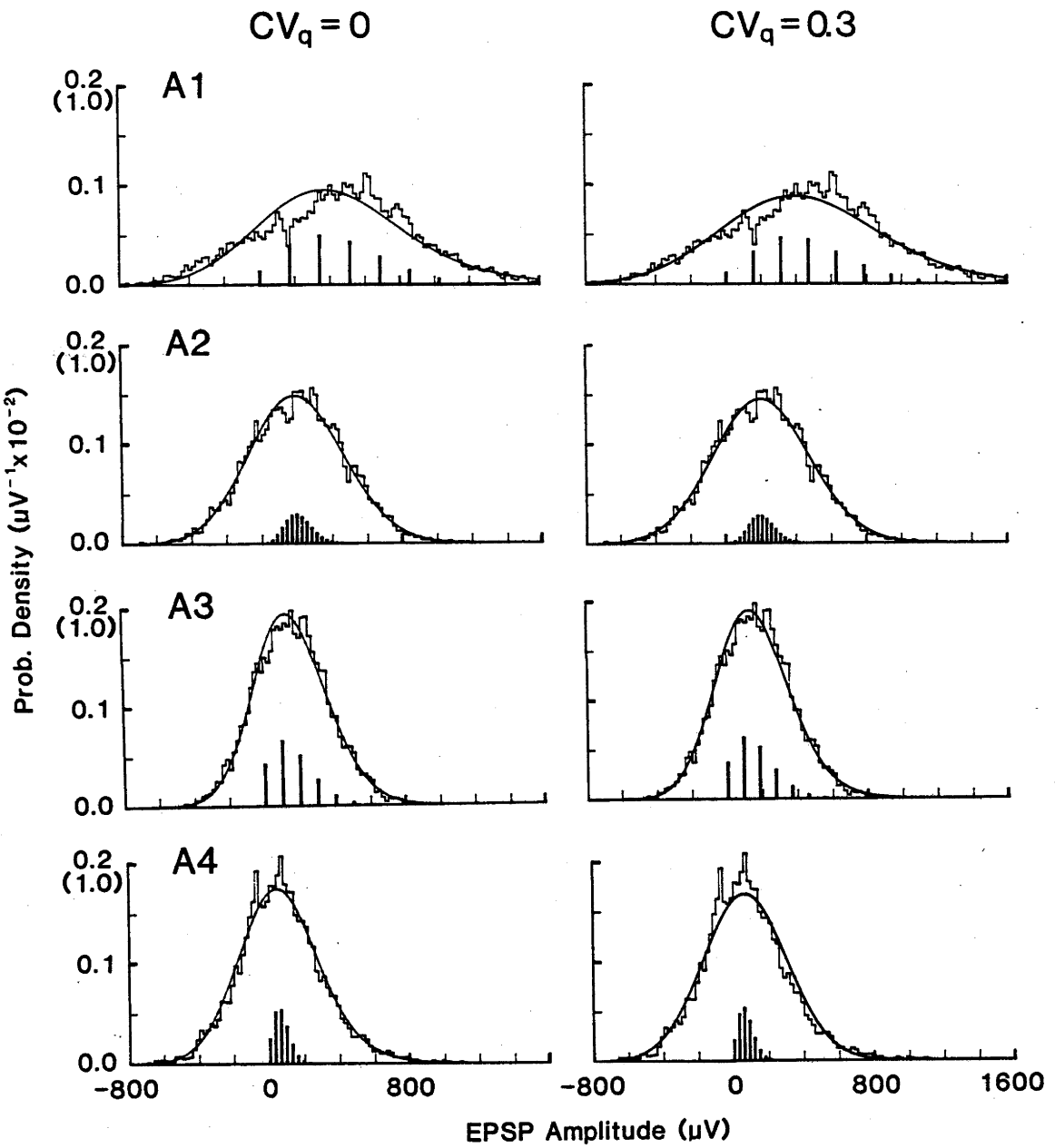
z = $\sqrt{N}\ \log(\sigma_E/\sigma_N)$, Fisher's z-approximation to the F-distribution (Johnson & Kotz, 1970). z is mormally distributed with variance = 1. N is the number of records used to make the histograms (listed in Table 4.3A).

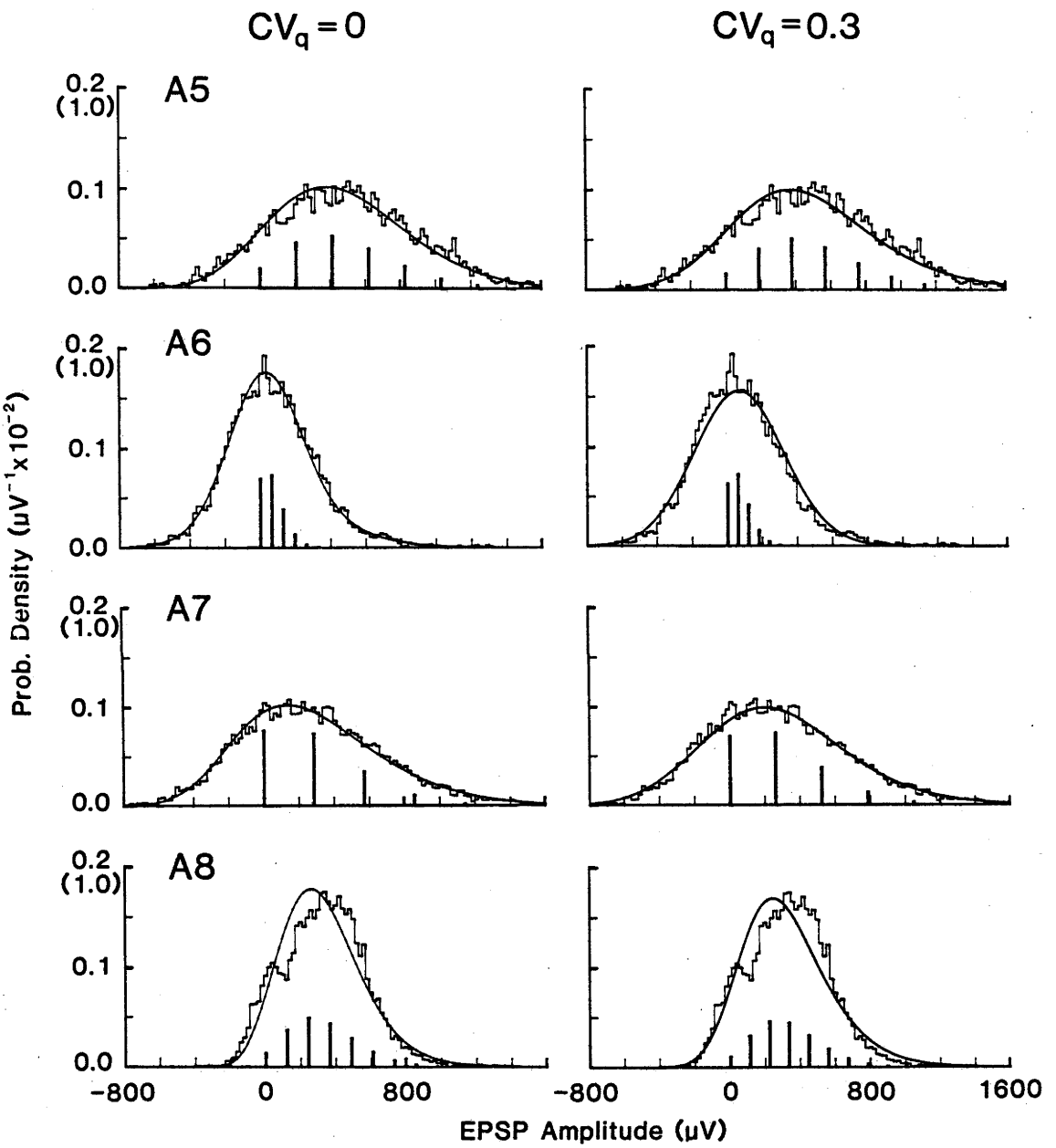
If the following is true:
there is no intrinsic variability in the EPSPs, so that σ_E and σ_N would be equal except for the effects of finite sampling,
then P is the expected probability of obtaining a z value equal to or greater than that given (and therefore σ_E and σ_N as different, or more different than obtained in the experiment), purely due to random sampling error.

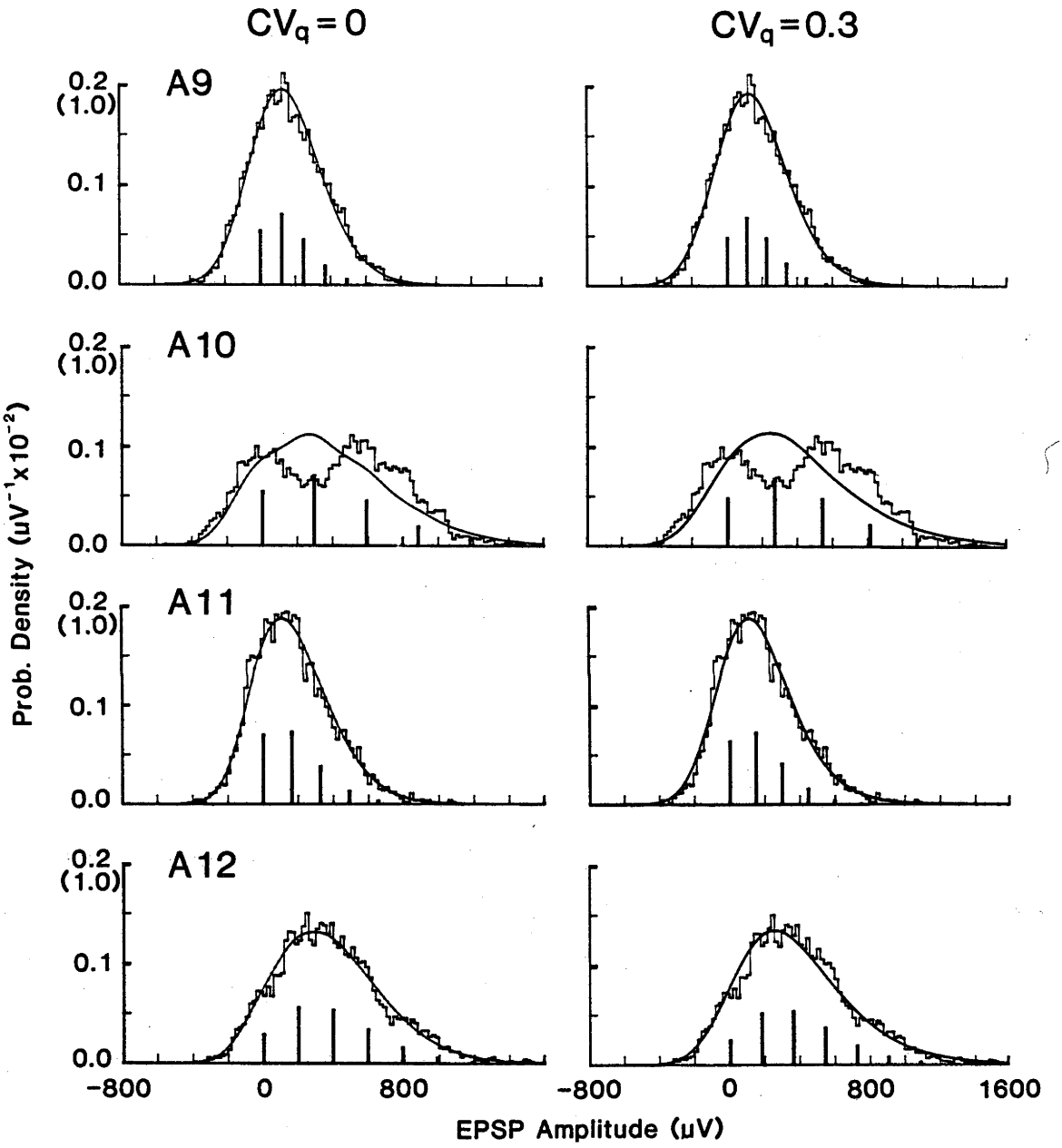
assumption of 30% variance about the mean quantal size (CV_q = 0.3). The calculated values for v_1 ranged from 28 to 295 μV (mean 149) for CV_q = 0, and from 26 to 271 μV (mean 137) for CV_q = 0.3. The parameter m ranged from 0.96 to 7.27 (mean 2.17) for CV_q = 0 and from 1.05 to 7.95 (mean 2.36) for CV_q = 0.3. m has been used in the formula for the Poisson distribution to calculate the probabilities associated with the discrete amplitudes (one at zero μV and the remainder at intervals of v_1). The noise-free amplitude distributions were then reconvolved with the sum of two Gaussian distributions fitted to the noise (for CV_q = 0) or with Gaussians having the appropriate variances for each discrete amplitude (for CV_q = 0.3). These histograms are illustrated in Fig. 4.7. The noise-contaminated probability density functions based on the Poisson distribution have been overlaid with the experimentally obtained histograms of the noise-contaminated EPSP amplitudes, to enable visual assessment of goodness of fit.

The chi-square distribution has been used to test more objectively whether the Poisson distributions for the calculated 'm's provide satisfactory fits to the experimental data. The noise-contaminated amplitude histograms constructed from the Poisson parameters provide the 'expected' frequencies for each bin, and the noise-contaminated histograms obtained in the experiments provide the 'observed' frequencies, when multiplied by the sample size (number of EPSP records). The question being asked for each EPSP is: if the Poisson distribution specified by the calculated m was the true underlying distribution, what are

Figure 4.7. (Following three pages) Results of quantal analysis by the method of variance, for the group A (unitary) EPSPs. The left-hand column is the results for the assumption of $CV_q = 0$, while the right has those for $CV_q = 0.3$. The vertical bars represent the noise free amplitudes, which are at intervals of v_1 and have probabilities following the Poisson distribution. Note that the vertical axis scale in parentheses (1.0) applies to these probabilities. The solid curves were produced by convolution of these probabilities with Gaussian distributions representing the noise. They are superimposed on the noise-contaminated EPSP amplitude histograms obtained in the experiments.


CVq = 0
CVq = 0.3
A1
A2
A3
A4
0.2
(1.0)
0.1
0.0
Prob. Density (μV⁻¹x10⁻²)
-800
0
800
1600
EPSP Amplitude (μV)


CV$_q$ = 0
CV$_q$ = 0.3
A5
A6
A7
A8
0.2
(1.0)
0.1
0.0
Prob. Density (μV^{-1}x10^{-2})
-800
0
800
1600
EPSP Amplitude (μV)


CVq = 0
CVq = 0.3
A9
A10
A11
A12
0.2
(1.0)
0.1
0.0
Prob. Density (μV⁻¹x10⁻²)
-800
0
800
1600
EPSP Amplitude (μV)

the chances that finite sampling would have produced the frequency distribution observed in the experiment? The values for P listed in Table 4.2 give an estimate of this, by indicating the proportion of equally sized samples from the 'expected' distribution which would produce equal or worse chi-square fits.

For seven of the 12 EPSPs (A2, A3, A5, A7, A9, A11 & A12), chi-square testing indicated fits that were quite good ($P > 0.5$) both with and without allowance for quantal variance. Within this group the P values were generally similar regardless of quantal variance; they were the same for one EPSP, slightly better without quantal variance for four and slightly better with quantal variance for two.

For three of the EPSPs (A1, A8 & A10), the fits were very poor ($P < 0.0005$) both with and without quantal variance. For the remaining two of the 12 EPSPs (A4 & A6) the fits were very good ($P > 0.975$) if no quantal variance was assumed, but very poor ($P < 0.0005$) for $CV = 0.3$, indicating a high degree of sensitivity to the amount of quantal variance chosen.

4.3.3. Quantal analysis by the deconvolution method

The 37 EPSPs analysed by the deconvolution method were from all three series of experiments (groups A, B and C). The most important difference between the groups is that the EPSPs in group A were elicited by activation of a single presynaptic cell, whereas those in groups B and C were evoked by extracellular stimuli to afferent fibres in the stratum radiatum. The range of mean EPSP amplitudes was similar for

all three groups, being 67-451, 94-395 and 67-396 μV for groups A, B and C respectively. The mean peak amplitudes were 256, 228 and 160 μV for the groups A, B and C.

The deconvolution procedure gives results in the form of noise-free EPSP amplitude distributions. These are listed as discrete amplitudes and their associated probabilities for the 37 EPSPs in Tables 4.3B, 4.4B and 4.5B. The most interesting parameter to be extracted from these data is the estimate of quantal size ($\bar{v}_1$), which is calculated as the mean separation between adjacent discrete amplitudes. The quantal size estimates are given in Tables 4.3A, 4.4A and 4.5A. These tables also list the number of records obtained and the standard deviation of the noise distribution for each EPSP. The signal-to-noise ratio $\bar{v}_1/\sigma_N$ is important for interpretation of the results.

In contrast to the analysis for the method of variance, the question is not whether a good fit has been obtained to the experimental data (the deconvolution procedure always finds a good fit), but rather whether the result provided can be considered reliable. It was shown in section 4.2.6 that as the signal-to-noise ratio of the underlying amplitude distribution is reduced, the errors due to finite sampling prevent reliable recovery of the true quantal size (similar errors occur for a reduction of sample size). Conversely, when the deconvolution analysis provides a solution which lies within the scatter of unreliable results (in terms of $\bar{v}_1/\sigma_N$), its status is uncertain. The solution given might be the correct one, but because other underlying amplitude distributions could give the same result (and there is no way

Table 4.3A. Deconvolution results for the unitary EPSPs (Group A).

EPSP No.	Number of records	$\bar{v}$ (μV)	$\bar{v}_1$ (μV)	σ_N (μV)	$\bar{v}_1/\sigma_N$	
A1.	5031	451	609	349	1.74	
A2.	2813	205	161	257	0.63	
A3.	4495	155	229	169	1.36	
A4.	3199	67	62	233	0.27	
A5.	2394	471	317	254	1.25	
A6.	3448	69	129	246	0.52	
A7.	4087	274	317	308	1.03	
A8.	4334	324	173	127	1.36	
A9.	3553	159	184	158	1.16	
A10.	3395	380	288	169	1.70	
A11.	2160	170	225	147	1.53	
A12.	2581	377	278	145	1.92	*

$\bar{v}$ = mean amplitude of EPSP
$\bar{v}_1$ = mean increment Between discrete amplitude values (quantal size)
σ_N = standard deviation of the noise histogram

Table 4.3B. Deconvolution results for the unitary EPSPs (Group A): discrete amplitudes and probabilities of each component. Only amplitudes with p>0.05 are listed.

	discrete amplitudes (μV) / probabilities				
A1.	33/0.33,	642/0.67			
A2.	101/0.36,	262/0.64			
A3.	13/0.41,	221/0.06,	242/0.50		
A4.	62/0.99				
A5.	43/0.25,	429/0.41,	723/0.20,	995/0.14	
A6.	3/0.50,	132/0.50			
A7.	43/0.44,	373/0.36,	677/0.15		
A8.	26/0.21,	250/0.30,	419/0.27,	546/0.17	
A9.	40/0.53,	214/0.28,	407/0.18		
A10.	-28/0.31,	190/0.15,	543/0.35,	836/0.19	
A11.	27/0.47,	220/0.38,	447/0.13		
A12.	17/0.19,	267/0.38,	523/0.30,	850/0.10	*

'*' indicates the EPSP for which the deconvolution result has been accepted as reliable

Table 4.4A. Deconvolution results for the small compound EPSPs in Group B.

EPSP No.	Stim	Number of records	$\bar{v}$ (μV)	$\bar{v}_1$ (μV)	σ_N (μV)	$\bar{v}_1/\sigma_N$	
B1.	prox	1718	170	224	115	1.94	*
B2.	dist	1818	164	179	127	1.41	
B3.	prox	1789	322	194	123	1.58	
B4.	dist	2191	294	213	138	1.54	
B5.	prox	2398	395	115	70	1.65	
B6.	dist	2396	203	85	71	1.20	
B7.	prox	3838	94	141	125	1.12	
B8.	dist	4817	131	120	131	0.92	
B9.	prox	1795	282	193	93	2.08	*
B10.	dist	2298	227	126	95	1.33	

$\bar{v}$ = mean amplitude of EPSP
$\bar{v}_1$ = mean increment between discrete amplitude values (quantal size)
σ_N = standard deviation of the noise histogram

Table 4.4B. Deconvolution results for the small compound EPSPs in Group B: discrete amplitudes and probabilities of each component. Only amplitudes with p>0.05 are listed.

		discrete amplitudes (μV) / probabilities	
B1.	prox	16/0.44, 240/0.44, 463/0.10	*
B2.	dist	28/0.34, 196/0.54, 386/0.13	
B3.	prox	25/0.08, 206/0.42, 395/0.34, 608/0.16	
B4.	dist	24/0.16, 232/0.51, 480/0.27, 663/0.07	
B5.	prox	179/0.11, 273/0.19, 382/0.31, 512/0.23, 640/0.11	
B6.	dist	46/0.15, 142/0.23, 171/0.17, 259/0.34, 386/0.07	
B7.	prox	-4/0.43, 131/0.42, 277/0.15	
B8.	dist	-17/0.18, 75/0.35, 196/0.37, 343/0.10	
B9.	prox	5/0.17, 184/0.36, 381/0.29, 585/0.13	*
B10.	dist	22/0.09, 100/0.22, 206/0.40, 356/0.21, 526/0.06	

'*' indicates EPSPs for which the deconvolution results have been accepted as reliable

Table 4.5A. Deconvolution results for the small compound EPSPs in Group C.

EPSP No.	Number of records	$\bar{v}$ (μV)	$\bar{v}_1$ (μV)	σ_N (μV)	$\bar{v}_1/\sigma_N$
C1.	7300	67	73	83	0.88
C2.	5400	120	94	80	1.18
C3.	5519	137	130	105	1.24
C4.	5798	166	145	121	1.19
C5.	2196	143	147	94	1.56
C6.	3999	146	159	91	1.75
C7.	2714	396	193	116	1.67
C8.	2399	163	83	99	0.83
C9.	2398	131	152	115	1.32
C10.	4139	141	109	99	1.10
C11.	3596	199	97	84	1.16
C12.	2400	173	103	61	1.69
C13.	2519	142	127	79	1.61
C14.	3598	148	66	62	1.06
C15.	3514	124	90	91	0.99

$\bar{v}$ = mean amplitude of EPSP
$\bar{v}_1$ = mean increment Between discrete amplitude values (quantal size)
σ_N = standard deviation of the noise histogram

Table 4.5B. Deconvolution results for the small compound EPSPs in Group C: discrete amplitudes and probabilities of of each component. Only amplitudes with p>0.05 are listed.

	discrete amplitudes (μV) / probabilities				
C1.	-34/0.07,	52/0.77,	185/0.158		
C2.	20/0.34,	85/0.19,	154/0.33,	302/0.13	
C3.	52/0.35,	160/0.55,	312/0.10		
C4.	38/0.33,	171/0.45,	327/0.19		
C5.	39/0.48,	173/0.25,	332/0.20		
C6.	24/0.56,	179/0.12,	345/0.18,	502/0.08	
C7.	0/0.37,	314/0.13,	489/0.23,	702/0.16,	894/0.07
C8.	88/0.36,	179/0.40,	253/0.24		
C9.	64/0.59,	216/0.39			
C10.	95/0.59,	204/0.41			
C11.	65/0.13,	158/0.39,	245/0.38,	357/0.09	
C12.	15/0.03,	112/0.42,	211/0.47,	325/0.08	
C13.	19/0.46,	139/0.23,	261/0.21,	400/0.06	
C14.	124/0.55,	190/0.41			
C15.	66/0.41,	156/0.56			

of knowing when this occurs), it must be rejected as unreliable. For example, turn to Fig. 4.3C and follow a line horizontally across from a result of 1.60 $\bar{v}_1/\sigma_N$. The possible true $\bar{v}_1/\sigma_N$ which could provide this result range from 0.9 to 2.5. For this sample size, and for three or more discrete amplitudes, a result of 1.60 $\bar{v}_1/\sigma_N$ is unreliable. For a result to be accepted there must be some degree of confidence that it lies above the range of solutions which give erroneous over- or underestimates of quantal size. For the conditions tested in Fig. 4.3A, results with $\bar{v}_1/\sigma_N$ = 1.6 would be acceptable, but for those tested in 4.3B and 4.3C, the threshold for acceptance would be closer to 1.9 $\bar{v}_1/\sigma_N$.

The number of discrete amplitudes in the deconvolution result with $p>0.05$ ranged from 1 to 5 for the 37 EPSPs, and $\bar{v}_1/\sigma_N$ ranged from 0.27 to 2.08 (mean 1.31). Figure 4.8 illustrates the range of signal-to-noise ratios by plotting, for each EPSP, the quantal size estimated by deconvolution analysis against the standard deviation of the noise. The solid line represents $\bar{v}_1/\sigma_N$ = 2.0, and the dotted line represents $\bar{v}_1/\sigma_N$ = 1.6. Although most of the results lie around or below $\bar{v}_1/\sigma_N$ = 1.6, the best three lie close to $\bar{v}_1/\sigma_N$ = 2.0. These three results, which correspond to EPSPs A12, B1 and B9, are the most likely to be reliable.

EPSP A12 was one of two EPSPs evoked in the CA1 neurone described as 'atypical' in Chapter 3 (section 3.3.8). Individual records for EPSP A12 were shown in Fig. 3.12. The left side of Fig. 4.9 illustrates the amplitude histograms for this EPSP while the corresponding histograms for the other EPSP recorded from this cell (A11) are shown on the

Figure 4.8. Quantal size ($\bar{v}_1$) estimated by the deconvolution method versus the standard deviation of the noise (σ_N), for the EPSPs in group A (triangles), group B (filled circles) and group C (open circles). The solid line represents $\bar{v}_1/\sigma_N = 2.0$ and the interrupted line represents $\bar{v}_1/\sigma_N = 1.6$.

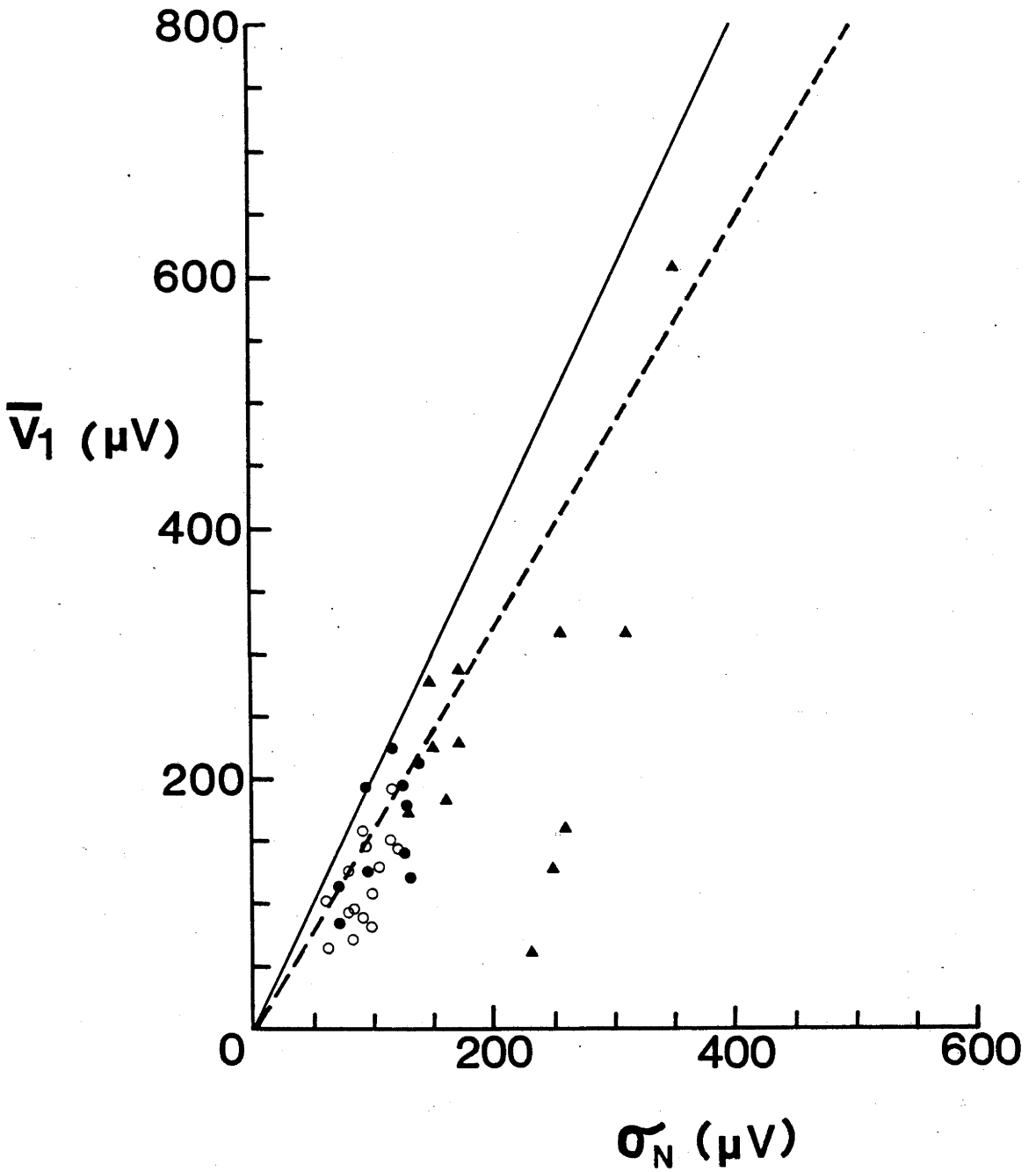
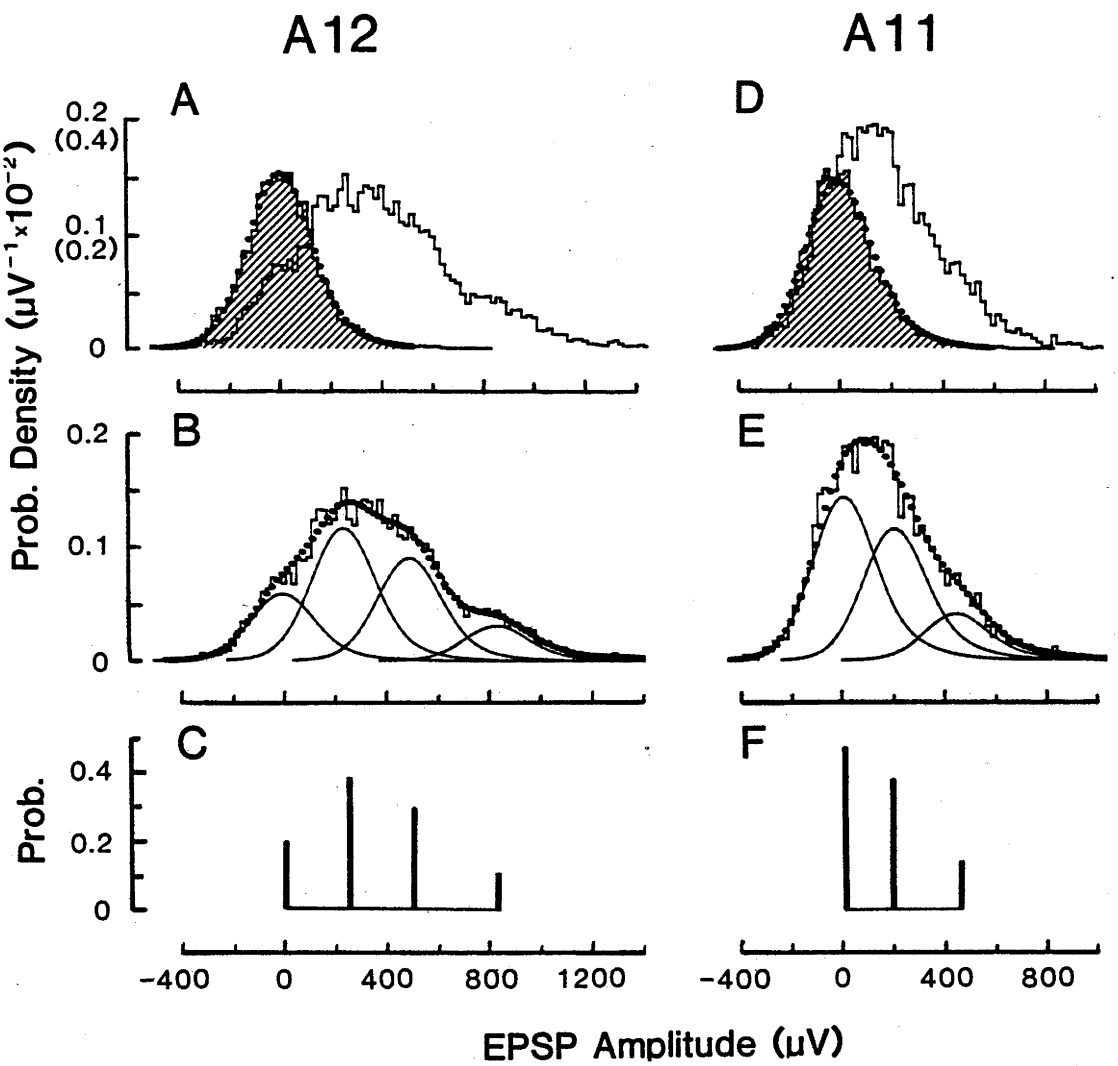

800
600
400
200
0
200
400
600
$\overline{V}_1$ (μV)
σ_N (μV)

Figure 4.9. Deconvolution analysis for EPSPs A12 and A11. **A**, the noise amplitude histogram (shaded) superimposed on the noise-contaminated EPSP amplitude histogram, for EPSP A12. The filled circles indicate the two-Gaussian distribution fitted to the noise amplitude histogram, used as the noise distribution by the deconvolution procedure. Note that the vertical scale is different for the noise histograms (parentheses). **B**, Filled circles indicate the reconvolved deconvolution result for EPSP A12, and were obtained by summing the four underlying curves. These points have been superimposed on the noise-contaminated EPSP amplitude histogram. The four underlying distributions have the same standard deviation (σ_N) as the measured noise distribution, their mean values are equal to each of the discrete amplitudes, and their areas are equal to the probabilities associated with the discrete amplitudes. **C**, Deconvolution results for EPSP A12, shown as a sequence of discrete amplitudes and associated probabilities. **D,E,F**, These correspond to **A,B** and **C**, but are for EPSP A11.


A12
A11
A
D
B
E
C
F
0.2
(0.4)
0.1
(0.2)
0
Prob. Density (μV⁻¹×10⁻²)
0.2
0.1
0
0.4
0.2
0
Prob.
-400
0
400
800
1200
-400
0
400
800
EPSP Amplitude (μV)

right side for comparison. Fig 4.9A shows the noise-contaminated EPSP amplitude histogram for A12, with the noise amplitude histogram superimposed (shaded area). The filled circles outline the two-Gaussian fit to the noise histogram, which was calculated during the first stage of the deconvolution procedure. Fig. 4.9C gives the results of the deconvolution analysis, shown as vertical bars. The discrete amplitudes and associated probabilities are listed in Table 4.3B (asterisked). For this EPSP $\bar{v}_1$ = 278 μV, and $\bar{v}_1/\sigma_N$ = 1.92 (Table 4.3A). Fig. 4.9B shows the reconvolution of these discrete amplitudes with the noise distribution, superimposed on the experimentally-obtained EPSP amplitude histogram. The two-Gaussian noise distributions, with standard deviations equal to that of the noise, and with means equal to the different discrete amplitudes, are scaled to have areas equal to the probability associated with each discrete amplitude. The sum of these distributions (filled circles) is the best fit to the measured histogram, using the maximum likelihood criterion. The deconvolution results for EPSP A11 are shown in Fig. 4.9E and 4.9F. $\bar{v}_1/\sigma_N$ for A11 was 1.53 (Table 4.3A).

EPSPs B1 and B9 were both evoked in CA1 pyramidal neurones by extracellular activation of stratum radiatum afferents which passed through proximal tissue bridges. Examples of individual records, and the averages of all records, are shown for these EPSPs in Figs. 4.10 and 4.11. The 10-90% rise times of the EPSPs B1 and B9, at 5.4 ms and 5.1 ms, were faster than the rise times of the distally evoked EPSPs in the same cells (B2 and B10), which were 7.3

Figure 4.10. Examples of single records and the averages of all records, for EPSPs B1 and B2 (proximally and distally stimulated EPSPs in the same CA1 neurone). Averaged extracellular records have been subtracted. The arrows indicate the time of the stimuli.

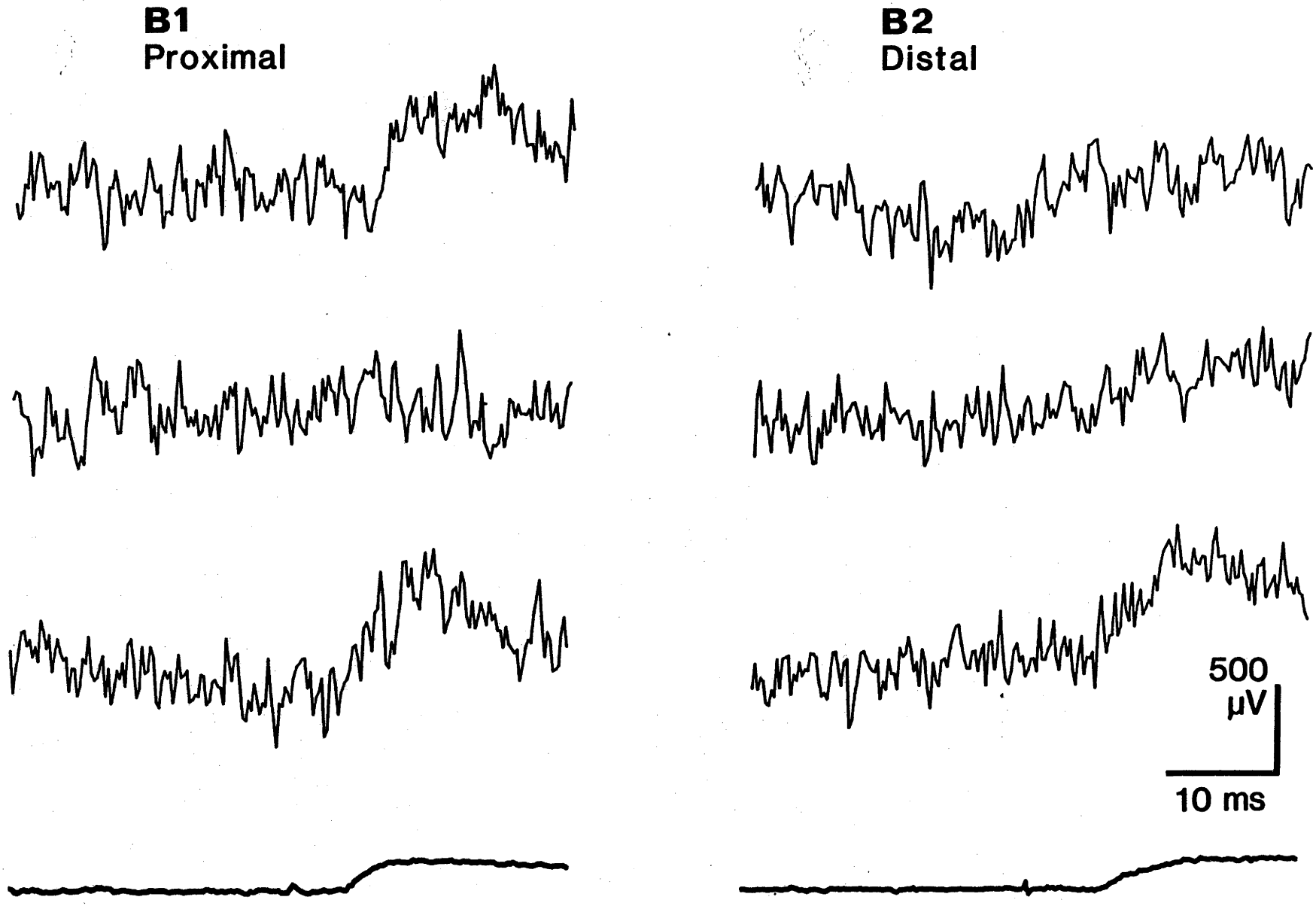
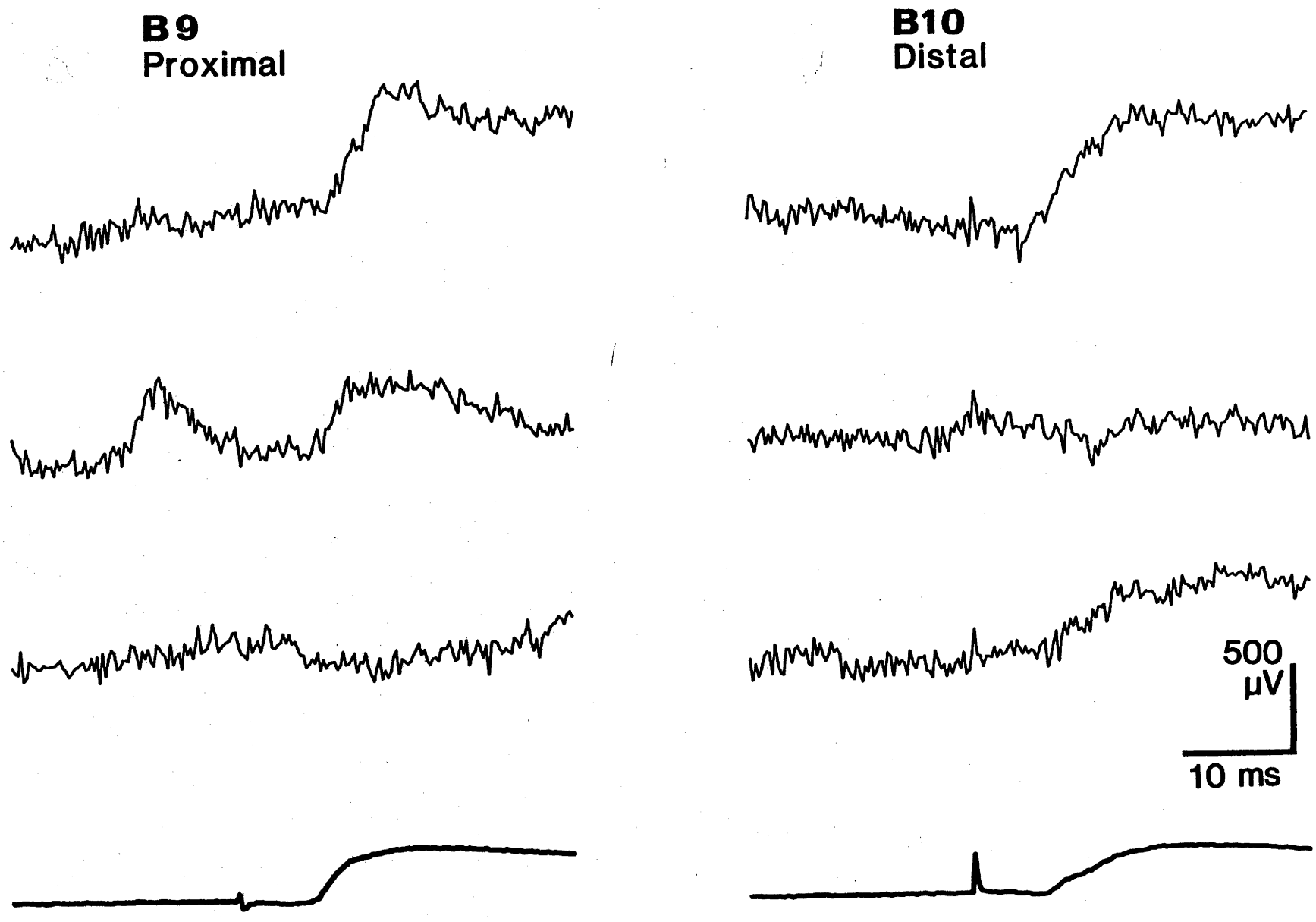

B1
Proximal
B2
Distal
500
μV
10 ms

Figure 4.11. Examples of single records and the averages of all records, for EPSPs B9 and B10 (proximally and distally stimulated EPSPs in the same CA1 neurone). Averaged extracellular records have been subtracted. The arrows indicate the time of the stimuli.


B9
Proximal
B10
Distal
500
μV
10 ms

ms and 7.8 ms respectively. This agrees with previous results for small proximally and distally evoked EPSPs in CA1 pyramidal cells (Turner, 1988). The amplitude histograms and deconvolution results for EPSPs B1 and B9 are given in the left-hand columns of Figs. 4.12 and 4.13 respectively. The corresponding histograms on the right side of these figures show for comparison the analysis for the 'distal' EPSPs from the same CA1 neurones (EPSPs B2 and B10). The discrete amplitudes and probabilities for all of these EPSPs are listed in Table 4.4B. For EPSP B1, $\bar{v}_1$ = 224 μV and $\bar{v}_1/\sigma_N$ = 1.94; for EPSP B9, $\bar{v}_1$ = 193 μV and $\bar{v}_1/\sigma_N$ = 2.08 (Table 4.4A). (For B2, $\bar{v}_1/\sigma_N$ = 1.41; for B10, $\bar{v}_1/\sigma_N$ = 1.33.)

In this kind of analysis, the question usually surfaces about which type of probability distribution is appropriate to describe the probabilities of the different peak amplitudes, with its attendant implications for the probabilities of release at different release sites. Taking the deconvolution results for EPSPs A12, B1 and B9 as the most likely true estimates of quantal size, we were interested to determine whether the probabilities associated with these quantal amplitudes agreed with the predictions of a simple binomial distribution. If so, this would indicate similar probabilities of quantal release at each release site.

For comparison with the results for the three EPSPs (A12, B1 and B9), a range of noise-free amplitude histograms were constructed in which the probabilities of the discrete amplitudes satisfied binomial statistics. Quantal size (v_1) was held constant at the values determined by deconvolution,

Figure 4.12. Deconvolution analysis for EPSPs B1 and B2. Histograms are to be interpreted as for Fig. 4.9.

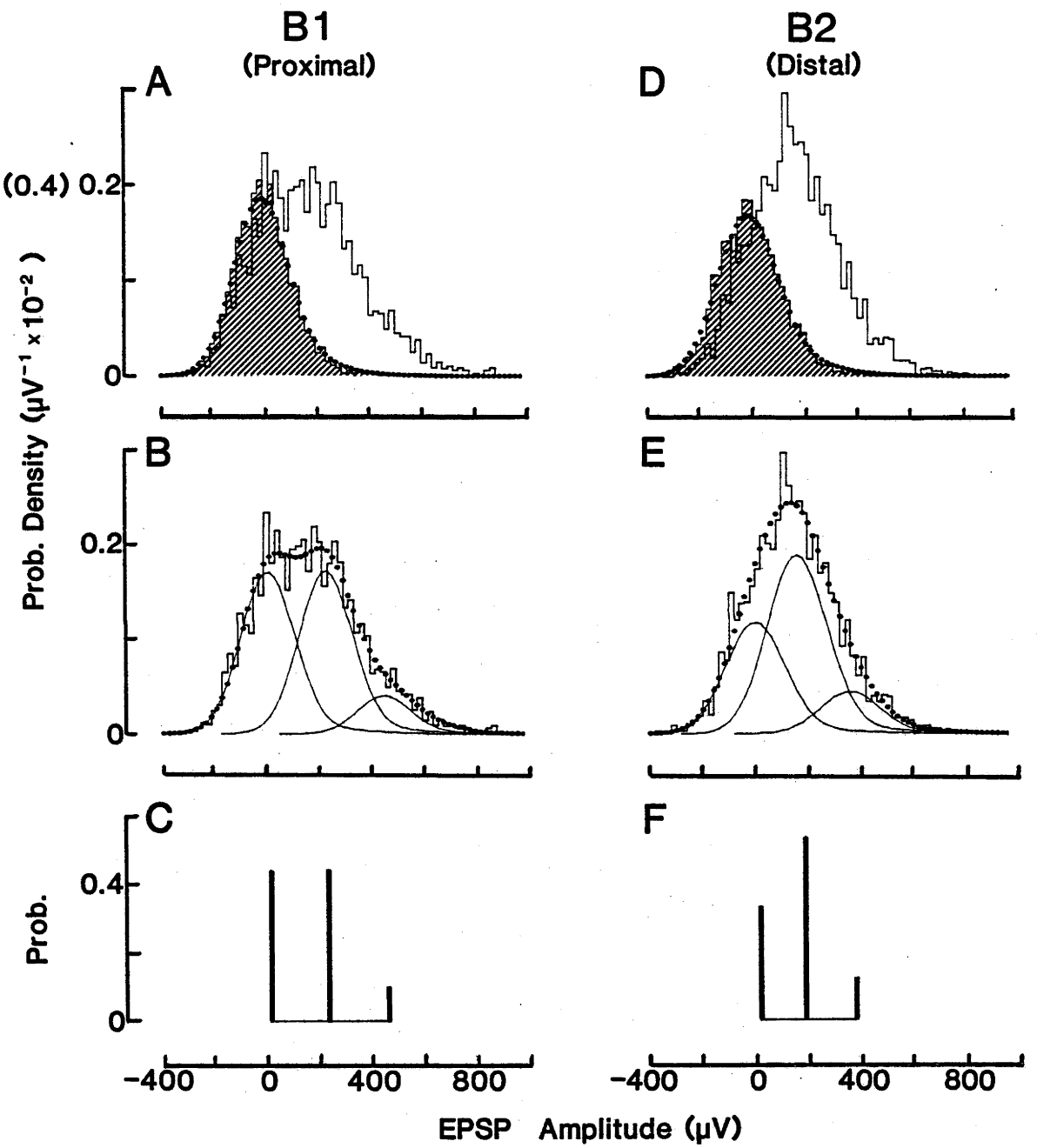
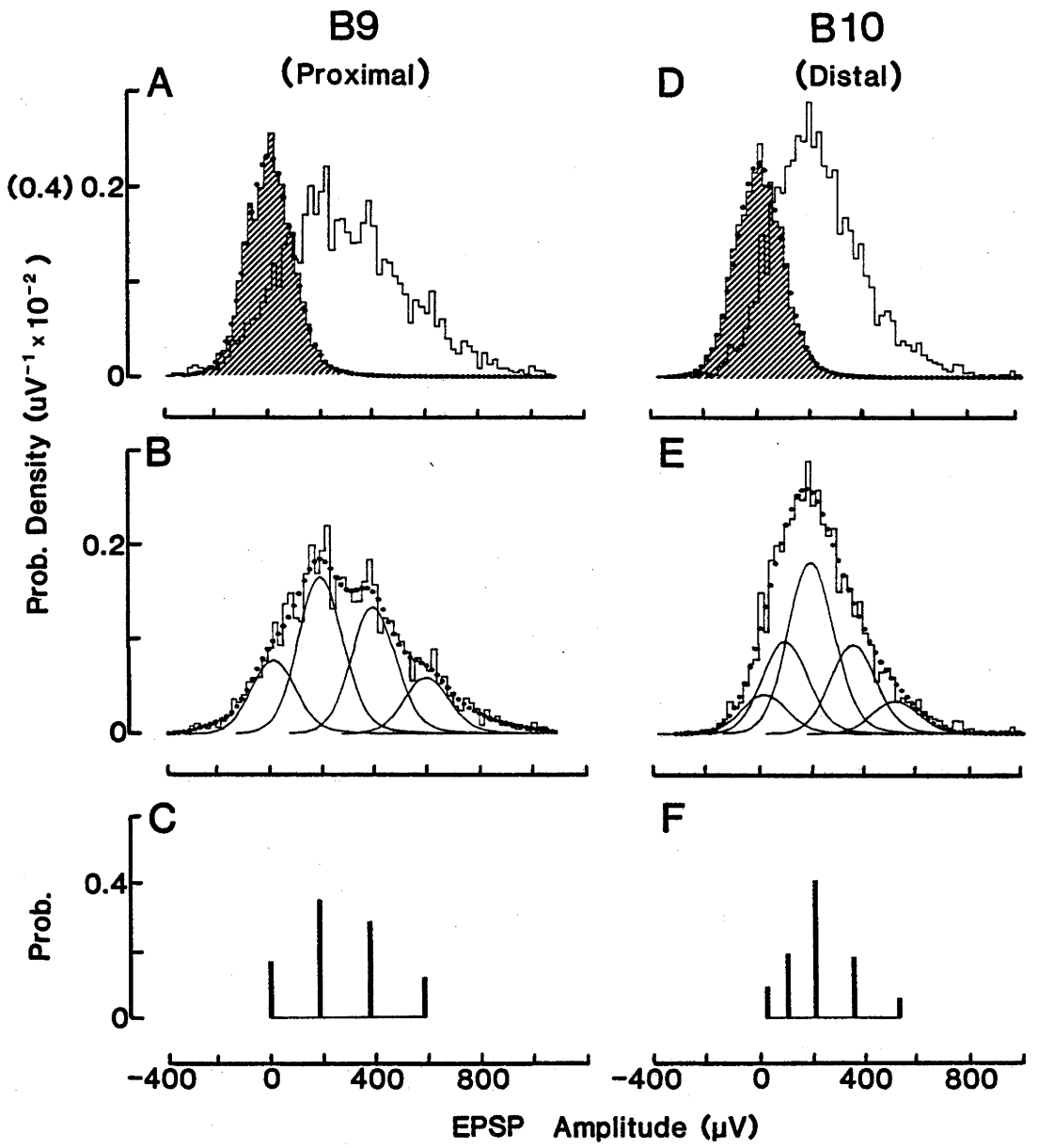

B1
(Proximal)
B2
(Distal)
A
D
(0.4) 0.2
0
Prob. Density (μV⁻¹ x10⁻²)
B
E
0.2
0
C
F
Prob.
0.4
0
-400
0
400
800
-400
0
400
800
EPSP Amplitude (μV)

Figure 4.13. Deconvolution analysis for EPSPs B9 and B10. Histograms are to be interpreted as for Fig. 4.9.


B9
(Proximal)
B10
(Distal)
A
D
B
E
C
F
(0.4) 0.2
0
0.2
0
0.4
0
Prob. Density (μV⁻¹ x 10⁻²)
Prob.
-400
0
400
800
-400
0
400
800
EPSP Amplitude (μV)

while the maximum number of discrete amplitudes (n) was varied within the range 2 to 50. The probabilites of release (p) were adjusted accordingly, so that $np = \bar{v}/v_1$, where $\bar{v}$ is the mean amplitude of the EPSP. The variable n was not restricted to the number of discrete amplitudes given by the deconvolution procedure, because as n is increased the probabilities of the larger discrete amplitudes become so small that they are unlikely to be resolved by the deconvolution procedure, or even to be sampled during an experiment.

The probabilities associated with the discrete amplitudes given by the deconvolution procedure were adjusted slightly before being tested against the binomial distributions. The small inacurracies in the location of the discrete amplitudes (particularly where they have low probabilities of occurrence) were compensated for by setting the deconvolved peak amplitudes near zero (representing failures) exactly at zero, and placing all the others (including those with $p < 0.05$) at intervals equal to the quantal size. The probabilities were then optimised (by MLE criteria) with a variant of the deconvolution procedure which did not allow the locations of the discrete amplitudes to vary. The adjusted amplitudes and probabilities are listed in Table 4.6. It was considered that this adjustment would allow the fairest comparison with the binomial distributions.

The probabilities of occurrence of the discrete amplitudes predicted by the binomial distribution were then compared to the corresponding 'observed' discrete amplitudes (deconvolution results) using the chi-square test. For EPSP

Table 4.6. Comparison of deconvolution results with binomial amplitude distributions, for EPSPs A12, B1 and B9.

	No. of quanta	deconv. results (μV)/prob.	adjusted deconv. results (μV)/prob.	best binomial approximation prob.	
A12	0.	17/0.193	0/0.177	0.206	
	1.	267/0.382	278/0.436	0.383	
	2.	523/0.296	556/0.260	0.285	
	3.	850/0.102	834/0.101	0.106	
	4.	1029/0.026	1112/0.026	0.021	for 4 & 5 quanta
Best binomial approximation: n=5, p=0.271					
Chi-square testing: X^2=38.8, d.f.=3, P<0.0005					
B1	0.	16/0.439	0/0.404	0.417	
	1.	240/0.443	224/0.463	0.424	
	2.	463/0.103	448/0.120	0.143	
	3.	640/0.015	672/0.013	0.016	
Best binomial approximation: n=3, p=0.253					
Chi-square testing: X^2=22.8, d.f.=2, P<0.0005					
B9	0.	5/0.166	0/0.195	0.199	
	1.	184/0.355	193/0.358	0.356	
	2.	381/0.287	386/0.273	0.279	
	3.	585/0.126	579/0.129	0.125	
	4.	754/0.033	772/0.037	0.042	for 4 to 8 quanta
	5.	925/0.012	965/0.008		
Best binomial approximation: n=8, p=0.183					
Chi-square testing: X^2=1.01, d.f.=3, 0.70<P<0.80					

A12, the lowest chi-square error occurred for n = 5 and p = 0.271; however even for these values the difference between the distributions was highly significant ($P < 0.0005$). Similarly for EPSP B1, the best fit with n = 3 and p = 0.253 gave $P < 0.0005$. However, the results for EPSP B9 could be fitted more closely. Binomial distributions with n between 6 and 16 (inclusive) were not significantly different at the 0.05 level of confidence from the discrete amplitude distribution given by the deconvolution procedure. The lowest chi-square value occurred for n = 8 and p = 0.183 ($0.70 < P < 0.80$).

4.4 DISCUSSION

4.4.1 EPSP variability from trial-to-trial

The first aim of this study was to determine the presence or absence of intrinsic amplitude variability in CA3-CA1 EPSPs. Visual inspection of the standard deviation records for 12 unitary EPSPs confirmed that these EPSPs do fluctuate from trial to trial more than can be attributed to baseline noise. For 11 of the 12 EPSPs, the peaks of the standard deviation records occurred at similar times to the peaks of the averaged EPSPs, indicating that they were not the spurious result of variations in EPSP latency. If they were, the maxima in the standard deviation records would have occurred at the rising phase of the averaged EPSP, as this has the greatest rate of change with time. For EPSP A9, the peak of the standard deviation record coincided with the

rising phase of the average, suggesting that in this case the latency variations may have contributed to the measured EPSP variability.

The amplitude fluctuations were also shown by comparing the standard deviations of the noise amplitude histograms with those of the noise-contaminated EPSP amplitude histograms. Although this method used voltage measurements from specified baseline and peak regions, rather than the whole time course of the EPSP, it enabled the statistical significance of the differences in the standard deviations to be shown. The differences were highly significant ($p < 0.0001$) for 9 of the 12 unitary EPSPs. It is possible that the other three EPSPs had no intrinsic variability, and that their amplitude histogram standard deviations exceeded those of the noise because of finite sampling errors. However, in view of the observations of the standard deviation records, this seems unlikely.

There were no EPSPs which could be shown with certainty not to have fluctuations in amplitude. This is an important point, because for the group Ia input to cat motoneurones, non-fluctuating EPSPs were used as evidence for neglible quantal variability ($CV_q < 0.05$, Edwards et al, 1976a; Jack et al, 1981). Our data cannot be used to support the assumption that the quantal EPSP at the CA3-CA1 synapse has neglible variability. (At the same time, it does not argue against it.)

As for the causes of EPSP amplitude fluctuation, two arguments can be made for some of the variability being due to intermittent failure of transmitter release, rather than

being entirely due to variability in the quantal size. The first is based upon the coefficients of variation of the unitary EPSPs. The CVs, listed in Table 4.1, range from 0.37 to 1.02 (mean 0.76). If an EPSP was generated by invariant release of a single quantum, the CV would be the coefficient of variation of the quantal unit (CV_q). The values we obtained were always greater than the CV_q measured at the neuromuscular junction, which is about 0.3 (Martin 1966). If an EPSP was generated by invariant release of more than one (N) quanta, then CV_q would need to be even higher to account for the measured CV:

$$\begin{aligned} CV_q &= \sigma_q / v_1 \\ &= (\sigma_E / \sqrt{N}) / (\bar{v}/N) \\ &= \sqrt{N}(\sigma_E / \bar{v}) \\ &= \sqrt{N}(CV) \end{aligned}$$

where σ_q and σ_E are the standard deviations of the quantal EPSP and the total EPSP respectively.

The second and probably stronger argument for intermittent failure to evoke an EPSP comes from the observation that some noise-contaminated EPSP amplitude histograms show prominent peaks over zero μV. The two best examples are for EPSPs A8 and A10 (Fig. 4.6), although there is also a suggestive peak for EPSP A12 (Fig. 4.6). All of the other unitary EPSP amplitude histograms have a large number of entries in the bins around zero μV, although distinct peaks for 'failures' cannot be resolved by eye.

Given that failures occur, it should not be automatically assumed that these are due to variability of the release mechanisms at the terminal. Other possibilities are that the action potential fails to propagate from the CA3 soma to the axon, or that block is occurring at axonal branch points. The former might happen if the action potential was shunted by tonic inhibitory conductances at the initial segment. (There is anatomical evidence for presumed inhibitory synapses onto the initial segment of pyramidal cell axons in the hippocampus; Kosaka, 1980 (rat); Somogyi et al, 1983a (cat); Somogyi et al, 1983b (monkey).) The evidence against this is that ~~suprathreshold~~ antidromic activation of CA3 axons reliably elicited somatic action potentials. There is no direct evidence against the possibility of axonal branch point block in the hippocampus, but there is from other preparations in which this question has been addressed. At the cat neuromuscular junction *in vitro*, Boyd and Martin (1956) found that the reduction of the endplate potential by 10 mM Mg^{2+} could be reversed by increasing the Ca^{2+} concentration. This was the opposite of the effect expected if branch point block were occurring, as both divalent cations suppress membrane excitability (Frankenhaeuser & Hodgkin, 1957). Kuno and Takahashi (1986) similarly found competitive rather than cooperative interactions between Ca^{2+} and Mg^{2+} in their effects on EPSPs in neonatal rat motoneurones *in vitro*. On the other hand, Henneman et al (1984) argued for alterations in conduction block within axonal arborizations as the cause of changes in

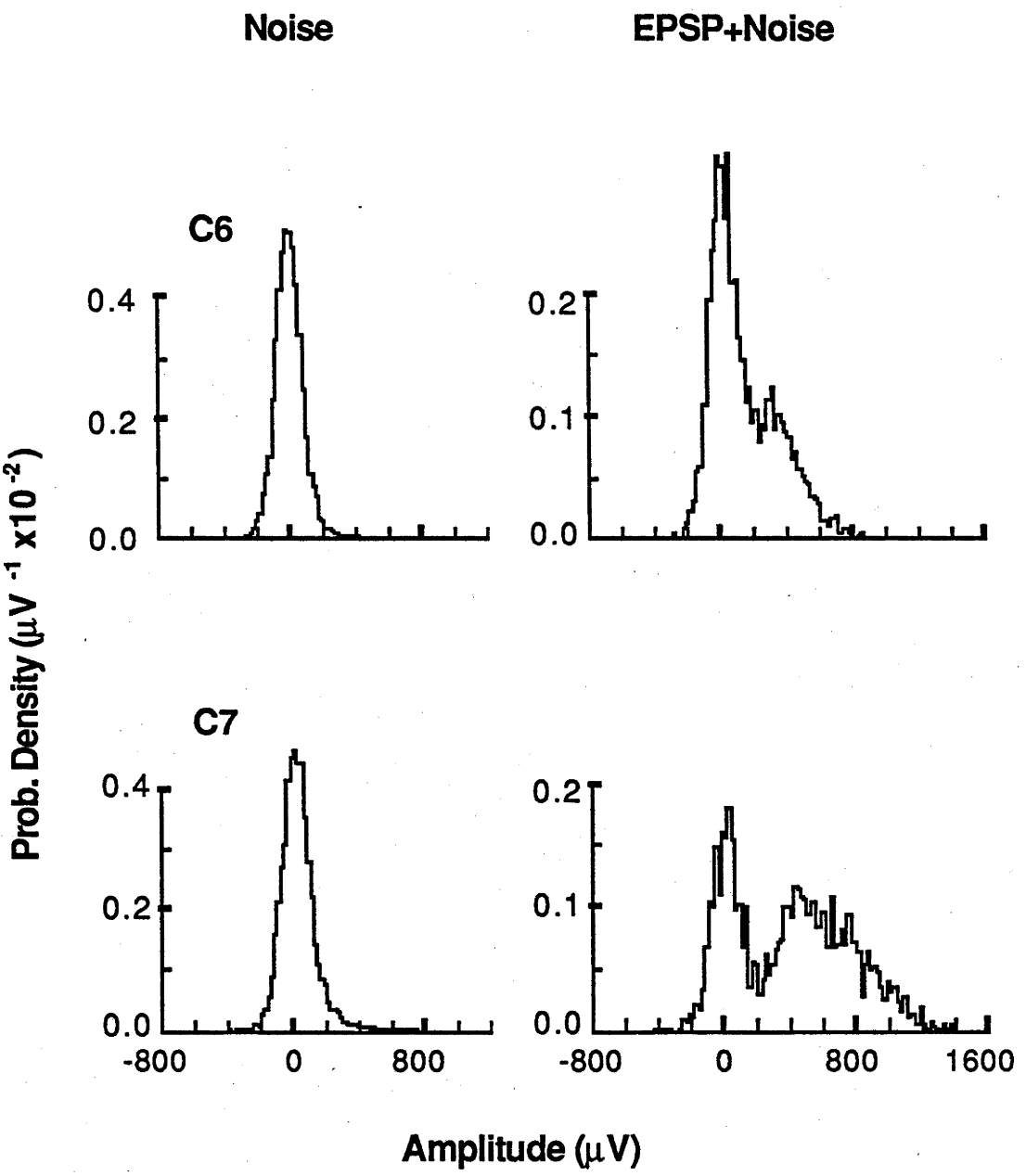
amplitude and time course of EPSPs recorded over 30-40 min in cat spinal motoneurones.

It is likely that some of the variability seen in the EPSPs evoked by stratum radiatum stimuli was due to afferents being near threshold for activation. This would have resulted in a disproportionate number of failures. Two of the EPSP amplitude histograms which were particularly suggestive of this are shown in Fig. 4.14. Note the clear peaks in the histograms at zero μV.

4.4.2 Quantal analysis by the method of variance

The method of variance was used to estimate parameters m and v_1 for the unitary EPSPs, and the reconvolved Poisson distributions were compared with the noise-contaminated EPSP amplitude histograms obtained in the experiments. It is worth establishing the appropriateness (or otherwise) of this method, because it is an extremely simple technique. However, it relies on the assumptions that there are a large number of quanta available for release and that their individual probabilities of release are very small (the Poisson approximation to the binomial distribution becomes accurate for $n>100$ and $p<0.05$; see Hoel, 1954). These assumptions hold for the neuromuscular junction when transmission is largely blocked by reduced Ca^{2+} and/or raised Mg^{2+}, but there is no independent evidence that they are true for CNS synapses in normal media. Several groups have nevertheless applied the method of variance to excitatory synaptic transmission in hippocampal slices (perforant path input to dentate granule cells: McNaughton et al, 1981; mossy

Figure 4.14. Noise and noise-contaminated EPSP amplitude histograms for EPSPs C6 and C7.


Noise
EPSP+Noise
C6
C7
0.4
0.2
0.0
0.2
0.1
0.0
-800
0
800
1600
Prob. Density (μV -1 x10 -2)
Amplitude (μV)

fibre input to CA3 neurones: Yamamoto, 1982; Higashima et al, 1986; Yamamoto et al, 1987; recurrent excitatory connections in CA3: Miles and Wong, 1986; compound EPSPs in CA1: Hess et al, 1987).

In this study, the Poisson parameters calculated by the method of variance provided good fits to the original EPSP amplitude distributions for seven of the 12 unitary EPSPs. On the other hand, for five EPSPs the fits were either poor or highly dependent upon the allowance made for quantal variance. The points that should be made about this result are (1) under the optimal conditions of obtaining a large number of EPSPs from a connection between single CA3 and CA1 neurones, this method frequently produced results which did not adequately fit with the experimental data, (2) even when a good fit was obtained, this did not neccessarily mean that the solution was the best or only one which could have fitted the data by chi-square criteria, and (3) if these EPSPs had been elicited by stimuli to the stratum radiatum and the number of failures had been disproportionately high (due to threshold variability), the variances of the distributions would have been greater, leading to a larger calculated quantal size. Relevant to this last point is the observation that the quantal sizes estimated by Hess et al (1987) using the variance method, for EPSPs in CA1 neurones evoked by stratum radiatum stimuli, were on average about twice those of this study (286 c.f. 149 or 137 μV).

4.4.3 Quantal size obtained by the deconvolution method

The deconvolution results for the majority of the 37 EPSPs fell into a signal-to-noise range which made their reliability uncertain. The three best results by this criteria had values for $\bar{v}_1/\sigma_N$ of 1.92, 1.94 and 2.08 and gave quantal size estimates of 273, 224 and 193 μV respectively. The first of these was for an EPSP evoked by activation of a single CA3 cell, while the other two were for EPSPs in pyramidal cells elicited by low-intensity stimuli to the stratum radiatum. It is interesting that the largest quantal size was for an EPSP in an 'atypical' CA1 neurone. The short time course for this unitary EPSP (see section 3.3.8) is suggestive of a shorter electrotonic distance between the synapse(s) and the recording site. This factor might have reduced the degradation of the quantal EPSP voltage between the site(s) of synaptic current injection and the electrode.

The quantal sizes determined here for CA1 pyramidal cells probably represent the upper end of the quantal size range, and for this reason they were resolvable. Even so, they were generally smaller than those calculated by Hess et al (1987) (v_1 = 240 ± 140 μV to 297 ± 129 μV; mean ± S.D., depending upon the method of calculation). The various formulae used by Hess et al (1987) are based on binomial or Poisson statistics, and they have been applied to histograms of EPSP amplitudes, constructed from about 100 records, which contain distinct peaks and troughs with approximately equal spacing. Only rarely did we observe histograms where this occurred, despite comparable noise levels. These differences are puzzling, but if the quantal size had been consistently greater than about 200 μV as reported by Hess et al, our

deconvolution methods would have routinely extracted it. In fact, our lowest noise recordings, with σ_N about 70 μV (Table 4.4A, EPSPs B5 and B6), would have resolved discrete amplitudes separated by 110 μV or more.

4.4.4 Quantal size of EPSPs evoked at different dendritic locations

For both group Ia and descending monosynaptic EPSPs in spinal motoneurons, the quantal size measured at the soma appears to be independent of the dendritic location of the synaptic contacts (Jack, et al, 1981; Edwards et al, 1983; Harrison et al, 1985). We adopted protocol 'B' because we were interested to determine whether this was the case for CA1 pyramidal cells, especially in view of the finding that CA1 pyramidal cells are discharged as readily by fibres running distally or proximally in the stratum radiatum (Andersen et al, 1980a). However, in this series we were never able to resolve discrete amplitude fluctuations for more than one EPSP in the same cell. The two EPSPs with the most reliable deconvolution results in this group (B1 and B9), were both evoked by stimulation of fibres running proximally in the stratum radiatum, so in these cells the 'proximal' quantal size may have been greater than the 'distal' quantal size.

4.4.5 Possible models for release underlying the EPSP amplitude distributions

Evidence from other systems (Jack et al, 1981; Redman & Walmsley, 1983b; Korn et al, 1982; Walmsley et al, 1987) suggests that the quantal EPSP may result from the release of

transmitter from a single synaptic release site. The amplitude histogram for EPSP A12, for example, could then be explained by an afferent which failed to release transmitter for 19% of trials, released transmitter from one release site for 38% of trials, from two sites for 30% of trials, and so on (for at least three release sites). The noise-free amplitude histogram could not be fitted to a simple binomial distribution, indicating that the underlying probabilities for each of these release sites were not equal. The interpretations for EPSPs B1 and B9 are clouded by the possibility that some or all of the variations in peak amplitude could have resulted from intermittent excitation of one or more afferents. For example, either one or two axons might have been involved in eliciting EPSP B1. If two were involved, the 240 μV amplitude (Fig. 4.12) could have occurred when either (a) both axons were excited but transmitter release only occurred at one of the two release sites, or (b) only one of the two axons was excited but it did release transmitter on that occasion. When both axons were excited and both released transmitter, the maximum amplitude would have occurred. Alternatively only one axon may have been involved, with two release sites.

A similar set of possibilities may be listed for EPSP B9, involving up to three axons. Binomial distributions were found which fitted the data for this EPSP and the best of these was for $n = 8$ and $p = 0.183$. This would correspond to eight transmitter release sites, each with a probability of release of 0.183. This model would not fit if some of the

amplitude fluctuations were due to failure to activate the axon(s).

4.4.6 Further comments on quantal analysis by the deconvolution method

The advantage of the deconvolution technique used in this study is that the discrete amplitudes and their associated probabilities are free to vary in any way to best fit the experimental data. If the solution then obtained has the features expected for the quantal theory for synaptic transmission, such as almost equally spaced components (including one near zero, for 'failures'), then this adds a measure of confidence that the solution represents a true phenomenon underlying the data, rather than one imposed upon it. There is now a considerable body of literature in support of non-uniformity of release probabilities for synapses both in the CNS (Jack et al, 1981; Redman & Walmsley, 1983b; Walmsley et al, 1987; but c.f. Korn et al, 1982) and at the neuromuscular junction (Hatt & Smith, 1976; D'Alonzo & Grinnell, 1985; Bennett et al, 1986; Robitaille & Tremblay, 1987). In view of this it seems unwise to use techniques for quantal analysis which impose uniform probabilities for release, such as those based on the binomial distribution or its Poisson approximation.

The deconvolution method does make an assumption which should be considered when interpreting the results. By fitting the experimentally-obtained EPSP amplitude histograms with discrete amplitudes convolved with the noise, the variance in the quantal EPSP is assumed to be negligible.

There is evidence for this at the group Ia connection to the motoneuron (Jack et al, 1981), and other studies in the CNS have ignored quantal variance in their analysis (e.g. Korn et al, 1982; Hess et al, 1987), but as more information becomes known about synapses in the hippocampus, this assumption may be shown to be false. If significant quantal variability is neglected, the quantal size calculated by the deconvolution technique will be incorrect (with a tendency to underestimate it).

Therefore there are several possible explanations for the difficulties in resolving quantal EPSPs in this study. The most obvious is that they may generally be too small to be detected above the level of the baseline noise. It could also be that there is significant quantal variability which has led to systematic underestimation of the quantal size. The noise-contaminated amplitude histograms for EPSPs A8 and A10 (Fig. 4.6), which had distinct peaks for failures, but not for other quantal amplitudes, might be explained by quantal variability. It would be feasible to implement a variant of the deconvolution procedure which would allow for quantal variance and adjust it to find the best fit to the data. However it is likely that the introduction of another variable (CV_q being unknown) would lead to multiple solutions with similar goodness of fit.

Discrete amplitudes would also be difficult to discriminate if there were significant differences between the amplitudes of the quantal EPSPs originating from different release sites in a synaptic connection, as the resultant multiple entries in the amplitude histogram might

be too close together to be resolved. If the differences were greater between release sites at the terminals of different afferents, protocols which allowed more than one axon to be activated (e.g. by stimulation of the stratum radiatum) would be a particularly disadvantaged. Hopefully, techniques will be developed to circumvent the above problems. For example, the reduction of baseline noise, and perhaps even the ability to measure EPSPs from connections involving a single release site, may become possible with some of the more recently-developed neuronal culture preparations in which synaptic connections are formed *in vitro* (e.g. Pun et al, 1986).

Chapter Five:

SYNAPTIC PLASTICITY: PAIRED-PULSE FACILITATION AND LONG-TERM POTENTIATION INVESTIGATED FOR SMALL EPSPS IN CA1 NEURONES

5.1 INTRODUCTION

One of the incentives for the application of quantal analysis to EPSPs in CA1 pyramidal cells is the information it ought to provide about the mechanisms underlying synaptic plasticity. Localisation of the altered processes to presynaptic or postsynaptic regions would be particularly valuable for LTP, because the locus of change for this form of plasticity is a controversial issue (see Chapter 1).

As a prerequisite for such a study, it is necessary to show that plasticity can be experimentally induced in EPSPs of small amplitudes. Preferably, unitary EPSPs should be used rather than small compound EPSPs, because the security of presynaptic activation associated with unitary EPSPs gives confidence to interpret any changes in the EPSP in terms of changes in release parameters. It is also interesting in itself to determine whether synaptic modifications are expressed at the level of the single cell-to-cell connection.

In this chapter, experiments are described which begin to address these issues. The emphasis is on LTP, but paired-pulse facilitation was examined in some experiments. Post-

tetanic augmentation and potentiation have not been investigated, as trial studies showed difficulties in achieving adequate resolution of these rapidly decaying processes. (The limitation is in obtaining sufficient records to gain noise-free averages over epochs of a few seconds.) The LTP studies included some initial experiments using extracellular fields and large compound EPSPs, to check that the induction protocols used were adequate. In a further series, a variety of paradigms were used in attempts to induce LTP in small compound EPSPs evoked by stratum radiatum stimuli. In the final experiments, LTP was compared for unitary EPSPs and large compound EPSPs evoked in the same CA1 neurones.

5.2 METHODS

5.2.1 Paired-pulse facilitation

The unitary EPSPs tested for paired-pulse facilitation were a sub-group of those presented in Chapter 3, and were obtained as described in Section 3.2. The CA3 cells were activated by short current pulses, adjusted to evoke single action potentials, delivered in pairs separated by 15-200 ms, in a 1 Hz cycle. A separation of 25 ms between the pulses was the first interval tested, and if the penetrations could be maintained, a range of paired-pulse intervals was tested. Averages were constructed off-line from the 200-300 records saved for each interval.

The peak of the second EPSP of each pair usually occurred during the decay phase of the first EPSP. Therefore the voltage contributed by the first EPSP to the peak amplitude of the second EPSP was calculated and subtracted, before determining the degree of facilitation. The voltage contributed by the first EPSP to the peak amplitude of the second EPSP was calculated from the decay of the same averaged unitary EPSP evoked by regular 2 Hz activation, obtained before and/or after the paired-pulse EPSPs. The percentage decay in amplitude between the time of the peak and the appropriate delay (paired-pulse interval) was measured for the single EPSP and applied to the peak voltage of the first EPSP in the pair. This voltage was then subtracted from the peak voltage of the second EPSP in the pair. The degree of facilitation of the second EPSP was then expressed as the percentage increase of its mean peak amplitude over that of the first EPSP.

5.2.2 Long-term potentiation

In all experiments with LTP, the same slice was never used to test more than one CA1 cell (or extracellular field, or CA3-CA1 pair), since the tetani delivered to the stratum radiatum would presumably have affected other cells in the slice. In addition, stimuli to the stratum radiatum were kept to a minimum while searching for cells, to avoid the possibility of inducing LTP prematurely.

For extracellular field recordings (4 experiments) the stimulating electrode was placed in the mid-stratum radiatum of CA1, and the recording electrode (filled with 2M NaCl and

broken back to a resistance of 10-20 MΩ) was positioned in the CA1 stratum pyramidale. Both the test and the tetanic stimuli were delivered through the same stimulating electrode. The test stimuli were 20-80 μA, 0.1 ms cathodal pulses delivered at 2 Hz. Each tetanus consisted of three trains of 20 pulses at 100 Hz (same intensity as the test stimuli), delivered at intervals of 10-15 s.

In the experiments involving compound intracellular EPSPs (but not unitary EPSPs), 10 μM bicuculline methiodide was added to the ACSF to reduce $GABA_A$-mediated synaptic inhibition. This was intended to serve two functions, (1) to reduce the contamination of the EPSPs by IPSPs, and (2) to facilitate the induction of LTP (Wigstrom & Gustafsson, 1985). As described in the previous chapter, the whole of area CA3 was cut away with a scalpel blade in these slices, to prevent the propagation of spontaneous activity from the disinhibited CA3 region.

For the experiments with small compound EPSPs, (mean peak amplitudes of less than 500 μV), low-intensity stimuli were delivered to the stratum radiatum (see Section 3.2.2). Another stimulating electrode was positioned in the CA1 stratum radiatum to provide additional synaptic input during the tetani. The advantage of this setup was that the test stimulus did not have to be adjusted for delivery of a strong tetanus (with the possibility of hysteresis on resetting it), because the strong synaptic depolarization was provided by the other input. It also eliminated concerns about local tissue damage due to the greater currents during the tetani, which might affect the test EPSP if they were delivered

through the same electrode. Each 'tetanus' consisted of 3-6 trains of stimuli, at 10-15 s intervals; each train being 20 impulses delivered at 100 Hz. The stimulus intensity for the additional electrode (active only during the tetani) was usually in the range 20-100 μA. This stimulating electrode was positioned 200-500 μm further away from the CA1 cell than the test electrode, but at the same distance from the stratum pyramidale, so that afferents projecting to the same region of the apical dendrites would be activated by both electrodes.

In some experiments the small compound EPSPs were conjoined with depolarizing current pulses injected into the CA1 neurone, rather than with a strong tetanus (see results).

The electrode placement for the unitary EPSP experiments was as shown in Fig. 3.1. After CA3-CA1 pairs with synaptic connections were found, the stimulating electrode in the CA1 stratum radiatum was used to (1) evoke a large compound test EPSP (2-8 mV), during the pre-tetanus and post-tetanus periods, and (2) to deliver a strong tetanic input at the same time as the unitary afferent was tetanized. Two constant current stimulators were connected to the electrode via a switch. The current strength could then be switched between the values used for the single stimulus and the tetanus, thus avoiding the problem of hysteresis.

Unitary EPSPs were evoked by activation of the CA3 cell at 2 Hz, and a large compound EPSP was evoked once every 15 s. These records were saved during a pre-tetanus control period of 10-20 min. Each tetanus consisted of 1-6 trains of

impulses, 10-15s apart, each train being 20 impulses delivered at 100 Hz. The current strength for tetani delivered through the stratum radiatum electrode ranged from 9-160 μA. The CA3 cell was activated during the tetani at the same frequency, by repeated short intracellular current pulses (20 for each train). Intracellular records during the tetani were saved, so that the CA3 records could be checked to ensure that the presynaptic neurone was repetitively activated.

In some cases postsynaptic depolarization during the tetanus was provided by injection of current into the CA1 cell, instead of by tetanization through the stratum radiatum electrode. Depolarizing current pulses (7-9 nA) of 300 ms duration were delivered to the CA1 neurone, commencing at the start of each train of short pulses delivered to the CA3 cell.

The regions for measurement of EPSP peak amplitude were selected as described in the previous chapter. The mean peak amplitudes of the EPSPs were calculated for successive 1 min intervals, and the minute-average plots were used to compare the EPSP amplitudes before and after the tetani.

EPSP amplitudes before and after tetanization were compared by calculating the mean amplitude during (1) the five minutes immediately prior to the tetanus and (2) the period 5-10 minutes following the tetanus. (Note that post-tetanic potentiation decays within 1-2 min in the hippocampus; McNaughton, 1982; Gustafsson & Wigstrom, 1988.)

5.3 RESULTS

5.3.1 Paired-pulse facilitation

Ten unitary EPSPs were tested for paired-pulse facilitation at an inter-pulse interval of 25 ms. Seven of the EPSPs showed facilitation of the mean peak amplitude of the second EPSP (ranging from 14% to 160%), while one showed a minimal change (3%) and two were depressed (-20% and -63%). The results for the ten EPSPs are listed in Table 5.1. The three examples of averaged EPSPs in Fig. 5.1 indicate the variability in the degree of facilitation for different unitary EPSPs. The average facilitation for the 25 ms inter-pulse interval was 35% (SD=58%, n=10).

In general, the CA1 neurones were not held for a sufficiently long time to examine the full time course of the facilitation at different intervals. However, five unitary EPSPs were tested for at least one other inter-pulse interval. These results are listed in Table 5.1.

5.3.2 LTP - extracellular field recordings

The initial experiments for the LTP studies involved recordings of extracellular fields from the CA1 stratum pyramidale of four different slices. The amplitude of the population spike was used as an indicator of the relative number of CA1 cells discharged by the test stimulus, before and after tetanization. Fig. 5.2A shows the averaged fields from one of the slices, with the responses before and after the (two) tetani superimposed. In this case there was almost no population spike present during the control period, with a

Figure 5.1. Paired-pulse facilitation of averaged unitary EPSPs. These EPSPs were evoked at 25 ms intervals in a 1 s cycle. **A**, an EPSP which showed marked facilitation (160%). **B**, one which showed little change (3%), and **C**, one which showed a depression of the second EPSP (-20%).

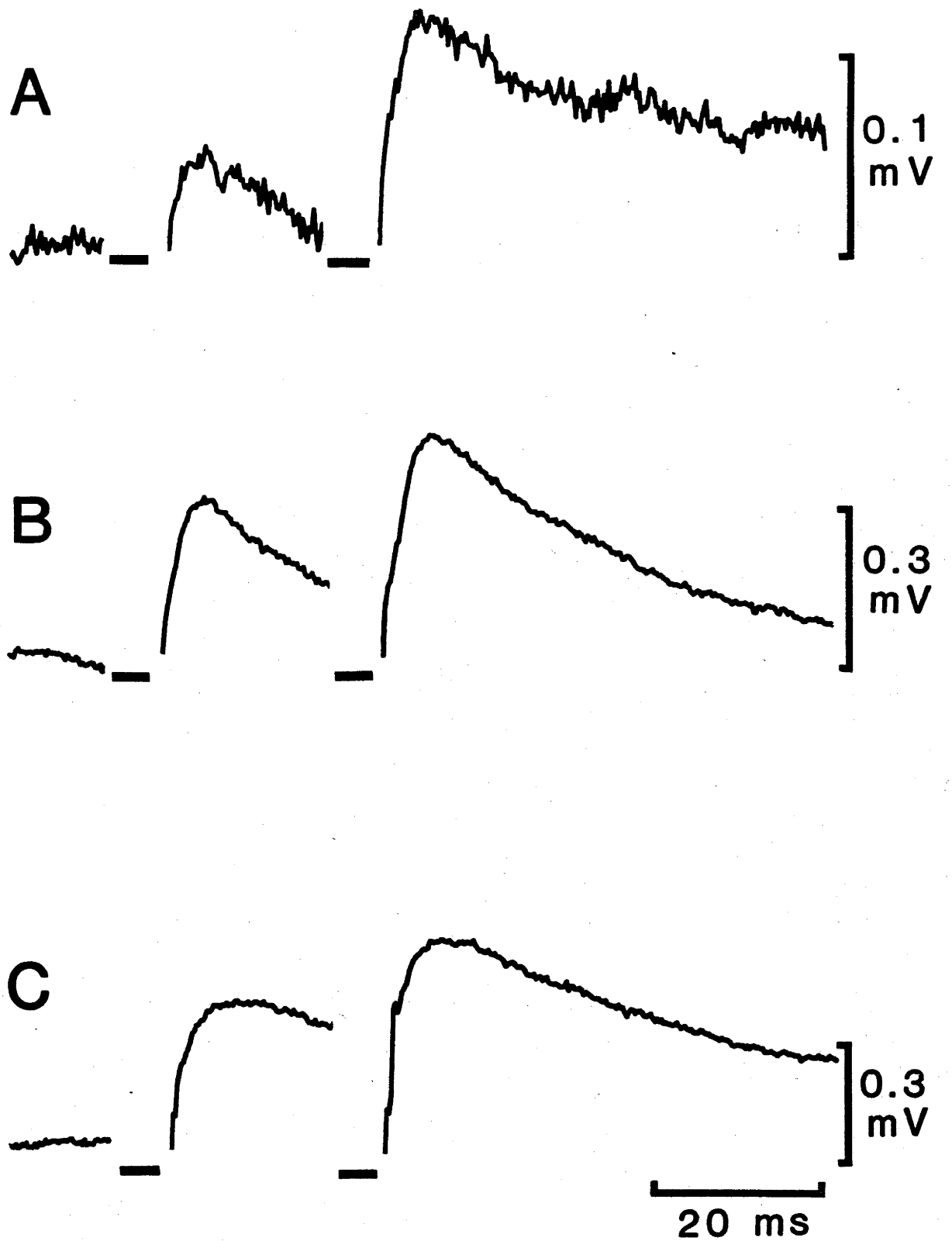
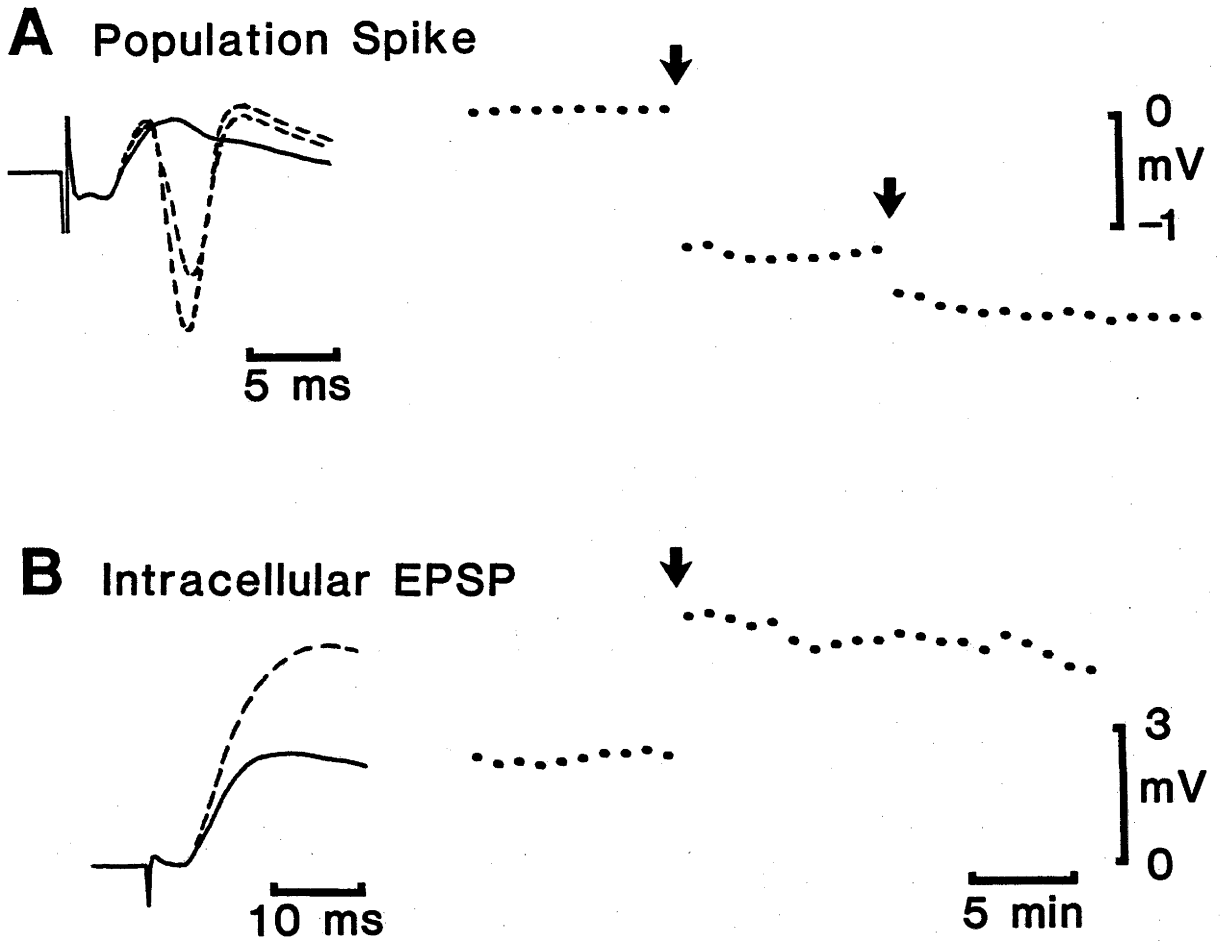

A
0.1
mV
B
0.3
mV
C
0.3
mV
20 ms

Table 5.1. Paired-pulse facilitation of averaged unitary EPSPs. (Percentage increase in amplitude of 2nd EPSP)

Interval (ms):	15	25	35	50	100	200
1		61				
2		35		17		
3		43				
4	-26	3	-13	-1	2	
5		14				
6		-63		23		
7		160				
8		88				
9		-20	-27	-22	12	-9
10	-11	24	8	-10		

Figure 5.2. LTP of an extracellular field and a large compound intracellular EPSP. Both were evoked at 2 Hz during the pre-tetanus and post-tetanus periods. In this and all subsequent figures, the arrows indicate the time of the tetani. **A**, the extracellular field recorded from the CA1 stratum pyramidale showed a sustained enhancement of the population spike after tetanization through the stratum radiatum electrode. The averaged post-tetanic fields (broken lines) are superimposed on the averaged pre-tetanus field (solid line). Each tetanus was three trains delivered at the test stimulus intensity, 55 μA. The minute-average shows the timing of the changes in (negative) amplitude of the population spike. **B**, superimposed averages of an intracellular EPSP before (solid line) and after (broken line) tetanization. The tetanus was delivered through two electrodes in the stratum radiatum (9.8 μA and 21 μA) and consisted of three trains. The minute-average shows the change in peak amplitude for this EPSP.


A Population Spike
0
mV
−1
5 ms
B Intracellular EPSP
3
mV
0
10 ms
5 min

growth to 1-2 mV after the tetani. Each shock in the tetanic trains was delivered at the same current intensity as the test stimulus (55 μA, 0.1 ms). The minute-average plot of the population spike amplitude indicates that the changes occured at the time of the tetanus, and were sustained for the duration of the recording. The superimposed fields also show that the slope of the rising phase of the underlying field EPSP was increased after the tetani.

The other three fields tested all showed persistent increases in the population spike amplitude following tetanic activation. Two of these had small population spikes initially, with subsequent large increases in amplitude (about 300% and 310% respectively. The third, which was obtained in the presence of 10 μM bicuculline methiodide, had a larger (1.5 mV) population spike initially. This showed only a 40% increase in amplitude, but following the tetanus a second spike appeared on the field waveform about 8 ms after the first, indicating that some of the CA1 neurones were discharging more than once for each stimulus.

5.3.3 LTP - large compound EPSPs

Although called 'large', the four compound EPSPs in these experiments were all well below the action potential theshold initially, with peak amplitudes of 1.5-2.5 mV during the pre-tetanus control period. In addition to the tetani given through the test electrode (same current strength as the test shocks, 8.5-10 μA), stronger tetani (13-200 μA) were delivered at the same time through a stimulating

electrode in the stratum radiatum, but on the other side of the apical dendrites.

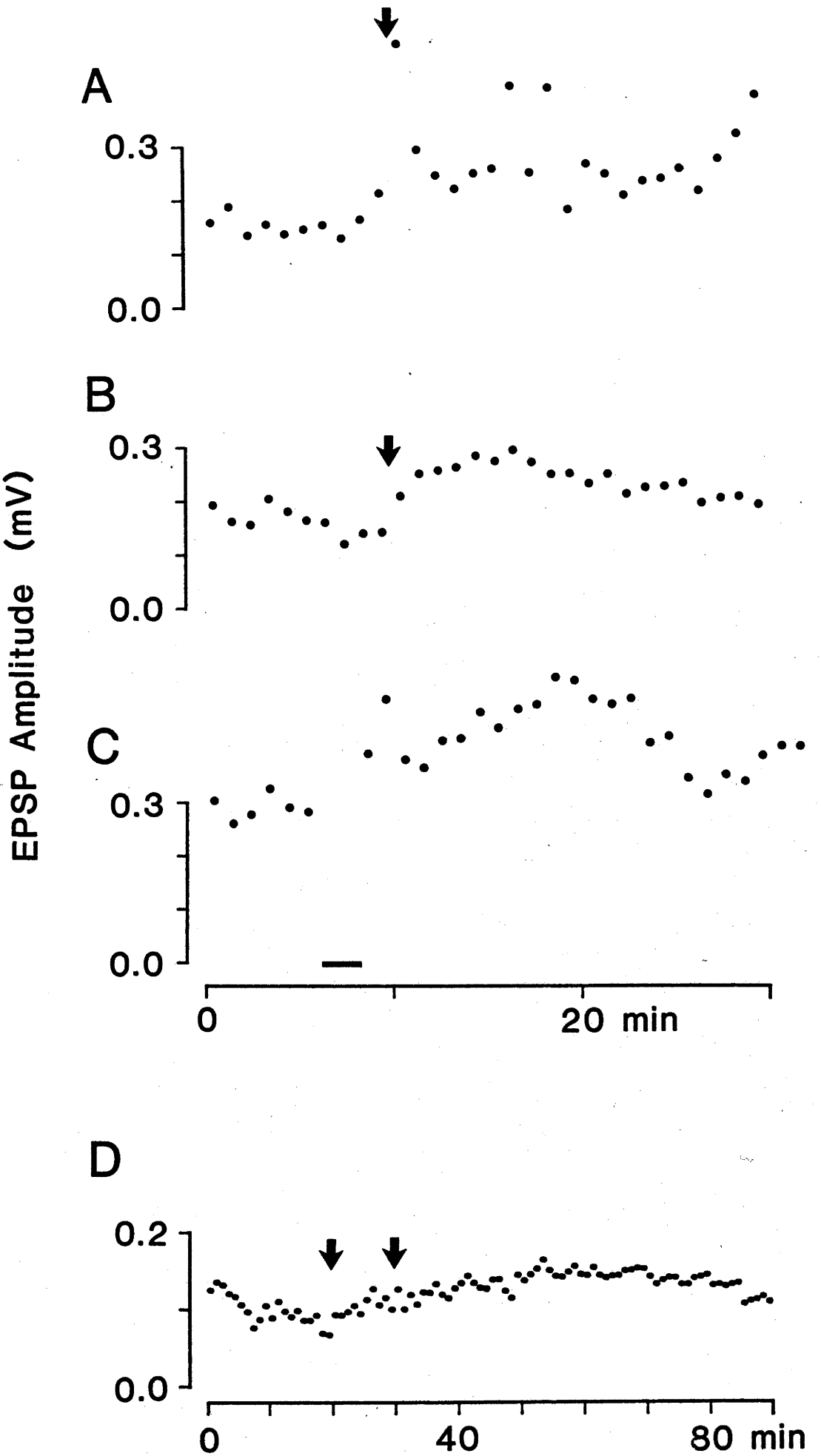
Three of the four EPSPs showed a sustained potentiation after the tetani. One of these is illustrated in Fig. 5.2B. The increase in mean peak amplitude, for the period 5-10 min after the tetanus compared to the control period, was 106% for this EPSP. The increases in amplitude for the two other enhanced EPSPs were 90% and 39%, for the same periods. One EPSP was unchanged by the tetani (4% difference between the post-tetanus and pre-tetanus mean amplitudes).

5.3.4 LTP - small compound EPSPs

Forty small compound EPSPs (mean peak amplitude <500 μV) evoked in CA1 pyramidal neurones were recorded before and after tetanization. The results are grouped according to the protocols used to deliver the tetani.

(1). Twenty-six cells were tetanized through the test electrode at the test stimulus strength, with a concurrent stronger (but identically-timed) tetanus delivered through another electrode close to the first in the stratum radiatum. For two of the 26 EPSPs, the mean peak amplitude increased following the tetani, with the onset of the changes coincident with the time of the tetani (Fig. 5.3A & B). The increments in amplitude from the 5 min pre-tetanus period to the 5-10 min post-tetanus period were 88% and 84% respectively. For the first of these EPSPs, the increased amplitude was sustained for the period of the recording (Fig. 5.3A). However, the second EPSP (Fig. 5.3B) showed a gradual

Figure 5.3. Minute-averages of the peak amplitudes for the four small compound EPSPs which were enhanced following tetanization or conjunction with postsynaptic depolarizing pulses. The protocols were **A**, three trains, 5.1 μA through the test electrode and 85 μA through the additional electrode in the stratum radiatum; **B**, three trains; 18 μA and 25 μA through the two electrodes; **C**, the small compund EPSP (5 μA stimulus) was conjoined with a 5 nA, 100 ms depolarizing pulse injected into the postsynaptic cell, for 3 minutes (bar). The stimulus rate was continued at 2 Hz. **D**, each tetanus consisted of three trains, 2.8 μA and 10 μA through the test and the additional tetanizing electrodes respectively, and in addition a 15 nA 300 ms depolarizing pulse injected into the postsynaptic cell (coincident with each train).


A
0.3
0.0
B
0.3
0.0
EPSP Amplitude (mV)
C
0.3
0.0
0
20 min
D
0.2
0.0
0
40
80 min

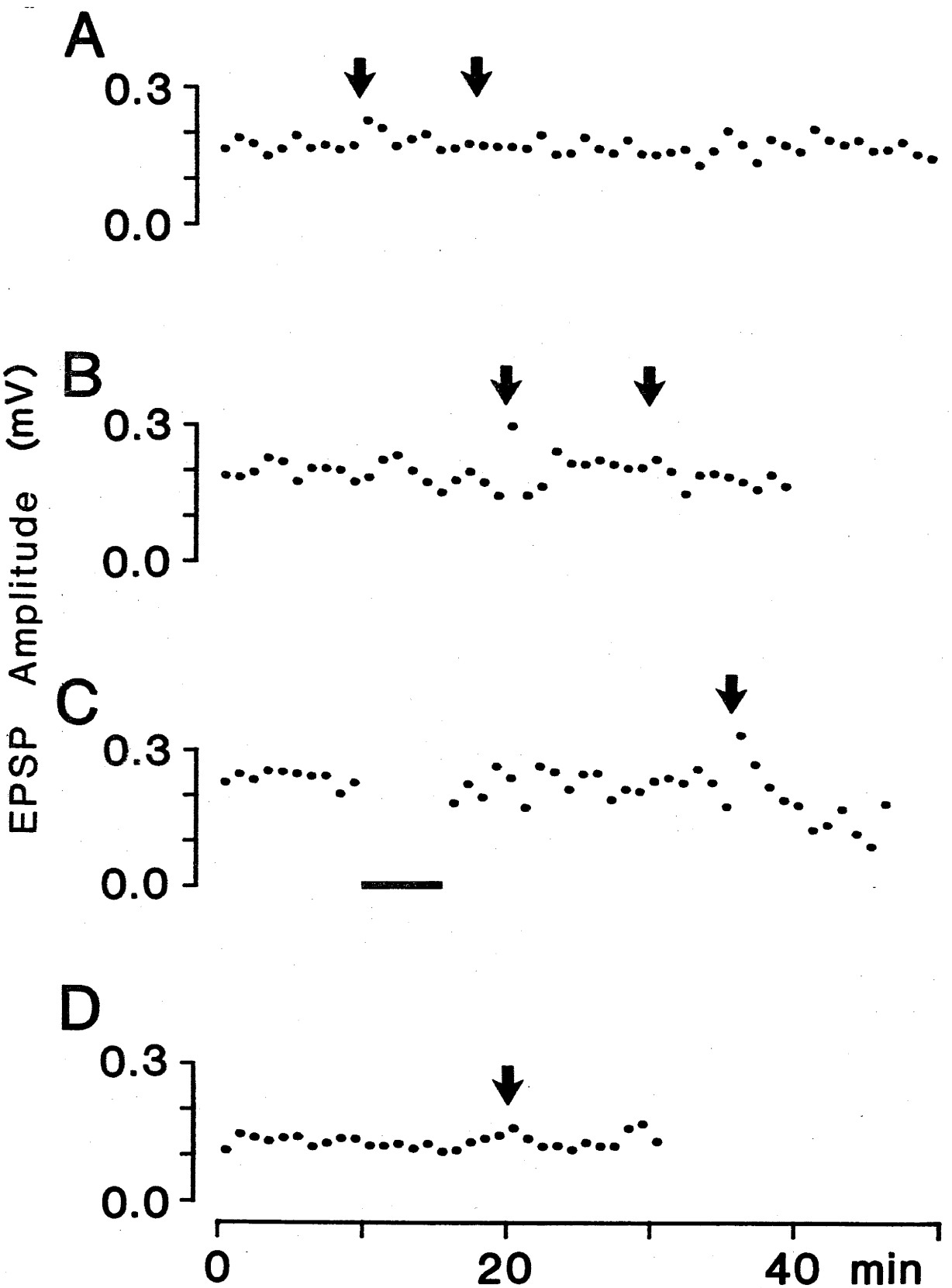
decline, almost returning to the initial control amplitude by 20 min after the tetanus.

The other 24 EPSPs tested with this protocol showed no change in mean peak amplitude which could be attributed to the tetani. The mean percentage change in amplitude from the control period to the 5-10 min post-tetanus period was 0.5% (SEM=6.1%, n=24). Lumping the data from this group of 24 EPSPs together, the mean EPSP amplitude before the tetanus was 223 μV, and 226 μV for the period following the tetanus (1.4% change). Where individual EPSPs showed drifts in their amplitude during the course of the recording, the timing of the changes was not related to the tetani. Examples of EPSPs showing no persistent response to tetani are illustrated in Fig. 5.4A and 5.4B. In some cases the EPSPs amplitudes were increased for 1-2 min following the tetani, before returning to the control value (e.g. Fig. 5.4A and 5.4B, first tetani for each).

(2). For five EPSPs, the inputs were not tetanized, but instead conjoined with depolarizing current pulses injected into the postsynaptic cell. Stimulation was continued at the test intensity and frequency (2 Hz), during the conjunction period, which lasted for 3-6 min. The current pulses injected into the CA1 cells were 5-7 nA, 100-400 ms in duration, and timed to start at the peak of the EPSP (protocol used by Wigstrom et al, 1986a; Gustafsson et al, 1987).

One EPSP showed an increase of 59% in mean peak amplitude for the period 5-10 min after the conjunction (Fig. 5.3C). Another increased in amplitude by 33% between the

Figure 5.4. Minute-averages for four examples of EPSPs which did not show sustained amplitude potentiations following tetanization or conjunction with postsynaptic depolarizing pulses. The protocols were **A**, three trains for each tetanus, 3.4 μA through the test electrode, and 44 μA and 60 μA through the additional stratum radiatum electrode for the first and second tetani respectively; **B**, three trains for each tetanus, test electrode 2.7 μA and the additional tetanizing electrode 200 μA in each case; **C**, the bar indicates a 6 min conjunction of the test stimulus (8 μA, continued at 2Hz), with a 7 nA 400 ms depolarizing pulse injected into the postsynaptic cell. The arrow indicates tetanization with the additional stratum radiatum electrode (85 μA). **D**, three trains, 3 μA and 50 μA through the stratum radiatum electrodes, conjoined with 10 nA 300 ms depolarizing pulses into the postsynaptic cell.


A
0.3
0.0
B
0.3
0.0
EPSP Amplitude (mV)
C
0.3
0.0
D
0.3
0.0
0
20
40 min

measurement regions, but it was apparent from observation of the minute-average plot that this was likely to be the continuation of a gradual increase which commenced during the initial control period. The remaining three EPSPs tested with this protocol showed slight declines in amplitude (1-12%). The minute-average plot for one of these is shown in Fig 5.4C. There was no persistent amplitude potentiation of this EPSP after it was later tetanized through the stratum radiatum electrodes (Fig. 5.4C).

(3). Nine cells were given a combination of strong tetanic activation and a postsynaptic depolarizing pulse during the tetanus. The tetani were delivered both through the test electrode (at the test intensity) and through the other stratum radiatum electrode (10-70 μA). The postsynaptic depolarizing pulses were 8-15 nA, 300 ms in duration, and commenced at the same time as the first shock in the tetanic train. The minute average for one of the nine EPSPs is shown in Fig. 5.3D. The amplitude of this EPSP increased (although gradually) following two tetani 10 min apart. The change in amplitude from the 5 min period immediately before the first tetanus, to the 5-10 post-tetanic period, was 41%. However, the maximum minute-average amplitude, 30-40 min following the tetani, was barely greater than during the first few minutes of the recording (Fig. 5.3D).

None of the other eight EPSPs tested with this protocol showed persistent changes in amplitude in response to the tetani. Fig. 5.4D is the minute average for one of these EPSPs. The mean percentage change in amplitude from the

control period to the 5-10 min post-tetanus period was -6.0% (SEM=8.8%, n=8). The overall mean amplitude for this group (n=8) showed a slight decline, from 126 μV to 117 μV (-7.0%). For five of these cells, the tetani were repeated 10-15 minutes after the first tetanus, without subsequent enhancement.

In summary, three different protocols were used in attempts to induce LTP in small compound EPSPs. Of the 40 EPSPs tested, only four showed persistent increases in their minute-average amplitude, subsequent to the tetani or conjunction period. The minute-averages for the four EPSPs which were potentiated are shown in Fig. 5.3.

5.3.5 LTP - unitary EPSPs

(a). Unitary EPSPs and large compound EPSPs tetanized together

The aim of these experiments was to compare the effects of tetani on unitary EPSPs and larger compound EPSPs, where both were evoked in the same neurone. In the event of difficulty in obtaining LTP for the unitary EPSPs, it was intended that the compound EPSPs would indicate whether conditions had been adequate for induction of LTP in at least some of the afferents.

Data from three cells were rejected because the minute-average amplitudes of the compound EPSPs and/or the unitary EPSPs were not stationary during the pre-tetanus baseline recordings. In several more cases the recordings were

abandoned because the tetani induced prolonged (about 30-60 s) depolarizations of the CA1 neurone. These were out-lasted by depressions of the synaptic responses (presumed spreading depression; see Dingledine, 1984, p. 425; Snow et al, 1983; Mody et al, 1987). This occurred particularly when the strongest current intensities were used during the tetani (e.g. >50 μA).

However, nine unitary EPSPs were successfully carried through the experimental protocol which included (a) a 10 -20 min initial control period, during which records were collected for both the unitary EPSP (evoked at 2 Hz) and the compound EPSP (evoked through the stimulating electrode once every 15 s), (b) tetanic activation of the CA3 neurone concurrent with tetanic stimuli delivered by the stimulating electrode, and (c) a period of at least 15 min following the tetanus during which records were collected for both the unitary and the compound EPSPs.

In two of the nine CA1 neurones, neither the compound EPSP nor the unitary EPSP showed more than a minimal increase in mean amplitude after the tetani. For one cell the unitary EPSP peak amplitude averaged 106 μV before the tetanus and 112 μV during the 5-10 min post-tetanus period. The compound EPSP averaged 4.51 mV and 5.40 mV during the same periods. The mean amplitudes of both EPSPs declined to the control values after a further 5-10 min. For the other neurone, both the unitary and the compound EPSPs were essentially unchanged by the tetani. The mean amplitudes of the unitary EPSP were 397 μV and 386 μV for the pre- and post-tetanus periods

respectively. The corresponding mean amplitudes for the compound EPSP were 1.64 mV and 1.60 mV.

In seven CA1 cells the tetani produced increases in the amplitudes of the compound EPSPs. The compound EPSPs remained larger than their control amplitude for the duration of the recording (17-90 min post-tetanization). Table 5.2 lists the mean amplitudes of both the compound and unitary EPSPs in these seven cells, during the five minutes prior to the tetani, and for the 5-10 min period following the tetani. The increases in peak amplitude for the compound EPSPs ranged from 37% to 266% (mean=83%, SEM=28, n=7).

In contrast, over the same interval three of the unitary EPSPs declined in mean amplitude (by 22-26%), three showed minimal change (0-5%), and only one was increased (32%). Even this EPSP returned to near its control amplitude within 15-20 min, when the corresponding compound EPSP was still more than 200% of its control amplitude. The mean percentage change in amplitude of these EPSPs was -3.1% (SEM=6.75%, n=7).

When the data for this group of seven neurones was lumped together, the overall mean amplitude of the compound EPSPs was 5.25 mV before the tetani, and 8.44 mV for the post-tetanus period (60% increase). The overall means for the pre- and post-tetanus periods for the unitary EPSPs were 277 μV and 258 μV respectively (7% decline).

The minute-averages for the EPSPs evoked in one neurone (no. 3 in Table 5.2) are shown in Fig. 5.5. This demonstrates a clear prolonged enhancement of the amplitude of the compound EPSP following the tetanus, with no

Table 5.2A. Effects of tetanization on compound and unitary EPSPs evoked in the same CA1 neurones.
Mean peak amplitudes (mV) for the 5 min period before tetanization (pre) and 5-10 min afterwards (post).

Expt. No.	Compound EPSPs pre	post	% change	Unitary EPSPs pre	post	% change
1.	7.54	10.29	+37	0.563	0.438	-22
2.	1.41	5.15	+266	0.187	0.246	+32
3.	4.33	7.13	+65	0.143	0.143	0
4.	6.67	9.53	+43	0.506	0.451	-11
5.	6.42	11.23	+75	0.089	0.066	-26
6.	8.34	12.69	+52	0.336	0.338	+1
7.	2.04	3.06	+50	0.115	0.121	+5
mean:	5.25	8.44		0.277	0.258	

Table 5.2B. Stimulus intensities for antidromic activation of the CA3 neurones, for evoking the compound EPSPs, and during the tetani.
(For the seven experiments above.)

Expt. no.	Antidromic threshold (μA)	Compound EPSP test stim. (μA)	Tetanic stim. (μA)	No. of trains
1.	90	16	160 *	2
2.	280	12	50	2
3.	45	40	80 *	3
4.	69	12.5	79 *	1
5.	240	21.5	50	3
6.	240	8	15	6
7.	<9	7	9 *	5

* Stimulus during the tetanus above the threshold for antidromic activation of the CA3 cell.

corresponding change in the unitary EPSP. The records obtained during the three tetanic trains delivered to this cell are shown in Fig. 5.6. The trains of current pulses injected into the CA3 cell elicited action potentials at the appropriate frequency. Except for the first pulse in each train, which discharged the CA3 cell twice, there is a single action potential on each pulse. The CA1 records illustrate the repetitive discharge as a result of the tetanus delivered through the stimulating electode (each shock was 80 μA, 0.1 ms duration). Averages of the compound and unitary EPSPs are shown in Fig.5.7, with the pre- and post-tetanus averages superimposed.

Another example (no.6 in Table 5.2) is presented in Fig. 5.8. Again, the enhancement of the compound EPSP is not matched by the unitary EPSP. Six tetanic trains were delivered to this neurone, through both the CA3 cell (short current pulses), and the stratum radiatum stimulating electrode (each shock 15 μA, 0.1 ms). The CA3 records (not shown) indicated reliable activation of the CA3 neurone.

The minute-average for unitary EPSP no. 5 in Table 5.2, is given in Fig. 5.9A, as a further example of a unitary EPSP with no amplitude change after tetanic activation. The tetanus was repeated 10 min later, with a stronger stimulus intensity, again without effect.

(b). Tetanization of the unitary afferents in conjunction with postsynaptic depolarizing pulses

In addition to the above protocol, attempts were made to induce LTP of the unitary EPSPs in five CA1 cells, by

Figure 5.5. Minute-averages of the peak amplitudes of compound and unitary EPSPs recorded in the same CA1 neurone (no.3 in Table 5.2). The tetanus consisted of three trains and was delivered through the stratum radiatum electrode (80 μA). The CA3 cell was simultaneously discharged by repetitive depolarizing current pulses. After the tetanus, LTP was only observed for the compound EPSP.

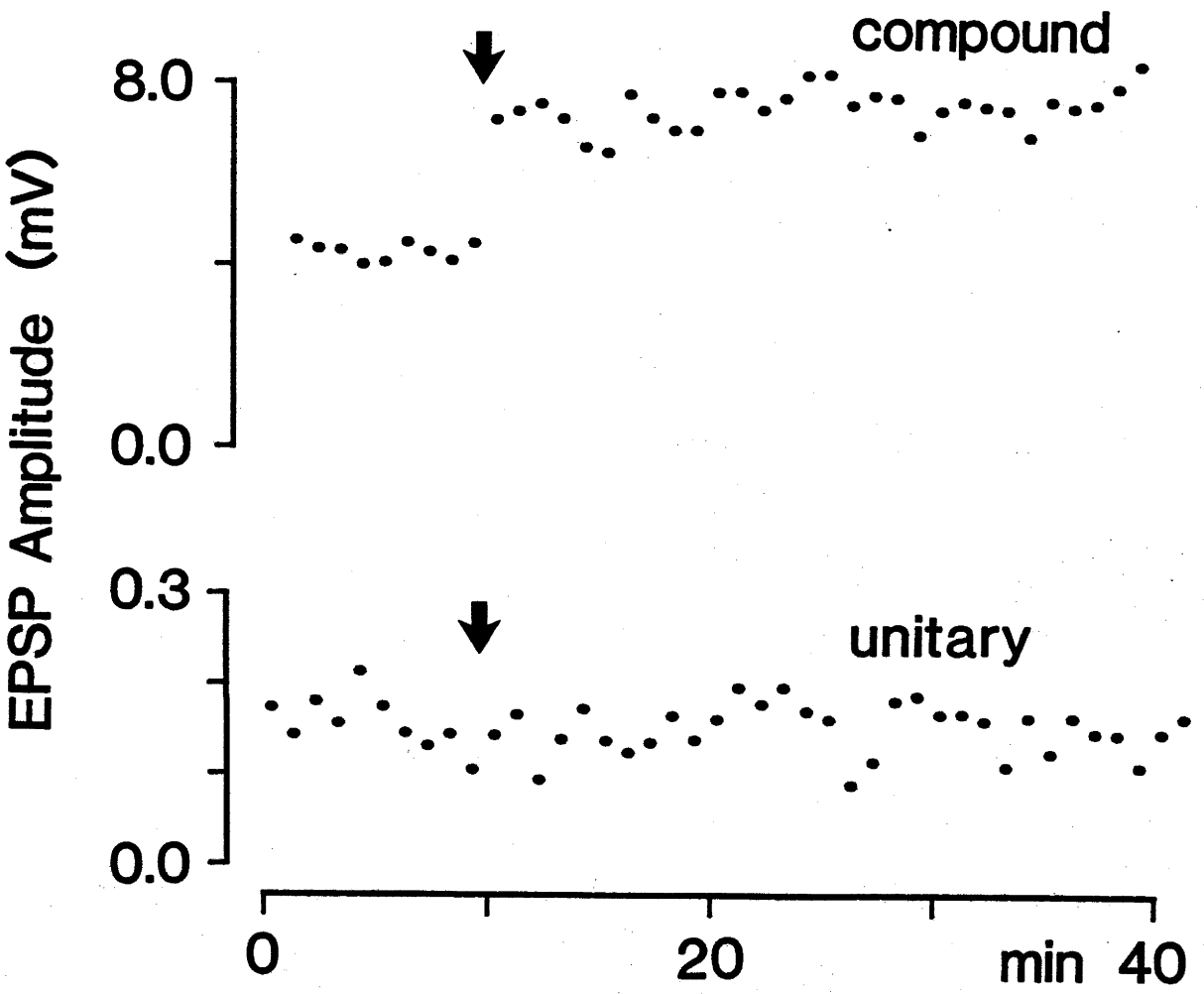

compound
8.0
0.0
EPSP Amplitude (mV)
0.3
unitary
0.0
0
20
min 40

Figure 5.6. Responses of the CA3 and CA1 neurones during the three-train tetanus (for no. 3 in Table 5.2). The interval between each train was 10-15s.

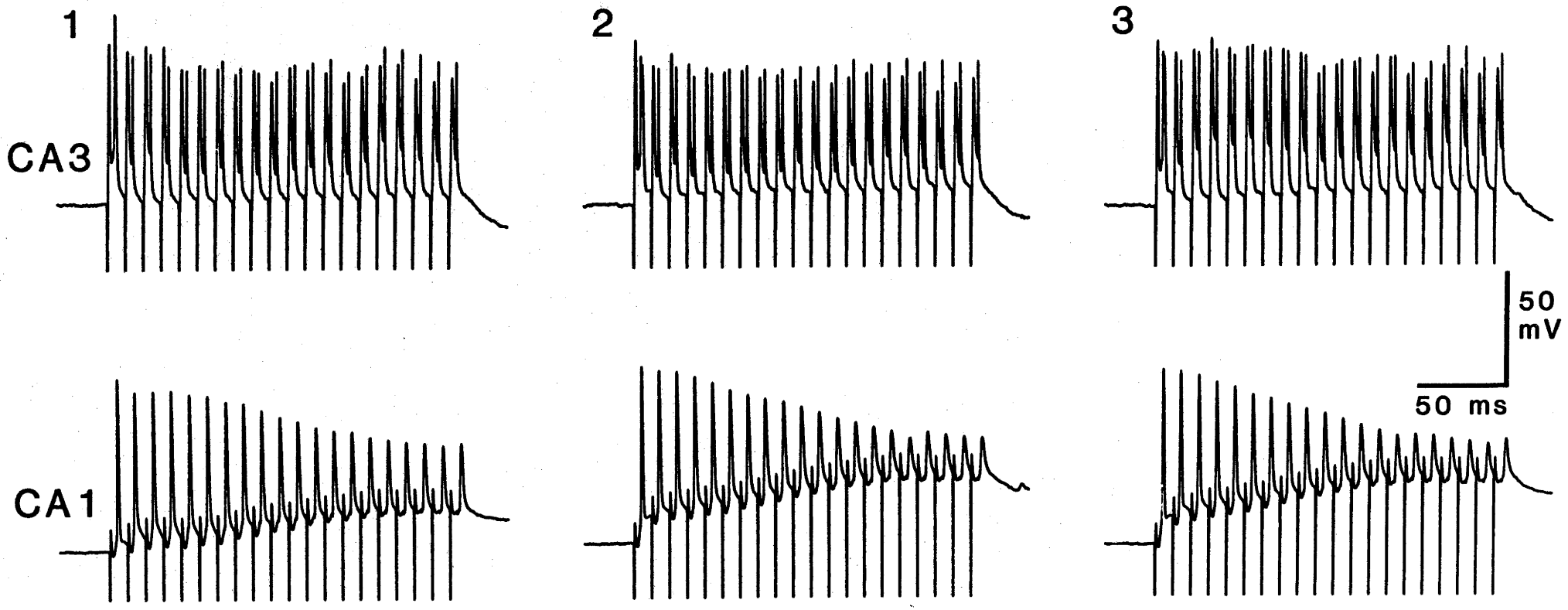

1
2
3
CA3
CA1
50
mV
50 ms

Figure 5.7. Averaged EPSPs before and after tetanization, for CA1 cell no. 3 in Table 5.2. (solid lines, before; dotted lines, after). **A**, averages of the compound EPSP, evoked by a 40 μA stimulus through the stratum radiatum electrode once every 15 s. **B**, averages of the unitary EPSP, evoked at 2 Hz by acvtivation of the CA3 neurone with a depolarizing current pulse.

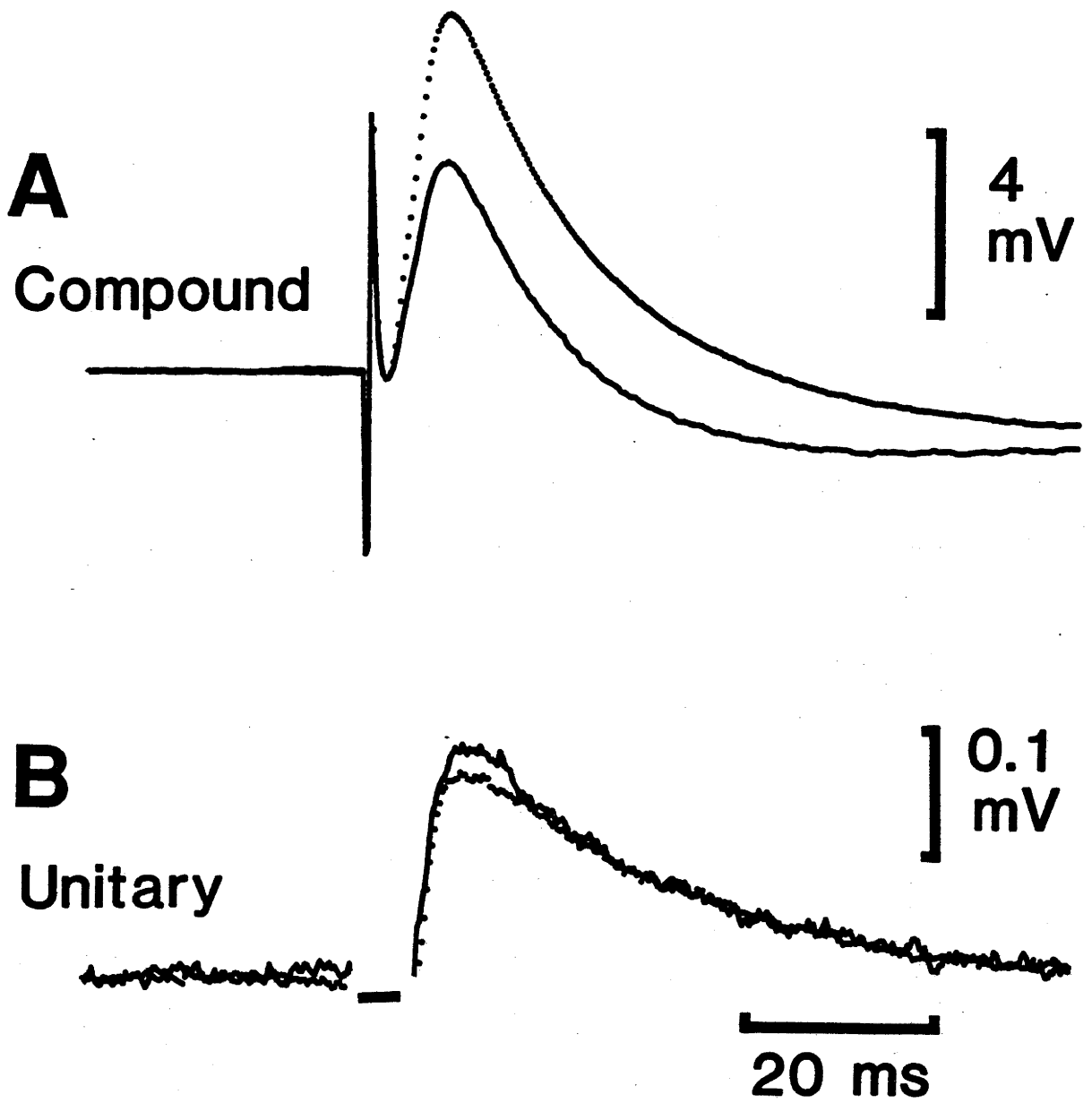

A
Compound
4
mV
B
Unitary
0.1
mV
20 ms

Figure 5.8. Minute-averages of the peak amplitudes for the compound and unitary EPSPs evoked in CA1 cell no. 6 (Table 5.2). The tetanus consisted of six trains through the stratum radiatum electrode (15 μA), with simultaneous repetitive activation of the CA3 cell by intracellular current pulses. Following the tetanus, only the compound EPSP maintained an increased amplitude. A technical problem prevented the collection of the compound EPSP records after 15 min post-tetanus.

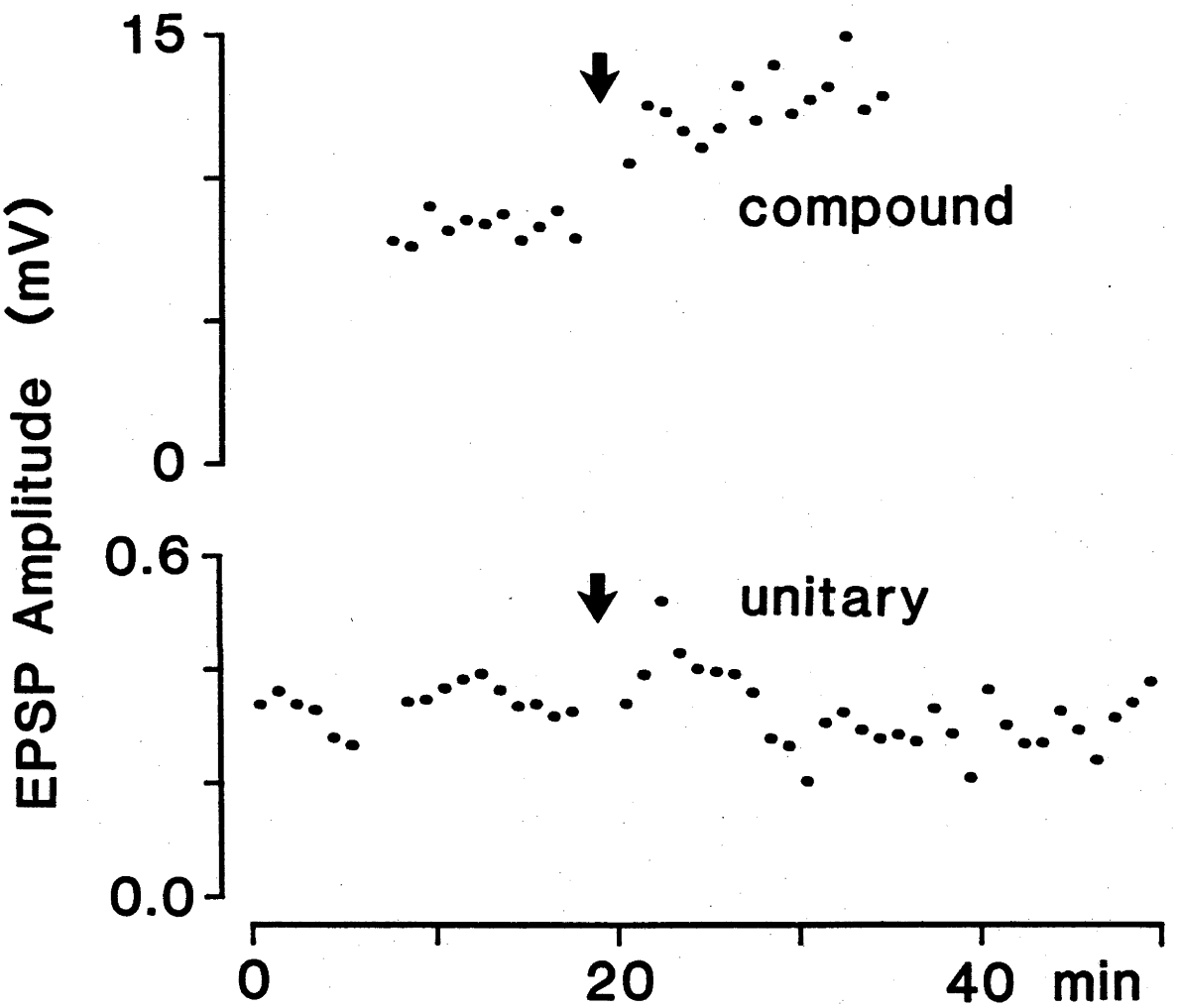
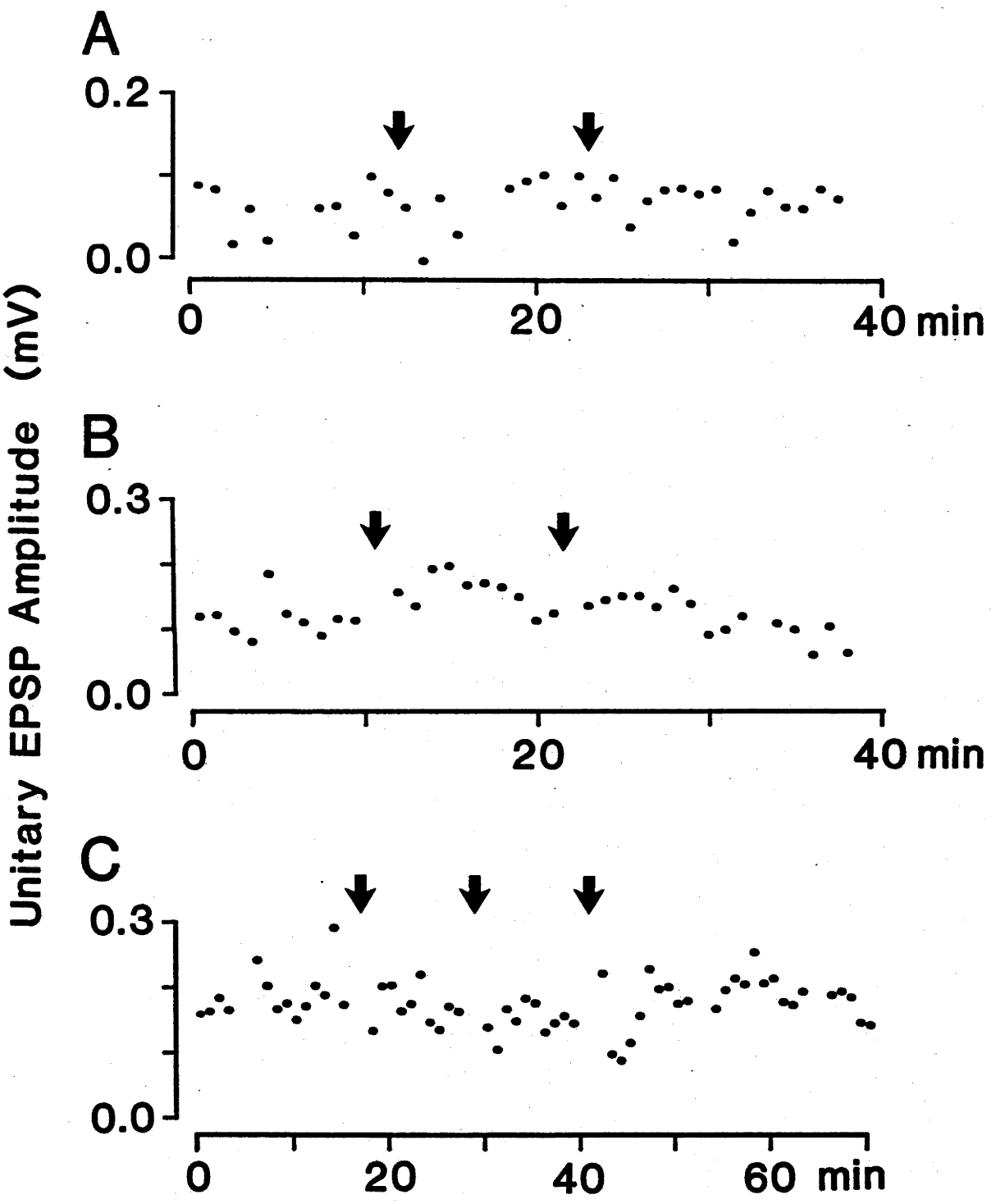

15
0
EPSP Amplitude (mV)
compound
0.6
0.0
unitary
0
20
40 min

Figure 5.9. Minute-averages for unitary EPSPs tetanized in conjunction with stratum radiatum inputs or postsynaptic depolarizing pulses. The protocols were: **A**, tetanization with three trains delivered to the stratum radiatum, 20 μA (first tetanus) and 50 μA (second tetanus). **B**, five trains, in conjunction with depolarizing current pulses injected into the CA1 neurone. The pulses were 7 nA, 300 ms for the first, and 8 nA, 500 ms for the second tetanus. During the second tetanus, the CA3 cell was activated at 50 Hz instead of the usual 100 Hz. **C**, the first and second tetani each consisted of five trains, in conjunction with 7 nA and 9 nA 300 ms postsynaptic depolarizing pulses respectively. The third tetanus was 10 trains, each at 50 Hz, with 9 nA 500 ms postsynaptic depolarizing pulses.


A
0.2
0.0
0
20
40 min
B
0.3
0.0
0
20
40 min
C
0.3
0.0
0
20
40
60 min
Unitary EPSP Amplitude (mV)

tetanizing the unitary afferents while depolarizing the CA1 cells with long intracellular current pulses. The stratum radiatum was not stimulated in this protocol.

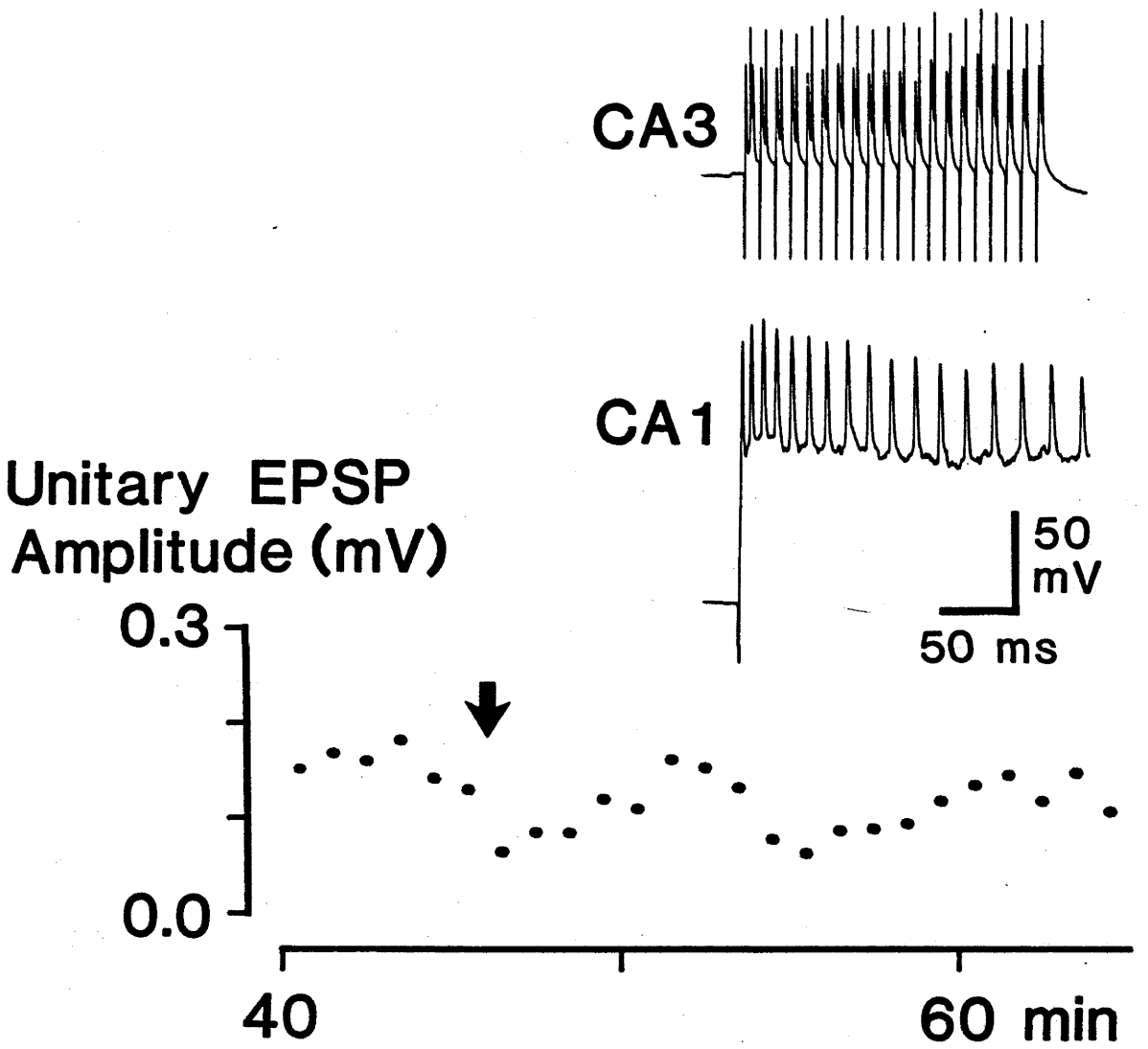
Three of the five unitary EPSPs were also tested with the protocol (1) above; they are nos. 3, 6 and 7 in Table 5.2. Nos. 3 and 6 were first tetanized according to protocol (1), with potentiation of the compound EPSPs but no effect upon the unitary EPSPs. No. 7 in Table 5.2 was tested in the reverse order (i.e. later with protocol (1)). The other two unitary EPSPs tested with protocol (2) had not been previously tetanized.

Of the five unitary EPSPs tested by the conjunction protocol, one showed a clear post-tetanic enhancement of its mean amplitude, and this increase in amplitude persisted for more than 20-30 min. The results for this EPSP will be presented last, and with more detail.

Fig. 5.10 is the minute-average for one EPSP which did not increase in mean amplitude in response to this tetanization protocol. This EPSP is no. 3 in Table 5.2, and the minute average in Fig 5.10 continues from that in Fig. 5.5. Three tetanic trains were delivered by activation of the CA3 neurone, in conjunction with long depolarizing current pulses (7 nA, 300 ms) injected into the CA1 neurone. The mean amplitude declined from 154 μV during the pre-tetanus period to 119 μV for the 5-10 min period following the tetanus. The insets in Fig. 5.10 show the CA3 and CA1 intracellular responses during a single tetanic train.

Fig. 5.9B and Fig 5.9C are the minute-averages for two further unitary EPSPs which were tetanized in conjunction

Figure 5.10. Minute-average for the unitary EPSP in CA1 cell no. 3 (Table 5.2), which was also tetanized in conjunction with a postsynaptic depolarizing pulse. This minute-average continues on from Fig. 5.5. The tetanus was three trains, each conjoined with a 7 nA, 300 ms depolarizing cuurent injection into the CA1 neurone. The insets show the responses of the CA3 and CA1 cells during one of the trains.

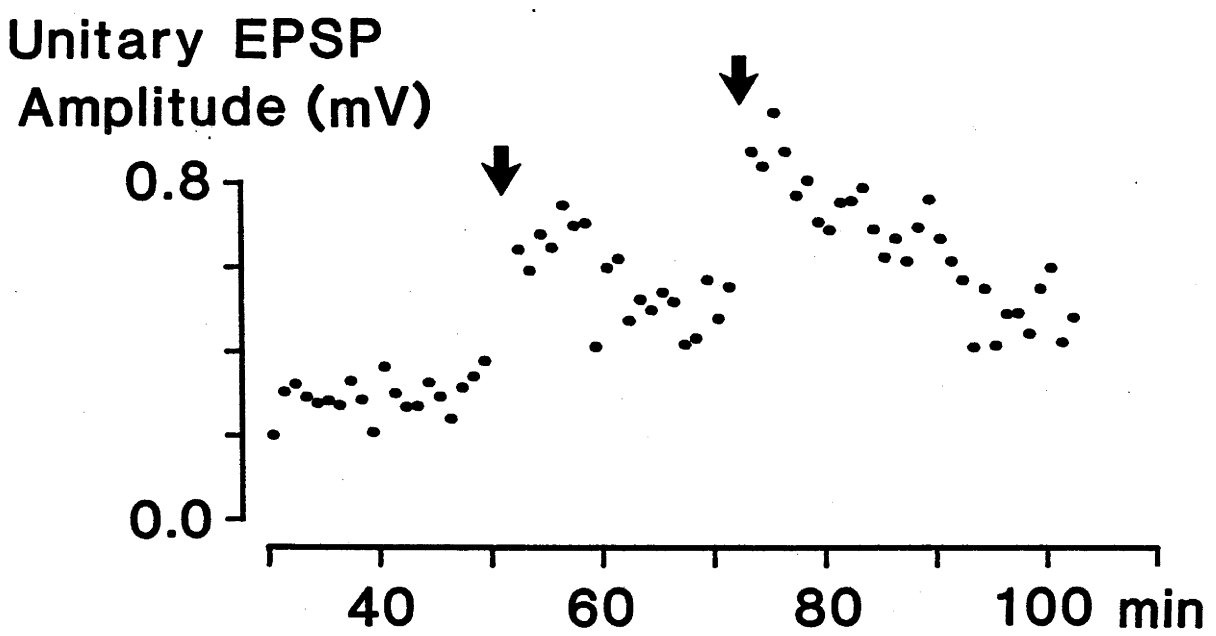

CA3
CA1
50
mV
50 ms
Unitary EPSP
Amplitude (mV)
0.3
0.0
40
60 min

with post-synaptic depolarizing pulses (7-9 nA, 300 ms). Each tetanus consisted of five trains of action potentials evoked by current pulses in the CA3 cell. One of these (Fig. 5.9B) showed an increase in amplitude folowing the first tetanus, but this declined during the 5-10 min post tetanus period, and there was no response to a second tetanus. The other EPSP (Fig. 5.9C) was tetanized three times at 10 min intervals, without effect.

One further EPSP (minute average not shown) was given a five-train tetanus in conjunction with 7 nA, 300 ms depolarizing pulses injected into the postsynaptic neurone. The post-tetanus mean amplitude was not enhanced, being 366 μV compared with 363 μV for the pre-tetanus period.

The unitary EPSP which was potentiated by the conjunction protocol, was previously tested with protocol (1) (no. 6, Table 5.2), without effect. The minute-average shown in Fig. 5.11 overlaps with that in Fig. 5.8. Six pairings of presynaptic trains with postsynaptic depolarizing pulses were given, at 10 s intervals (the first arrow in Fig. 5.11). The depolarizing current pulses injected into the CA1 cell were 7 nA, and 300 ms duration. The result was a clear enhancement of the unitary EPSP amplitude (Fig. 5.11). The mean peak amplitude grew from 316 μV prior to the tetanus, to 610 μV for the 5-10 min period after the tetanus (93% increase). The minute-average amplitudes then declined during the subsequent 15 min, but were still about 50% above the control amplitude, when the conjunction tetani were repeated (Fig. 5.11, second arrow). The mean amplitude for the 5-10 min

Figure 5.11. Minute average for the unitary EPSP which was potentiated by conjunction with postsynaptic depolarizing pulses. This EPSP had been previously tetanized in conjunction with a tetanus to the stratum radiatum (no. 6, Table 5.2), and this minute-average overlaps that in Fig. 5.8. Each tetanus consists of six trains of repetitive activation of the CA3 neurone, in conjunction with 7 nA, 300 ms pulses to the CA1 cell.


Unitary EPSP
Amplitude (mV)
0.8
0.0
40
60
80
100 min

period following the second tetanus was 747 μV, which is 136% greater than the control period before the first tetanus. The maximum minute-average was 971 μV, and this occurred in the third minute after the second tetanus. There was then a gradual decline in the minute-average, to about 50% greater than the control amplitude, at 20-30 min after the second tetanus. The CA1 cell was lost 30 min after the second tetanus.

The minute-average points for this unitary EPSP were divided into three groups, one for the control period, and two to include the earlier and later phases of the amplitude declines after the tetani (Fig. 5.12A). The division of the points following the tetani was somewhat arbitrary, but was done for the purpose of lumping together records from periods with similar mean amplitudes. This allowed enough individual records to be accumulated in the groups for relatively noise-free averages to be obtained for examination of the EPSP time course (Fig. 5.12B), and for amplitude histograms to be constructed for this EPSP (Fig. 5.13).

The time course parameters for this EPSP, for the three minute-average groups, are listed in Table 5.3. There was essentially no change in the time course following the tetani. The slight shortening of the time course parameters following the tetani (group 1 to group 2) were not reversed as the mean EPSP amplitude declined (group 2 to group 3). Similarly, there was little difference between the time course of averages made from subgroups of records made to compare the periods following the first and the second tetani (not listed).

Figure 5.12. Grouping of records for comparison of time courses and amplitude histograms, for the potentiated unitary EPSP. **A**, records within the indicated borders (broken lines) were lumped together to form three groups; one before the potentiation and two afterwards. The groups after the tetani were formed on the basis of similar minute-average amplitudes rather than the time post-tetanus. **B**, averages constructed from the records comprising the three groups.

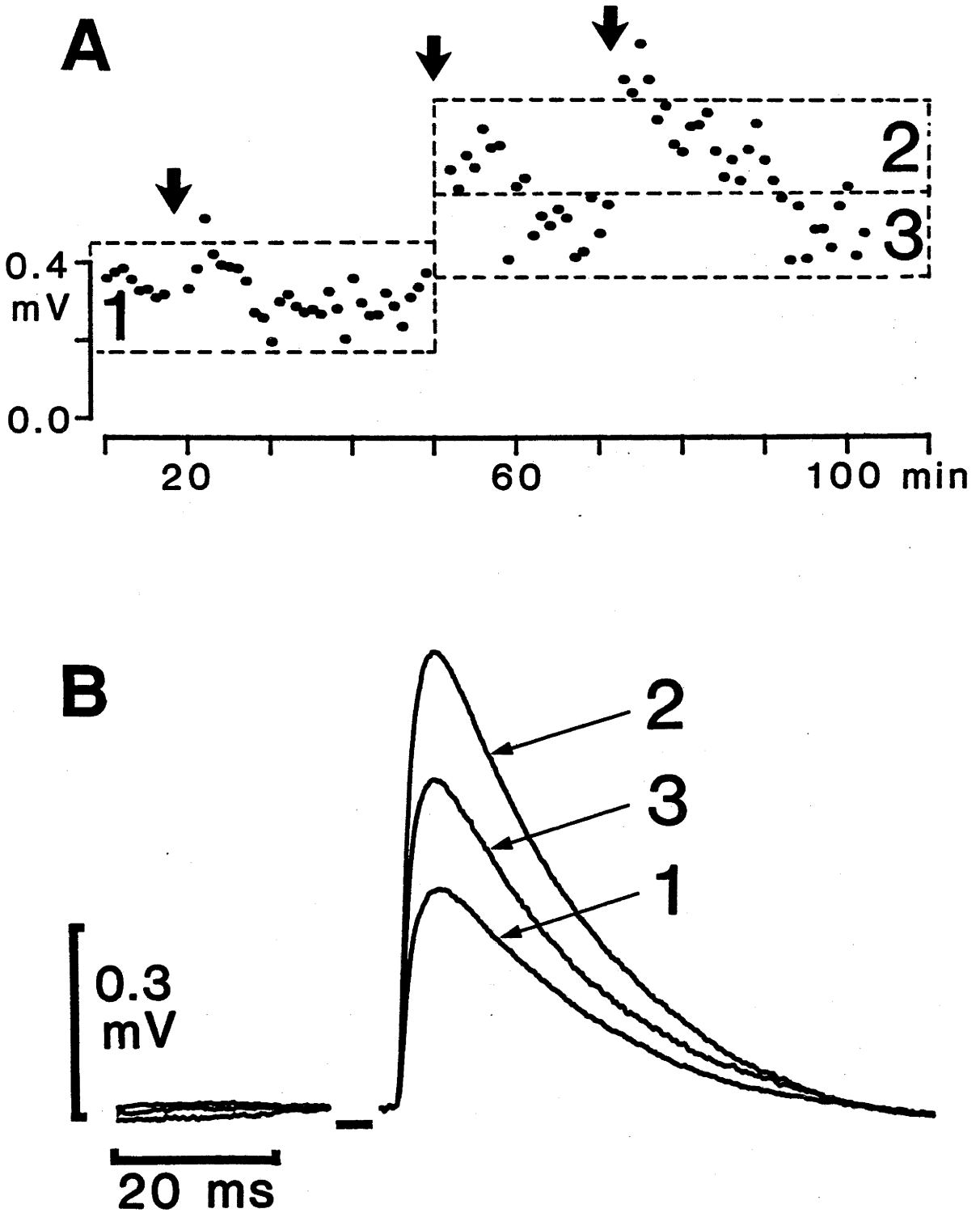

A
0.4
mV
0.0
1
2
3
20
60
100 min
B
2
3
1
0.3
mV
20 ms

Table 5.3. Time course parameters for the potentiated unitary EPSP, before and after tetanization.

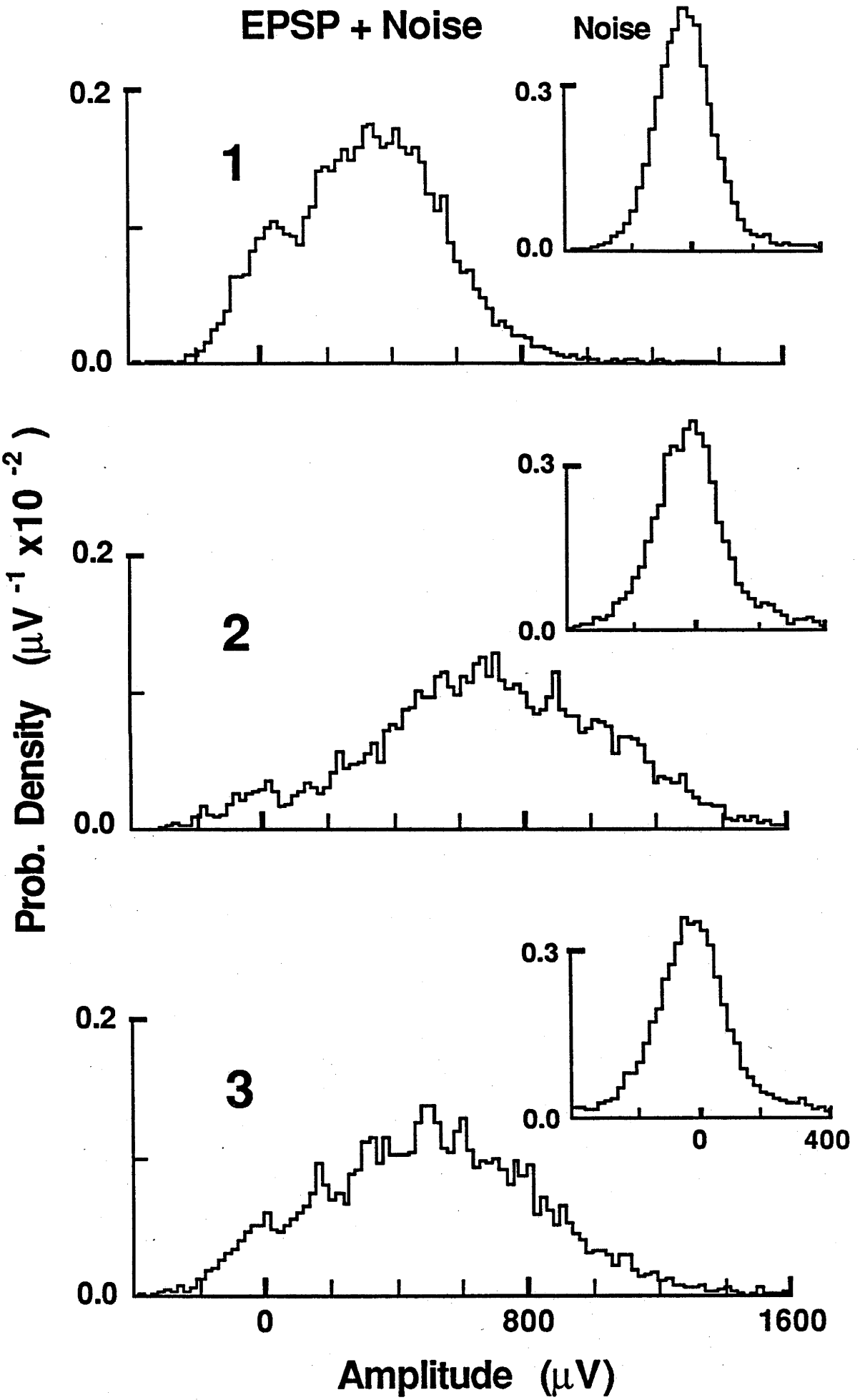
	Pre-tet. Group 1	Post-tet. Group 2	Post-tet. Group 3
10-90% rise time (mS):	2.68	2.43	2.29
Half-width (ms):	19.04	17.75	17.69
Time constant of final EPSP decay (ms):	14.73	15.57	15.56
Time to EPSP peak amplitude (ms):[1]	9.25	8.75	8.50
(Peak amplitude, μV:	335	702	503)

[1]Time to EPSP peak amplitude was measured from the peak of the CA3 action potential.

The noise-contaminated EPSP amplitude histograms constructed from the individual records in the three groups are shown in Fig. 5.13. The insets are the corresponding noise amplitude histograms. The histograms for the pre-tetanus control period (no. 1 in Fig. 5.13) have already been presented in Chapter 4, where this EPSP was referred to as no. A8. The deconvolution results for this EPSP (during the control period) were judged to be unreliable ($\bar{v}_1/\sigma_N$ =1.36). Similarly, when the deconvolution procedure was applied to the post-tetanus histograms, the discrete amplitudes in the results were not sufficently separated with respect to the noise for us to have confidence in the results. For histogram no. 2, $\bar{v}_1/\sigma_N$ was 1.68 (5 discrete amplitudes in the result), and for histogram 3 (Fig. 5.13), $\bar{v}_1/\sigma_N$ was 1.52 (4 discrete amplitudes). However, even in the absence of reliable deconvolution results, useful observations can be made from the shape of these histograms. Note that the noise-contaminated EPSP amplitude histograms for the post-tetanus records (nos. 2 and 3, Fig. 5.13) have entries over a wider range of amplitudes. For example, amplitudes of greater than 1000 μV were extremely rare during the control period, but were frequent after the tetani (see the Discussion for the implications of these changes).

To summarise the experiments with unitary EPSPs, (1) in seven CA1 neurones, simultaneous tetanization of the unitary afferent and a stronger synaptic input produced LTP of the large compound EPSPs, but not of the unitary EPSPs, and (2) tetanization of the unitary afferent, conjoined with

Figure 5.13. Noise-contaminated EPSP amplitude histograms for the records from groups 1, 2 and 3 (Fig. 5.12). The mean amplitude for each of these histograms is 324 μV, 687 μV and 495 μV (groups 1, 2 and 3). The number of records in each group (1-3) is 4334, 2697 and 2261. The insets are the corresponding noise histograms.


EPSP + Noise
Noise
0.2
0.0
1
0.3
0.0
2
3
Prob. Density (μV -1 x10 -2)
0
800
1600
400
Amplitude (μV)

depolarizing pulses injected into the postsynaptic neurone, resulted in a persistent increase in the unitary EPSP amplitude for one out of the five CA1 neurones tested.

5.4 DISCUSSION

5.4.1 Paired-pulse facilitation

In this study, the mean facilitation of the peak amplitude for the ten unitary EPSPs tested with paired stimuli (25 ms interval) was 35% (SD=58%). This degree of facilitation is comparable to that observed for extracellular (field) EPSPs in the hippocampus. Facilitation of about 40% has been reported for field EPSPs evoked with paired stimuli in CA1 (20 ms interval, Creager et al, 1980), and EPSPs evoked in dentate granule cells by perforant path activation show paired-pulse facilitation of about 22% for a 30 ms interval (McNaughton, 1982). One intracellular study in CA1 (Hess et al, 1987), which attempted quantal analysis of the control and facilitated EPSPs, had a mean facilitation of 148% for inter-pulse intervals of 40-50 ms. However, it is not made clear whether EPSPs were selectively included in the analysis because they showed strong facilitation.

In comparison with other CNS synapses, the mean facilitation for the CA1 unitary EPSPs is mid-range. For example, paired-pulses separated by 1-2 ms produced a mean facilitation of 11% for unitary Ia afferents to the cat motoneurone (Hirst et al, 1981), while minimal corticomotoneuronal EPSPs in the monkey showed an average of

about 60% facilitation for inter-pulse intervals of 2 ms (Muir & Porter, 1973). Lin and Faber (1988b) have recently reported a mean facilitation of 99% for chemical synaptic transmission at single club endings on the goldfish Mauthner cell (interval 1.6-4.0 ms).

In the present study, there was a wide variability in the degree of facilitation observed for individual unitary EPSPs. Three of the ten EPSPs showed either no facilitation or a depression, while those that did facilitate had amplitude increases ranging from 14-160%. This kind of variability has also been found for other unitary or minimal EPSPs. Of 18 unitary Ia afferent EPSPs tested for paired-pulse facilitation in cat motoneurones by Hirst et al (1981), five were not facilitated (one was depressed), and the others were facilitated by between 10% and 31%. Muir and Porter (1973) give examples of facilitation ranging from 30% to 100% for individual corticomotoneuronal EPSPs.

Given the evidence from a number of different preparations that the facilitation of the second EPSP is due to an increased probability of transmitter release (Zucker, 1973; Korn et al, 1984; Hirst et al, 1981), the variability in the facilitation observed for individual unitary EPSPs suggests that there may be marked differences in the 'resting' probabilities of release at different synapses. An active site with a probability of transmitter release close to one (in response to a single presynaptic action potential), will make a very small contribution to facilitation, whereas an active site with a low release probability has a greater potential to contribute to

facilitation. In the present study, insufficient records were obtained for each EPSP to construct useful amplitude histograms, but it would be interesting in future experiments to test these ideas by correlating the proportion of failures in the first EPSP (where this was resolvable) with the degree of paired-pulse facilitation. If the above scheme was correct, EPSPs with a higher proportion of failures following single presynaptic action potentials, would show greater paired-pulse facilitation.

5.4.2 LTP compared for small and large EPSPs

The sequence of these experiments was (1) fields and large EPSPs were tetanized to ensure that LTP could be induced in our slice preparation with a high 'success rate', (2) attempts were made to induce LTP in small compound EPSPs, using three different protocols, but LTP was observed only infrequently (4/40 occasions), and (3) more definitive experiments were performed in which the post-tetanic responses of both large compound and unitary EPSPs could be observed in the same CA1 neurones. The third series of experiments confirmed the (separate) results for the first two: that the test and tetanization protocols used here are much more effective at inducing (or expressing, see below) LTP in large synaptic inputs than in minimal or unitary inputs. The first part of this discussion will focus on the rarity of the small compound and unitary EPSPs being enhanced, and the features of the unitary EPSP which did show a prolonged post-tetanic enhancement will be discussed later.

Possible reasons for the low incidence of LTP observed in small EPSPs

The first concern is whether the small compound and unitary EPSPs may have been consistently enhanced, but by a proportion too small to be seen above the 'noise' of the minute-to-minute variations in mean amplitude. A given percentage increment in amplitude would be more obvious for the large compound EPSPs, which had a higher signal to noise ratio. Could the small EPSPs which were judged to be non-enhanced, be ones which had increases in mean amplitude hidden by the minute-average variability?

This concern was the reason for lumping together the mean amplitudes of the EPSPs in the non-enhanced category. A consistent trend, distinct from individual variability, should be detected in the averaged values; however the mean changes in these groups were all close to zero or slightly negative. This argues against small (but frequently-occurring) potentiations having gone unnoticed.

A related question is whether the occasional small compound and unitary EPSPs which were potentiated could account for the magnitude of the changes observed in the large compound EPSPs (assuming the large EPSPs are linearly summed unitary EPSPs). To answer this, averaged mean amplitudes (before and after the tetani) have been calculated for the small and large EPSPs, including both potentiated and non-potentiated EPSPs. In the initial experiments, the mean amplitude of the large compound EPSPs increased from 1.89 mV to 3.22 mV (+63% change, n=4). The small compound EPSPs averaged 0.200 mV before the tetani, and 0.212 mV afterwards

(+5%, n=40). In the experiments with large compound and unitary EPSPs together, the mean amplitude of the compound EPSPs increased from 4.77 mV to 7.34 mV (+54%, n=9), while the unitary EPSPs declined from 0.271 mV to 0.256 mV (-5.5%, n=9). Clearly, the few small EPSPs which were potentiated contributed too little to the overall averages to account for the percentage change observed in the large EPSPs.

Another possibility is that the potentiation of the large compound EPSPs is due to very large increases in synaptic strength of only a few afferents, and that by chance none of these were sampled in the experiments with unitary or small compound EPSPs. This might be tenable if the unitary EPSP experiments are considered alone, but the larger sample size of the experiments with small compound EPSPs makes this seem unlikely. Certainly no 'super-potentiating' EPSPs were ever observed; the maximum potentiation obtained for any of the small EPSPs was 136% (Figs. 5.11, change measured from control to period after the second tetanus/conjunction).

Possible problems with the LTP induction protocols

It is worth considering whether the rarity of the LTP observed in small EPSPs could be due to some inadequacy of the induction protocols. As described in Chapter 1, the necessary conditions for the induction of LTP are believed to be the conjunction of presynaptic activity with postsynaptic depolarization. Under this paradigm, failure to induce LTP would imply either an insufficient number of presynaptic volleys during the period of depolarization, or inadequate

depolarization at the postsynaptic region local to the synaptic connection(s), or both of the above.

Firstly, relating to the experiments involving tetanization of small compound EPSPs, Wigstrom and Gustafsson (1985) have shown that with inhibition reduced by picrotoxin (100 μM), the major part of the capacity for potentiation was used up after 20-30 stratum radiatum stimuli. The tetani in their experiments were delivered at 50 Hz and at the test stimulus intensity. Although the concentration of GABAa antagonist used in our experiments was less (10 μM bicuculline methiodide), our standard tetanus regime involved at least twice as many volleys (three trains of 20 stimuli, often repeated after 5-10 min). The tetani in our experiments would also be expected to be more effective because they were delivered at the higher frequency of 100 Hz (Dunwiddie & Lynch, 1978), presumably secondary to the increased NMDA receptor-mediated component of the depolarization at the higher stimulus frequency (Collingridge et al, 1988b). The postsynaptic depolarizations during the tetani were supplemented by strong tetanic stimuli (50-100 μA), delivered through electrodes in the stratum radiatum near the test electrodes. These stimuli were stronger than those commonly used for induction of LTP, as in most studies the test electrode is used to provide the tetani, without the stimulus intensity being changed. For 10 of the 40 small compound EPSPs tested in the present study, the postsynaptic depolarization was further boosted by injection of current (7-15 nA) through the recording electrode.

Secondly, in the experiments involving small compound EPSPs which were conjoined with depolarizing pulses alone, rather than being tetanized, the protocol of Gustafsson et al (1987) was followed. Gustafsson et al (1987) reported potentiation for more than 70% of the EPSPs conjoined with 5 nA depolarizing pulses, reaching a maximum after only 20-30 conjunction events in most cases. The average increase in the initial slope of the EPSPs in their study was 76%. Gustafsson et al (1987) do not give the initial mean peak amplitudes for the EPSPs they tested, but they illustrate one example which had a pre-conjunction peak amplitude of 5-10 mV. The input resistances of the CA1 cells they tested were presumably in a similar range to the ones here, as they used the same acceptance criterion (20 MΩ). However, despite being subjected to between 360 and 720 conjunction events (3-7 min at 2 Hz), four of the five small compound EPSPs tested in the present study were not potentiated. The one EPSP which did show a clear increase in amplitude (Fig. 5.3C), returned to close to the control amplitude after 15-20 min.

For the CA1 neurones in which both large compound and unitary EPSPs were evoked, the compound EPSP provided a control input to indicate that the tetanization protocol had been adequate to induce LTP in at least some of the tetanized afferents. Although in two of the nine cells tested, neither of the inputs were potentiated, this does not necessarily indicate that the tetanization paradigms were inadequate. Most investigators report some failures to induce LTP, even in extracellular field studies; however there is little

published information on 'failure rates' of intracellularly-monitored LTP to compare with the present study. Gustafsson et al (1987) could not show LTP for approximately one third of their intracellular EPSPs, even when tetanization of the stratum radiatum potentiated field EPSPs. Gustafsson et al (1987) suggested that the trauma of electrode penetration may have damaged the cells which did not show LTP.

The number of tetanic trains used to induce LTP in the seven (out of nine) large compound EPSPs ranged from one to six (Table 5.2B). It is likely that the relatively high stimulus intensities used in some cases caused sufficient postsynaptic depolarization (and therefore NMDA receptor-mediated channel opening) for as few as one or two trains to be effective. One of the reasons for deliberately using such strong stimuli was to involve as many axons as possible in the tetani (in some instances this included the 'unitary' afferent), in the hope that these would spread the postsynaptic depolarization over a wide region of the dendritic tree (see below). However, when using high stimulus intensities, we prefered to minimise the number of tetani delivered, to reduce the chances of local tissue trauma (the tetanizing electrode was also the test electrode for the large compound EPSP in these experiments), and to reduce the likelihood of inducing spreading depression or epileptiform activity. When lower stimulus intensities were used during the tetanus, five or six trains were delivered (cells 6 and 7, Table 5.2B).

Electrotonic separation of the two inputs

One of the concerns during these experiments was that the unitary afferent might make its synaptic connection(s) at a dendritic location distant from the inputs belonging to the group of axons activated during the tetani. If so, the postsynaptic depolarization during the tetanus close to the synapse(s) mediating the unitary input, might be significantly less than in the other regions of the dendrites, where many of the afferents involved in the compound EPSP presumably make their connections. The decay of the depolarization between the different dendritic regions might be due to the electrotonic distances involved, and may also be enhanced by the local shunting effects of synaptic inhibition.

For four of the seven CA3-CA1 pairs, this was less likely to have been a problem, because the stimulus strength during the tetanus was above the threshold for antidromic activation of the CA3 cell (Table 5.2B). The axon (or at least a branch of that axon) making the connection between the CA3 and the CA1 neurone, was therefore amongst the group of afferents providing the tetanic depolarization. While this axon may have had a branch deviating away from the rest of the group to a more remote region of the dendritic tree, it would be no more likely to do this than any of the other activated axons. For such an axon to synapse at a less depolarized region of dendrite should therefore be an exception rather than the rule.

However, three of the seven CA3-CA1 pairs would be potential candidates for this problem (nos. 2, 5 and 6 in

Table 5.2). These had high thresholds for antidromic activation of the CA3 cell (>200 μA), implying that the axon was some distance away from the stratum radiatum electrode. These were not activated by the stimulating electrode during the tetani, although they were still tetanized via the CA3 intracellular current pulses. In a worst case situation, the unitary afferent might be making a synaptic connection to the basal dendrites in the stratum oriens, while the large compound and strongly tetanized afferents projected to the apical dendrites. Of relevance here is the finding by Gustafsson and Wigstrom (1986) that tetanization of the basal dendrites potentiated a conjoined single volley to the apical dendrites, only when inhibition was blocked by picrotoxin. That is, the combination of electrotonic distance and inhibition was sufficient to block the cooperativity between widely separated inputs.

When the unitary input to the CA1 cell in experiment no.6 (Table 5.2) was tetanized in conjunction with the strong stratum radiatum input, it was not potentiated (Fig 5.8). However, when it was tetanized in conjunction with 7 nA depolarizing current pulses injected into the CA1 soma, a clear potentiation was observed (Fig. 5.11). This argues strongly for the situation of separated inputs, as described above, having occurred for this particular CA1 cell. The intracellular current injection may have been more effective than the synaptically-induced depolarization because the unitary input was electrotonically closer to the soma than to the site of the strong synaptic input, or because the amount

of inhibition during the unitary input tetanus alone would have been considerably less.

However, other evidence suggests that the problem of separated inputs was an occasional complicating factor, rather than the overall cause of the low incidence of LTP observed in small EPSPs. Five unitary EPSPs were tetanized in conjunction with postsynaptic depolarizing pulses, but a convincing change in peak amplitude was only seen for one of them. It seems unlikely that there was insufficient spread of the depolarization from the soma to the site of the synapse(s), because the time courses of the five unitary EPSPs indicated that their electrotonic distances from the soma were relatively short. The EPSP with the longest normalized time course had a normalized rise time of 0.20 and a normalized half-width of 1.14. From the modelling data of Turner (1984a,b, 1988), the normalized time courses for all five unitary EPSPs lie within the predicted values for 'proximal' EPSPs. In the model (Turner 1984b, 1988), proximal inputs were on average 0.32 (± 0.18, SD) length constants from the soma in the model. Assuming passive cable properties, 73% of the depolarization induced by steady current at the soma should be transmitted to a synaptic location at an electrotonic distance of 0.32 length constants. While these estimates rely on many assumptions, it would be difficult to argue that the synapses involved in the unitary EPSPs were electrotonically 'remote'.

Furthermore, the success rate for LTP was no higher in the experiments with small compound EPSPs. In those experiments separation of the inputs would be expected to be

less of a problem, because (1) inhibition was reduced by bicuculline, (2) when strong tetani were delivered through the stratum radiatum electrodes (35 cells), these electrodes were close to the test electrodes, so in most cases they should have activated afferents projecting to the same region of the dendritic tree as the test afferent(s). Finally, when the small compound EPSPs were tetanized in conjunction with depolarizing current pulses (5 cells), or with both depolarizing current pulses and strong tetani (10 cells), LTP was still only seen rarely (two out of 15 cells).

Collision of action potentials

Two other aspects of the protocol for the combined unitary EPSP/large compound EPSP experiments need to be briefly considered. Firstly, in some cases the CA3 afferent was activated during the tetanus both antidromically (through the stratum radiatum electrode) and orthodromically (repetitive current pulses injected into the CA3 cell). This occurred when the stimulus intensity during the tetanus was above the threshold for antidromic activation of the CA3 cell (no.s 1, 3, 4 and 7 in Table 5.2). It might be argued that direct activation of the CA3 cell by current pulses during the tetanus was unnecessary in this situation. However, in trial experiments (not dual recording) when the CA3 axon was tetanized through the stratum radiatum electrode alone, the CA3 cell hyperpolarized and failed to discharge during the later part of the train. The hyperpolarization and block of the action potentials is likely to be due to recurrent inhibition within CA3 (Miles & Wong, 1984; Miles & Wong

1987b), but because the failure of activation of the axon at the CA1 end could not be ruled out, it was considered safer to always activate the CA3 cell with depolarizing pulses as well. Collision of the action potentials originating from the two ends of the axon should not affect the depolarizations at the terminals, as all parts of the axon must be invaded by one or other of the action potentials. Related to this point, there is no reason to believe that antidromic action potentials should be any less effective in depolarizing the terminals than orthodromic action potentials. LTP was induced without difficulty for the large compound EPSPs, which were evoked via antidromic activation of the axons in the stratum radiatum.

Test stimulus rate

Secondly, one difference between the unitary EPSPs and the large compound EPSPs was the rate at which they were evoked during the test (non-tetanus) periods. Could the faster activation rate (2 Hz) of the unitary EPSPs have prevented them from showing LTP? The fast rate was desirable for the unitary EPSPs because they are small relative to the baseline noise, and as many records as possible are required to make the minute-averages relatively noise-free. However, most studies of LTP use much slower test rates (e.g. 0.33 Hz or less), although Gustafsson & Wigstrom (1988) obtained LTP in field EPSPs evoked at 1 Hz without any difficulty.

The clearest indication that the 2 Hz test rate ought not to be a problem, was provided by the initial experiments in the present study, in which LTP was obtained for

extracellular fields and large compound EPSPs evoked at 2 Hz. Furthermore, two arguments as to why the fast test stimulus rate might reduce LTP, can be rebutted:

(1) Auto-induction of LTP at the test rate (i.e. before the tetanization), is unlikely because such a weak input, even if tetanized at much higher frequencies (i.e. without providing additional depolarization), would not be expected to show LTP (Barrionuevo & Brown, 1983; Kelso & Brown, 1986). For larger EPSPs, a 2 Hz activation rate is too slow for LTP induction under normal circumstances (Dunwiddie & Lynch, 1978; McNaughton, 1983), although with inhibition supressed a sufficiently strong input might be potentiated (Abraham et al, 1986).

(2) Depletion of transmitter from the terminals as result of the tetanization, perhaps due to less transmitter in reserve at the 2 Hz test rate than at lower frequencies, ought not to occur. While setting the equipment for the tetani (and resetting it afterwards), the preparation was always 'rested' for at least 20-30 s, and similarly between each train delivered, there were no stimuli for 10-15 s. Each train consisted of twenty impulses, the equivalent of 10 s activation at the 2 Hz test frequency. Therefore, over the whole tetanization period, there was a net decline in stimulus rate, rather than an added burden on the presynaptic transmitter reserve.

Other possible explanations for the low incidence of LTP in small EPSPs

Having argued above that the rarity of LTP observed in small EPSPs is not due to inadeqate protocols for LTP induction, it is appropriate to make some speculative suggestions about possible mechanisms for LTP which would be consistent with the results of the present study.

(a). Presynaptic mechanisms

If tetanization induced the formation of new synapses, and these predominantly formed between previously non-connected presynaptic and postsynaptic cells, then the method used for the unitary EPSP experiments would usually fail to detect the change. Instead of tetanizing connected CA3-CA1 pairs, it would be more appropriate to tetanize CA3 cells which did not have initially-apparent connections to the simultaneously impaled CA1 neurones. However, it is unlikely that this would be a fruitful experimental paradigm, without some means of identifying CA3 cells with axons running very close to the dendrites of the impaled CA1 neurone.

The available evidence indicates such a scheme is unlikely for LTP, at least in CA1. Electron microscopic comparisons of the CA1 stratum radiatum before and after tetanization, have found no change in the number of synapses onto dendritic spines (Lee et al, 1980; Chang & Greenough, 1984). While both studies reported an increase in the number of synapses directly onto dendritic shafts, these make up less than 5% of the total number of synapses (Lee et al, 1980; Chang & Greenough, 1984), and it is not known whether

these represent new connections or transformations of spine synapses, or what proportion of these are on pyramidal cells rather than interneurones.

The experiments with small compound EPSPs should also have had a higher yield of LTP, if new synapses were formed preferentially from non-connected presynaptic and postsynaptic elements. Although the low-intensity stimuli to the stratum radiatum probably activate only a few afferents to the impaled CA1 cell, many other axons must be stimulated as well. Some of these active axons would run close to the apical dendrites of the impaled CA1 cell, and should have the opportunity to make connections (if that was the result of tetanization), thereby enhancing the post-tetanized EPSP.

A mechanism for LTP which would fit with the lack of structural changes, would be the activation of previously inactive or 'silent' synapses. There is good evidence in other systems for synaptic boutons which appear to physically contact the postsynaptic cell, but which do not release transmitter in the presence of activity in the presynaptic axon (some group Ia synapses to the cat motoneurone, Redman & Walmsley, 1983b; single club endings on the goldfish Mauthner cell, Lin & Faber, 1988a,b). Lin & Faber (1988b) found that the proportion of active chemical synapses was greater when the presynaptic axons were impaled by electrodes filled with 4-aminopyridine. This implied that synapses could be 'turned on' by changed conditions within the terminal. However, if LTP were entirely due to the activation of silent synapses, the same objection as described above would apply; the

changes should have been more frequently observed in the experiments with small compound EPSPs.

A synergistic action between the presynaptic terminals could be proposed, perhaps by extrasynaptic spread of transmitter to neighbouring synapses. However, it is difficult to accept that released transmitter could diffuse through the extracellular space rapidly enough to reach other terminals activated during the same volley. There is evidence for presynaptic receptors for excitatory amino acids in CA3, but these appear to antagonise transmitter release (Cotman et al, 1986).

(b). Postsynaptic mechanisms

An interesting suggestion for a postsynaptic mechanism for LTP has recently come from a study of Ca^{2+} fluxes in isolated adult CA1 neurones (Connor et al, 1988). Long-lasting Ca^{2+} gradients, measured by fura-2 fluorescence, were induced in the apical dendrites subsequent to brief local applications of glutamate or NMDA. The sustained gradients were blocked by previous treatment with the protein kinase C inhibitor sphingosine. Connor et al (1988) propose that these results are best explained by a C kinase-mediated modification of voltage-dependent channels. Their evidence for the channels being voltage-dependent was that the Ca^{2+} gradients were reduced by application of GABA, which was presumed to hyperpolarize the cells from their resting membrane potentials (which were depolarized relative to CA1 neurones in slices).

If the major synaptic modification underlying LTP is the enhancement of a voltage-dependent postsynaptic inward current in the postsynaptic spine (or local dendritic region), the results of the present study might be explained. An EPSP which is only a few hundred μV at the soma, may not cause sufficient depolarization (either in amplitude or duration) at the location of the voltage dependent channels to activate them significantly. The channels might be modified as a result of the tetanization, but the modification would not be expressed unless they were depolarized above their activation threshold by subsequent test inputs.

The feasibility of this scheme depends upon two unknown factors. Firstly, there is no precise information on the voltage dependence of the Ca^{2+} channels proposed by Connor et al (1988), so the depolarization required to activate them is uncertain. A transient Ca^{2+} current with a threshold of about -55 mV has been reported for CA1 neurones in vitro (Halliwell, 1983), in addition to the persistent Ca2+ current activated at more depolarized potentials (Johnston et al, 1980; Brown & Griffith, 1983). The activation thresholds for different sub-types of voltage-dependent channels in other neurones vary from about -70 to -10 mV (see Miller, 1987 for review). In the Aplysia bag cell neurone, the covert voltage-dependent Ca^{2+} channels which are recruited by activators of protein kinase C, require depolarizations of 20-30 mV from the resting potential for activation (Deriemer et al, 1985; Strong et al, 1987).

Secondly, the voltage transients within spines or nearby dendritic shafts cannot be measured with currently available techniques. Cable model estimates of the voltage transient evoked within a spine by a single synaptic input, are particulary susceptible to inaccuracies due to the wide variablity of spine dimensions, and to the possible variability in the membrane resistivity at different regions within the cell (Durand et al, 1983; Clements & Redman, 1986). Turner (1984b) predicts a transient of about 10 mV peak amplitude within an 'average' spine, while Gamble & Koch (1987) estimate one of 45-50 mV. In both cases the waveforms are predicted to return to the membrane potential of the adjacent dendrite within 1-2 ms.

Depending on the relative settings of the above factors, it is conceivable that a single spine transient alone might not reach the voltage threshold for the active channel, and that it might exceed it if aided by depolarization from its parent dendrite. The depolarization induced by a large compound EPSP in a single spine, would not only be greater in amplitude, but also more prolonged, due to both the local cable properties of the dendrites and due to the probable asynchrony of the many synaptic inputs due to the varying conduction delays from the site of stimulation. This might also lead to increased currents through the voltage dependent channels. Occasionally, a single spine input might be above the threshold for activation of the Ca^{2+} channel, depending on the synaptic current, and the spine and local dendrite cable properties. Only in these cases would the modification induced by the tetanus (LTP) be expressed for a single input.

Note that active processes in spines (including action potentials) have been previously modelled for spiny neurons, generally with regard to putative amplification mechanisms for distal dendrites (Shepherd et al, 1985; Perkel & Perkel, 1985; Rall & Segev, 1987). The effects of various active currents, and spine and dendrite geometries, are dealt with in detail by those authors. Shepherd et al (1985) also stressed the importance of these issues to possible mechanisms underlying learning and memory.

The results of Connor et al (1988) pointed to modification of a voltage-dependent Ca^{2+} channel in the CA1 apical dendrites, so the emphasis of this discussion has been on Ca^{2+} currents. It should be pointed out, however, that alteration of other voltage-dependent ion channels (e.g. enhancement of Na^{+}, inhibition of K^{+} or Cl^{-}), would be equally consistent with the results of the present study taken alone. Madison et al (1986) reported a Cl^{-} current in hippocampal pyramidal cells which was active at the resting potential and turned off by depolarization. However, this current was turned off, and lost its voltage dependence, after activation of protein kinase C by phorbol esters. This change would not explain a differential enhancement of small and large EPSPs following tetanization. As yet there is no evidence that the enhancement of CA1 EPSPs in LTP is associated with alterations in voltage-dependent Na^{+} or K^{+} channels.

Despite the attractiveness of the postsynaptic mechanism for LTP described above, it should not be forgotten that

there is good evidence for a sustained increase in transmitter release following tetanization, at least in the dentate gyrus (Dolphin et al, 1982; Bliss et al, 1986). These results imply that at least some of the mechanisms underlying the expression of LTP are presynaptic. Having argued above against the presynaptic mechanisms which would allow for differences in LTP observed between unitary and large compound EPSPs, it is difficult to reconcile the results of the present study with increased transmitter release. The rise in glutamate release occurs within 10-15 min of after tetanization in the dentate gyrus (Dolphin et al, 1982; Bliss et al, 1986), so it cannot be argued that a presynaptic mechanism occurs during the later phase of LTP expression, after the period monitored in our experiments.

5.4.3 Features of the unitary EPSP which showed LTP

In this final section of the discussion, some comments will be made about the one unitary EPSP which was enhanced for a prolonged period after the tetanus.

Although the minute-average for this unitary EPSP showed a decay towards the baseline amplitude (Fig. 5.11), the duration of the enhanced response was certainly too long for it to be attributed to post-tetanic potentiation. Post-tetanic potentiation at hippocampal synapses lasts less than 1-2 min (McNaughton, 1982; Gustafsson & Wigstrom, 1988), and furthermore, this unitary input had been previously tetanized without showing the same kind of response (Fig. 5.8). There is apparently a relationship between the strength of the induction procedure and the duration of LTP; Linden et al

(1987) found that LTP induced by two trains (eight shocks each) decayed within two hours, while the enhancement persisted longer if eight trains were delivered. Gustafsson et al (1987) noted that LTP induced by conjunction of single volleys with depolarizing pulses was more persistent for the stronger depolarizing currents. It is therefore reasonable to expect a variation in decay times for different induction protocols, and it is not suprising that the time course of decay for the unitary EPSP should differ from that seen for the large compound EPSPs. Despite the decline in amplitude, the unitary EPSP was still potentiated by about 50% at the end of the recording (30 min after the second conjunction tetanus).

With reference to the discussion about possible postsynaptic voltage-dependent channels, it is worth considering the amplitude and time course parameters for this particular EPSP. The normalized rise time for this EPSP was 0.20, and at the time the average was taken for measurement of the time course, the mean peak amplitude was 300 μV. These values are plotted in Fig. 3.11A. For its rise time, this EPSP has one of the largest amplitudes. Assuming that common rise times indicate similar electrotonic distances between the dendritic location of the spine(s) involved and the soma, this suggests that even before tetanization, this EPSP was probably one of the largest at its dendritic origin. It would therefore be one of the best candidates for activation of a voltage-dependant channel in the dendrites.

However, as mentioned above, there is considerable uncertainty about the effects of spines on the amplitudes and time courses of EPSPs. It could be that the cable properties of the spine head and neck attenuate the EPSP amplitude out of proportion to the effect on the time course of the transient (which may be mostly shaped by the dendrites). If that were the case, it would be dangerous to make assumptions about the amplitude of the depolarization within the spine(s) for this unitary EPSP, relative to the others. For the same reason, the absence of a change in time course for this EPSP following tetanization, does not rule out the possibility that alterations in the spine geometry may have caused the increased amplitude of the EPSP. However, a change in the time course would have been expected if the greater amplitude was secondary to an increased dendritic membrane resistivity following inactivation of chloride channels (Madison et al, 1986).

Although the deconvolution procedure was not able to reliably resolve discrete amplitudes in the amplitude histograms for this unitary EPSP (Fig. 5.13), there is some useful information to be obtained from them. Note that the noise-contaminated EPSP histograms have spread to the right following the tetani, with entries at amplitudes where there were previously no entries. For example, compare the entries at 1200 μV for the three histograms. Before the tetani (histogram 1) the very rare entries at this amplitude appear to be the extreme values of distributions centered at much lower amplitudes. In the first histogram after tetanization

(2), there are a large number of entries at 1200 μV, which would be consistent with a noise-free EPSP amplitude somewhere in the region 800-1200 μV. The third histogram shows a return towards the appearance of the first. This series of histograms cannot be explained by a simple change in the probabilities of release for already-active release sites. This would have resulted in an increase in the proportion of (non-failures) amplitudes already present in the first histogram, without such a major shift to the right.

Without reliable quantal analysis, it is difficult to be certain whether or not the proportion of failures is different in the three histograms. The failures peak appears larger in histograms 1 and 3 (Fig. 5.13), but perhaps only because this peak is additive to the tails of the noise-comtaminated distributions for the smaller non-failure amplitudes. As these are shifted to the right (histogram 2), the entries around zero μV become more purely comprised of true failures to release. The trend is reversed in histogram 3, as the small amplitude (noise-contaminated) EPSPs again contibute more entries to the bins around zero μV.

Changes at the synapse(s) following the tetani, which these histograms would be consistent with, are: (1) an increase in the quantal size, which could be either presynaptic (more transmitter released on each occasion when release occurred) or postsynaptic (increased postsynaptic current, including active currents in the spines or dendrites, or reduced attenuation of the voltage change evoked by that current due to changed cable properties), (2) an increase in the number of quanta available for release

(this would include new connections being formed, or the activation of previously inactive synapses) and (3) an increase in the probability of transmitter release (at normally releasing synapses) in combination with any of the above, but not alone.

Chapter Six:
CONCLUSIONS AND SUGGESTIONS FOR EXTENSIONS OF THIS STUDY

The general features of averaged unitary PSPs obtained in simultaneous CA3-CA1 intracellular recordings were described in Chapter Three. This investigation is the first to directly measure the synaptic strength of unitary connections between CA3 and CA1 neurones. The average amplitude of the unitary EPSPs recorded at the pyramidal soma was 131 μV, with a range of 30 to 665 μV. Previous estimates by Andersen (1982, 1986) were shown to remarkably accurate, and our results support the contention that synchronous input from about 100 excitatory afferents would be sufficient to discharge a CA1 pyramidal cell which was initially at the resting potential (Andersen, 1986). The convergence required to activate a CA1 neurone would of course be more variable in the natural situation. A greater number of afferents would need to be involved if the inputs were asynchronous or with increasing levels of postsynaptic inhibition (EPSP summation is less than linear when inhibition is intact; Langmoen & Andersen, 1983). Fewer synchronous inputs would be required to bring the neurone to discharge in the presence of asynchronous background excitation, if the inputs were facilitated by repetitive activation, or if regenerative processes brought about greater than linear summation. Note

that the potential for synchronized discharge of CA3 neurones is indicated by the demonstration of recurrent excitatory connections within CA3 (MacVicar & Dudek, 1980; Miles & Wong, 1986) and by the generation of synchronous burst discharges within CA3 when inhibition is blocked (Dichter & Spencer, 1969; Wong & Traub, 1983).

The time courses of the unitary EPSPs were compared with those of the 'minimal' EPSPs obtained by stimulation of afferents in the stratum radiatum (Turner, 1988), and with the time courses predicted by Turner (1984b, 1988) for inputs to single spines. On average the time courses of the unitary EPSPs were more similar to those evoked by proximal rather than distal stimulation of the stratum radiatum (Turner, 1988), although there was considerable individual variability. In addition, a comparison of the normalized shape-index plots for the three kinds of EPSP (minimal, unitary and modelled single spine inputs) indicated that the scatter of normalized half-widths for any given rise time was greatest for the minimal EPSPs (Turner, 1988), intermediate for the unitary EPSPs, and least for the single spine inputs modelled by Turner (1988). This finding would be consistent with some of the unitary connections involving more than one synapse (at different electrotonic locations), but on average involving fewer synapses than the minimal EPSPs of Turner (1988).

The demonstration that three PSPs consisted of predominant hyperpolarizations emphasizes the pervasiveness of the inhibitory circuitry in the CA1 region. It was surprising to find hyperpolarizing responses following

activation of single CA3 neurones, even though IPSPs have previously been found to be associated with small compound EPSPs evoked by stimulation of the stratum radiatum (Turner, 1985, 1988).

In Chapter Four, the intrinsic trial-to-trial variability of the unitary EPSPs was established. By comparison with other systems, it was argued that the coefficient of variation of the EPSPs was too great to be accounted for by variation in the quantal EPSP alone, implicating intermittent failure to release as one source of the variability. This was confirmed by the presence of distinct 'failures' peaks in some of the noise-contaminated EPSP amplitude histograms.

The method of variance, which is a form of quantal analysis based on Poisson statistics, provided results which did not aquately fit the experimental data for a sizeable proportion of the EPSPs. For this reason, and because of theoretical objections, it was difficult to justify further application of this method to the variations in amplitude of the CA1 EPSPs.

An unconstrained deconvolution method of quantal analysis was applied to the amplitude variations of both unitary EPSPs and small compound EPSPs evoked in CA1 neurones. In three cases the signal to noise ratios of the results gave confidence that discrete amplitudes were accurately resolved from the noise-contaminated EPSP amplitude histograms. For these EPSPs the quantal size estimates were 278 μV, 224 μV and 193 μV (for the unitary EPSP and two small compound EPSPs respectively). It is

suggested that the failure to resolve discrete amplitudes in the other noise-contaminated EPSP amplitude histograms could be due to (1) the small amplitude of the quantal EPSPs relative to the noise, (2) significant quantal variability or (3) significant differences between the amplitudes of quantal EPSPs originating from different release sites in the synaptic connections.

Synaptic plasticity was investigated for unitary EPSPs and compound EPSPs in the experiments described in Chapter Five. A surprising finding was the low incidence of LTP observed in small compound and unitary EPSPs after induction protocols which caused sustained enhancements of larger compound EPSPs. It is argued that this is unlikely to be secondary to any problems associated with the testing or induction protocols. It is suggested that one possible postsynaptic mechanism for LTP consistent with these results would be the activation a voltage-dependent channel, such as the modification of the Ca^{2+} channel as proposed by Connor et al (1988). If this is the case, then one of the interesting implications is that LTP may require some degree of cooperativity for its expression as well as for its induction. That is, a synapse which is potentiated might only express its modification in the presence of sufficient postsynaptic depolarization, provided by other synaptic inputs.

To make sense of such a mechanism, it could be proposed that a unitary afferent, activated in isolation, does not provide a functionally 'meaningful' input to a CA1 pyramidal cell. The other primary findings of this study, (1) that the

amplitude of a unitary EPSP is very small relative to the depolarization required to bring the neurone from the resting potential to the threshold for discharge, and (2) that the evoked response to a unitary connection is highly variable and frequently subject to failures, would both be consistent with this proposal. If the functionally 'meaningful' event consisted instead of discharge of a whole group of CA3 neurones which converged to a single CA1 cell (or group of CA1 cells) the evoked response would be of significant amplitude and would also be more reliable. If the expression of LTP were cooperative, the larger EPSP would be enhanced, but the modification induced in the unitary EPSP would not be expressed when it was activated alone. It might be advantageous for a unitary connection not to show its modification when not activated in synchrony with the other afferents, because the 'noise' induced by spontaneous release or asynchronous activation of the afferent would be reduced.

This rule could not apply absolutely to all unitary connections, as evidenced by the one unitary EPSP which was clearly potentiated. Some useful information was gained from that EPSP; there was no significant change in the time course with the change in amplitude, and from the amplitude histograms it was apparent that the potentiation was not solely due to a change in the release probabilities of already active release sites. Changes in other quantal parameters could not be ruled out, and these may have occurred in combination with alterations of the probabilities of transmitter release.

Suggestions for further experiments

The results from the investigation of LTP were particularly interesting, and this aspect of the study would take first priority for further experiments. As one of the concerns relating to the induction protocols was that there may have been insufficient spread of the postsynaptic depolarization to the synaptic site(s) involved in the unitary connection, it would be useful to try one of the methods of inducing potentiation which are not specific to the activated inputs. For example, both the application of phorbol esters (Malenka et al, 1986) and brief elevations of the extracellular Ca^{2+} concentration (Turner et al, 1982; Reymann et al, 1986; Williams & Bliss, 1988) induce sustained increases of EPSP amplitude similar to that seen in LTP. These should act equally at all synapses, and therefore would have the same opportunity to modify the synapses involved with both the unitary and the large compound EPSPs. It would be preferable to use the method of Ca^{2+} elevation, because the evidence that this activates the same mechanisms as those underlying LTP is more convincing than the evidence for phorbol ester activation of LTP mechanisms (Gustafsson & Wigstrom, 1988).

If these experiments confirmed the results of the present study (i.e. a differential effect on large and small EPSPs), it would be worth testing a wider range of compound EPSPs of different amplitudes in the same CA1 neurone. If EPSP amplitude versus stimulus current plots were made before and after tetanization, the threshold amplitude required for the expression of LTP could be determined. It might be

possible to show that this threshold was voltage-dependent, perhaps by showing it to be sensitive to depolarizing or hyperpolarizing current injections. Similarly, two EPSPs just below the amplitude threshold, and evoked by inputs to nearby regions of the dendritic tree, might show a cooperative enhancement when activated synchronously after tetanization, but not if activated separately. Similar EPSPs more separated in the dendritic tree should not show the same cooperativity. It might be possible to demonstrate LTP more frequently for unitary EPSPs in cells depolarized by current injection, although the increased electrode noise caused by passing current would require more records to be averaged for reliable measurement of the EPSP amplitude.

As explained in Chapter Four, the single most useful improvement for quantal analysis in CA1 pyramidal cells would be gained by a reduction of the background noise. One way to do this would be to use patch electrodes either in thin slices (with improved optics) or in fragments of tissue with exposed somata but intact dendritic regions. Cultures of hippocampal cells with synaptic connections might serve the same purpose, and might also have lower background levels of synaptic release.

Finally, there is still much to be learnt about the anatomy and physiology of the synaptic connections between single CA3 and CA1 neurones. The ideal experiment would involve combined physiology and intracellular labelling of the presynaptic and postsynaptic elements, as has been done for the group Ia afferent connection to the motoneurone (Redman & Walmsley, 1983a,b), for the inhibitory interneurone

input to the goldfish Mauthner cell (Korn et al, 1982) and in fetal mouse cell cultures (Pun et al, 1986). However this kind of experiment faces several major difficulties in the hippocampal slice. It more difficult to inject tracers such as HRP into individual somata, because they are closely packed in the stratum pyramidale, and spill into neighbouring cells is common. Another problem is that the synapses are so small in the hippocampus that electon microscopy is mandatory to verify the synaptic connections. In the slice preparation, there is always a difficult trade-off between maintaining the slices long enough to allow transport of the intracellular tracers, and at the same time avoiding deterioration (and ultrastuctural pathology) of the tissue. However, the usefulness of the information potentially provided by such a study would justify trial experiments.

REFERENCES

Abraham, W.C., B. Gustafsson, and H. Wigstrom (1986) Single high strength afferent volleys can produce long-term potentiation in the hippocampus *in vitro*. Neurosci. Lett. 70:217-222.

Abraham, W.C., B. Gustafsson, and H. Wigstrom (1987) Long-term potentiation involves enhanced synaptic excitation relative to synaptic inhibition in the guinea-pig hippocampus. J. Physiol. 394;367-380.

Akers, R.F., D.M. Lovinger, P.A. Colley, D.J. Linden, and A. Routtenberg (1986) Translocation of protein kinase C activity may mediate hippocampal long-term potentiation. Science 231:587-589.

Alger, B.E., and R.A. Nicoll (1982a) Feed-forward dendritic inhibition in rat hippocampal pyramidal cells studied *in vitro*. J. Physiol. 328:105-123.

Alger, B.E., and R.A. Nicoll (1982b) Pharmacological evidence for two kinds of GABA receptor on rat hippocampal pyramidal cells studied *in vitro*. J. Physiol. 328:125-141.

Andersen, P. (1975) Organization of hippocampal neurons and their interconnections. In The Hippocampus, Vol 1., R.L. Isaacson and K.H. Pribram, ed., Plenum Press.

Andersen, P. (1982) Synaptic control and modulation of hippocampal neurones. Adv. Biol. Psych. 8:40-55.

Andersen, P. (1986) Factors influencing the efficiency of dendritic synapses on hippocampal pyramidal cells. Neurosci. Res. 3:521-530.

Andersen, P., T. Blackstad, G. Hulleberg, M. Trommald, and J.L. Vaaland (1987a) Dimensions of dendritic spines of rat dentate granule cells during long-term potentiation (LTP). J. Physiol. 390:264P.

Andersen, P., T.V.P. Bliss, and K.K. Skrede (1971) Lamellar organization of hippocampal excitatory pathways. Exp. Brain Res. 13:222-238.

Andersen, P., J.C. Eccles, and Y. Loyning (1963) Recurrent inhibition in the hippocampus with identification of the inhibitory cell and its synapses. Nature 198:540-542.

Andersen, P., J.C. Eccles, and Y. Loyning (1964a) Location of postsynaptic inhibitory synapses on hippocampal pyramids. J. Neurophysiol. 27:592-607.

Andersen, P., J.C. Eccles, and Y. Loyning (1964b) Pathway of postsynaptic inhibition in the hippocampus. J. Neurophysiol. 27:608-619.

Andersen, P., P. Greengard, G.-Y. Hu, O. Hvalby, and S.I. Wallaas (1987b) Injection of protein kinase C in rat hippocampal pyramidal cells *in vitro* induces plastic changes similar to long-term potentiation. J. Physiol. 390:18P.

Andersen, P., and T. Lomo (1966) Mode of activation of hippocampal pyramidal cells by excitatory synapses on dendrites. Exp. Brain Res. 2:247-260.

Andersen, P., H. Silfvenius, S.H. Sundberg, and O. Sveen (1980a) Acomparison of distal and proximal dendritic synapses on CA1 pyramids in guinea-pig hippocampal slices *in vitro*. 307:273-299.

Andersen, P., J. Storm, and H.V. Wheal (1987c) Thresholds of action potentials evoked by synapses on the dendrites of pyramidal cells in the rat hippocampus *in vitro*. J. Physiol. 383:509-526.

Andersen, P., S.H. Sundberg, O. Sveen, J.W. Swann, and H. Wigstrom (1980b) Possible mechanisms for long-lasting potentiation of synaptic transmission in hippocampal slices from guinea-pigs. J. Physiol. 302:463-482.

Ascher, P., and L. Nowak (1986) Calcium permeability of the channels activated by N-methyl-D-aspartate (NMDA) in isolated mouse central neurones. J. Physiol. 377:35P.

Ascher, P., and L. Nowak (1987) Electrophysiological studies of NMDA receptors. Trends in Neurosci. 10:284-288.

Ashwood, T.J., B. Lancaster, and H.V. Wheal (1984) *In vivo* and *in vitro* studies on putative interneurones in the rat hippocampus: possible mediators of feed-forward inhibition. Brain Res. 293:279-291.

Barrionuevo, G., and T.H. Brown (1983) Associative long-term potentiation in hippocampal slices. Proc. Natl. Acad. Sci. USA 80:7347-7351.

Barrionuevo, G., S. Bench, and T.H. Brown (1985) Quantal analysis of postsynaptic current fluctuations in hippocampus. Soc. Neurosci. Abstr. 11:88.12.

Baudry, M., M. Oliver, R. Creager, A. Wieraszko, and G. Lynch (1980) Increase in glutamate receptors following repetitive electrical stimulation in hippocampal slices. Life Sci. 27:325-330.

Benardo, L.S., L.M. Masukawa, and D.A. Prince (1982) Electrophysiology of isolated hippocampal pyramidal dendrites. J. Neurosci. 2:1614-1622.

Bennett, M.R., P. Jones, and N.A. Lavidis (1986) The probability of quantal secretion along visualized branches at amphibian (*Bufo Marinus*) neuromuscular synapses. J. Physiol. 379:257-274.

Blackstad, T. (1956) Commissural connections of the hippocampal region of the rat, with special reference to their mode of termination. J. Comp. Neurol. 105:417-538.

Blackstad, T.W., K. Brink, J. Hem, and B. Jeune (1970) Distribution of hippocampal mossy fibres in the rat. An experimental study with silver impregnation methods. J. Comp. Neurol. 138:433-450.

Bliss, T.V.P., R.M. Douglas, M.L. Errington, and M.A. Lynch (1986) Correlation between long-term potentiation and release of endogenous amino acids from dentate gyrus of anaesthetized rats. J. Physiol. 377:391-408.

Bliss, T.V.P., and A.R. Gardner-Medwin (1973) Long-lasting potentiation of synaptic transmission in the dentate area of the unanaesthetised rabbit following stimulation of the perforant path. J. Physiol. 232:357-374.

Bliss, T.V.P., and T. Lomo (1973) Long-lasting potentiation of synaptic transmission in the dentate area of the anaesthetised rabbit following stimulation of the perforant path. J. Physiol. 232:331-356.

Boyd, I.A., and A.R. Martin (1956) The endplate potential in mammaliam muscle. J. Physiol. 132:74-91.

Brown, D.A., and W.H. Griffith (1983) Persistent slow inward calcium current in voltage-clamped hippocampal neurones of the guinea-pig. J. Physiol. 337:303-320.

Brown, T.H., R.K.S. Wong, and D.A. Prince (1979) Spontaneous miniature synaptic potentials in hippocampal neurones. Brain Res. 177:194-199.

Burke, R.E. (1967) Composite nature of the monosynaptic excitatory postsynaptic potential. J. Neurophysiol. 30:1114-1137.

Burke, R.E., and P.G. Nelson (1966) Synaptic activity in motoneurones during natural stimulation of muscle spindles. Science 151:1088-1091.

Buzsaki, G., and E. Eidelberg (1982) Direct afferent excitation and long-term potentiation of hippocampal interneurons. J. Neurophysiol. 48:597-607.

Chang, F.-L.F., and W.T. Greenough (1984) Transient and enduring morphological correlates of synaptic activity and efficacy change in the rat hippocampal slice. Brain Res. 309:35-46.

Christian, E.P., and F.E. Dudek (1988) Electrophysiological evidence from glutamate microapplications for local excitatory circuits in the CA1 area of rat hippocampal slices. J. Neurophysiol. 59:110-123.

Clements, J.D. (1986) Synaptic transmission and integration in spinal motoneurones. Ph.D. thesis, Australian National University.

Clements, J.D., I.D. Forsythe, and S.J. Redman (1987) Presynaptic inhibition of synaptic potentials evoked in cat spinal motoneurones by impulses in single group Ia axons. J. Physiol. 383, 153-169.

Clements, J.D., and S.J. Redman (1986) Electrical and geometrical non-uniformities in motoneurone cable properties. Soc. Neurosci. Abstr. 12:235.4.

Coan, E.J., and G.L. Collingridge (1987) Characteristics of an N-methyl-D-aspartate receptor component of synaptic transmission in rat hippocampal slices. Neuroscience 22:1-8.

Collingridge, G.L., C.E. Herron, and R.A.J. Lester (1988a) Synaptic activation of N-methyl-D-aspartate receptors in the Schaffer collateral-commissural pathway of rat hippocampus. J. Physiol. 399:283-300.

Collingridge, G.L., C.E. Herron, and R.A.J. Lester (1988b) Frequency-dependent N-methyl-D-aspartate receptor-mediated synaptic transmission in rat hippocampus. J. Physiol. 399, 301-312.

Collingridge, G.L., S.J. Kehl, and H. McLennan (1982) The action of an N-methylaspartate antagonist on synaptic processes in the rat hippocampus. J. Physiol. 338:27P.

Collingridge, G.L., S.J. Kehl, and H. McLennan (1983a) The antagonism of amino acid-induced excitations of rat hippocampal CA1 neurones *in vitro*. J. Physiol. 334:19-31.

Collingridge, G.L., S.J. Kehl, and H. McLennan (1983b) Excitatory amino acids in synaptic transmission in the Schaffer collateral-commissural pathway of the rat hippocampus. J. Physiol. 334:33-46.

Connor, J.A., W.J. Wadman, P.E. Hockberger, and R.K.S. Wong (1988) Sustained dendritic gradients of Ca^{2+} induced by excitatory amino acids in CA1 hippocampal neurons. Science 240:649-653.

Cotman, C.W., J.A. Flatman, A.H. Ganong, and M.N. Perkins (1986) Effects of excitatory amino acid antagonists on evoked and spontaneous excitatory potentials in guinea-pig hippocampus. J. Physiol. 378:403-415.

Cotman, C.W., and L.L. Iversen (1987) Excitatory amino acids in the brain - focus on NMDA receptors. Trends in Neurosci. 10:263-265.

Cotman, C.W., D.T. Monaghan, O.P. Ottersen, and J. Storm-Mathisen (1987) Anatomical organization of excitatory amino acid receptors and their pathways. Trends in Neurosci. 10:273-280.

Cotman, C.W., and J.V. Nadler (1981) Glutamate and aspartate as hippocampal transmitters: biochemical and pharmacological evidence. In Glutamate: transmitter in the central nervous system. P.J. Roberts, J. Storm-Mathisen, and G.A.R. Johnston, eds., John Wiley & Sons, Chichester.

Creager, R., T. Dunwiddie, and G. Lynch (1980) Paired-pulse and frequency facilitation in the CA1 region of the *in vitro* rat hippocampus. J. Physiol. 299:409-424.

D'Alonzo, A.J., and A.D. Grinnell (1985) Profiles of evoked release along the length of frog motor nerve terminals. J. Physiol. 359:235-258.

Del Castillo, J., and B. Katz (1954) Quantal components of the end-plate potential. J. Physiol. 124:560-573.

Dempster, A.P., N.M. Laird, and D.B. Rubin (1977) Maximum likelihood from incomplete data via the EM algorithm. J. R. Statist. Soc. B 39:1-21.

Deriemer, S.A., J.A. Strong, K.A. Albert, P. Greengard, and L.K. Kaczmarek (1985) Enhancement of calcium current in *Aplysia* neurones by phorbol ester and protein kinase C. Nature 313:313-316.

Dichter, M., and W.A. Spencer (1969) Penicillin-induced interictal discharges from the cat hippocampus. I. Characteristics and topological features. J. Neurophysiol. 32:649-662.

Dingledine, R., ed., (1984) Brain slices. Plenum Press, New York.

Dolphin, A.C., M.L. Errington, and T.V.P. Bliss (1982) Long-term potentiation of the perforant path *in vivo* is associated with increased glutamate release. Nature 297:496-498.

Dunwiddie, T. and G. Lynch (1978) Long-term potentiation and depression of synaptic responses in the rat hippocampus: localization and frequency dependency. J. Physiol. 276:353-367.

Dunwiddie, T. and G. Lynch (1979) The relationship between extracellular calcium concentrations and the induction of hippocampal long-term potentiation. Brain Res. 169:103-110.

Durand, D., P.L. Carlen, N. Gurevich, A. Ho, and H. Kunov (1983) Electrotonic parameters of rat dentate granule cells measured using short current pulses and HRP staining. J. Neurophysiol. 50:1080-1097.

Dutar, P., and R.A. Nicoll (1988) A physiological role for $GABA_B$ receptors in the central nervous system. Nature 332, 156-158.

Eccles, J.C. (1964) The physiology of synapses. Springer-Verlag, Berlin.

Edwards, F.R., J.J.B. Jack, and D.M. Kullmann (1983) The relationship between amplitude and time course of single fibre group Ia excitatory postsynaptic potentials in cat spinal motoneurones. J. Physiol. 345:58P.

Edwards, F.R., S.J. Redman, and B. Walmsley (1976a) Statistical fluctuations in charge transfer at Ia synapses on spinal motoneurones. J. Physiol. 259:665-688.

Edwards, F.R., S.J. Redman, and B. Walmsley (1976b) Non-quantal fluctuations and transmission failures in charge transfer at Ia synapses on spinal motoneurones. J. Physiol. 259:689-704.

Errington, M.L., M.A. Lynch, and T.V.P. Bliss (1987) Long-term potentiation in the dentate gyrus: induction and increased glutamate release are blocked by D(-)aminophosphonovalerate. Neuroscience 20:279-284.

Finch, D.M., N.L. Nowlin, T.L. Babb (1983) Demonstration of axonal projections of neurons in the rat hippocampus and subiculum by intracellular injection of HRP. Brain Res. 271:201-216.

Frankenhaeuser, B., and A.L. Hodgkin (1957) The action of calcium on the electrical properties of squid axons. J. Physiol. 137:218-244.

Fyffe, R.E.W., and A.R. Light (1984) The ultrastructure of group Ia afferent fibre synapses in the lumbosacral cord of the cat. Brain Res. 300:201-209.

Gamble, E., and C. Koch (1987) The dynamics of free calcium in dendritic spines in response to repetitive synaptic input. Science 236:1311-1315.

Groen, T.V., and J.M. Wyss (1988) Species differences in hippocampal commissural connections: studies in rat, guinea pig, rabbit and cat. J. Comp. Neurol. 267:322-334.

Gustafsson, B., and H. Wigstrom (1986) Hippocampal long-lasting potentiation produced by pairing single volleys and brief conditioning tetani evoked in separate afferents. J. Neurosci. 6:1575-1582.

Gustafsson, B., and H. Wigstrom (1988) Physiological mechanisms underlying long-term potentiation. Trends in Neurosci. 11:156-162.

Gustafsson, B., H. Wigstrom, W.C. Abraham, and Y.-Y. Huang (1987) Long-term potentiation in the hippocampus using depolarizing current pulses as the conditioning stimulus to single volley synaptic potentials. J. Neurosci. 7:774-780.

Haas, H.L., and G. Rose (1984) The role of inhibitory mechanisms in hippocampal long-term potentiation. Neurosci. Lett. 47:301-306.

Hablitz, J.J., and I.A. Langmoen (1986) N-methyl-D-aspartate receptor antagonists reduce synaptic excitation in the hippocampus. J. Neurosci. 6:102-106.

Halliwell, J.V. (1983) Caesium-loading reveals two distinct Ca-currents in voltage-clamped guinea-pig hippocampal neurones *in vitro*. J. Physiol. 341:10-11P.

Hanker, J.S., P.E. Yates, C.B. Metz, and A. Rustioni (1977) A new specific, sensitive and noncarcinogenic reagent for the demonstration of horseradish peroxidase. J. Histochem. 9:789-792.

Harris, E.W., and C.W. Cotman (1986) Long-term potentiation of guinea pig mossy fibre responses is not blocked by N-methyl-D-aspartate antagonists. Neurosci. Lett. 70, 132-137.

Harris, K.M., and J.K. Stevens (1987) Study of dendritic spines by serial electron microscopy and three-dimensional reconstructions. In Intrinsic determinants of neuronal form and function. R.J. Lasek, and M.M. Black, eds., Alan R. Liss, New York.

Harrison P.J., J.J.B. Jack, and D.M. Kullmann (1985) Independence of quantal size and synaptic location of descending monosynaptic excitatory post-synaptic potentials in cat spinal motoneurones. J. Physiol. 369:25P.

Hasselblad, V. (1966) Estimation of parameters for a mixture of normal distributions. Technometrics 8:431-444.

Hatt, H. and D.O. Smith (1976) Non-uniform probabilities of quantal release at the crayfish neuromuscular junction. J. Physiol. 259:395-404.

Henneman, E., H.R. Luscher, and J. Mathis (1984) Simultaneously active and inactive synapses of single Ia fibres on cat spinal motoneurones. J. Physiol. 352:147-161.

Herron, C.E., R.A.J. Lester, E.J. Coan, and G.L. Collingridge (1986) Frequency-dependent involvement of NMDA receptors in the hippocampus: a novel synaptic mechanism. Nature 322:265-268.

Hess, G., U. Kuhnt, and L.L. Voronin (1987) Quantal analysis of paired-pulse facilitation in guinea pig hippocampal slices. Neurosci. Lett. 77:187-192.

Higashima, M., S. Sawada, and C. Yamamoto (1986) A revised method for generation of unitary postsynaptic potentials for quantal analysis in the hippocampus. Neurosci. Lett. 68:221-226.

Hirst, G.D.S., S.J. Redman, and K. Wong (1981) Post-tetanic potentiation and facilitation of synaptic potentials evoked in cat spinal motoneurones. J. Physiol. 321:97-109.

Hjorth-Simonsen, A. (1973) Some intrinsic connections of the hippocampus in the rat: an experimental analysis. J. Comp. Neurol. 147:145-162.

Hoel, P.G. (1954) Introduction to mathematical statistics. John Wiley & Sons, New York.

Hubbard, J.I., R. Llinas, and D.M.J. Quastel (1969) Electrophysiological analysis of synaptic transmission. Edward Arnold Publishers, London.

Ito, M., and T. Oshima (1965) Electrical behaviour of the motoneurone membrane during intracellularly applied current steps. J. Physiol. 180:607-635.

Jack, J.J.B., S. Miller, R. Porter, and S.J. Redman (1971) The time course of minimal excitatory post-synaptic potentials evoked in spinal motoneurones by group Ia afferent fibres. J. Physiol. 215:353-380.

Jack, J.J.B., and S.J. Redman (1971) The propagation of transient potentials in some linear cable structures. J. Physiol. 215:283-320.

Jack, J.J.B., S.J. Redman, and K. Wong (1981) The components of synaptic potentials evoked in cat spinal motoneurones by impulses in single group Ia afferents. J. Physiol. 321:65-96.

Jarvilehto, M., I.A. Meinertzhagen, and S.R. Shaw (1986) Anti-adhesive coating for glass microelectrodes. J. Neurosci. Meth. 17:327-334.

Johnson, N.L., and S. Kotz (1970) Continuous univariate distributions, 2nd Edition. Houghton-Mifflin, Boston.

Johnston, D. (1981) Passive cable properties of hippocampal CA3 pyramidal neurons. Cell. Mol. Neurobiol. 1:41-55.

Johnston, D., J.J. Hablitz, and W.A. Wilson (1980) Voltage clamp discloses slow inward current in hippocampal burst-firing neurones. Nature 286:391-393.

Kaczmarek, L.K. (1987) The role of protein kinase C in the regulation of ion channels and neurotransmitter release. Trends in Neurosci. 10:30-34.

Kelso, S.R., and T.H. Brown (1986) Differential conditioning of associative synaptic enhancement in hippocampal brain slices. Science 232:85-87.

Kelso, S.R., A.H. Ganong, and T.H. Brown (1986) Hebbian synapses in hippocampus. Proc. Natl. Acad. Sci. USA 83:5326-5330.

Knowles, W.D., and P.A. Schwartzkroin (1981) Local circuit synaptic interactions in hippocampal brain slices. J. Neurosci. 1:318-322.

Kohno, K., and N. Noguchi (1986) Large myelinated club endings on the Mauthner cell in the goldfish: a study with thin sectioning and freeze-fracturing. Anat. Embryol. 173:361-370.

Korn, H., Y. Burnod, and D.S. Faber (1987) Spontaneous quantal currents in a central neuron match predictions from binomial analysis of evoked responses. Proc. Natl. Acad. Sci. USA 84:5981-5985.

Korn, H., D.S. Faber, Y. Brunod, and A. Triller (1984) Regulation of efficacy at central synapses. J. Neurosci. 4:125-130.

Korn, H., A. Mallet, A. Triller, and D.S. Faber (1982) Transmission at a central inhibitory synapse. II. Quantal description of release, with a physical correlate for binomial n. J. Neurophysiol. 48:697-707.

Korn, H., A. Triller, A. Mallet, and D.S. Faber (1981) Fluctuating responses at a central synapse. n of binomial fit predicts number of stained presynaptic boutons. Science 213:898-901.

Kosaka, T. (1980) The axon initial segment as a synaptic site: ultrastructure and synaptology of the initial segment of the pyramidal cell in the rat hippocampus (CA3 region). J. Neurocyt. 9:861-882.

Kuhnt, U., A. Mihaly, and F. Joo (1985) Increased binding of calcium in the hippocampal slice during long-term potentiation. Neurosci. Lett. 53:149-154.

Kuno, M. (1964) Quantal components of excitatory synaptic potentials in spinal motoneurones. J. Physiol. 175:81-99.

Kuno, M., and T. Takahashi (1986) Effects of calcium and magnesium on transmitter release at Ia synapses of rat spinal motoneurones *in vitro*. J. Physiol. 376:543-553.

Lacaille, J., A.L. Mueller, D.D. Kunkel and P.A. Schwartzkroin (1987) Local circuit interactions between oriens/alveus interneurons and CA1 pyramidal cells in hippocampal slices: electrophysiology and morphology. J. Neurosci. 7:1979-1993.

Lacaille, J., and P.A. Schwartzkroin (1988a) Stratum lacunosum-moleculare interneurons of hippocampal CA1 region. I. Intracellular response characteristics, synaptic responses, and morphology. J. Neurosci. 8:1400-1410.

Lacaille, J., and P.A. Schwartzkroin (1988b) Stratum lacunosum-moleculare interneurons of hippocampal CA1 region. II. Intrasomatic and intradendritic recordings of local circuit synaptic interactions. J. Neurosci. 8:1411-1424.

Langmoen, I.A., and P. Andersen (1983) Summation of excitatory postsynaptic potentials in hippocampal pyramidal cells. J. Neurophysiol. 50:1320-1329.

Lee, K.S. (1983) Cooperativity among afferents for the induction of long-term potentiation in the CA1 region of the hippocampus. J. Neurosci. 3:1369-1372.

Lee, K.S., F. Schottler, M. Oliver, and G. Lynch (1980) Brief bursts of high-frequency stimulation produce two types of structural change in rat hippocampus. J. Neurophysiol. 44:247-258.

Levy, W.B., and O. Steward (1979) Synapses as associative memory elements in the hippocampal formation. Brain Res. 175:233-245.

Levy, W.B., and O. Steward (1983) Temporal contiguity requirements for long-term associative potentiation/depression in the hippocampus. Neuroscience 8:791-797.

Lin, J.-W., and D.S. Faber (1988a) Synaptic transmission mediated by single club endings on the goldfish Mauthner cell. I. Characteristics of electrotonic and chemical postsynaptic potentials. J. Neurosci. 8:1302-1312.

Lin, J.-W., and D.S. Faber (1988b) Synaptic transmission mediated by single club endings on the goldfish Mauthner cell. II. Plasticity of excitatory postsynaptic potentials. J. Neurosci. 8:1313-1325.

Linden, D.J., F.-S. Sheu, K. Murakami, and A. Routtenberg (1987) Enhancement of long-term potentiation by *cis*-unsaturated fatty acid: relation to protein kinase C and phospholipase A_2. J. Neurosci. 7:3783-3792.

Lorente de No, R. (1934) Studies on the structure of the cerebral cortex. II. Continuation of the study of the ammonic system. J. Psychol. Neurol. 46:113-176.

Lovinger, D.M., K.L. Wong, K. Murakami, and A. Routtenberg (1987) Protein kinase C inhibitors eliminate hippocampal long-term potentiation. Brain Res. 436:177-183.

Lynch, G., and M. Baudry (1984) The biochemistry of memory: a new and specific hypothesis. Science 224:1057-1063.

Lynch, M.A., and T.V.P. Bliss (1986) On the mechanism of enhanced release of [^{14}C]glutamate in hippocampal long-term potentiation. Brain Res. 369:405-408.

Lynch, G.S., V.K. Gribkoff, and S.A. Deadwyler (1976) Long-term potentiation is accompanied by a reduction in dendritic responsiveness to glutamic acid. Nature 263:151-153.

Lynch, G., S. Halpain, and M. Baudry (1982) Effects of high-frequency synaptic stimulation on glutamate receptor binding studied with a modified *in vitro* hippocampal slice preparation. Brain Res. 244:101-111.

Lynch, G., J. Larson, S. Kelso, G. Barrionueuo, and F. Schottler (1983) Intracellular injections of EGTA block induction of hippocampal long-term potentiation. Nature 305:719-721.

MacDermott, A.B. and N. Dale (1987) Receptors, ion channels and synaptic potentials underlying the integrative actions of excitatory amino acids. Trends in Neurosci. 10:280-284.

MacDermott, A.B., M.L. Mayer, G.L. Westbrook, S.J. Smith, and J.L. Barker (1986) NMDA-receptor activation increases cytoplasmic calcium concentration in cultured spinal cord neurones. Nature 321:519-522.

MacVicar, B.A. and F.E. Dudek (1980) Local synaptic circuits in rat hippocampus: interactions between pyramidal cells. Brain Res. 184:220-223.

Madison, D.V., R.C. Malenka, and R.A. Nicoll. (1986) Phorbol esters block a voltage-sensitive chloride current in hippocampal pyramidal cells. Nature 321:695-697.

Malenka, R.C., D.V. Madison, and R.A. Nicoll (1986) Potentiation of synaptic transmission in the hippocampus by phorbol esters. Nature 321:75-177.

Malinow, R. and J.P. Miller (1986) Postsynaptic hyperpolarization during conditioning reversibly blocks induction of long-term potentiation. Nature 320:529-530.

Martin, A.R. (1966) Quantal nature of synaptic transmission. Physiological Rev. 46:51-66.

Martin, A.R. (1977) Junctional transmission II. Presynaptic mechanisms. In Handbook of Physiology, Vol. 1, Sect. 1, E. Kandel, ed., pp. 329-355. The American Physiological Society, Bethesda.

Masukawa, L.M. and D.A. Prince (1984) Synaptic control of excitability in isolated dendrites of hippocampal neurones. J. Neurosci. 4:217-227.

Mayer, M.L. and G.L. Westbrook (1988) the action of N-methyl-D-aspartic acid on mouse spinal neurones in culture. J. Physiol. 361:65-90.

McLachlan, E.M. (1978) The statistics of transmitter release at chemical synapses. In International Review of Physiology. Neurophysiology III, Vol. 17, R. Porter, ed., University Park Press, Baltimore.

McNaughton, B.L. (1982) Long-term synaptic enhancement and short-term potentiation in rat fascia dentata act through different mechanisms. J. Physiol. 324:249-262.

McNaughton, B.L. (1983) Activity dependent modulation of hippocampal synaptic efficacy: some implications for memory process. In Neurobiology of the hippocampus, W. Seifert, ed. Academic Press, London.

McNaughton, B.L., C.A. Barnes, and P. Andersen (1981) Synaptic efficacy and EPSP summation in granule cells of rat fascia dentata studied *in vitro*. J. Neurophysiol. 46:952-966.

McNaughton, B.L., R.M. Douglas, and G.V. Goddard (1978) Synaptic enhancement in *fascia dentata*: cooperativity among coactive afferents. Brain Res. 157:277-293.

Miles, R. and R.K.S. Wong (1984) Unitary inhibitory synaptic potentials in the guinea-pig hippocampus *in vitro*. J. Physiol. 356:97-113.

Miles, R. and R.K.S. Wong (1986) Excitatory synaptic interactions between CA3 neurones in the guinea-pig hippocampus. J. Physiol. 373:397-418.

Miles, R. and R.K.S. Wong (1987a) Latent synaptic pathways revealed after tetanic stimulation in the hippocampus. Nature 329:724-726.

Miles, R. and R.K.S. Wong (1987b) Inhibitory control of local excitatory circuits in the guinea-pig hippocampus. J. Physiol. 388:611-629.

Miller, R.J. (1987) Multiple calcium channels and neuronal function. Science 235:46-52.

Miyakawa, H. and H. Kato (1986) Active properties of dendritic membrane examined by current source density analysts in hippocampal CA1 pyramidal neurons. Brain Res. 399:303-309.

Mody, I., J.D.C. Lambert, and U. Heinemann (1987) Low extracellular magnesium induces epileptiform activity and spreading depression in rat hippocampal slices. J. Neurophysiol. 57:869-888.

Monaghan, D.T. and C.W. Cotman (1982) the distribution of [3H]Kainic acid binding sites in rat CNS as determined by autoradiography. Brain Res. 252:91-100.

Monoghan, D.T., V.R. Holets, D.W. Toy, and C.W. Cotman (1983) Anatomical distributions of four pharmacologically distinct ^{3}H-L-glutamate binding sites. Nature 306:176-179.

Monaghan, D.T., D. Yao, and C.W. Cotman (1984) Distribution of [^{3}H]AMPA binding sites in rat brain as determined by quantitative autoradiography. Brain Res. 324:160-164.

Muir, R.B. and Porter, R. (1973) the effect of preceding stimulus on temporal facilitation at corticomotoneuronal synapses. J. Physiol. 228:749-763.

Neale, E.A., P.G. Nelson, R.L. MacDonald, C.N. Christian, and L.M. Bowers (1983) Synaptic interactions between mammalian central neurones in cell culture III. Morphophysiological correlates of quantal synaptic transmission. J. Neurophysiol. 49:1459-1468.

Newberry, N.R. and R.A. Nicoll (1984) A bicuculline-resistant inhibitory post-synaptic potential in rat hippocampal pyramidal cells *in vitro*. J. Physiol. 348:239-254.

Newberry, N.R. and R.A. Nicoll (1985) Comparison of the action of baclofen with y-amino butyric acid on rat hippocampal pyramidal cell *in vitro*. J. Physiol. 360:161-185.

Nowak, L., P. Bregestovski, P. Ascher, A. Berbet, and A. Prochiantz (1984) Magnesium gates glutamate-activated channels in mouse central neurones. Nature 307:462-465.

Perkel, D.H. and D.J. Perkel (1985) Dendritic spines: role of active membrane in modulating synaptic efficacy. Brain Res. 325:331-335.

Pun, R.Y.K., E.A. Neale, P.B. Guthrie, and P.G. Nelson (1986) Active and inactive central synapses in cell culture. J. Neurophysiol. 56:1242-1256.

Racine, R.J., N.W. Milgram, and S. Hafner (1983) Long-term potentiation phenomena in the rat limbic forebrain. Brain Res. 260:217-231.

Rainbow, T.C., C.M. Wieczorek, and S. Halpain (1984) Quantitative autoradiography of binding sites for [3H]AMPA, a structural analogue of glutamic acid. Brain Res. 309:173-177.

Rall, W. (1967) Distinguishing theoretical synaptic potentials computed for different soma-dendritic distributions of synaptic inputs. J. Neurophysiol. 30:1138-1168.

Rall, W. (1977) Core conductor theory and cable properties of neurons. In Handbook of Physiology - The Nervous System I, American Physiological Society, Bethesda.

Rall, W. and J. Rinzel (1973) Branch input resistance and steady attenuation for input to one branch of a dendritic neuron model. Biophys. J. 13:648-688.

Rall, W. and I. Segev (1987) Functional possibilities for synapses on dendrites and dendritic spines. In Synaptic function, Edelman, Fall & Cowan, eds., John Wiley & Sons.

Ramon y Cajal, S. (1893) The structure of Ammon's horn. Charles C. Thomas, Springfield, Illinois. (English translation, published 1968)

Ramon y Cajal, S. (1911) Histologie du systeme nerveux de l'Homme et des Vertebres, A. Maloine, Paris.

Redman, S.J. (1973) The attenuation of passively propagating dendritic potentials in a motoneurone cable model. J. Physiol. 234:637-664.

Redman, S.J. (1979) Junctional mechanisms at group Ia synapses. Prog. Neurobiol. 12:33-83.

Redman, S. and B. Walmsley (1983a) The time course of synaptic potentials evoked in cat spinal motoneurones at identified group Ia synapses. J. Physiol. 343:117-133.

Redman, S. and B. Walmsley (1983b) Amplitude fluctuations in synaptic potentials evoked in cat spinal motoneurones at identified group 1a synapses. J. Physiol. 343:135-145.

Rethelyi, M. (1970) Ultrastructural synaptology of Clarke's column. Exp. Brain Res. 11:159-174.

Reymann, K.G., H.K. Matthies, U. Frey, V.S. Vorobyev and H. Matthies (1986) Calcium-induced long-term potentiation in the hippocampal slice: characterization of the time course and conditions. Brain Res. Bull. 17:291-296.

Richardson, T.L., R.W. Turner, and J.J. Miller (1987) Action-potential discharge in hippocampal CA1 pyramidal neurons: current source-density analysis. J. Neurophysiol. 58:981-996.

Robitaille, R. and J.P. Tremblay (1987) Non-uniform release at the frog neuromuscular junction: evidence of morphological and physiological plasticity. Brain Res. Rev. 12:95-116.

Schwartzkroin, P.A. and D.D. Kunkel (1985) Morphology of Identified interneurones in the CA1 regions of guinea pig hippocampus. J. Comp. Neurol. 232:205-218.

Schwartzkroin, P.A. and L.H. Mathers (1978) Physiological and morphological identification of a nonpyramidal hippocampal cell type. Brain Res. 157:1-10.

Schwartzkroin, P.A. and D.A. Prince (1980) Changes in excitatory and inhibitory synaptic potentials leading to epileptogenic activity. Brain Res. 183:61-76.

Shepherd, G.M., R.K. Brayton, J.P. Miller, I. Segev., J. Rinzel, and W. Rall (1985) Signal enhancement in distal cortical dendrites by means of interactions between active dendritic spines. Proc. Natl. Acad. Sci. USA 82:2192-2195.

Simonson, L., M. Baudry, R. Siman, and G. Lynch (1985) Regional distribution of soluble calcium activated proteinase activity in neonatal and adult rat brain. Brain Res. 327:153-159.

Skrede, K.K. and D. Malthe-Sorenssen (1981) Increased resting an evoked release of transmitter following repetitive electrical tetanization in hippocampus: a biochemical correlate to long-lasting synaptic potentiation. Brain Res. 208:436-441.

Skrede, K.K. and R.H. Westgaard (1971) The transverse hippocampal slice; a well-defined cortical structure maintained *in vitro*. Brain Res. 35:589-593.

Smith, S.J. (1987) Progress on LTP at hippocampal synapses: a post-synaptic CA^{2+} trigger for memory storage? Trends in Neurosci. 10:142-144.

Snow, R.W., C.P. Taylor and F.E. Dudek (1983) Electrophysiological and optical changes in slices of rat hippocampus during spreading depression. J. Neurophysiol. 50:561-572.

Somogyi, P., A.D. Smith, M.G. Nunzi, A. Gorio, H. Takagi, and J.Y. Wu (1983a) glutamate decarboxylase immunoreactivity in the hippocampus of the cat: distribution of immunoreactive synaptic terminals with special reference to the axon initial segment of pyramidal neurons. J. Neurosci. 3:1450-1468.

Somogyi, P., M.G. Nunzi, A. Gorio, and A.D. Smith (1983b) A new type of specific interneuron in the monkey hippocampus forming synapses exclusively with the axon initial segments of pyramidal cells. Brain Res. 259:137-142.

Spencer, W.A. and E.R. Kandel (1961) Electrophysiology of hippocampal neurons IV. Fast prepotentials. J. Neurophysiol. 24:272-285.

Strong, J.A., A.P. Fox, R.W. Tsien, and L.K. Kaczmarek (1987) Stimulation of protein kinase C recruits covert calcium channels in *Aplysia* bag cell neurons. Nature 325:714-717.

Swanson, L.W. and W.M. Cowan (1977) An autoradiographic study of the organization of the efferent connections of the hippocampal formation in the rat. J. Comp. Neurol. 172:49-84.

Swanson, L.W., P.E. Sawchenko and W.M. Cowan (1980) Evidence that the commissural, associational and septal projections of the regio inferior of the hippocampus arise from the same neurons. Brain Res. 197:207-212.

Swanson, L.W., J.M. Wyss, and W.M.Cowan (1978) An autoradiographic study of the organisation of intrahippocampal association pathways in the rat. J. Comp. Neurol. 181:681-716.

Tamamaki, N., K. Watanabe, and Y. Nojko (1984) A whole image of the hippocampal pyramidal neuron revealed by intracellular pressure-injection or horseradish peroxidase. Brain Res. 307:336-340.

Taube, J.S. and P.A. Schwartzkroin (1987) Intracellular recording from hippocampal CA1 interneurons before and after development of long-term potentiation. Brain Res. 419:32-38.

Taube, J.S. and P.A. Schwartzkroin (1988) Mechanisms of long-term potentiation: EPSP/spike dissociation, intradendritic recordings, and glutamate sensitivity. J. Neurosci. 8:1632-1644.

Teyler, T.J. and P. DiScenna (1987) Long-term Potentiation. Ann. Rev. Neurosci. 10:131-161.

Tracey, D.J. and B. Walmsley (1984) Synaptic input from identified muscle afferents to neurones of the dorsal spinocerebellar tract in the cat. J. Physiol. 350:599-614.

Triller, A. and H. Korn (1982) Transmission at a central inhibitory synapse. III. Ultrastructure of physiologically identified terminals. J. Neurophysiol. 48:708-736.

Turner, D.A. (1984a) Segmental cable evaluation of somatic transients in hippocampal neurons (CA1, CA3 and dentate). Biophys. J. 46:73-84.

Turner, D.A. (1984b) Conductance transients onto dendritic spines in a segmental cable model of hippocampal neurons. Biophys. J. 46:85-96.

Turner, D.A. (1985) The influence of feed-forward ipsps on small epsps in hippocampal CA1 pyramidal cells *in vitro* - timing and interactions. Neurosci. Lett. Suppl. 22, S511.

Turner, D.A. (1988) Waveform and amplitude characteristics of evoked reponses to dendritic stimulation of CA1 guinea-pig pyramidal cells. J. Physiol. 395:419-439.

Turner, D.A. and P.A. Schwartzkroin (1980) Steady-state electrotonic analysis of intracellularly stained hippocampal neurons. J. Neurophysiol. 44:184-199.

Turner, R.W., K.G. Baimbridge, and J.J. Miller (1982) Calcium-induced long-term potentiation in the hippocampus. Neuroscience 7:1411-1416.

Tuttle, R., S. Masuko and Y. Nakajima (1986) Freeze-fracture study of the large myelinated club ending synapse on the goldfish Mauthner cell: Special reference to the quantitative analysis of gap junctions. J. Comp. Neurol. 246:202-211.

Walmsley, B., F.R. Edwards, and D.J. Tracey (1987) The probabilistic nature of synaptic transmission at a mammalian excitatory central synapse. J. Neurosci. 7:1037-1046.

Walmsley, B., F.R. Edwards, and D.J. Tracey (1988) Non-uniform release probabilities underlie quantal synaptic transmission at a mammalian excitatory central synapse. J. Neurphysiol. In press.

Walmsley, B., E. Wieniawa-Narkiewicz, and M.J. Nicol (1985) The ultrastructural basis for synaptic transmission between primary muscle afferents and neurons in Clarke's column of the cat. J. Neurosci. 5:2095-2106.

Watkins, J.C. and H.J. Olverman (1987) Agonists and antagonists for excitatory amino acid receptors. Trends in Neurosci. 10:265-272.

Westrum, L.E. and T.W. Blackstad (1962) An electron microscopic study of the stratum radiatum of the rat hippocampus (regio superior, CA1) with particular emphasis on synaptology. J. Comp. Neurol. 119:281-309.

Wickens, J.R. (1988) Electrically coupled but chemically isolated synapses: dendritic spines and calcium in a rule for synaptic modification. Prog. Neurobiol. In press.

Wigstrom, H. and B. Gustafsson (1985) Facilitation of hippocampal long-lasting potentiation by GABA antagonists. Acta. Physiol. Scand. 125:159-172.

Wigstrom, H., B. Gustafsson, Y.-Y. Huang, and W.C. Abraham (1986) Hippocampal long-term potentiation is induced by pairing single afferent volleys with intracellularly injected depolarizing current probes. Acta. Physiol. Scand. 126:317-319.

Wigstrom, H., B. Gustafsson, and Y.-Y. Huang (1986) Mode of action of excitatory amino acid receptor antagonists on hippocampal long-lasting potentiation. Neuroscience 17:1105-1115.

Wigstrom, H., B. Gustafsson, and Y.-Y. Huang (1985) A synaptic potential following single volleys in the hippocampal CA1 region possibly involved in the induction of long-lasting potentiation. Acta. Physiol. Scand. 124:475-478.

Williams, J.H. and T.V.P. Bliss (1988) Induction but not maintenance of calcium-induced long-term potentiation in dentate gyrus and area CA1 of the hippocampal slice is blocked by nordihydroguaiaretic acid. Neurosci. Lett. 88:81-85.

Wong, K. and S. Redman (1980) The recovery of a random variable from a noisy record with application to the study of fluctuations in synaptic potentials. J. Neurosci. Meth. 2:389-409.

Wong, R.K.S. and D.A. Prince (1979) Dendritic mechanisms underlying penicillin induced epileptiform activity. Science 204:1228-1230.

Wong, R.K.S., D.A. Prince, and A.I. Basbaum (1979) Intradendritic recordings from hippocampal neurons. Proc. Natl. Acad. Sci. U.S.A. 76:986-990.

Wong, R.K.S., and R.D. Traub (1983) Synchronized burst discharge in disinhibited hippocampal slice. I. Initiation in CA2-CA3 region. J. Neurophysiol. 49:442-458.

Yamamoto, C. (1982) Quantal analysis of excitatory postsynaptic potentials induced in hippocampal neurons by activation of granula cells. Exp. Brain Res. 46:170-176.

Yamamoto, C., M. Higashima. and S. Sawada (1987) Quantal analysis of potentiating action of phorbol ester on synaptic transmission in the hippocampus. Neurosci. Res. 5:28-38.

Zucker, R.S. (1973) Changes in the statistics of transmitter release during facilitation. J. Physiol. 229:787-810.